INFORMATION TO USERS

This manuscript has been reproduced from the microfilm master. UMI films the text directly from the original or copy submitted. Thus, some thesis and dissertation copies are in typewriter face, while others may be from any type of computer printer.

The quality of this reproduction is dependent upon the quality of the copy submitted. Broken or indistinct print, colored or poor quality illustrations and photographs, print bleedthrough, substandard margins, and improper alignment can adversely affect reproduction.

In the unlikely event that the author did not send UMI a complete manuscript and there are missing pages, these will be noted. Also, if unauthorized copyright material had to be removed, a note will indicate the deletion.

Oversize materials (e.g., maps, drawings, charts) are reproduced by sectioning the original, beginning at the upper left-hand corner and continuing from left to right in equal sections with small overlaps. Each original is also photographed in one exposure and is included in reduced form at the back of the book.

Photographs included in the original manuscript have been reproduced xerographically in this copy. Higher quality 6" x 9" black and white photographic prints are available for any photographs or illustrations appearing in this copy for an additional charge. Contact UMI directly to order.

UMI

A Bell & Howell Information Company
300 North Zeeb Road, Ann Arbor MI 48106-1346 USA
313/761-4700 800/521-0600

Université d'Ottawa · University of Ottawa

STUDY OF MUTATIONS ARISING *IN VIVO* AND *IN VITRO* IN A NEW MURINE TUMOR MODEL SYSTEM: THE ROLE OF REACTIVE OXYGEN AND NITROGEN SPECIES

Jagdeep K. Sandhu

Thesis submitted to the Department of Microbiology and Immunology in partial fulfillment of the requirements for the degree Doctor of Philosophy

University of Ottawa
Ottawa, Ontario, Canada
January, 1998

ABSTRACT

The initiation and progression of cancer is associated with mutational events that may be either small-scale (base changes) or large-scale (amplification, loss of chromosome fragments or chromosome rearrangements). The mechanism by which these changes occur is not well understood. We have hypothesized that factors present in the tumor microenvironment, such as products of inflammatory cells (reactive oxygen and nitrogen species) may be mutagenic and/or clastogenic and thereby contribute to tumor progression. A transplantable murine tumor model system has been established in our laboratory to study the contribution of the tumor microenvironment in tumor progression using the hypoxanthine phosphoribosyltransferase (*HPRT*) gene as a marker of chromosome fragmentation or loss. MN-11 was identified as the most stable clone with a low spontaneous mutant frequency (MF) and 1000 times increased sensitivity than the parental line in detecting mutagenic events induced by ^{60}Co γ-rays. This cell line can grow *in vitro* and *in vivo* as a subcutaneous tumor in syngeneic C57BL/6 mice. This model system allows the *ex vivo* detection of mutants that may arise *in vivo* in tumors. Such mutants are resistant to the cytotoxic drug, 6-thioguanine when grown *in vitro*. The frequency of mutants arising in MN-11 cells grown as subcutaneous tumors was found to be 4-fold higher than that in otherwise identical cells grown in culture. The mutant frequency of individual tumors varied considerably in a non-gaussian manner. These results suggest that the conditions within solid tumors are mutagenic and/or clastogenic.

Solid tumors are comprised of malignant cells plus infiltrating host cells. Histochemical analysis of MN-11 tumors showed the presence of granulocytes, macrophages, mast cells and lymphocytes. Biochemical measurements of total nitric oxide

synthase (NOS) activity in tumor homogenates demonstrated a positive correlation between NOS activity and MF. The expression of inducible (iNOS) was estimated by Western blot analysis and localized by immunohistochemistry. The synthase was present in some tumors as a 130 kDa band, similar to the human iNOS, but not in others. The iNOS-positive cells included predominantly granulocytes and not tumor cells, lymphocytes or vascular endothelial cells. Granulocytes were found mainly in necrotic areas, less frequently in non-necrotic and at the periphery of the tumor. A positive correlation was observed between the number of infiltrating granulocytes and MF. A positive correlation was also observed between % tumor necrosis and MF. These results are consistent with the notion that endogenously generated nitric oxide (NO·) or a related species by tumor-infiltrating phagocytic cells may contribute to the observed increase in MF in MN-11 tumors. Administration of an antioxidant, vitamin E to tumor-bearing mice resulted in a significant decrease in MF by 50%.

Using this model system, a series of nitrogen monoxide (NO)-donating drugs that differed in their rate of NO· release was tested to induce mutants both *in vitro* and *in vivo*. The results show that NO-donating drugs can induce mutants in MN-11 cells but they varied widely in their mutagenic potential. Glyceryl trinitrate and sodium nitroprusside were found to be mutagenic in MN-11 cells. The mutation can be blocked *in vitro* by pretreatment with vitamin E. As a positive control, exposure of tumor-bearing mice to ionizing radiation and cisplatin also showed an increase in MF. Administration of glyceryl trinitrate to tumor-bearing mice produced a large increase in MF that could also be blocked by vitamin E. In summary, the MN-11 tumor model system has allowed sensitive detection of mutants both *in vitro* and *in vivo*. NO· or a related species generated endogenously by tumor-infiltrating

granulocytes may induce mutations in MN-11 cells grown as tumors. In this manner NO· or a related species may contribute to genetic instability in MN-11 tumors leading to tumor progression.

This thesis is dedicated to

my husband, our children and my parents, especially my mother who has given me the strength and support to complete these studies

ACKNOWLEDGMENTS

The completion of my Ph.D. thesis has been a long and strenuous journey of my life. I started as a Master's student in Dr. Birnboim's laboratory and upgraded to the Ph.D. program. During the course of these studies I was blessed with two children. Balancing between the laboratory and family life was hard. The one who made all this possible is my mother and I owe a huge debt of gratitude to her. She is a symbol of strength and encouragement that got me through difficult times and without whose constant love and inspiration these studies would never have been completed. Thanks a lot to my father who has been very understanding and supportive of my never-ending enthusiasm in science. I also thank my sister for her kindness to give loving care to my children. Special thanks to my husband, whose patience, enduring support and love got me through this experience.

Now, I would like humbly to thank Dr. Hyman Chaim Birnboim, my thesis supervisor under whose supervision I have accomplished this work. He deserves special acknowledgment for the excellence he brought to this project, for his expertise, encouragement, constructive criticism and continuous support throughout these studies. I am indebted for his patience, for his willingness to devote his valuable time and answering all my naive questions anytime.

Thanks are also due to Drs. R. Korneluk, E.Brown, and K. Dimock, members of my advisory committee, for their valuable advice and helpful suggestions. Special thanks to our collaborators, Dr. David Blakey for the fluorescence *in situ* hybridization studies, Dr. Susan Robertson for providing the iNOS antibody and Dr. George Wenckebach for photomicrography and histopathological studies of the tumors. The technical help provided by Louise Kobylinski and Zaida Ticas with histochemical and immunohistochemical analysis of tumors is greatly appreciated. I also acknowledge Dr. Anthony Krantis for helping me with the nitric oxide synthase assays and Dr. Wally McNaughton for assistance with nitrite measurements. Thanks to Dr. Alvin Chan for the gift of vitamin E used in these studies and the generous supply of cytokines by Dr. Mark Freedman. Many thanks to the dedicated staff of the Animal Care and services for helping me with the animal experiments.

I especially thank all the members of the lab for their support and friendship and being like a family to me throughout the years. Thanks to: Amy Yamazaki, Amanda Reid, Diana Wilkinson, Donna Grant, Helen Privora, Randy Cowling, Steffany Bennett and other members, past and present of the Birnboim lab. The technical assistance of Cai-Ying Zhou, Sylvie and Rick Pilon is also greatly acknowledged. As for the thesis writing, many thanks to my nephew, J. Singh, for his expertise in computers and my son, Asees, for being quiet around me. Once again thanks to all my family members for their forbearance and support throughout this project that consumed much time that would otherwise have been spent with them.

Finally, and most important, I would like to thank **God** with all my love.

PREFACE

Genomic instability is a characteristic of malignant tumors, but the underlying mechanisms are only partially understood. Factors *intrinsic* to the tumor cells have been extensively studied which may predispose these cells to further instability. In contrast, this thesis explores the possibility that factors *extrinsic* to the tumor cells presumably present in the tumor environment, such as reactive oxygen and nitrogen species may enhance genetic instability. These reactive species may be presumably produced by tumor-infiltrating phagocytic cells that may cause mutagenic and/or clastogenic damage to the neighbouring tumor cells leading to tumor progression. The tumor milieu and inflammatory milieu are characterized by increased recruitment of phagocytic cells to sites of tissue destruction. Transient release of proinflammatory mediators is necessary for the body to fight infection and help in wound repair. However, sustained release of these mediators can result in pathophysiological conditions such as rheumatoid arthritis, ulcerative colitis, gastritis etc. There is a expanding body of literature that suggests that many of these disorders have been associated with an increased predisposition to the development of cancers. The specific focus of this thesis is to examine the role of reactive oxygen and reactive nitrogen species, with emphasis on nitric oxide as potential contributors to the increased genetic instability commonly observed within solid tumors. The organization of the thesis is as follows:

There is one combined abstract and list of abbreviations for all the chapters at the beginning of the thesis. Materials, suppliers and solution composition are detailed in the text and/or Appendix II. Preparation of fixatives and antibody solutions is detailed in Appendix III. A general Methods section is not included and the Methods common to all the chapters are described in Appendix IV. The thesis begins with a general introduction section and the results section is divided into five chapters. Except Materials being listed elsewhere, each chapter is organized as a typical research paper with abstract, introduction, Methods, Results and Discussion section. The first chapter introduces the reader to a review of the literature on different toxic species elaborated by cells and mechanisms by which they can promote genetic instability. The next chapter describes the development of the novel *in vitro/in vivo/ex vivo* murine model system (MN-11) used to study genetic instability *in situ* in growing tumors and chapter 3 describes the biology of this tumor. The next three chapters focus on the role of reactive oxygen and reactive nitrogen species in inducing mutations in this model system. Chapter 6 describes the use of a lipophilic antioxidant, vitamin E to block the mutations induced by reactive nitrogen species. The thesis ends with a general discussion section which ties all the chapters with overall conclusions of the study and future direction. I hope that by organizing the material in this way readers can gain a better understanding of the role of reactive nitrogen species in promoting genomic instability underlying tumor progression.

TABLE OF CONTENTS

LIST OF FIGURES AND ILLUSTRATIONS

CHAPTER 1

CHAPTER 2

CHAPTER 3

CHAPTER 4

CHAPTER 5

CHAPTER 6

CHAPTER 7

LIST OF TABLES

CHAPTER 1

CHAPTER 2

CHAPTER 4

CHAPTER 6

LIST OF ABBREVIATIONS

(Terms are defined when they first appear in text. The following abbreviations are used upon subsequent citation)

AI	Apoptotic index
ANOVA	Analysis of variance
5-Aza-Cyd	5-azacytidine
BLI	BrdU labeled index
BrdU	5-bromo-2'-deoxyuridine
CDTA	*trans*-1,2,-diamine-cyclohexane-*N,N,N',N'*,-tetraacetic acid
cNOS	constitutive nitric oxide synthase
D_0	dose that reduces survival to 37%
DEA/NO·	diethylamine dinitric oxide
DMSO	dimethylsulfoxide
EDRF	endothelium-derived relaxing factor
EGTA	ethylene glycol-bis (β-amino ethyl ether)-*N, N, N', N'*,-tetraacetic acid
eNOS	endothelial nitric oxide synthase
FCS	fetal calf serum
GTN	glyceryl trinitrate
h	hour(s)
HAT	hypoxanthine, aminopterin, thymidine
HPRT	hypoxanthine phosphoribosyltransferase gene
$HPRT^-$	cells with a functional *HPRT* gene, manifested as HAT-resistance
$HPRT^-$	cells with a nonfunctional (mutant) *HPRT* gene, manifested as 6-TG-resistance
HT	hypoxanthine, thymidine
IL	interleukin (e.g., IL-8)
iNOS	inducible nitric oxide synthase
i.p.	intraperitoneal
L	litre(s)
LPS	lipopolysaccharide
MF	mutant frequency

µg	micrograms
MI	mitotic index
min	minute(s)
µL	microlitres
mL	millilitres
µM	micromolar
mM	millimolar
MNU	*N*-methyl-*N*-nitrosourea
MOL	molsidomine or N-carboxy-3-morpholino-sydnonimine-ethylester
mRNA	messenger ribonucleic acid
neo	neomycin resistance gene
nNOS	neuronal nitric oxide synthase
NO·	nitric oxide
NOS	nitric oxide synthase
oxyHb	oxyhaemoglobin
PB	phosphate buffer
PBS	phosphate buffered saline
RNS	reactive nitrogen species
ROS	reactive oxygen species
S-phase	synthetic-phase
s.c.	subcutaneous
SD	standard deviation
SDS	sodium dodecyl sulfate
SEM	standard error of mean
SIN-1	active metabolite of MOL
SNAP	*S*-nitroso-*N*-acetyl-D,L-penicillamine
SNP	sodium nitroprusside
SOD	Cu,Zn-superoxide dismutase
SPER/NO·	spermine bis (NO·) adduct
TBS	50 mM tris-buffered saline, pH 7.6
TK	thymidine kinase gene
TPA	12-*O*-tetradecanoylphorbol-13-acetate (also known as PMA, phorbol 12-myristate 13-acetate)
6-TG	6-thioguanine

CHAPTER 1

GENERAL INTRODUCTION

ABSTRACT

A hallmark of tumor cells is genomic instability, manifested as increased chromosomal aberrations, amplification, deletions and at the gene level as mutations. The basis for this genomic instability in cancer has not been fully established. Much recent work has been directed in investigating the role of critical genes such as the tumor suppressor gene *p*53, which may predispose to genomic instability via alterations in the cell cycle and in deoxyribonucleic acid (DNA) repair. In contrast, we and others have postulated that the microenvironment of a developing tumor might itself contribute to genomic instability and mutagenesis, leading to tumor progression. The tumor milieu and the inflammatory milieu are very similar in many aspects. Both are characterized by changes in vasculature, by tissue destruction and the presence of an inflammatory infiltrate such as granulocytes, mast cells, macrophages and lymphocytes. These cells release a variety of proinflammatory agents such as interleukins, arachidonic acid metabolites, platelet activating factor (PAF), reactive oxygen (ROS) and reactive nitrogen species (RNS) that cause damage to the neighbouring cells.

Our laboratory has established a novel tumor model system (MN-11) [1] to study mutations that arise *in situ* in growing tumors (Figure 1-1). The salient features of this model system are as follows: (i) the cells can be grown *in vitro* or (ii) grown as subcutaneous tumors in syngeneic C57BL/6 mice, and (iii) mutations at the *HPRT* gene can be detected with high sensitivity. Such mutations are indicators of genetic damage and provide no growth advantage or disadvantage to the mutant cells [1].

1.1 GENOMIC INSTABILITY AND CANCER

There is increasing evidence that the pathogenesis of cancer proceeds in a step-wise

Figure 1-1 **MN-11 tumor model system to examine mutational events in the tumor microenvironment.** MN-11 cells were grown in culture and then injected in C57BL/6 mice to form subcutaneous tumors. Following 2 weeks of growth, tumors were excised and examined for the appearance of mutant cells in culture.

Figure 1-1

***IN VITRO/IN VIVO/EX VIVO* MN-11 TUMOR MODEL SYSTEM**

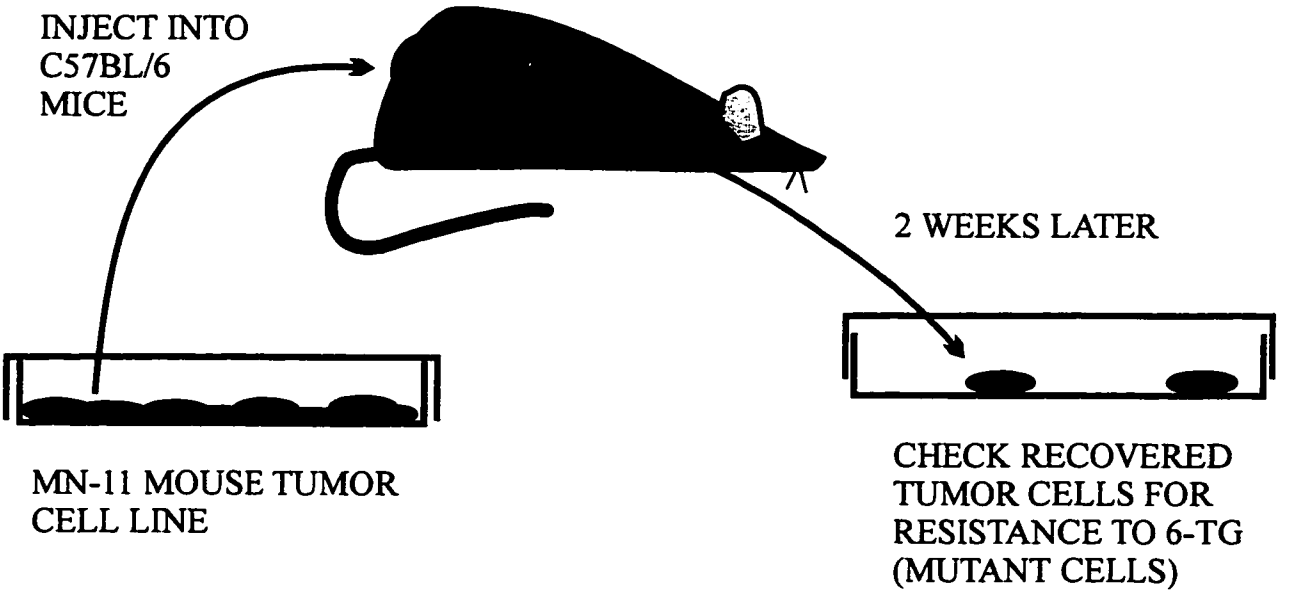

fashion. A number of genetic changes are required for a normal cell to become an invasive metastatic tumor [2-5]. Normal cells generally exhibit a stable karyotype, while genomes of cancer cells are unstable showing increased "*genomic instability*". Multiple pathways exist in normal cells that allow accurate duplication and distribution of DNA to progeny cells. In contrast, genomic instability in cancer cells may arise by mutational or exogenous interference with the pathways that ensure normal cellular homeostasis and genetic continuity. In fact, a large number of mutations is often found in malignant cells; these mutations cannot be accounted for by the low spontaneous mutation rate in rapidly growing normal cells [6] and has been ascribed to a "mutator phenotype". The mutator phenotype in tumor cells may be one cause of genomic instability. These processess are thought to underlie tumor heterogeneity and progression [3]. Genomic instability is associated with cancer and tumor progression [7,8]. The genomic alterations associated with tumor progression include, point mutations and deletions, chromosomal aberrations, gene amplifications, alteration of microsatellite sequences, replication errors and epigenetic changes such as DNA methylation. Mutations in genes that cause a generalized increased frequency of single base substitutions, insertions, or deletions are commonly called *mutator mutations*. Other mutations may lead to an increased frequency of aneuploidy or structural chromosomal aberrations and are called *chromosomal mutations*. These mutations result in increased genomic instability and may together be called *genomic instability mutations* [9].

1.1.1 *Genomic instability and tumor progression*

The idea that genomic instability mutations may play an important role in human cancer is supported by three lines of observations: (i) the incidence of most adult cancers

exhibits an exponential rate of increase with age, suggesting a series of events each rendered more likely by the occurrence of a previous event [10]; (ii) there is increasing evidence that multiple genetic alterations occur in tumors to generate a solid metastatic tumor. A cell with enhanced genomic instability would traverse this evolutionary pathway more rapidly than a cell with normal stability; individual colon cancers, for example, have been reported to involve four to five sequential chromosomal changes [11]; (iii) human cancer-prone syndromes such as Fanconi's anaemia, xeroderma pigmentosum (XP), Bloom's syndrome, and ataxia-telangiectasia (AT), characterized by chromosome instability, provide striking evidence that genomic instability can be heritable and that such instability is associated with a predisposition to cancer [12,13]. Although many studies show the existence of genomic instability in tumors, *in vivo* factors affecting its activation are not known, and a causal relationship between genomic instability and tumor progression remains to be established [9].

1.1.2 *p53 and genomic instability*

Alterations of the *p*53 tumor suppressor gene have been reported in a wide variety of human cancers, suggesting that it plays an important role in the formation of tumors [14-17].

(i) *p*53 functions in the G1-S checkpoint: Proliferating cells have several mechanisms for repairing DNA damage. DNA damage can be detected in at least two stages in the cell cycle: at the G1-S transition and at the G2-M transition. These transitions serve as check points to allow repair of damage before entering either S phase, when damage would be perpetuated, or M phase, when breaks would result in the loss of genetic material. A number of studies have implicated the *p*53 protein in the G1-S arrest in response to DNA damage [18-20]. Cells with DNA damage rapidly increase the content of *p*53 protein levels

by a post-transcriptional mechanism. Induction of *p*53 results in transcriptional activation of GADD45, MDM2 and CIP1/WAF1/SD11 and inhibits the activity of cyclin-dependent kinases (CDKs), thus inducing either arrest in G1 or apoptosis. Cells with abnormal *p*53 do not activate *p*21 and do not show the normal G1 arrest necessary for repair following exposure to DNA-damaging agents, leading to increased genomic instability.

Evidence supporting a role for the *p*53 protein in G1-S checkpoint pathway in the development of human cancers is provided by studies on adenocarcinomas in esophageal epithelium [21,22]. In this cancer type, cellular damage leads to cell cycle arrest, but when loss of a cell cycle checkpoint occurs, genetic instability develops and the cells progress to a malignant phenotype. Abnormal expression of cyclins D, E, and A in some cancers [23-25] and altered associations of various cyclin-CDK proteins in *p*53-deficient cells [26], may provide additional mechanisms of abrogating the G1-S checkpoint during tumorigenesis.

(ii) *p*53 and gene amplification: Cells homozygous for mutant *p*53 are genetically unstable and can undergo gene amplification [18,27]. When challenged with the uridine biosynthesis inhibitor N-phosphonacetyl-L-aspartate (PALA), these cells gain the capacity to amplify at high frequency the gene encoding CAD (a trifunctional polypeptide containing carbamoyl phosphate synthetase, aspartate transcarbamylase and dihydroorotase). Germ line mutations in the *p*53 gene are found in families with the Li-Fraumeni cancer syndrome. Normal somatic cells from these patients are heterozygous for *p*53, whereas tumor cells have no wild-type *p*53 gene. Cells homozygous for *p*53 mutations amplify the CAD gene at high frequency, while heterozygous and wild-type cells do not, suggesting that loss or alteration of both copies of the *p*53 gene is needed for amplification to occur [18,27].

1.1.3 *DNA repair and genomic instability*

Mutations in DNA repair genes (mismatch repair and excision repair) predispose to cancer, presumably by increasing genomic instability. Several human genetic disorders including XP, Bloom's syndrome and Fanconi's anaemia involve faulty DNA repair pathways. These predispose affected individuals to the development of various malignancies [12,13]. Recently, a more common form of DNA repair deficiency (termed RER phenotype, for replication errors) was described that may account for a large portion of genetic instability in hereditary nonpolyposis colorectal cancers (HNPCC). However, a small percent of sporadic colorectal tumors also exhibit RER phenotype [28-30]. The RER is manifested by instability in microsatellite repeat sequences (CA repeats). RER phenotype in HNPCC (Lynch syndrome) involves germline mutations in mismatch repair (MMR) genes. The four MMR genes known to be mutated in the germline of HNPCC patients are the mutS-related gene, *hMSH2*, and the bacterial mutL-related genes *hMLH1*, *hPMS1* and *hPMS2* [31-36]. In families with HNPCC, a mutation in one gene copy is inherited, and a somatic mutation in the second copy is associated with microsatellite instability in the tumor [32-35]. The RER phenotype has been observed in many familial and sporadic cancers, suggesting that the RER phenotype may represent a common feature of neoplasia [37,38]; however, not all human tumors examined exhibit the RER phenotype and microsatellite instability [39,40]. Muir-Torre syndrome, an inherited predisposition to sebaceous gland tumors and to colorectal carcinomas, is associated with microsatellite instability [41]. The observed genomic instability is compatible with a mutator phenotype, which predisposes patients to the development of various malignancies. How the change in the microsatellite sequences contributes to tumor development and tumor progression is unknown and is under

investigation.

1.1.4 *Other mechanisms*

As opposed to the *endogenous* mechanisms of genomic instability discussed above, recently attention has been paid to the *exogenous* factors in the tumors that would enhance genomic instability and contribute to the progression of the tumor to a more malignant state. Our laboratory has been interested in the factors in the tumor environment, such as reactive oxygen and nitrogen species generated by tumor-infiltrating phagocytic cells that may be mutagenic/clastogenic. Using the MN-11 tumor model our laboratory was the first to demonstrate an increased MF in cells grown as s.c. tumors as compared with cells cultured for the equivalent time [1]. Work from two laboratories independently also demonstrated genomic instability *in vivo* in tumors. Paquette and Little [42] used the C3H/10T½ cell line as a model and showed that the frequency of genomic rearrangements was higher in clones grown as tumors than among clones passaged *in vitro*. In another study, LN12 cells were used to show an increase in MF in cells grown as subcutaneous tumors than cells in culture [43]. These studies suggest that the conditions within solid tumors are mutagenic and suggest that genetic instability induced by the tumor microenvironment is important in tumor progression.

1.2 INFLAMMATION

Inflammation is the reaction of vascularized tissue to local injury from a variety of physical, chemical, microbial or immunological agents. An inability to produce an inflammatory response leads to a compromised host. On the other hand, inappropriate

activation of the inflammatory cascade, or more important, absence of a "stop" signal in an otherwise normal inflammatory process leads to debilitating inflammatory diseases. The mechanisms that may "turn on" or "turn off" an inflammatory signal remain essentially unknown. The inflammatory response consists of acute and chronic phases. Acute inflammation is directed toward neutralizing the damaging agents and restoration of the tissue to normal functions. The characteristic features of acute inflammation are the formation of an inflammatory exudate that has three principal constituents: fibrin, serum and leukocytes, predominantly neutrophils. The formation of the inflammatory exudate involves three vascular phenomena: (i) dilation of local blood vessels (ii) increased vascular permeability permitting plasma proteins to pass into the tissue (iii) migration of leukocytes from blood vessels into the areas of the damaged tissue. The duration and intensity of each reaction is determined by the concentration of proinflammatory agents present at the site of injury. In some circumstances, a damaging agent may persist over a prolonged period despite the tissue responses directed at destroying or neutralizing it resulting in continuous tissue damage. This process is known as chronic inflammation. It is marked by increased infiltration of macrophages, lymphocytes and plasma cells at the site of the injury. Macrophages continue the phagocytic work begun by neutrophils and ultimately mop up the degenerate neutrophils and fibrin strands. The duration and intensity of this response depends upon the elaboration of immune molecules by inflammatory cells at the site of injury. Under normal conditions, inflammation is transient progressing through acute and chronic phases before dissipating. However, under pathological conditions, the stimulus responsible for activating the inflammatory response fails to be eradicated and the entire cycle is perpetuated and/or exacerbated.

1.2.1 *Inflammation and cancer*

Chronic infection, injury and inflammation have long been recognized as risk factors for a variety of human cancers. How does an inflammatory response contribute to tumor development and tumor progression? This subject was first reviewed in 1975 by Templeton [44] and more recently by Ohshima and Bartsch [45]. As shown in Table 1-1, the association between inflammation and cancer has been observed in many different tissues. Inflammation may arise due to viral, bacterial, or parasitic infections or due to autoimmune diseases. In each case the inflammation is prolonged and the cancer usually develops at the site of inflammation. It has been proposed that agents generated in chronically inflamed tissues can cause injury to target cells and damage DNA, which could contribute to tumor development. It is unknown whether transient or recurrent inflammatory reactions are associated with increased cancer risk. Nor it is known to what extent chemical and physical agents present in the environment are acting in humans to increase tumorigenesis by stimulating inflammatory reactions. Many irritants thought to increase cancer development by stimulation of cell proliferation may also act by aggravating inflammation in the tissue and *vice versa*. Depending upon their concentrations, endogenously generated proinflammatory agents may exert physiological or pathophysiological effects. At low concentrations or with limited exposure, they act as signalling molecules and are important for normal physiological functions. However, at high concentrations or with extended exposure they can stimulate cell replication and/or act as endogenous carcinogens.

Table 1-1 Possible role of inflammatory mediators in an increase in cancer incidence in patients with chronic inflammation

Inflammatory Disorder	Source/site of inflammation	Cancer site	Inflammatory mediators	Mechanism of action
Bacterial infection	*Helicobacter pylori* Urinary infection Tuberculosis	stomach bladder lung	ROS RNS	Chromosomal abnormalities DNA damage ↑ cell replication
Parasitic infection	*S. haematobium* *S. mansoni* *S. japonicum* *Opisthorchis viverrini* *Clonorchis sinensis* Malaria	bladder liver colon biliary tract biliary tract Burkitt's lymphoma	*N*-nitroso compounds ROS RNS	Chromosomal abnormalities DNA damage ↑ cell replication cell death fibrosis
Viral infection	Hepatitis viruses Human papilloma virus Herpes simplex virus- type 2 Cytomegalovirus Epstein-Barr virus Human T-cell leukemia virus Human immunodeficiency virus	liver cervix Burkitt's lymphoma Adult T-cell leukemia Kaposi's sarcoma, non-Hodgkin lymphoma	*N*-nitroso compounds ROS	DNA damage
Crohn's disease	inflammation of the ileumn and/or colon	colon	ROS RNS PAF	DNA damage ↑ cell replication
Ulcerative colitis	inflammation of mucous membranes	colon	ROS RNS	DNA damage ↑ cell replication
Rheumatoid arthritis	inflammation of synovium	lymphoma	ROS RNS	DNA damage ↑ cell replication
Atrophic gastritis	inflammation of the stomach with atrophy of mucosa and glands	stomach	ROS	DNA damage ↑ cell replication

Particles (e.g. silica dust. asbestos)	inflammation of the exposed tissues	lung	ROS RNS nitrosamines	Chromosomal abnormalities DNA damage ↑ cell replication
Chronic injury (burns. heat. smoking)	Recurrent cystitis chronic skin ulcers Repeated abrasions	throat lung. bladder skin	ROS	Chromosomal abnormalities DNA damage ↑ cell replication

Adapted from references [53. 45. 54, 55].

(i) Chronic inflammatory disorders associated with cancers: There is clear evidence from human studies that "inflammatory conditions" i.e., in the absence of exposure to environmental carcinogens, may predispose individuals to the development of cancer (Table 1-1). A rare form of acne predisposes to squamous cell carcinoma [46]. Chronic gastritis due to *Helicobacter pylori* infection is strongly associated with increased risk of non-cardia gastric adenocarcinoma and gastric lymphoma [47-52]. There is an increase in acute and chronic inflammatory cells in the patients with *H. pylori* infection, such as neutrophils, lymphocytes, macrophages and plasma cells. The increased risk of cancer development is presumed to be mediated by agents released by inflammatory cells.

Schistosomiasis is a common parasitic disease that occurs in humans. Three major species infect man and each is associated with an increase in cancer (Table 1-1). *S. haematobium* infection is strongly associated with increased incidence of bladder cancer [54,56]. Individuals become infected with the larvae (termed cercariae or metacercariae) that can penetrate the skin. The adult worms inhabit the veins of the perivesical plexus, where the female lays eggs. The eggs can either penetrate through the bladder mucosa to be excreted in the urine or become trapped in the epithelial cell lining of the bladder. A chronic

inflammatory reaction is initiated with infiltration of histiocytes and other inflammatory cells into the bladder, the formation of granuloma and eventually fibrosis. Thus, the infection is long term and the eruption of eggs through the mucosa stimulate urothelial hyperplasia and cell turnover which could be associated with increased risk of tumor development. Epidemiological and experimental studies describe a strong relationship between infection with the liver fluke, *Opisthorchis viverrini*, and cholangiocarcinoma in humans [55]. The flukes chronically infect the intrahepatic bile ducts and cause long term inflammation leading to increased risk of tumor development.

Colorectal carcinoma risk is increased in patients with longstanding ulcerative colitis and Crohn's disease [57]. Patients with rheumatoid arthritis, a chronic inflammatory autoimmune disease, have an increased incidence of development of haematopoietic cancers of B cells and myelocytes, including lymphoma, and multiple myeloma [58]. Epidemiological studies suggest a strong association between chronic hepatitis and cirrhosis caused by infections of hepatitis B virus (HBV) and hepatocellular carcinoma in humans [53]. The mechanism by which HBV increases liver cancer is unknown but may be related to alteration of cellular DNA directly or indirectly by the virus. However, the integration of the HBV DNA into hepatocyte DNA is not adjacent to known protooncogenes. Whether inflammation *per se* contributes to the increase in the incidence of liver cancer is unknown. Furthermore, in some situations where there may be an environmental carcinogen implicated (such as tobacco in lung cancer or head and neck cancer), there also may be an associated chronic inflammation, which may contribute to cancer development.

Besides these clinical observations, there is abundant literature describing controlled animal experiments where inflammation contributes to cancer development in the presence

of a known carcinogenic agent. The 'classic' animal model to examine the relationship between inflammation and cancer is the well-known mouse skin tumor initiation/promotion/progression system [59]. TPA (12-*O*-tetradecanoylphorbol-13-acetate), a widely used activator of protein kinase C, was first identified as the active inflammatory and tumor promoting agent in croton oil in this model system. A plasmacytoma model has been developed by Potter and colleagues in which an irritating but chemically inert agent 2,6,10,14 tetramethylpentadecane (pristane) was injected into the peritoneal cavity of mice [60]. The chronic peritoneal inflammation lead to the development of plasmacytomas, and it was suggested that neutrophils present in the inflamed area may contribute to the development of plasmacytomas. Other experimental models have also been examined. Colitis induced by chemotactic peptides (formylmethionyl-leucyl-phenylalanine (FMLP) and formylnorleucyl-leucyl-phenylalanine (FNLP)) enhances colon carcinogenesis in the rat [61,62]. Instillation of these peptides caused increased infiltration of neutrophils resulting in acute mucosal inflammation, followed by ulceration and necrosis. In none of these systems has a critical inflammatory component(s) been identified that is responsible for the increase in malignancy. The inflammatory milieu is an extremely complex environment in which abnormally high levels of interleukins, eicosanoids, PAF, ROS and RNS [63] may be present. Which of these, singly or in combination, may be causally related to the increase in cancer frequency is not known with certainty and is currently being investigated in different laboratories.

1.3 REACTIVE OXYGEN SPECIES

This brief review discusses the mechanisms by which inflammation may lead to the development of cancer, mainly focussing on the role of ROS and RNS in mutation induction.

ROS are free radical species produced by every cell type constitutively, and in certain cases they are produced in sufficient quantities to act as cytotoxic and genotoxic agents. Some blood cells, for example, phagocytic cells are activated to synthesize ROS during acute and chronic inflammation. ROS encompass superoxide anion ($O_2^{\cdot-}$), hydrogen peroxide (H_2O_2) and/or hydroxyl radical ($OH\cdot$). These species are toxic and can attack cellular biomolecules resulting in damage to lipids, proteins, and nucleic acids. Because of the toxic nature of these radicals, cells have evolved pathways to eliminate $O_2^{\cdot-}$ and H_2O_2, thereby eliminating the formation of $OH\cdot$. These include superoxide dismutase (SOD) for superoxide [64] and peroxidases and catalase for hydrogen peroxide (Figure 1-2). In spite of these antioxidant mechanisms, endogenous or exogenous sources of these toxic products could contribute to the development of many pathologic conditions [65-69].

Various studies have implicated ROS in the induction of gene mutations. Moody and Hassan [70] have shown that ROS produced by the intracellular metabolism of paraquat was mutagenic in *Salmonella typhimurium*. ROS generated chemically, enzymatically or by phagocytic cells have been shown to be genotoxic to mammalian cells. They produce effects that include cytotoxicity, DNA strand breaks, specific-locus mutations, chromosome aberrations, sister-chromatid exchanges, and transformation [70-74]. Human neutrophils activated by TPA induce mutations at the *HPRT* locus in CHO cells [72]. Phillips et al. [76] observed an increase in mutation frequency (MF) in CHO cells exposed to the xanthine oxidase/xanthine system. Catalase, but not SOD, prevented the induction, indicating that externally generated H_2O_2 is the mutagenic agent. Mutations were also observed at this locus when a large number of V79 cells were exposed to millimolar concentrations of H_2O_2

Figure 1-2 **Reactions showing the formation and elimination of ROS.** The sequential four-electron reduction of molecular oxygen to water is depicted in which superoxide, hydrogen peroxide and hydroxyl radical are intermediates. Enzymatic pathways to control superoxide and hydrogen peroxide are also shown. Adapted from [75].

Figure 1-2

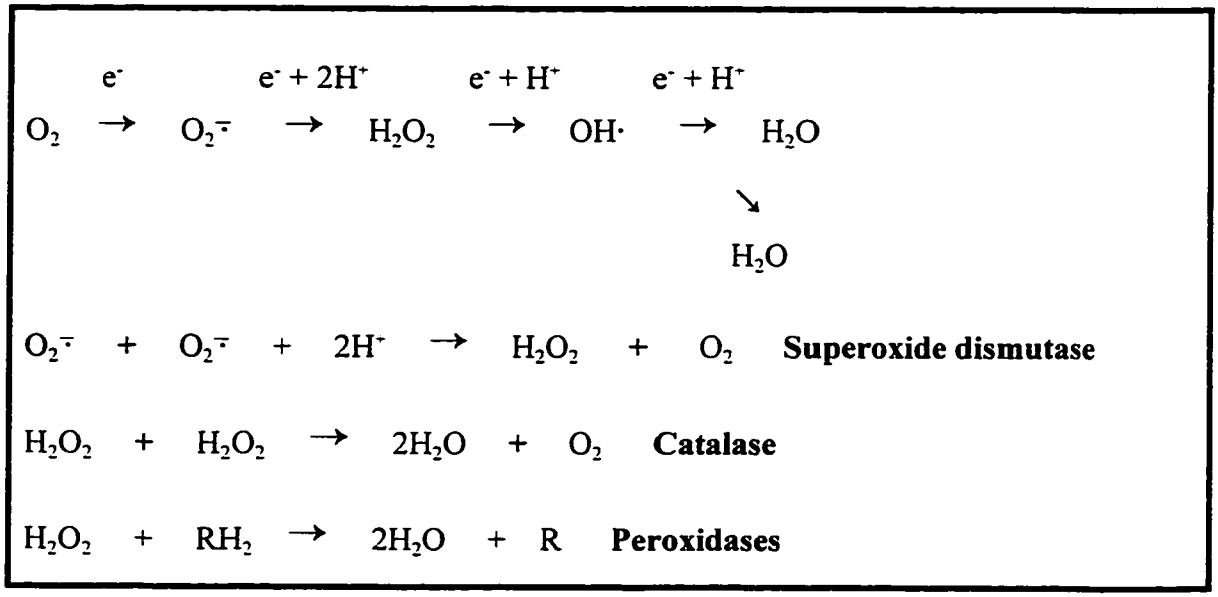
e⁻
e⁻ + 2H⁺
e⁻ + H⁺
e⁻ + H⁺
O2 → O2⁻· → H2O2 → OH· → H2O
↘
H2O
O2⁻· + O2⁻· + 2H⁺ → H2O2 + O2 Superoxide dismutase
H2O2 + H2O2 → 2H2O + O2 Catalase
H2O2 + RH2 → 2H2O + R Peroxidases

[77,78]. Hsie et al. [79,80] were able to detect mutants in CHO cells and its clone AS52 (contain a single copy of the bacterial *GPT* transgene instead of the *HPRT* gene) following exposure to ROS. When investigated, most of the mutations observed have been point mutations, either due to base substitution or frameshift base deletions.

A diffusible clastogenic factor (CF) has been identified in the medium of TPA-activated human granulocytes that causes chromosome aberrations and sister-chromatid exchanges [81-83]. V79 cells have also been shown to produce CF when exposed to TPA that induced sister-chromatid exchanges and mutations in these cells [84,85]. The formation of CF can be diminished by catalase or SOD [81,82]. Hence, it is thought that CF comprises a mixture of H_2O_2 and oxidized lipids, in particular oxidative intermediates of arachidonic acid. Unlike $O_2^{\cdot-}$ and $OH^{\cdot}$ radicals, which are unstable and have a very short half-life, CF possesses a half-life of several hours and penetrates cell membranes. Human monocytes stimulated with TPA produce increased amounts of hydroperoxy-arachidonic acid that is clastogenic for cultured rodent fibroblasts [86,87]. Understanding the molecular nature of these species may provide insight into the mechanism of action of these species and methods for their elimination.

1.4 REACTIVE NITROGEN SPECIES

More recently, there has been considerable interest in the effects of $NO^{\cdot}$ and related species. Like ROS in the prior decade, interest has been spurred by the recognition that these reactive chemicals are formed within the body in a regulated manner. $NO^{\cdot}$ is formed by many cell types in the body for intercellular communication or as part of the immune or inflammatory response by macrophages and endothelial cells. It is an important

neurotransmitter and NOS activity has been found in endothelial tissue of the cardiovascular system and in the central nervous system, suggesting an important role for NO· in human physiology and pathophysiology [88,89].

1.4.1 *NO·: the endogenous nitrovasodilator*

NO· is now known as a mediator of blood vessel relaxation. Acetylcholine, bradykinin, adenosine triphosphate, and other stimuli that dilate blood vessels act on receptors located on the surface of endothelial cells to trigger the release of local hormones that diffuse to adjacent smooth muscle to evoke relaxation. One of the most potent substances released by the vascular endothelium in this process is endothelium-derived relaxing factor (EDRF). The chemical nature of EDRF has now been identified as NO· or a labile nitroso precursor to NO· [90]. NO· relaxes smooth muscle in blood vessels by activating soluble guanylate cyclase (sGC) and thereby stimulating the formation of cyclic guanosine 3', 5'-monophosphate (cGMP) (Figure 1-3). This increase in intracellular cGMP concentrations leads to a reduction in intracellular Ca^{2+} levels through a multitude of proposed cascade events, resulting in myosin light-chain kinase phosphorylation and relaxation of vascular smooth muscle cells, resulting in vasodilation. NO· is now considered to be the endogenous nitrovasodilator and the names NO· and EDRF are used interchangeably.

NO· can also be generated by nitric oxide-donating drugs (NO-donating drugs) that are widely used for the treatment of coronary artery disease to substitute for diminished EDRF/NO· production. Among the most widely used is glyceryl trinitrate (GTN) and sodium nitroprusside (SNP). NO-donating drugs can be classified into the following

Figure 1-3 **Mechanism of NO· mediated vasodilation.** cNOS is activated in response to various stimuli such as bradykinin or acetylcholine by activation of surface receptors on vascular endothelial cells. These cells release EDRF, which diffuses to adjacent smooth muscle cells and produces vascular smooth muscle cell relaxation and vasodilation. In 1987 EDRF was found to be identical to NO·. NO-donating drugs also release NO·, that is used to substitute for a diminished EDRF/NO· production. cNOS = constitutive nitric oxide synthase

Figure 1-3

VASCULAR RELAXATION MEDIATED BY NITRIC OXIDE

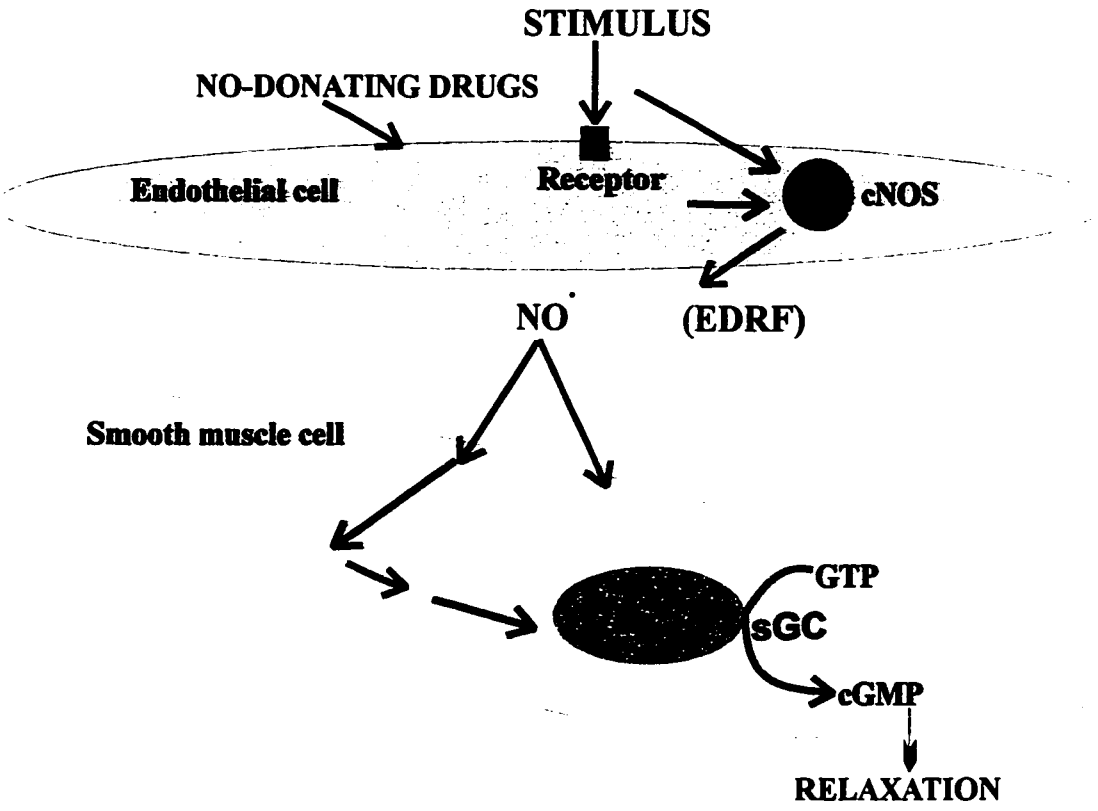

categories: organic nitrates, organic nitrites, floxane derivatives, iron-nitrosyls, S-nitrosothiols and sydnonimines. The pathway leading to NO· formation differs among individual compounds; some compounds require enzymatic biotransformation while others are spontaneous generators [91]. An alternative series of NO-donating drugs, termed "NONOates" have been described recently [92]. These agents are nitric oxide/nucleophile complexes that release NO· spontaneously.

1.4.2 *Biosynthesis of NO·*

NO· is produced by the oxidation of the amino acid L-arginine by an enzyme, NO synthase (NOS). The oxidation of L-arginine to NO· and citrulline uses NADPH and O_2. Flavin mononucleotide (FMN), flavin adenine dinucleotide (FAD), haem, and tetrahydrobiopterin are essential cofactors of this reaction (Figure 1-4). To date, several isoforms of NOS have been isolated and cloned and they generally fall into one of two categories: constitutive (cNOS) or inducible (iNOS). The cNOS is cytosolic, Ca^{2+}/calmodulin dependent, and releases NO· for short periods in response to receptor or physical stimulation. The NO· released by this enzyme act as a transduction mechanism underlying physiological responses. For instance, the neuronal form of NOS, which is activated by glutamate neurotransmission acting on *N*-methyl-D-aspartate (NMDA) receptors, is clearly constitutive. The endothelial form of NOS is also constitutive, being activated by increase in intracellular Ca^{2+} levels. Kobzik et al. [94,95] have described the existence of neuronal NOS in skeletal muscle, where it is concentrated in fast fibres and seems to have a physiological role in relaxing muscle. Neuronal and endothelial forms of NOS are also inducible in the sense that in the response to certain stimuli, new enzyme

Figure 1-4 **Biosynthesis of NO· from arginine.** NO· formation by NOS involves conversion of L-arginine to L-citrulline. The enzyme is a homodimeric protein, though only one subunit is illustrated here. Several cofactors are necessary for enzymatic activity, including flavones (FAD, FMN) and tetrahydrobiopterin. The catalytic cycle produces hydroxyarginine as an intermediate, which remains bound to the enzyme for further oxidation to citrulline and NO·. NOS is inhibited competitively by arginine analogs. Adapted from [93].

Figure 1-4

BIOSYNTHESIS OF NITRIC OXIDE FROM ARGININE

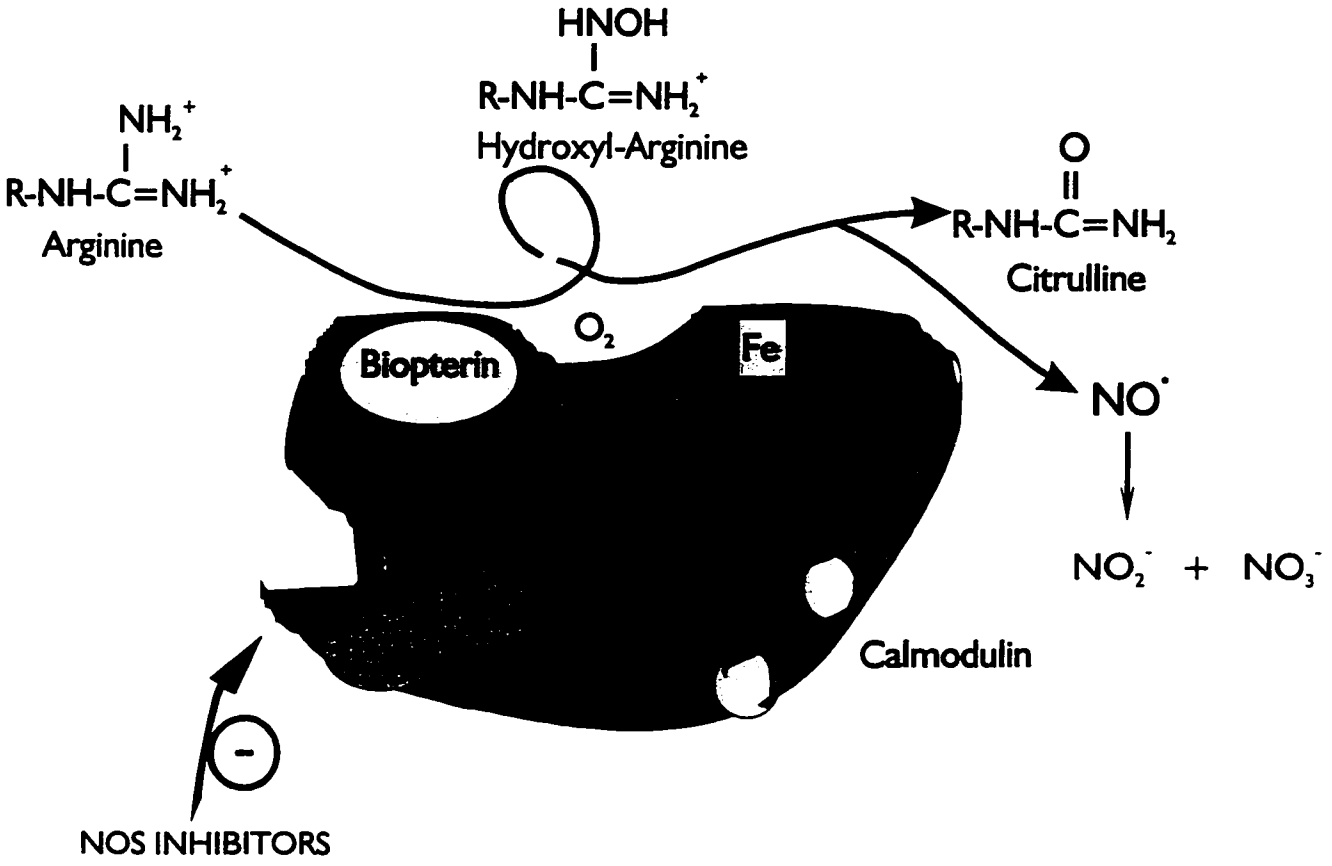

protein synthesis occurs. The inducible NOS (iNOS) was originally isolated from activated macrophages [96], which is not expressed in normal resting cells. Both *in vivo* and *in vitro* stimulation with a variety of cytokines and bacterial lipopolysaccharide (LPS) have been shown to induce NOS [97] and once expressed, synthesize enormous amounts of NO· for long periods. Furthermore, this enzyme is cytosolic, Ca^{2+} independent, it requires tetrahydrobiopterin as well as other cofactors, and its induction is inhibited by glucocorticoids, transforming growth factor-β, IL-4, and IL-10. No physiologic agents have been found that inhibit the enzyme activity of either cNOS or iNOS. Inducible NOS of macrophages is not stimulated by Ca^{2+}, but surprisingly, inducible NOS enzymes do possess calmodulin recognition sites. A number of other cell types including endothelial cells, brain astrocytes and microglia possess iNOS, which is also induced by a variety of cytokines [98,99]. Induction of iNOS in astrocytes and microglia may account for the tissue damage associated with a number of neurological disorders.

The molecular and cell biology of the constitutive and inducible NOS isoforms has recently been elucidated [100-102]. The rat brain and macrophage NOS isoforms are soluble, dimeric enzymes, each comprising two identical subunits. NOS appear to comprise a reductase domain and an oxygenase domain, each representing roughly one-half of the protein molecule. A binding sequence for the Ca^{2+}-binding protein calmodulin is invariably located between the NOS reductase and oxygenase domains. All NOS reductase domains contain binding sites for NADPH as well as for FMN and FAD [88,102,103]. Cytochrome P-450 reductase (CPR) is the only other mammalian enzyme known to contain recognition sites for NADPH, as well as for both FMN and FAD. The carboxyl-terminal half of NOS is 60% homologous to CPR. All NOS isoforms cloned share homology with CPR, and this

probably reflects the oxidative nature of NO· biosynthesis. Overall sequences, similarity between the constitutive endothelium and neuronal NOS isoforms is approximately 50%, and both are roughly 50% identical to inducible macrophage NOS [104]. The genes for human nNOS, eNOS, and iNOS are located on chromosomes 12, 7 and 17, respectively. Inducible NOS cloned from various cells (macrophages, hepatocytes, chondrocytes, and smooth muscle) are highly homologous (roughly 80-90%), perhaps reflecting their localization on a single chromosome.

A number of NOS inhibitors have been identified that are analogs of L-arginine and inhibit the enzymatic production of NO· by NOS [105-113]. These include N^G-monomethyl-L-arginine (L-NMMA), N^G-nitro-L-arginine (L-NOARG), N^G-nitro-L-arginine methyl ester (L-NAME), and N^G-iminoethyl-L-ornithine (L-NIO), all of which are extremely useful in revealing the role of endogenous NO· in various physiological and pathological processes.

1.4.3 *Chemistry of NO·*

NO· exists as a highly reactive free radical with an unpaired electron. As a result, NO· is assumed directly to attack many molecules like DNA or thiols, whereas the reaction rates are very slow and probably not of great biological significance. NO· reacts with molecular oxygen (O_2) to produce NO_2, which forms the nitrosating agents N_2O_3 and N_2O_4 (Figure 1- 5A). Both N_2O_3 and N_2O_4 can react with H_2O to yield NO_2^- and NO_3^-. Stamler et al. [114] proposed that NO may exist in the following three forms, NO·, nitrosonium cation (NO^+), and the nitronyl anion (NO^-) in a biological system. The half-life of NO· in biological systems is estimated to be 4-50 sec. NO· is uncharged and can migrate freely in and out of the cells similar to O_2. Therefore, there should be time for NO· to diffuse several

Figure 1-5 **Reactions showing reactivity of NO· with biomolecules.** (A), Autooxidation of NO· leads to the formation of nitrosating agents (N_2O_3 and N_2O_4). (B), Nitrosation of secondary amine results in the formation of nitrosamine. (C), Nitrosation of primary amines leads to deamination. (D), Peroxynitrite formation in the presence of NO· and $O_2^{\cdot-}$. Adapted from [53].

Figure 1-5

A. Formation of nitrosating agents

$$2NO\cdot + O_2 \rightarrow 2NO_2\cdot$$

$$2NO_2\cdot \rightarrow N_2O_4 \rightarrow NO_2^- + NO_3^- + 2H^+$$

$$NO\cdot + NO_2\cdot \xrightarrow{H_2O} N_2O_3 \rightarrow 2NO_2^- + 2H^+$$

B. Nitrosation of a secondary amine

$$N_2O_3 + R_2NH \rightarrow R_2N\text{-}N{=}O + HNO_2$$

C. Deamination of a primary amine

$$N_2O_3 + R\text{-}NH_2 \rightarrow R^+ + N_2 + NO_2^- + H_2O$$

$$R^+ + H_2O \rightarrow R\text{-}OH + H^+$$

D. Peroxynitrite formation

$$NO\cdot + O_2^{\cdot-} \rightarrow ONOO^-$$

$$ONOO^- + H^+ \rightarrow ONOOH$$

$$ONOOH \rightarrow OH\cdot + NO_2\cdot$$

cell diameters to reach target sites before being consumed by O_2. It is also likely that biological carriers of NO· such as S-nitrosothiols exist *in vivo* [115]. These carriers may allow NO· to move via circulation to tissues distant from the origin of the NO·.

N_2O_3 and N_2O_4 are formed from NO· and O_2 rapidly nitrosate amines at neutral and basic pH (Figure 1-5A,B). However, NO· without O_2 is unreactive towards amines. NO· can form carcinogenic *N*-nitroso compounds including *N*-nitrosodialkylamines from secondary and tertiary amines *in vivo*. Nitrosation of primary amines results in deamination via diazonium ions or diazohydroxides. Acidic NO_2^- can deaminate purines, pyrimidines, and various forms of RNA and DNA (Figure 1-5C). Deamination of guanine to xanthine, for example, can result in depurination to form abasic sites in DNA and consequent single-strand breaks or misrepair. NO· rapidly reacts with $O_2^{\cdot-}$ to form a powerful and relatively stable oxidant, peroxynitrite ($ONOO^-$) which can react with DNA, proteins and cell membrane lipids [116, 117]. It is not stable at physiological pH and results in the formation of peroxynitrous acid (ONOOH) with a half-life of less than 1 s that decomposes spontaneously to form OH· and NO_2 (Figure 1-5D).

1.4.4 *Pathological roles of NO·*

(I) NOS and inflammation: There is now ample evidence to indicate that NO· may be generated by the enzyme iNOS in various inflammatory disorders by infiltrating leukocytes and resident tissue cells [118-129]. The role of NO· during inflammation is unclear and *in vivo* it may have both pro-inflammatory and anti-inflammatory functions. Under experimental conditions NO· has been implicated in both acute and chronic inflammation, and in many disease states these phases merge into a continuous pathological

process. Table 1-2 summarizes inflammatory diseases in which there is evidence for the presence of iNOS. RNS may cause tissue damage and vascular leakage in septicaemia, rheumatoid arthritis and inflammatory bowel disease [68,131]. The precise mechanisms of these cytotoxic effects are unknown but RNS are implicated since nitrotyrosine has been detected in serum and synovial fluid from rheumatoid arthritis patients [132]. Patients with

Table 1-2 ***In vivo*** **evidence for a role of NO· in inflammatory diseases**

Animal studies				Human studies
Infections	**Skin**	**Endotoxaemia**	**Immune diseases**	
Malaria Viral encephalitis Leishmaniasis	Carrageenan Ultraviolet light	Septic shock Hepatic necrosis model Glomerular thrombosis Chronic ileitis Arthritis-adjuvant	Vasculitis Streptococcal arthritis Allograft rejection Graft verus host Glomerulonephritis Experimental-encephalomyelitis	Arthritis Asthma Atherosclerosis Crohn's disease Ulcerative colitis Cystic fibrosis obliterative-bronchiolitis IL-2 therapy Sepsis

Adapted from [130].

active ulcerative colitis and Crohn's disease show a marked increase in NOS activity in the inflamed colonic mucosa [133]. Acute respiratory distress syndrome (ADRS) which often results from severe infection, may also involve RNS generation in the lung as evidenced by the presence of nitrotyrosine [134].

(ii) NOS and cancer: Several human cancers are associated with chronic viral, bacterial and parasitic infections (section 1.2.1 (I), [45]). NO· formation is elevated in these infections. Long term exposure to elevated NO· in cells resulting from chronic infections

could have cytotoxic and genotoxic effects on hosts. Although the flux of radicals per unit time is low, an inflammatory condition that continues for years becomes a significant risk factor for cell transformation. The relative contributions of various radicals in tumor development and progression must be assessed through both chemical analysis of DNA and through genetic and molecular analysis of mutations in surviving exposed cells. NOS activity has been shown in pathological specimens of human ovarian and breast cancer [135,136] and colorectal carcinomas [137,138]. Increased NOS activity in human ovarian cancers correlated with increased malignancy. Recent studies have suggested a role for NO· in causing increased tumor blood flow, edema, and vascular permeability especially in the tumors of the central nervous system [139]. Inducible NOS mRNA expression has been demonstrated in human brain tumors [140], considerably higher in the glioblastomas than meningiomas [141].

(iii) NOS and neurodegenerative disease: Under conditions of excessive formation, NO· may be neurotoxic and contribute to the pathology of neurodegenerative disorders including, stroke, epilepsy, trauma, Huntington's disease, Parkinson's disease, Alzheimer's disease, and amyotrophic lateral sclerosis [68,142-147]. Activation of the NMDA receptors results in the influx of calcium into the cell, which binds calmodulin and activates nNOS. In pathologic conditions, microglia (analogous to macrophages), on activation, may generate excess ROS and RNS and it is possible that most of the neurotoxic actions of NO· are mediated by $ONOO^-$. NO· may play a role in the pathogenesis of acquired AIDS dementia as the coat protein, gp 120, which is shed by the virus, kills neurons in primary cortical cultures, in part, via activation of NO· [148,149]. Overproduction of NO· may also play a pathological role in inflammatory disorders of the

central nervous system. Induction of iNOS in demyelinating regions of brains with multiple sclerosis [150] has been observed and may be directly toxic to the myelin-producing oligodendrocytes [151]. Increased levels of NO· production have been observed in bacterial meningitis, suggesting that excessive production of NO· may participate in the neurological sequelae associated with meningitis [152]. Recent studies suggest that migraine sufferers have supersensitivity to NO·, and this may be an important mechanism of migraine-associated pain [153].

1.4.5 *DNA damage by NO·*

Long-term exposure to elevated NO· in cells could have potential genotoxic effects on hosts. There are at least three mechanisms by which intracellular elevated NO· could exert genotoxic affects after reacting with O_2. The first results from the formation of carcinogenic N-nitroso compounds that can, in turn, alkylate DNA. The second is by reacting directly with the primary amino groups of DNA resulting in deamination. The third results from the formation of $ONOO^-$ and/or OH· radicals that can cause oxidative DNA damage.

(I) Endogenous-formation of N-Nitroso compounds: N_2O_3, which arises via reaction of NO· with O_2 (described in section 3.3), is an effective nitrosating agent for primary, secondary and tertiary amines. Nitrosation of secondary and tertiary amines to form N-nitrosamines can result in DNA damage followed by oxidative metabolism to an alkylating species [154-156].

(ii) Deamination of DNA: Spontaneous deamination of DNA occurs with extremely low frequency. However, high concentrations of NO· (delivered using NO-

donating drugs or NO· gas) has been shown to deaminate DNA [157,158]. Nitrosation of primary amines such as purines and pyrimidines results in rapid deamination via diazonium ions or diazohydroxides which subsequently hydrolyze to alcohols (section 1.4.3). For example, deamination of cytosine will lead to the formation of uracil. Removal of uracil by uracilglycosylase without restoration of cytosine would leave an abasic site in DNA and consequent single-strand breaks or misrepair. Misrepair would produce the observed G:C → A:T transition. Methylation of cytosine to form 5-methylcytosine and subsequent deamination would result in the formation of thymine in the DNA chain. Deamination of guanine to xanthine could explain the G:C → T:A and G:C → C:G transversions. Reaction of the aryldiazonium ion of the base undergoing deamination with a nucleophilic site on an adjacent macromolecule could lead to crosslinking with other nucleic acids or with proteins [155,156].

(iii) DNA oxidative damage: Macrophages activated with *E. coli* LPS and mouse interferon-gamma (IFN-γ) to produce NO· show evidence of both oxidative damage and deamination of DNA. The DNA oxidation products 5-hydroxymethyluracil, 2,6-diamino-4-hydroxy-5-formamidopyrimidine, and 8-oxoguanine were inhibited by a NOS inhibitor [159]. Reaction of NO· with $O_2^{\cdot-}$ leads to DNA oxidative damage due to the formation of $ONOO^-$ which may have OH· radical-like oxidizing potential [116]. It has been reported that $ONOO^-$ can be formed by rat macrophages activated with TPA [160]. $ONOO^-$ has strong oxidizing properties toward biomolecules including protein and non-protein thiols, deoxyribose and membrane phospholipids [161]. Such reactions have been shown to induce several types of DNA damage including DNA strand breaks and apoptosis in rat thymocytes [162,163]. Another possible mechanism of oxidative damage by NO· could be the

mobilization of free iron by NO· which could ultimately cause Fenton-type reactions.

In summary, the chemistry of DNA damage by NO· is highly complex with respect to the overall mechanism. The mechanisms described above are based on both *in vitro* and *in vivo* data obtained at high NO· concentrations. Whether or not NO· is an important factor in tumor development and progression will require evaluation of NO· concentrations more representative of the *in vivo* situation.

1.4.6 *Cytotoxic effects of NO·*

RNS have cytotoxic roles, such as in macrophage and natural killer (NK) cell killing of tumor cells, macrophage killing of intracellular parasites and granulocyte killing of bacteria [96,164-167]. Mitochondrial aconitase and ribonucleotide reductase are two important cell targets for killing by RNS [96,166,168]. NO· inactivates these enzymes by binding to the iron/sulfur centers and directly inactivating these centers. Although the exact mechanism of cell death may vary from one type of cell to another, in most cell lines investigated NO· cytotoxicity may involve an apoptotic mechanism. Apoptosis has been demonstrated in cultured macrophages [169], osteoblasts and osteoclasts [170], leukaemia HL-60 cells [171], glial cells [172], MEF 23.5 cells (hybrid neuroblastoma cell line) [173] and other cell types. Tamir et al. [174] have shown evidence of apoptotic cells next to NO· producing cells *in vivo* in the spleen of the SJL mouse. Cytotoxicity in macrophages and rat smooth muscle cells exposed to $ONOO^-$ is mediated by DNA strand breakage and the subsequent activation of the DNA repair enzyme poly (ADP-ribose) synthetase (PARS), a nuclear enzyme that synthesizes poly (ADP-ribose) from NAD [175]. This in turn leads to inhibition of mitochondrial respiration and a decline of intracellular NAD and ATP. 3-

Aminobenzamide, a inhibitor of PARS led to inhibition of these effects. Most of the evidence suggests that toxic effects of NO· occur directly or through its breakdown product $ONOO^-$.

1.4.7 *Genotoxicity of NO·*

Several workers have explored the genotoxic and mutagenic potential of RNS. RNS are usually delivered to biological test systems as NO· gas or as drugs thought to produce NO·, either spontaneously or after metabolic activation. DNA bases are damaged by high concentrations of NO· gas: saturated solutions of NO· deaminate deoxyribonucleosides, nucleotides, purines and calf thymus DNA [157,158]. Exposure of plasmid DNA to NO· gas or $ONOO^-$, followed by passage through human Ad293 cells or *E. coli*, also showed deamination of bases [176,177]. In a tester strain of *S. typhimurium*, NO· and nitrogen dioxide (NO_2) gases and SPER/NO· and DEA/NO· were strongly mutagenic while glyceryl trinitrate (GTN) and sodium nitrite ($NaNO_2$) were weakly mutagenic [178,179]. Lung cells of rats exposed *in vivo* to NO· gas showed a small increase in ouabain-resistant mutants [62]. Mutagenicity of NO· has also been shown in mammalian cells. In human TK6 lymphoblasts, very high concentrations of NO· gas induced mutations at both the *HPRT* and *TK* loci and induced DNA strand breaks [158]. By contrast, no mutants were induced at the *HPRT* locus in human epithelial cells by DEA/NO·, a spontaneous generator of NO· [180]. Thus, the evidence concerning the mutagenic potential of RNS is somewhat contradictory. There is clear agreement that deamination of DNA bases can occur. The number of studies employing mammalian cell systems is limited and these seem to show a relatively weak mutagenic response to RNS. Moreover, most of the studies employed large amounts of

external NO· than intracellularly produced NO·.

Study of the pathophysiological roles of RNS in biological systems represents a significant challenge since they are unstable and reactive. Identification of the precise species that may participate in a given reaction is difficult even under defined chemical conditions and extremely difficult under biological conditions. This explains some of the controversy in the literature about which species are actually involved in a biological setting.

1.5 THE NEED FOR NEW MODEL SYSTEMS: *Gene mutations (point mutations, small deletions) vs chromosome mutations (large deletions, multi-locus deletions)*

The absence of a mutagenic effect in a given system by RNS does not imply that RNS may not be mutagenic; different systems may be insensitive to different classes of mutations. To address this, one laboratory has very recently used a transgenic mouse bearing a plasmid-based lacZ gene as a mutational marker [181]to study NO· toxicology *in vivo* [182]. This system tolerates slightly larger deletions (up to 3 kb) than phage lambda-based shuttle vector systems [181,183]. The SJL mouse was crossed with the transgenic strain bearing a lacZ plasmid and lymphoma cells were injected. A small increase in MF was found in the DNA from the spleen (where the lymphoma cells lodge), which was abrogated by administration of a NOS inhibitor. Although the effect was very small, these results suggest that NO· may be involved in inducing mutants *in vivo*.

The MN-11 system has allowed detection of mutations both *in vitro* and *in vivo*. The advantage of MN-11 system in detecting mutants is illustrated in Figure 1-6. The centre panel shows mutant induction in a hemizygous state: one X chromosome bearing one *HPRT* gene. Mutations entirely within the gene do not affect cell viability and are therefore scored.

Figure 1-6 **Distinction between Gene mutations (point mutations, small-scale deletions) and Chromosomal mutations (multi-locus deletions).** Recovery of mutants in a functionally heterozygous (*TK* $^{-/-}$), hemizygous (*HPRT* $^{-/0}$) and MN-11 (*HPRT* $^{-/-/-}$) model system are shown.

Figure 1-6

RECOVERY OF MUTANTS AT HETEROZYGOUS AND HEMIZYGOUS LOCI

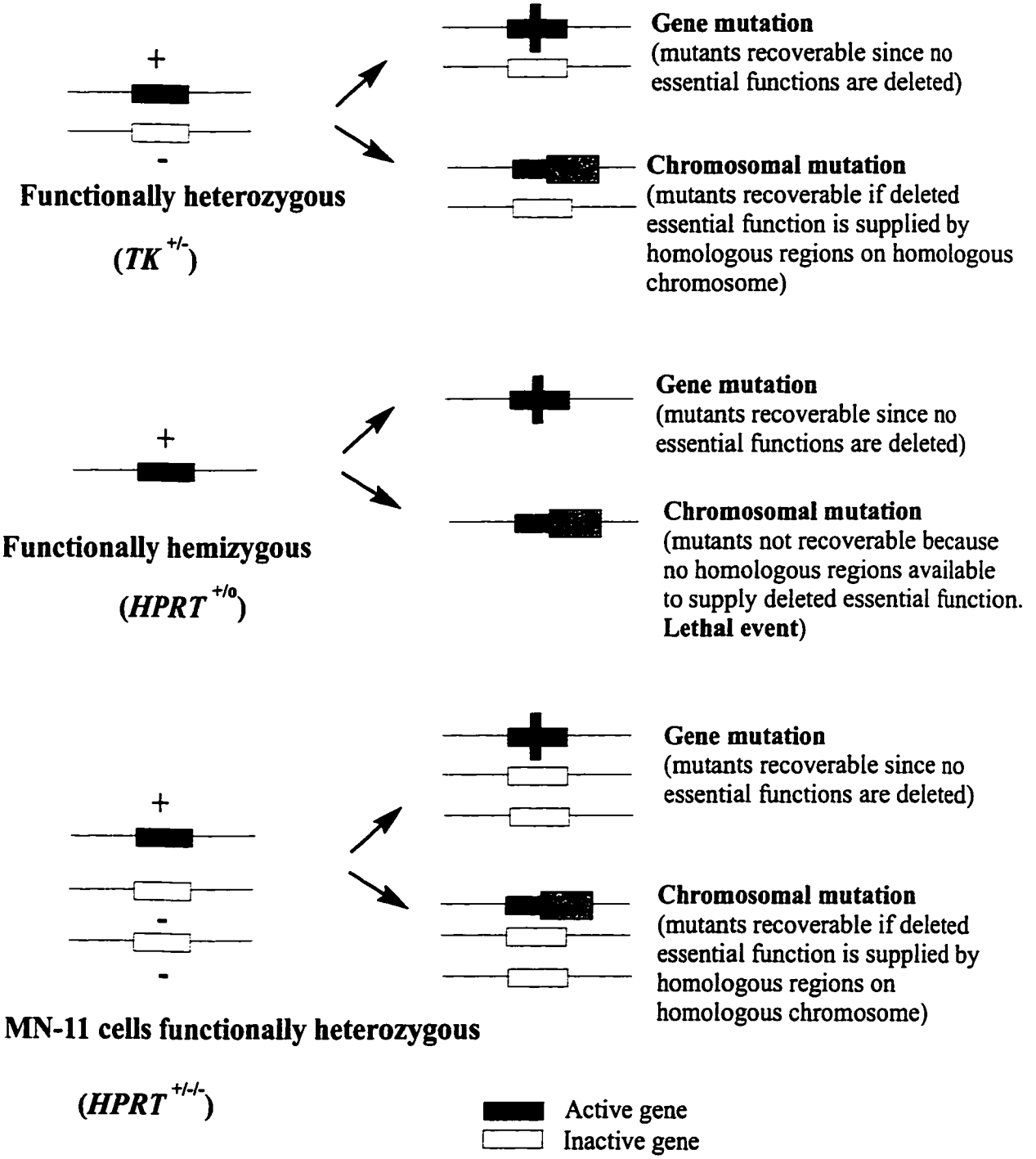

Large-scale mutations affecting the *HPRT* gene that concomitantly loses an essential gene in an adjoining chromosomal region produce non-viable cell and are therefore not scored. In a functionally heterozygous condition (top panel), loss of an essential gene on one chromosome may be compensated by the homologous chromosome. Therefore, the mutant cell will be scored. MN-11 cells (bottom panel) are functionally heterozygous, although they originated from a male mouse. Three copies of the X chromosome are present, presumably due to a non-disjunction event. Two of the three copies of the *HPRT* gene were inactivated, leaving "backup" copies of essential genes on the other X chromosomes. Thus, large deletions (chromosomal mutations) affecting the single functional *HPRT* gene can be tolerated and such mutants are viable. This model system is currently being used in our laboratory to study the contribution of tumor-infiltrating phagocytic cells in tumor progression.

1.6 HYPOTHESIS AND THESIS OBJECTIVES:

Tumor progression is frequently associated with evidence of genetic damage, such as gene amplification, loss of chromosome fragments and/or chromosome rearrangements. The cause of these large-scale changes commonly observed in tumors is not known. Our laboratory has hypothesized that tumor-infiltrating phagocytic cells (macrophages and granulocytes) may contribute to tumor progression by generating ROS and RNS, which in turn may induce DNA strand-breaks in the neighbouring tumor cells that may have cytotoxic and genotoxic effects. To test this hypothesis, we have developed the MN-11 tumor model system [1] in which loss of a marker gene (*HPRT*) could be detected with high sensitivity. Using this model system, a 4-fold increase in MF was observed *in vivo* in tumors than *in*

vitro for an equivalent time. It is my hypothesis that NO· or related species released by phagocytic cells might be partially responsible for this observed increase and these species may induce chromosomal mutations (large, multi-locus deletions) as opposed to gene mutations (small-scale deletions or point mutations). NO· is a multifaceted molecule that has been implicated in a wide variety of processes such as neurotransmission, smooth muscle relaxation, platelet aggregation, cytotoxic/inflammatory responses, and cellular proliferation and differentiation. However, its role in tumor progression is not yet clear. Solid tumors are known to be infiltrated with phagocytic cells and the presence of NOS has been recently shown in human tumors [135-137,139]. Once NOS is induced in phagocytic cells, it can produce large quantities of NO· for sustained periods. NO· may react with other radicals and mediate cytotoxicity and genotoxicity in the neighbouring tumor cells. It has been shown to induce deaminations, DNA strand-breaks, alkylations and oxidations (Figure 1-7). However, the induction of mutants by RNS in solid tumors is not known, and this could be a potential mechanism of NO· genotoxicity in tumors. In our laboratory we are investigating the role of RNS *in vitro* and *in vivo* with a goal of applying this knowledge to understand human cancers.

My objective was to determine whether there exist factors in the tumor milieu that may be mutagenic and/or clastogenic and to identify such factors, this thesis is divided into five sections designed to investigate the following:

1. To test if the model system is sensitive to detect mutations *in vitro* and *in vivo* and to determine if the tumor microenvironment is mutagenic and/or clastogenic (Chapter 2).
2. To study if the MN-11 tumor is infiltrated with phagocytic cells and to identify them histochemically (Chapter 3).

Figure 1-7 **The role of NO· in tumor progression.** Factors present in the tumor microenvironment stimulate phagocytic cells to produce NO· by the enzyme iNOS. NO· destroys tumor cells by inhibiting the energy-producing Krebs cycle and electron transport activities as well as DNA synthesis. It can also produce DNA damage that may underlie tumor progression. NO· reacts rapidly with $O_2^{\cdot-}$ to form peroxynitrite, which may be cytotoxic by itself or decompose to the highly reactive and toxic OH· radical and NO_2 species that may have diverse effects on cells.

Figure 1-7

POSSIBLE INVOLVEMENT OF NITRIC OXIDE IN TUMOUR PROGRESSION

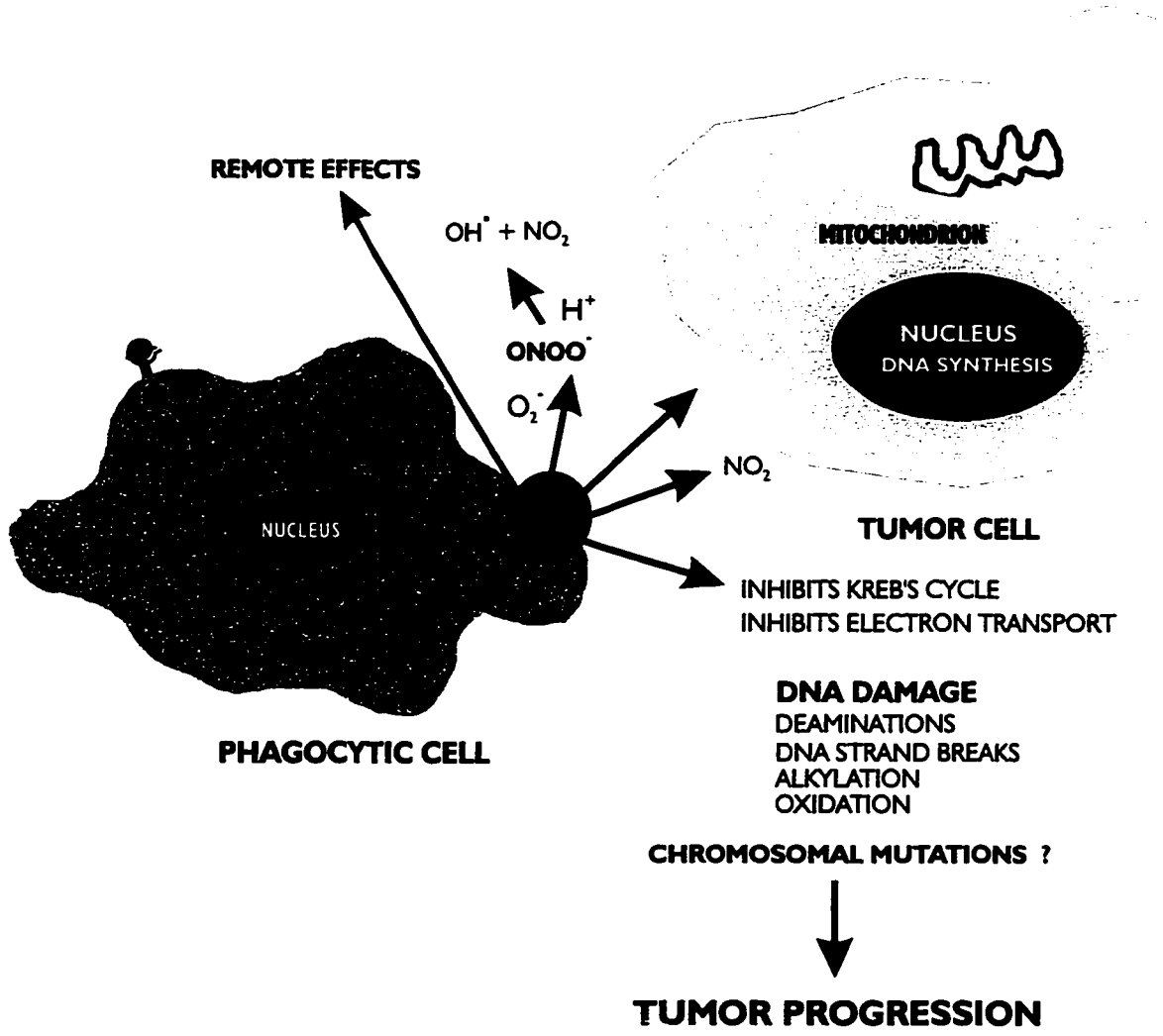

3. To determine if ROS and RNS can cause mutagenicity and cytotoxicity in MN-11 cells *in vitro* (Chapter 4).

4. To determine if endogenously generated NO· or other RNS may be mutagenic *in situ* in growing tumors (Chapter 5).

5. To determine if the mutagenicity and cytotoxicity of NO-donating drugs *in vitro* and *in vivo* could be inhibited by vitamin E (Chapter 6).

CHAPTER 2

DEVELOPMENT OF A TUMOR MODEL SYSTEM THAT ALLOWS SENSITIVE DETECTION OF *IN VIVO* AND *IN VITRO* MUTATIONS

ABSTRACT

It is well established that cancer can result from a series of mutational events. The mechanism(s) by which these occur is only partially understood. My hypothesis is that *exogenous* factors, such as products of inflammatory cells (ROS and RNS) are present in the tumor microenvironment and that these are clastogenic and/or mutagenic. To test this hypothesis, a transplantable murine tumor cell line (MN-11) has been developed that allows sensitive detection of mutational events arising *in vivo* in growing tumors and in cultured cells. *HPRT*, a non-essential gene in the purine "salvage" pathway, was used as a marker of mutations. MC-TGS17-51, which expressed a heterozygous *HPRT* locus, transfected with a *neo* gene was the starting point for my studies. $G418^R$ clones were screened to identify one (MN-11) having a low spontaneous rate of gene loss ($0.46 \times 10^{-5} \pm 0.27 \times 10^{-5}$ per day); it was similar to MC-TGS17-51 in sensitivity to induction of mutants by ^{60}Co γ-rays. Like MC-TGS17-51, these cells were 1000 times more sensitive than the parental cells (MC1A-C1, containing multiple copies of the *HPRT* gene) to induction of mutants by ^{60}Co γ-rays. At D_0, ^{137}Cs γ-rays induced about 170 mutants per 10^5 cells compared with 136 for ^{60}Co γ-rays. The frequency of mutations arising *in vivo* at the *HPRT* locus could be estimated by culturing explanted tumor cells in the presence of 6-TG, where G418 selection was used to distinguish tumor from host cells. The frequency of mutants in MN-11 cells grown as subcutaneous tumors was 3.64-fold higher than in the same cells maintained *in vitro* for an equivalent period, suggesting that mutagenic/clastogenic factors are present within the tumors. There was considerable variability in mutant frequency in tumors from different animals and in multiple tumors from the same animals.

2.1 INTRODUCTION

As cancers develop, they often become more malignant in their behaviour, a process termed tumor progression. This phenomenon has been associated with genomic instability, which is manifested as evolution of tumor cell populations with increasing numbers of genomic alterations [184]. Genomic instability includes all mechanisms that accelerate the accumulation of damage or modifications to DNA, such as gene amplification, epigenetic changes such as altered patterns of DNA methylation, small-scale (intralocus) and large-scale (multilocus) mutational events [185,186]. Karyotypic alterations, including whole chromosome loss or gain, and a variety of chromosomal aberrations are also common in cancer cells. Although the instability of tumor cells is clearly documented, the mechanisms involved are not yet defined. Mutations in the genes required to maintain chromosomal stability could result in a mutator phenotype and contribute to genomic instability [6,9,187]. Recently, much attention has been paid to the significance of specific gene defects that lead to genomic instability in mammalian cells. Examples include the DNA repair (mismatch repair and excision repair) implicated in hereditary forms of colon cancer [31,188-190] and the *p*53 gene associated with a variety of cancers [15,16,191]. In contrast, we and others have postulated that the tumor microenvironment of a developing tumor might itself contribute to genomic instability and mutagenesis, leading to tumor progression and an evolution of a more malignant phenotype [1,43,54,56,85,192-196].

Our laboratory has been interested in understanding the contribution to tumor progression of factors such as ROS and RNS generated by phagocytic cells, presumed to be present in the tumor environment. To study these factors, our laboratory has developed an *in vitro/in vivo* tumor model system highly sensitive to detection of mutational/clastogenic

events at the heterozygous *HPRT* gene. A transplantable mouse fibrosarcoma tumor (MC1A) was chosen as the starting point. This tumor was originally isolated from a male C57BL/6 mouse that had been treated with 500 μg of methylcholanthrene [197,198]. MC1A could not grow *in vitro* but a variant, MC1A-C1 that could grow arose spontaneously after these cells were maintained in culture for several weeks. The *HPRT* gene(s) in MC1A-C1 were inactivated by treatment with N-methyl-N-nitrosourea (MNU) (125 μM) for 1 h and growth in the presence of 0.5 μM 6-TG for several weeks. Eighteen 6-TG^R (HPRT$^-$) mutants were selected and tested for tumorigenicity in syngeneic C57BL/6 female mice. Of those tested MC-TGR17 was chosen. The next step was to reactivate one of what was believed to be two or more inactive copies of the *HPRT* gene. Spontaneously arising revertants to hypoxanthine/aminopterin/thymidine-resistance (HAT^R) were selected and labeled as MC-TGS17-1 to MC-TGS17-54. These clones were further characterized for their stability of *HPRT* expression, mutant induction by ^{60}Co γ-rays and tumorigenicity in syngeneic animals. Of these, MC-TGS17-51 was selected since it exhibited the lowest spontaneous reversion rate, maintained tumorigenicity and was 1000 times more sensitive to induction of mutants by ^{60}Co γ-rays. This clone was then transfected with a neomycin (*neo*) gene to allow distinction of tumor cells from the contaminating host cells [1]. These studies were carried out before my starting this project. This chapter describes the isolation of clones that were HAT^R and G418^R, labeled as MN-1 to MN-18 (development of these cell lines is represented in a flow chart in Appendix I). These were characterized with respect to tumorigenicity in syngeneic mice, spontaneous mutation rates and sensitivity to induction of mutants by the known clastogenic agent, ^{60}Co γ-rays. MN-11 was the most promising and was used to study the contribution of tumor microenvironment in mutant induction.

2.2. MATERIALS AND METHODS

A listing of the materials, chemical suppliers and composition of solutions is found in Appendix II.

2.2.1 *Cells and culture conditions*

MC1A-C1, MC-TGS17-51 and its *neo* derivatives (MN-clones) were grown in non-selective medium, HAT-medium, HT-medium or 6-TG-medium as defined in Appendix IV, section IV.1.

2.2.2 *Isolation of MN-clones*

Eighteen clones (MN-1 to MN-18) were derived from MC-TGS17-51 by a "spotting" method developed in our laboratory. MC-TGS17-51 cells were trypsinized and seeded in 96 well dishes at approximately 1 cell/well. Ten μL of cell suspension (containing 100 cells/mL) was carefully deposited in the center of each well. After approximately 3 h, each well was examined microscopically to identify those that contained a single cell. When cells had attached, 90 μL of non-selective medium was added. Following an incubation period of 7 days, colonies were washed with PBS, transferred to 24-well for another week and then to 6-well dishes. All the clones were grown in the presence of G418 (an antibiotic toxic to cells that do not have the *neo* gene) to ensure that they harbored the *neo* gene before freezing (the presence of the *neo* gene was confirmed by Northern slot-blot analysis by Diana Wilkinson).

2.2.3 *Tumorigenicity assay*

Six MN-clones (MN-12, 11, 5, 3, 2, 1) and the parental clone (MC-TGS17-51) were

grown in non-selective medium. A cell suspension of 5×10^5 viable cells (in 0.1 mL PBS) was inoculated subcutaneously (s.c.) into the flanks of C57BL/6 female mice, 8-10 weeks of age. Tumorigenicity was determined by the development of palpable tumors and the tumor size was measured using a caliper on day 7 and 14.

2.2.4 *Reconstruction experiment to determine conditions to minimize metabolic cooperation*

A reconstruction experiment was carried out by seeding 200 6-TG^R cells per 10 cm dish with increasing numbers of 6-TG sensitive (6-TG^S) MN-11 cells in the presence of 50 μM 6-TG. Following an incubation period of 12 days, colonies were fixed, stained and counted as described in Appendix IV, section IV.4.

2.2.5 *Determination of spontaneous mutant frequency*

MC-TGS17-51 and its G418^R derivatives were cultured in the presence of HAT-medium for 7 days to eliminate any pre-existing mutants (as described in Appendix IV, section IV.1.) and transferred to HT for 2 days. On day 0, 1×10^5 cells were challenged with 6-TG to determine the spontaneous rate of loss of the *HPRT* gene function. A more detailed estimate of the rate of spontaneous loss of *HPRT* gene function was carried out on three selected clones (MN-5, MN-11 and MN-12). Cultures were maintained in non-selective medium for up to 28 days. At weekly intervals a fraction of cells from each of the clones were removed from non-selective medium and incubated in the presence of 6-TG. MC-TGS17-51 was used for comparison. Following an incubation period of 12 days, colonies were fixed, stained and counted as described in Appendix IV, section IV.4.

An experiment was done to estimate the growth rate of 6-TG^R mutants (HPRT$^-$) in the presence of wild type MN-11 cells (HPRT$^-$). Five spontaneously arising 6-TG^R mutants were cloned and established in non-selective medium. One thousand mutant cells from each clone was mixed with 5×10^5 6-TG^S MN-11 cells. On day 0, 1×10^5 cells were challenged with 6-TG. The other cultures were grown in non-selective medium for up to 20 days, following which 6-TG^R colonies were scored as described in Appendix IV, section IV.4.

2.2.6 *Irradiation*

MC1A-C1, MC-TGS17-51, MN-5, MN-11 and MN-12 were grown as described above. Irradiation was carried out in non-selective medium in an ice bath with ^{60}Co γ-rays (dose rate, 1.8-1.4 Gy/min), Theratron 780, Atomic Energy of Canada Limited or at room temperature with a ^{137}Cs source (dose rate, 1.15 Gy/min), Gammacell-40, Atomic Energy of Canada Limited . Following an incubation period of 16 h, cultures were washed with PBS and trypsinized. Cytotoxicity was determined by seeding 200-1000 cells in 10 cm dishes and mutant frequency (MF) was determined as described in Appendix IV, section IV.2, using an expression time of 7 or 8 days for ^{137}Cs γ-irradiation. Unirradiated (control) cells were treated similarly, without irradiation. The effect of expression time on MF was also determined by challenging MN-11 cells with 6-TG on days 3, 6, 8 and 10 following ^{60}Co γ ray treatment.

2.2.7 *Treatment of MN-11 cells with caffeine*

5×10^5 cells were seeded in 10 cm dishes and treated with caffeine (0.5 mM) for 2 h at 37°C. Cells were then irradiated in an ice bath at doses of 0-5 Gy with ^{60}Co γ source

and incubated for 16 h before analysis of cytotoxicity and MF. Control cells were treated under similar conditions, without irradiation. Cytotoxicity and MF were determined as described in section 2.2.6.

2.2.8 *Determination of* in vivo *mutant frequency*

MN-5, MN-11 and MN-12 were grown as described above. Tumors were allowed to form following s.c. injections as described in section 2.2.3 (in some experiments MN-11 cells were injected at 2 sites). When tumors reached approximately 1 cm in size (14 days) for MN-12 and MN-5 and (12-18 days) for MN-11 cells, animals were sacrificed by cervical dislocation, tumors recovered and processed. For all experiments, an *ex vivo* expression period of 2-4 days was employed, following which MF was determined as described in Appendix IV, section IV.2.

2.2.9 In vitro *growth rate determination*

In vitro growth rate of MC-TGS17-51 and MN-clones was determined by plating 1 $\times$ 10^4 cells in replicate 3 cm dishes and counting trypsinized cell suspensions at daily intervals for 7 days using a Model ZM Coulter counter (Coulter Electronics Ltd, Luton, England). Cell doubling times were estimated from the logarithmic phase of the growth curve. Growth rate of selected mutant colonies was also determined similarly.

2.2.10 *Statistical analysis*

Data from animal experiments are expressed as mean $\pm$ SEM, but was analyzed using non-parametric tests such as Kruskal-Wallis ANOVA and Mann-Whitney test, as applicable.

Following detection of a statistically significant F value, *post hoc* Dunn's test of significance was used. In some cases, parametric test (One-way factorial ANOVA, followed by Tukey-Kramer test) was used where the data appeared to follow a Gaussian distribution. A 2 tailed p value of ≤ 0.05 was considered to be significant (shown as *) or $p \leq 0.01$ was considered to be highly statistically significant (shown as **). Statistical calculations were carried out using GraphPad Instat version 2.0.

2.3 RESULTS

2.3.1 *Derivation of MN-clones and determination of tumorigenicity*

MC-TGS17-51 cells harboring a *neo* gene were used (origin and properties of this cell line are detailed in the Ph.D. thesis of Diana Wilkinson). The presence of this gene permitted distinction between tumor and host cells when cells were recovered from s.c. tumors. Eighteen clones that were resistant to HAT and the drug G418 were isolated as described in section 2.2.2 and named MN-1 to MN-18. Since it was our intention to study the contribution of the tumor microenvironment to mutation induction, it was important to establish that the cell lines were tumorigenic. Tumorigenicity of six MN-clones and the parental MC-TGS17-51 clone was monitored by s.c. injection of 5×10^5 cells and measuring tumor size on day 7 and 14. Table 2-1 shows that the parent clone and all MN-clones examined were equivalently tumorigenic; there were no statistically significant differences seen in the size or rate of tumor growth in different MN-clones (ANOVA, $p > 0.05$).

2.3.2 *Metabolic cooperation*

When cells are plated at high cell density, it is possible that some 6-TG^R cells are killed by 6-TG because of direct contact between 6-TG^R and 6-TG^S cells. It is believed that

Table 2-1 **Tumorigenicity of MC-TGS17-51 and MN-clones.** Tumorigenicity of each clone was determined by injecting 5×10^5 cells s.c. in syngeneic animals and monitoring tumor growth. On day 7 no palpable tumors were observed in any of the injected animals. Tumor size was measured on day 14 and is expressed as mean ± S.D. (n = 3).

Table 2-1

Clone injected	Tumor formation	Size of the tumor after 14 days (cm)
MC-TGS 17-51	+, +, +	0.77 ± 0.45
MN-1	+, +, -	0.4 ± 0.53
MN-2	+, +, -	0.83 ± 0.76
MN-3	+, +, -	1.0 ± 0.2
MN-5	+, +, +	0.77 ± 0.68
MN-11	+, +, +	1.07 ± 0.12
MN-12	+, +, +	0.77 ± 0.25

Symbol -, represents no tumor formation.

the toxic metabolite, 6-TG nucleotide, can be transferred through gap junctions from 6-TG^S to 6-TG^R cells [199]. A "reconstruction" experiment was carried out using MN-11 cells to determine the cell density at which this effect could be minimized. Figure 2-1 shows that the recovery of 6-TG^R colonies was unchanged in the presence of up to 1×10^5 6-TG^S cells per 10 cm dish. Above this cell number, there was a clear decrease in the recovery of 6-TG^R colonies such that at 1×10^6 cells, very few colonies were recovered. It is concluded that at 1×10^5 cells per 10 cm dish the transfer of 6-TG nucleotide is minimized.

The number of cells on a 10 cm dish might be increased by growing cells in a semisolid media since individual cells would remain separate [200]. I attempted to grow MN-11 cells in soft agarose and/or methocel but all attempts failed, since these cells appeared to be unable to grow in an anchorage-independent fashion (data not shown). All future experiments were conducted at cell concentrations not exceeding 1×10^5 cells per 10 cm dish.

2.3.3 *Spontaneous mutation frequency*

Spontaneously occurring mutants constitute a background which decreases the sensitivity of detecting induced mutants. All clones were first cultured in HAT-medium for 7 days to kill any pre-existing HPRT$^-$ mutants (5 days was found to be ineffective). Before transfer to non-selective medium, cells were first cultured in HT-medium. If cells were directly transferred from HAT-medium to non-selective medium, poor cloning efficiency (< 5%) was obtained (data not shown). Table 2-2 shows the rate of spontaneous loss of HPRT function of six MN-clones and MC-TGS17-51. Clones MN-5, MN-11 and MN-12 appeared to be more stable (and were also tumorigenic), so they were compared in greater

Figure 2-1 **Effects of cell density on metabolic cooperation.** Two hundred 6-TG^R cells were seeded onto 10 cm dishes with increasing numbers of 6-TG^S cells (as indicated on the x-axis). The cells were grown in the presence of 6-TG for 12 days, following which 6-TG^R colonies were scored as described in Materials and Methods. Mean cloning efficiency of 200 6-TG^S cells (first bar) and the mean cloning efficiency of 200 6-TG^R cells (second bar) is shown. All other bar represents the mean number of 6-TG^R colonies. Error bars represent the SEM of the average 5-6 replicate dishes.

Figure 2-1

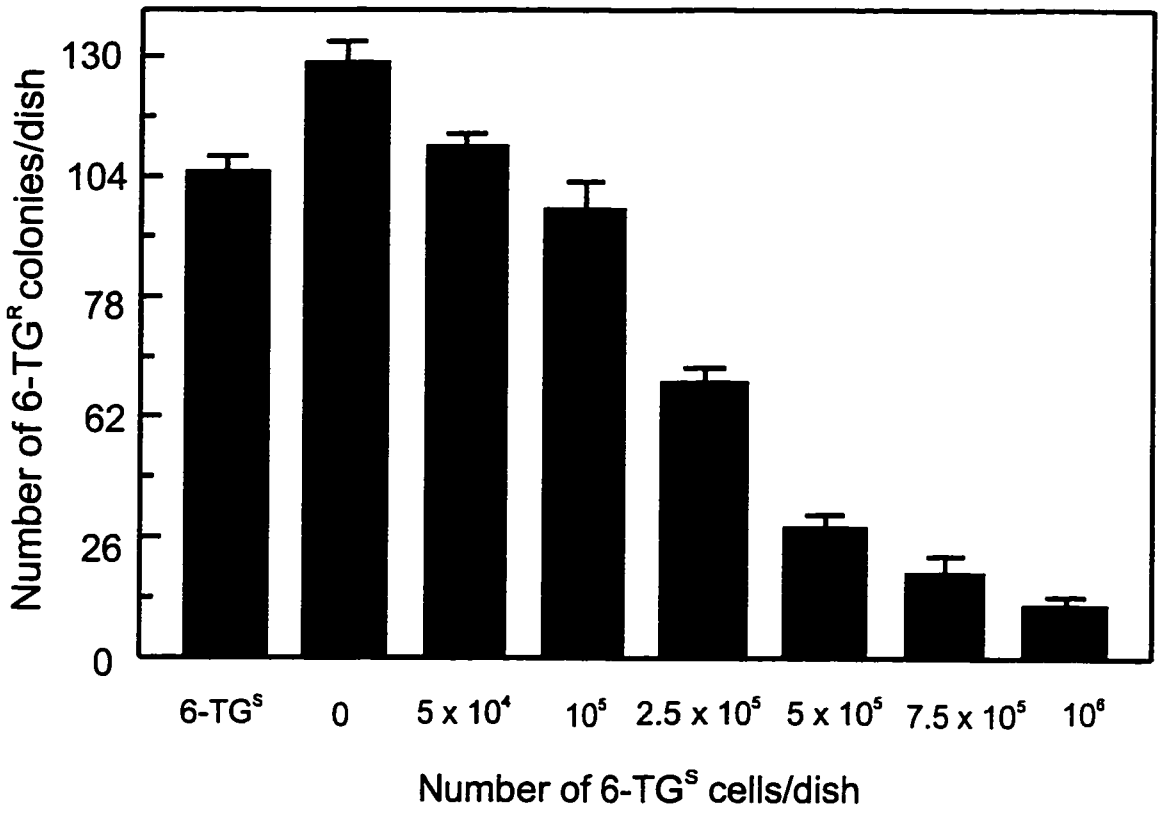
Number of 6-TG^R colonies/dish
130
104
78
62
26
0
6-TG^S
0
5 x 10^4
10^5
2.5 x 10^5
5 x 10^5
7.5 x 10^5
10^6
Number of 6-TG^S cells/dish

Table 2-2 **Spontaneous generation of 6-TG^R mutants.** MC-TGS17-51 and MN clones were grown in the presence of HAT-medium for one week (to eliminate any accumulated 6-TG^R spontaneous mutants) followed by growth in HT for 2 days. At day 0, 1×10^5 viable cells were seeded onto 10 cm dishes and challenged with 6-TG. Following growth for 12 days, 6-TG^R colonies were scored. Data shown is mean ± S.D. of the average of 7-8 replicate dishes from a single experiment.

Table 2-2

Clone	Mutant Frequency Mean ± S.D.
MC-TGS17-51	0.57 ± 0.79
MN-12	0.13 ± 0.35
MN-11	0 ± 0
MN-5	0 ± 0
MN-3	1.43 ± 1.13
MN-2	2.0 ± 1.53
MN-1	6.13 ± 1.73

detail for rate of spontaneous loss of HPRT function. At times up to 28 days following removal of HAT-medium, clones were challenged with 6-TG (Figure 2-2). In all cases, there was an increase in the number of 6-TG^R colonies seen as a function of time in non-selective medium. The spontaneous mutation rate for MC-TGS17-51 was estimated to be $0.89 \times 10^{-5} \pm 0.18 \times 10^{-5}$ per day. The spontaneous mutation rate for MN-5 and MN-12 was $0.72 \times 10^{-5} \pm 0.20 \times 10^{-5}$ and $0.93 \times 10^{-5} \pm 0.19 \times 10^{-5}$ per day, respectively. MN-11 exhibited a statistically significantly lower mutation rate, $0.46 \times 10^{-5} \pm 0.27 \times 10^{-5}$. All three MN-clones had a significantly lower doubling time (15-16 h) than the parental clone (19 h). When corrected for differences in doubling times, the rate of mutation was estimated to be 0.76×10^{-5} cells per generation for MC-TGS17-51, 0.50×10^{-5}, 0.30×10^{-5} and 0.62×10^{-5} cells per generation for MN-5, MN-11 and MN-12 respectively.

2.3.4 *Induced mutant frequency*

The main objective of this set of experiments was to select a clone which could detect induced mutants with high sensitivity, that is, which had a high ratio of induced to spontaneous mutations. Ionizing radiation is a well characterized cytotoxic and clastogenic agent. Preliminary experiments were performed in which MN-5, MN-11 and MN-12 were assessed for induction of 6-TG^R mutants by ^{60}Co γ-rays. There was a clear dose-dependent increase in the number of 6-TG^R colonies in all cases. However, MN-11 appeared to be the most useful, since it exhibited the highest ratio of induced/spontaneous mutants (Figure 2-3). MN-11 was compared to MC-TGS17-51 and MC1A-C1 in terms of sensitivity to mutation induction by ^{60}Co γ-rays (Figure 2-4A). Dose-dependent increase in the number of 6-TG^R colonies were observed in the case of MC-TGS17-51 and MN-11. No 6-TG^R colonies were

Figure 2-2 **Spontaneous generation of 6-TG^R mutants.** MC-TGS17-51 and three different G418^R clones (MN-5, MN-11 and MN-12) were grown in non-selective medium for up to 28 days. At weekly intervals, 1×10^5 cells were challenged with 6-TG and scored for the generation of 6-TG^R colonies. Mean absolute cloning efficiency of all cultures was 50%. Results are shown as mean ± SEM of 3-7 independent experiments, each involving 8-10 replicate dishes. Other details as described in Materials and Methods.

Figure 2-2

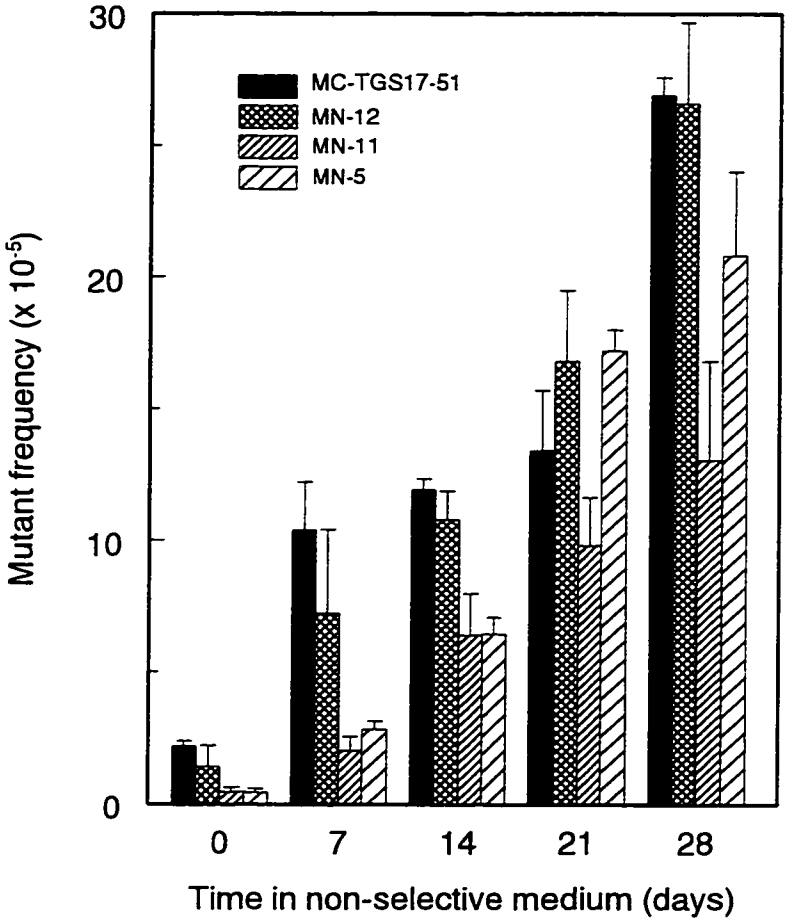
30
20
10
0
MC-TGS17-51
MN-12
MN-11
MN-5
Mutant frequency (x 10-5)
0
7
14
21
28
Time in non-selective medium (days)

Figure 2-3 **Generation of 6-TG^R mutants by ^{60}Co γ-rays in the G418^R clones.** MN-12, MN-11 and MN-5 were exposed to ^{60}Cobalt γ-irradiation at the indicated doses and the MF was determined after an expression time of 7 days. Results are shown as the mean ± SEM of 2-4 independent experiments each involving 5-7 replicate dishes. Data is not corrected for cloning efficiency.

Figure 2-3

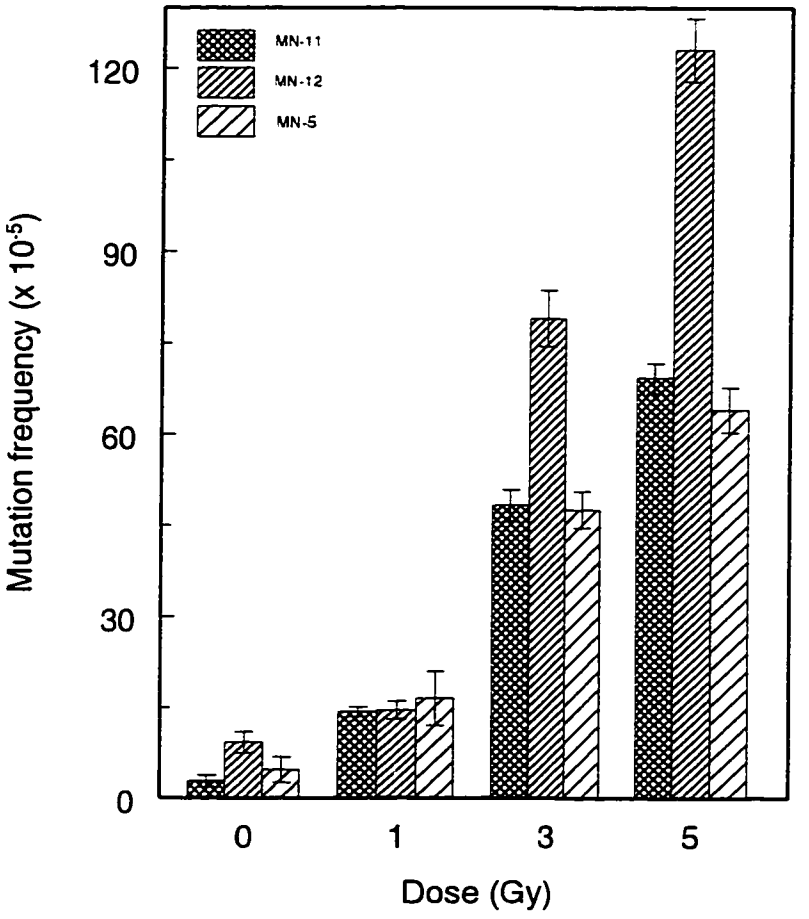
MN-11
MN-12
MN-5
120
90
60
30
0
Mutation frequency (x 10-5)
0
1
3
5
Dose (Gy)

Figure 2-4 **Mutagenic and cytotoxic effects of ^{60}Co γ-rays on MC1A-C1, MC-TGS17-51 and MN-11 cells.** Cell cultures were exposed to ^{60}Co γ-rays. Following overnight incubation, cultures were washed with PBS, mutagenicity and cytotoxicity determined as described in Materials and Methods. For (A) and (B), ▲, MC-TGS17-51; ○, MN-11; ■, MC1A-C1 parental cells. (A) Generation of 6-TG^R mutants. Error bars represent mean ± SEM of 2 independent experiments, each involving 3-8 replicate dishes at each experimental point. MF is corrected for cloning efficiency. The cloning efficiency of cells irradiated at 3 and 5 Gy was 81% and 53% of control respectively, after an expression time of 7 days (data not shown). (B) Dose-survival curves of MC1A-C1, MC-TGS17-51 and MN-11 cells. Mean absolute cloning efficiency of sham treated cultures was 45.2 ± 3.4% for MC-TGS17-51, 43 ± 3.5% for MN-11 and 41 ± 1.1% for MC1A-C1, respectively. Error bars represent the mean ± SEM of 2-7 independent experiments, each involving 5-8 replicate dishes. Dose (Gy) is plotted *versus* the survival (%) on the logarithmic scale.

Figure 2-4

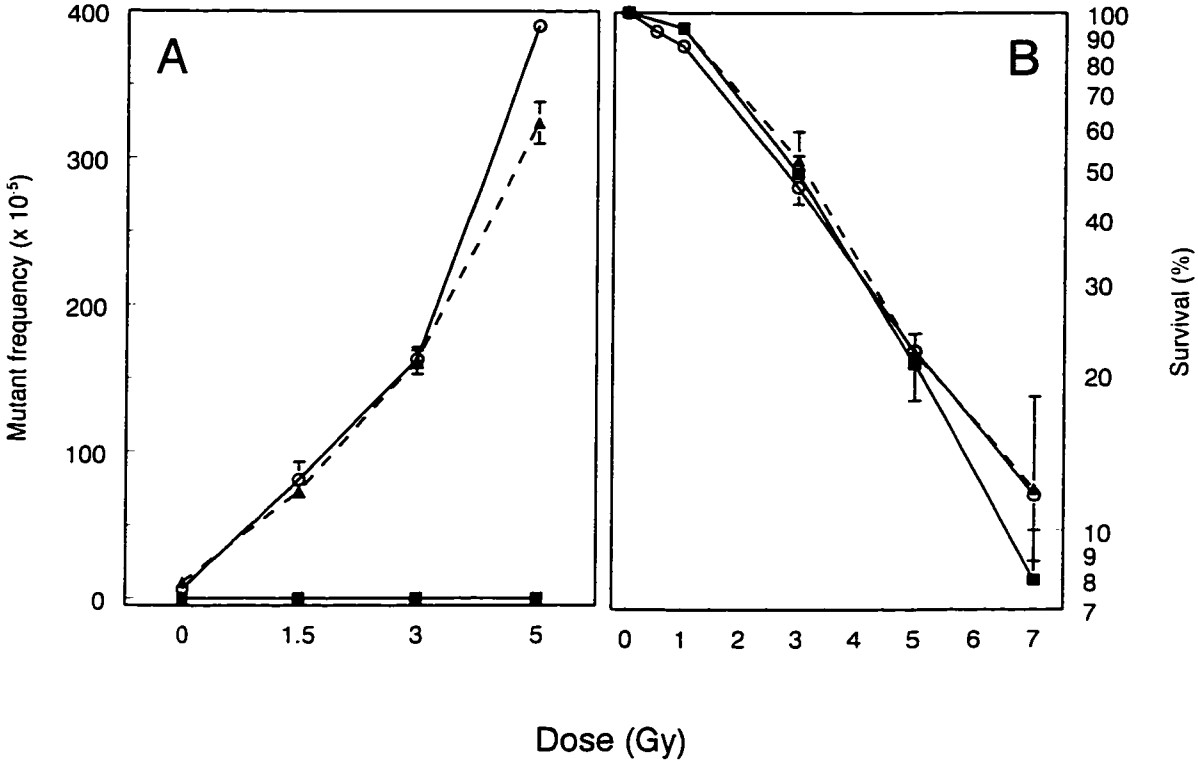
A
B
Mutant frequency (x 10⁻⁵)
Survival (%)
400
300
200
100
0
100
90
80
70
60
50
40
30
20
10
9
8
7
0
1.5
3
5
0
1
2
3
4
5
6
7
Dose (Gy)

observed in the parental MC1A-C1 cells in two independent experiments involving a total of 3.0×10^6 unirradiated and 1.2×10^7 irradiated (1.5-5 Gy). The calculated increase in MF in MC-TGS17-51 and MN-11 was 63 and 74 per 10^5 clonable cells per Gy respectively (calculations done using linear regression analysis, r = 0.976 and 0.958 for MC-TGS17-51 and MN-11, respectively). At 5 Gy, the estimated induced number of 6-TG^R colonies was at least 1000-fold greater than in the parental MC1A-C1 cells. Figure 2-4B shows that the survival curves exhibit a typical shoulder, indicating a capacity for repair of sub-lethal damage; at higher doses, an exponential decrease in cell viability was observed. The sensitivity to cell killing by ^{60}Co γ-rays was similar for all the three cell lines studied, D_0 = 3.6 Gy for MN-11; 3.0 Gy for MC1A-C1 and 3.5 Gy for MC-TGS17-51. The other two MN-clones, MN-12 and MN-5 also showed a similar sensitivity to cell killing, D_0 = 3.7 Gy (data not shown). The effects of ^{137}Cs γ-rays on cytotoxicity and mutant induction was also tested in MN-11 cells (Figure 2-5A). As observed for ^{60}Co γ-rays, ^{137}Cs γ-rays exhibited similar survival curve with an exponential decrease in cell viability at higher doses. The D_0 for ^{137}Cs γ-rays at room temperature was 2.0 Gy. ^{137}Cs γ-irradiation was also mutagenic in MN-11 cells, causing a dose-dependent increase in the number of $HPRT^-$ mutant colonies; at D_0, and an expression time of 8 days, the number of mutants induced was about 170 per 10^5 cells.

Mutations are "fixed" or an acentric chromosome fragment or HPRT protein is lost from a cell during the 'expression time'. The optimal expression time following ^{60}Co γ irradiation at 0°C was investigated (Figure 2-5B). Cultures were challenged with 6-TG on days 3, 6, 8 and 10 following ^{60}Co γ ray treatment. The number of mutants increased with time at doses of 1 to 3 Gy for expression times of 6-10 days. At higher doses, fewer mutants

Figure 2-5 **Cytotoxic and mutagenic effects of ionizing radiation on MN-11 cells.** (A), Cytotoxic (●) and mutagenic (○) effects of ^{137}Cs γ-rays. Cell cultures were exposed to ^{137}Cs γ-rays. Following overnight incubation, cultures were washed with PBS, cytotoxicity and mutagenicity determined as described in Materials and Methods. Mean absolute cloning efficiency of the sham treated cultures was 36 ± 8.5%. Error bars indicate the mean ± range of 2 experiments involving 3-5 replicate dishes at each experimental point. (B) Effect of expression time ((○), 3; (●), 6; (▼), 8; (■), 10 days) on MF by ^{60}Co γ-rays. Cell cultures were exposed to ^{60}Co γ-rays. Following overnight incubation, cultures were washed with PBS, cytotoxicity and mutagenicity determined as described in Materials and methods. Mean absolute cloning efficiency of the sham treated cultures was 43.4 ± 13%. Error bars indicate mean ± SEM of a single experiment (n = 4-6 replicate dishes). MF is not corrected for plating efficiency.

Figure 2-5

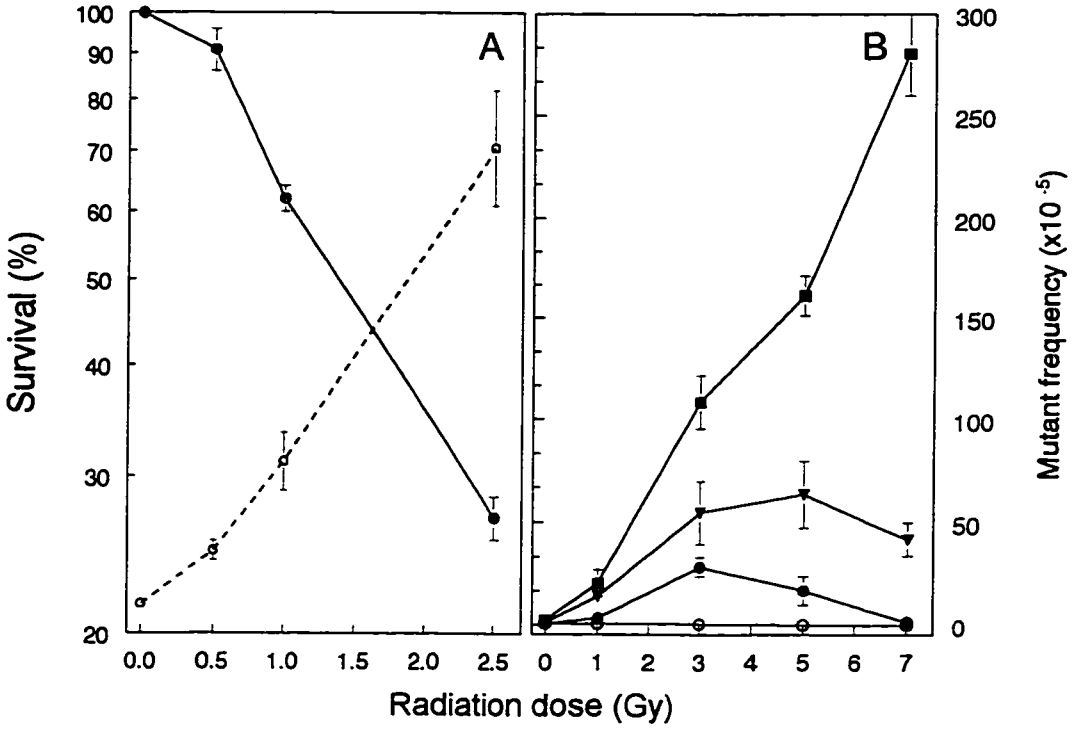
A
B
Survival (%)
Mutant frequency (x10 -5)
Radiation dose (Gy)
100
90
80
70
60
50
40
30
20
300
250
200
150
100
50
0
0.0
0.5
1.0
1.5
2.0
2.5
0
1
2
3
4
5
6
7

were recovered for expression times of 6 and 8 days. However, there was a marked increase in MF when the expression time was 10 days. No mutants were detected at any dose with a 3-day expression time. At D_o, the number of mutants induced was about 25, 60 and 130 per 10^5 cells on days 6, 8 and 10, respectively. Similar increase in MF was obtained for MN-5 and MN-12 (data not shown).

The presence of "small" colonies (≤ 0.3 mm) have previously been associated with large-scale deletions at the *TK* locus in mouse L5178Y lymphoma cells [201-203]. A bimodal distribution of colony size was also seen in $HPRT^-$ mutants of MN-11 cells. The number of "small" colonies as a percentage of total $HPRT^-$ mutants in irradiated and control MN-11 cells was determined. After 5 Gy of ^{60}Co γ rays, 46.6 ± 7.3% (n = 10, mean ± SD) of mutants formed "small" colonies and after 7 Gy, 63.0 ± 11.3% (n = 10) of mutant colonies were "small". The doubling time of selected "small" and "large" colonies was determined, as described in Materials and Methods. Five "large" colonies had an average doubling time of 12.0 ± 0.4 h and 3 "small" colonies had an average doubling time of 24.9 ± 5.2 h. "Small" colonies also accounted for 48.1 ± 2.1% (n = 34; mean ± SEM) of spontaneously arising mutants.

The average growth rate of a pool of five spontaneously arising $6\text{-}TG^R$ mutant clones cultured in the presence of wild type MN-11 cells was examined. It was found that the growth rate of the mutant clones was not detectably different from the wild type MN-11 cells, suggesting that at least *in vitro* there is no selective bias for the recovery of spontaneous mutants cells.

2.3.5 *Effect of Caffeine on radiation-induced cytotoxicity and mutagenicity in MN-11 cells*

Caffeine (1, 3, 7-trimethylxanthine) is known to inhibit DNA synthesis and repair, enhancing the cytotoxicity and mutagenicity of DNA-damaging agents such as radiation [204,205]. The effect of caffeine on cytotoxicity and mutagenicity induced by ^{60}Co γ-rays was tested on MN-11 cells. Treatment of MN-11 cells with caffeine (0.5 mM) for 18 h caused a low level of cytotoxicity (survival of 80.8 ± 10.4%, n = 3). Irradiation of MN-11 cells in the presence of caffeine did not cause any statistically significant increase in cytotoxicity at the doses tested (Figure 2-6A). Caffeine itself was not mutagenic in MN-11 cells, 6 mutants per 10^5 cells were induced. No increase in MF was seen at the lower dose (1.5 Gy); small but statistically significant increase in MF was observed at 3 Gy (2-tailed p = 0.042) and 5 Gy (2-tailed p = 0.037), respectively (Figure 2-6B).

2.3.6 *Detection of* in vivo *mutant frequency*

The primary use of the developed cell line was to determine the rate at which mutational events occur at the *HPRT* locus when these cells are grown as subcutaneous tumors in syngeneic animals. To investigate whether the tumor microenvironment may be mutagenic, three clones (MN-5, MN-11 and MN-12) were used. Clones were depleted of pre-existing mutants by culture in HAT-medium. Cells were then injected s.c. into the flanks of 5 mice to generate tumors. An equal number of cells were placed in culture and grown in non-selective medium. Tumors were collected when they reached a volume of 1 cm^3, estimated from measurements of the tumor diameters. Tumors of a volume ≥ 1 cm^3 yield approximately 10^8 total cells and were used for the determination of MF; however, tumors

Figure 2-6 **Effect of caffeine on radiation-induced cytotoxicity and mutagenicity on MN-11 cells.** Cultures were trypsinized, seeded at 5×10^5 cells per 10 cm dishes with or without caffeine for 2 h and then exposed to ^{60}Co γ-rays. Following an incubation of 16 h, cultures were washed with PBS, cytotoxicity and mutagenicity determined as described in Materials and Methods. Mean absolute cloning efficiency of the sham treated cultures with and without caffeine was 30.7% and 24.8%, respectively. Error bars show the mean ± SEM of a single experiment involving 3 independent dishes each analyzed in 3 replicate dishes. Panel (A) shows the cytotoxicity and (B) shows the mutagenicity curve. Solid line represents the dose-response curve without caffeine and broken line represents the dose-response curve with caffeine.

Figure 2-6

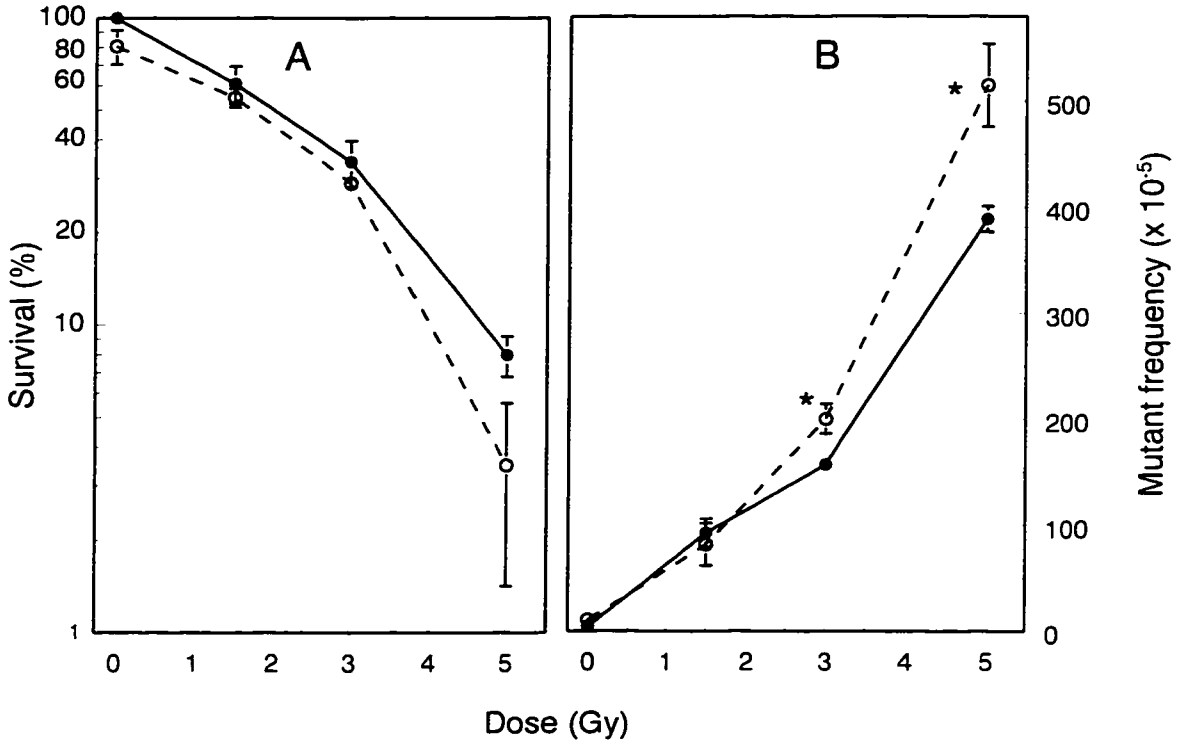
A
B
Survival (%)
100
80
60
40
20
10
1
0
1
2
3
4
5
Dose (Gy)
Mutant frequency (x 10-5)
500
400
300
200
100
0
*
*

< 1 cm^3 did not yield enough cells and were discarded. Figure 2-7 shows that all three clones demonstrated an increase in MF in cells recovered from tumors compared to cells grown in culture for an equivalent time. However, a large variance in MF was observed in cells recovered from different tumors. A more detailed comparison of *in vitro* and *in vivo* mutation frequencies was conducted using clone MN-11, which has a low background of spontaneous MF. The MF of cells from 50 tumors (12-18 days of *in vivo* growth) and 13 independent cultures were compared (Figure 2-8). Most of the tumor samples had a MF above that of any of the cell cultures. The overall 3.64-fold elevation in MF was highly significant ($p < 0.0001$, Mann-Whitney test). The MF was also examined as a function of time required for tumors to reach 1 cm diameter; no statistically significant differences were detected ($p = 0.0514$, Kruskal-Wallis test) (Figure 2-8, inset). In some cases, 2 tumors were produced in a single animal. No statistically significant correlation was observed in the tumors on the right and left flank of the same animal ($p = 0.4624$, Kruskal-Wallis test) (Figure 2-9).

2.4 DISCUSSION

Genomic instability is a commonly observed feature of cancer cells [9,40,206-213], but the reasons for this are still largely unknown. Factors intrinsic to the cancer cells (such as alterations of the *p*53 tumor suppressor gene) may predispose these cells to further genomic instability [17,191,214-219]. Our laboratory was interested in the development of a transplantable mouse model system in which loss of the *HPRT* gene function could be readily monitored. A mouse fibrosarcoma known to be infiltrated with macrophages and granulocytes was used in this study [197,198]. A clonal variant was selected by its ability

Figure 2-7 **Detection of 6-TG^R mutants arising *in vivo* in different MN tumors.** Solid bars represent the spontaneous *in vitro* MF of cells grown under standard tissue culture conditions (16-18 days) before being challenged with 6-TG. Results are shown as mean ± SEM of 5-8 replicate dishes. Hatched bars represent *in vivo* MF of cells recovered from different s.c. tumors. Data shown are mean ± SEM (n = 5 animals, each tumor analyzed in 5-8 replicate dishes). No statistically significant differences were detected between any of the clones (p = 0.0514, Kruskal-Wallis test).

Figure 2-7

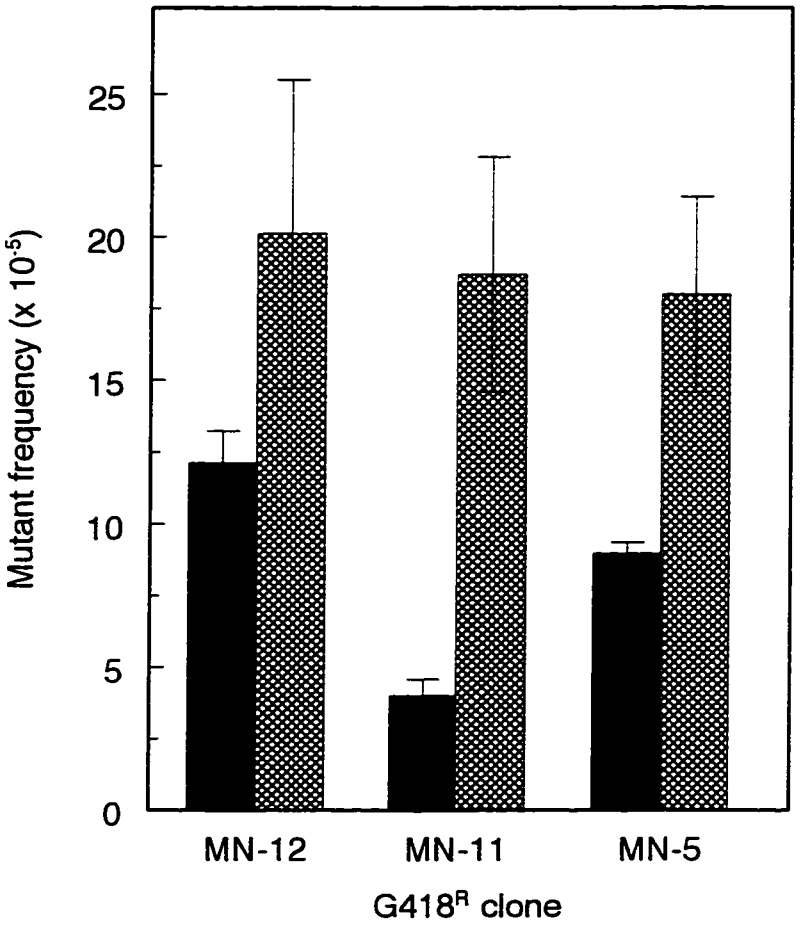
Mutant frequency (x 10-5)
25
20
15
10
5
0
MN-12
MN-11
MN-5
G418R clone

Figure 2-8 **Detection of 6-TG^R mutants arising *in vivo* in MN-11 tumors.** Main panel: solid bar represents the mean MF of MN-11 cells grown *in vitro* under standard culture conditions for 12-18 days before being analyzed for mutation induction. The error bar indicates the SEM of 13 independent cultures, each involving 5-8 replicate dishes. Hatched bar represents the mean MF of cells recovered from s.c. tumors at 12-18 days after tumor cell injection. The error bar indicates the SEM of 50 separate tumors each analyzed in 4-8 replicate dishes. MF is corrected for the percentage of cells (75-95%) which were G418^R and the cloning efficiency of the tumor cells. MF of the cells recovered from tumors was 17.83×10^{-5} *versus* 4.89×10^{-5} for the cultured cells. The respective median values were 16.25 and 5.53. Mutation frequencies in cultured and tumor cells were compared using the Mann-Whitney test; 2 tailed $p < 0.0001$. Inset: the pooled tumor data in the main panel, shown by time of *in vivo* growth. The error bars indicate the SEM, where the number of tumors examined is indicated in parentheses.

Figure 2-8

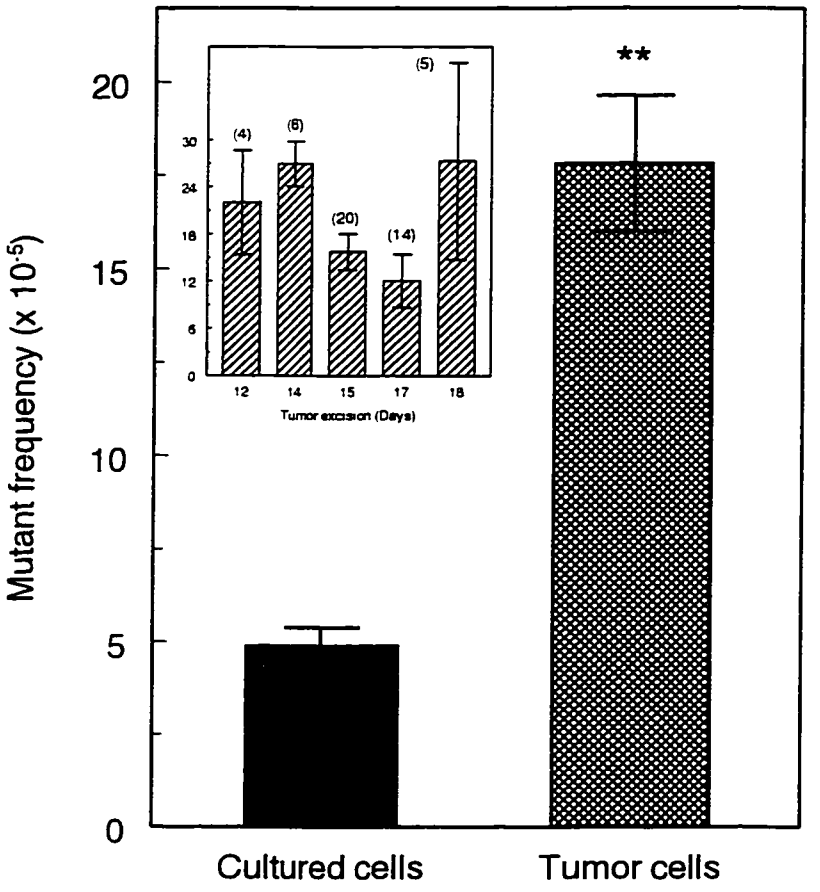
Mutant frequency (x 10⁻⁵)
20
15
10
5
0
**
(4)
(6)
(20)
(14)
(5)
30
24
18
12
6
0
12
14
15
17
18
Tumor excision (Days)
Cultured cells
Tumor cells

Figure 2-9 **Comparison of 6-TG^R mutants arising *in vivo* in MN-11 tumors injected on the right and left flanks of the same animal.** 5×10^5 MN-11 cells were injected on the right and left flanks of mice. Tumors were allowed to form for 14 days and MF determined. MF is corrected for percentage of cells which were G418^R and cloning efficiency of tumor cells. Results are expressed as mean ± SEM where each tumor was analyzed in 4-8 dishes. In the graph, tumors grown on the right flank were ordered in terms of increasing MF. The corresponding MF of the tumor grown on the left flank is plotted beside it. No statistically significant correlation was observed between the MF of the two tumors grown in the same animal (Kruskal-Wallis test, $p = 0.4624$).

Figure 2-9

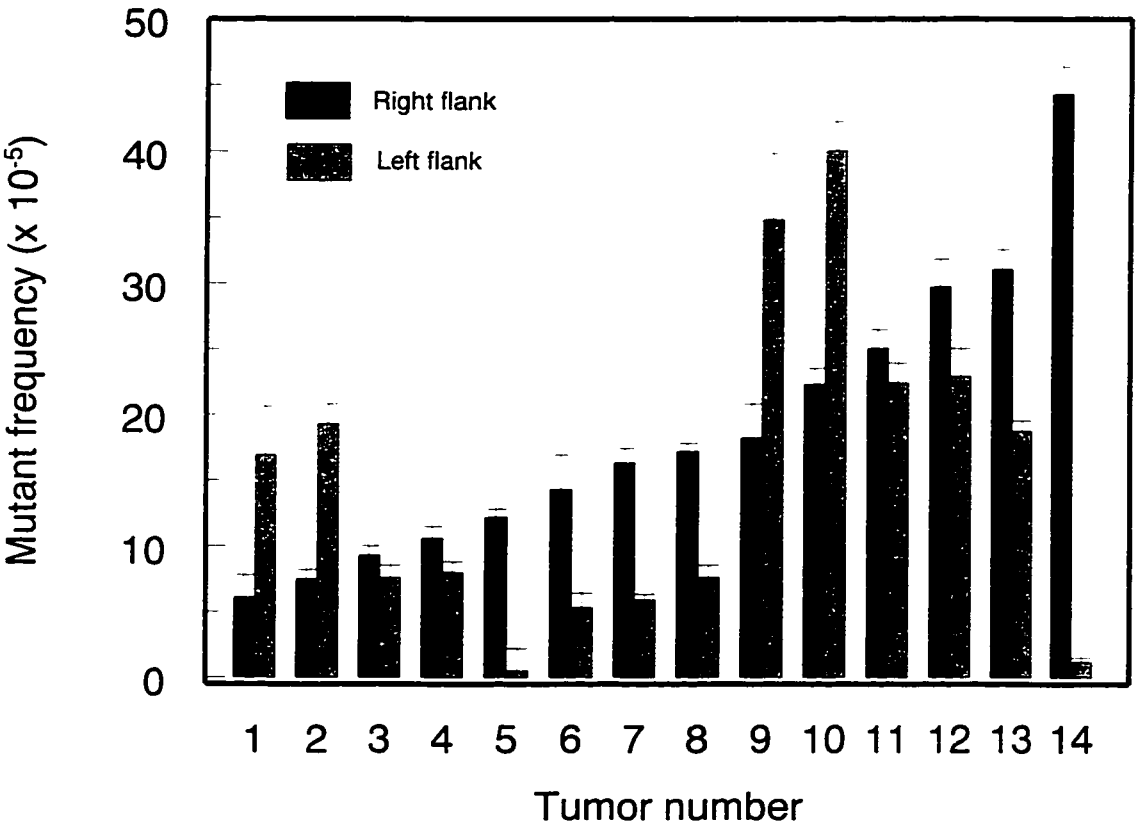
Mutant frequency (x 10-5)
50
40
30
20
10
0
Right flank
Left flank
1 2 3 4 5 6 7 8 9 10 11 12 13 14
Tumor number

to grow under tissue culture conditions, verified to be tumorigenic and further genetically manipulated to result in a clone, MC-TGS17-51 and its $G418^R$ derivative, MN-11.

The *HPRT* locus, located on the X chromosome, has been used as an important marker gene for the study of mammalian cell mutagenesis, including man [220-223]. It was chosen as a marker for detecting mutational events since the presence or absence of this enzyme can be readily scored by growing cells in HAT-medium or 6-TG-medium, respectively. One of the limitations of the use of the *HPRT* locus is that its hemizygous X-chromosome location is such that makes it insensitive to detection of clastogenic events (e.g., those caused by ionizing radiation) due to loss of essential genes. By definition, such mutants will not be scored because they are non-viable, resulting in a lowered sensitivity for detecting induced mutations. Interestingly, this is less of a problem in Chinese hamster and human cells, possibly because the gene locus is more centromere-proximal in a mouse than in other species. Evans *et al.* (1986) has demonstrated that the autosomal *TK* locus in mouse L5178Y lymphoma cells was 100-fold more sensitive in detecting mutations (by a clastogenic agent) than the hemizygous *HPRT* gene. The greater sensitivity of the *TK* locus to mutation induction by ionizing radiation compared to the *HPRT* locus is likely to be due to recovery of an additional class of mutants, possibly ones containing large-scale mutational events. Our own observation was that no $HPRT^-$ mutants could be induced by ^{60}Co γ-rays in MC1A-C1 parental mouse tumor cells (Figure 2-4A). A possible explanation was provided by karyotypic analysis of the MC1A-C1 cells, carried out in collaboration with Dr. Tucker's laboratory, Lawrence Livermore National Laboratory, Livermore, California, USA. These cells were found to be hypotetraploid with three copies of the X chromosome, suggesting that they have more than one active chromosome with more than one active

HPRT gene [1]. Thus multiple copies of the *HPRT* gene had to be mutated to result in an HPRT$^-$ phenotype. Treatment of MC1A-C1 cells with the mutagen, MNU, and growth in low concentrations of 6-TG eventually resulted in the inactivation of all the copies of the genes. The mechanism of inactivation of the *HPRT* genes in these cells is unknown. MNU is a point mutagen but it can also cause gene silencing by methylation [224-226]. 6-TG^R mutants obtained by this treatment were then passaged through the mouse and the most tumorigenic (MC-TGR17) was selected. This clone exhibited a high spontaneous reversion frequency in HAT-medium, suggesting reactivation of the *HPRT* gene (refer to Diana Wilkinson's thesis). One of the spontaneous revertants, MC-TGS17-51, was most stable with respect to spontaneous and induced MF. It was further infected with a viral construct carrying the *neo* gene.

Six HAT^R, G418^R clones were verified to be tumorigenic and further assessed for spontaneous mutation frequencies. Of these, three (MN-5, MN-11 and MN-12) were selected on the basis of their tumorigenicity in syngeneic animals and low spontaneous mutant frequencies. All clones displayed similar spontaneous mutation rates, $< 1.0 \times 10^{-5}$ mutants per generation. A more detailed characterization of these clones was conducted by examining the induced MF following exposure to ^{60}Co γ-rays. MN-11 demonstrated the highest induced to spontaneous ratio and a low spontaneous MF. This clone was then compared to mutant induction by ^{60}Co γ-rays to MC1A-C1 and MC-TGS17-51 (Figure 2-4). MN-11 cells exhibited a large increase in sensitivity (> 1000-fold) to mutation-induction by radiation than the parental line; however, the sensitivity was similar to MC-TGS17-51. ^{137}Cs γ-irradiation was also a very effective mutagen, as shown for ^{60}Co γ-irradiation. At equivalent cytotoxicities, ^{137}Cs γ-irradiation was slightly more effective

(170 compared to 130 mutants per 10^5 cells at D_o), but the difference could be due to differences in expression time, temperature at which cells were irradiated, or other factors. Our lines have a similar dose-response curve for induction of HPRT mutations by ionizing radiation as observed for mutations at known heterozygous loci, such as endogenous *TK* in mouse L5178Y cells and CHO-K1 cells [227,228], transfected bacterial GPT in CHO-10T5 cells and V79 cells[228,229] and retrovirally-introduced human *HPRT* in mouse VH-12 fibroblasts [230]. Ionizing radiation is known to be an efficient inducer of large-scale deletions (chromosomal mutations) [79,228,231-233]. About 50% of radiation-induced $HPRT^-$ mutants in MN-11 cells exhibited a "slow-growth" phenotype, as has been described for large-scale deletions at the heterozygous *TK* locus in mouse L5178Y lymphoma cells [201-203]. Taken together, these lines of evidence indicate that MN-11 cells have a heterozygous *HPRT* gene in which relatively large deleted regions (hundreds or thousands of base-pair deletions) can be tolerated. Parental lines from which MN-11 was derived contain 3 copies of the X chromosome [1]. Karyotype analysis of MN-11 cells using the X centromeric-specific probe have also shown that these cells have maintained the 3 X chromosomes (Chapter 6). Based upon their phenotype, MN-11 cells appear to have heterozygous *HPRT* gene ($HPRT^{+/-/-}$ genotype).

The effect of caffeine, an agent that can enhance cell killing and mutagenesis, was investigated after irradiation of MN-11 cells [204,205,234]. The results indicate that caffeine does not act synergistically with radiation in increasing cytotoxicity in MN-11 cells. This could be due to the difference in the concentration of caffeine (0.5 mM) used in these studies; a higher concentration (2 mM) was employed in other studies [234,235]. Exposure to caffeine alone at concentrations up to 5 mM for 18 h, produced dose-

dependent decreases in cell survival (at 5 mM, survival of 32 ± 3.1%, n = 2; data not shown). So a concentration of 0.5 mM was used in these studies. At higher doses of radiation, caffeine potentiates the mutagenic effect of radiation (Figure 2-6B). However, mutagenicity is not accompanied by strong cytotoxicity in these cells.

Using the MN-11 *in vitro/in vivo* model I have compared multiple tumor samples and multiple cell culture replicates, and consistently observed an increase in MF in the tumors. Clone MN-11 exhibited the lowest *in vitro* spontaneous MF and high induced MF. Therefore, it was chosen to analyze the contribution of the tumor microenvironment to mutant induction. The other two clones MN-12 and MN-5 also showed an increase in MF as compared with *in vitro* cultures, but they had a higher spontaneous MF. Therefore, measuring small increases in MF over a high background of spontaneous MF would be difficult (Figure 2-7). When cells from the tumors were analyzed for mutations, a highly statistically significant 3.64-fold increase in MF was observed (Figure 2-8). However, a large variance in MF was observed among different tumors, compared with the small variance in replicates of a single tumor cell suspension. This was seen for all the three clones studied, suggesting Luria-Delbrück type of fluctuation [236]. Since identical, clonally derived, HAT-cleaned cells were used to establish the tumors and the parallel cell cultures, the only variable between the two experimental groups was the condition of cell growth (in tumors *versus* in culture). Therefore, the differences between tumors and the cell cultures in MF can be attributed to the growth conditions, suggesting that the tumor microenvironment is mutagenic. No correlation in MF was found in the right and left tumors of the same animal. This observation suggests that each tumor may be unique in accumulating mutational events, possibly due to the differences in the tumor cell infiltrate.

In support of these findings, two recent publications from different laboratories have shown that the tumor microenvironment can contribute to genomic instability, although our laboratory was the first to show directly that factors in the tumor microenvironment may cause mutations at the *HPRT* locus [1]. Paquette and Little [42] reported the development of an *in vitro/ex vivo* model to examine instability in the minisatellite sequences. They transformed C3H/10T½ cells by x-irradiation and injected tranformed foci into syngeneic mice. After 3-5 months, clones derived from tumors were examined for changes in oligonucleotide repeat markers. These workers observed changes in a higher proportion of clones isolated from tumors than in subclones from cells grown *in vitro*. It is of interest that similar changes in oligonucleotide repeat markers have been described in human colorectal cancer and attributed to defects in DNA repair genes [29,31,210,237]. More recently, Reynolds et al. [43] described another *in vitro/ex vivo* model to study genetic instability in solid tumors. They used a tumorigenic mouse cell line (LN12, carrying a chromosomally based λsupF shuttle vector) that grows *in vitro* and as subcutaneous tumor in athymic nude mice. Following *in vivo* growth of 6-21 weeks, tumors were excised, genomic DNA exposed to an *in vitro* λ packaging extract and mutations analyzed in the *supF* gene. They found a 5-fold increase in MF in tumors than the cultured cells and they suggest that the hypoxia found within tumors may be responsible for this effect.

Although the mutation frequencies in tumors and in culture are clearly different, calculation of a true mutation rate (mutations per cell division) is complicated by possible differences between the growth rates of cells in culture and in solid tumors. The number of cell doublings in culture can be readily determined, but determining precisely the

number of doublings undergone by tumor cells is impossible, since tumors represent a heterogeneous cell population, with mixtures of growing, nondividing, and dying cells. Therefore, the data is represented as MF, i.e., mutants per total number of clonable cells, not mutation rates. It is worth noting that MN-11 cells have a very rapid doubling time (16 h); therefore, it is improbable that the observed increase in MF can be solely explained by increased number of cell divisions *in vivo* compared with *in vitro*. This is supported by other experimental tumor models, where the tumor cell populations consistently have longer mean cell cycle times than do parallel cultures grown *in vitro* under optimal culture conditions [238,239]. Hence, the number of cell divisions over a given period is likely to be lower in tumors than in cultures. This means that the difference in the true mutation rate would be even greater than the observed difference in mutation frequency.

Although it has been well known for many years that chronic inflammatory conditions predisposes to the development of cancer [44-46,55,57], a mechanism has yet to be established. Most solid tumors, including human tumors, are infiltrated with leukocytes and some of these cells are known to release a variety of oxidants that might cause further genetic damage in tumor cells, contributing to tumor progression [54,56,127,195,240-242]. On the one hand, mutations in critical genes, such as *p*53, may predispose to genomic instability via alterations in the cell cycle and in DNA repair [27,243-245]. On the other hand, the work presented in this Chapter shows that the tumor microenvironment itself may be mutagenic and may therefore be an important contributor to tumor progression. It is likely that the genomic instability in tumors may be mediated through a number of different mechanisms that are not necessarily mutually exclusive and may vary in different tumors.

CHAPTER 3

BIOLOGY OF SUBCUTANEOUS MN-11 TUMORS IN C57BL/6 MICE

ABSTRACT

Progression of cancer is associated with genetic instability. Our laboratory has hypothesized that phagocytic cells found within solid tumors may contribute to genetic instability by generating ROS, RNS and other clastogenic agents. To study these factors, a transplantable murine tumor cell line (MN-11) that grows in culture and as s.c. tumors in syngeneic mice has been developed. Injection of 5×10^5 viable cells formed tumors in essentially 100% of the animals by day 14 with an estimated tumor volume-doubling time of 2.7 days. MN-11 cells form solid tumors exhibiting properties of a malignant fibrosarcoma, which may be locally invasive but does not metastasize. The number of viable cells recovered from tumors decreases markedly with the age of the tumor. Immunohistochemical localization of BrdU labeled cells and the analysis of mitotic and apoptotic cells were used to study the dynamics of cell growth and death within the tumor. The number of cells in S-phase decreased ($p < 0.01$) and the number of cells undergoing apoptosis increased ($p < 0.001$) between days 12 to 18, both at the periphery and in the core. Histochemical analysis of MN-11 tumors has shown the presence of granulocytes, macrophages, mast cells and lymphocytes. Granulocytes are the major component of the infiltrate, found mainly in necrotic areas; however, macrophages, mast cells and lymphocytes are found in fewer numbers at the periphery of the tumor.

3.1 INTRODUCTION

Experimental tumor model systems are now available for the study of the genetic instability that may be an important cause of tumor progression [42,43,246]. These studies have focussed on different aspects of the tumor microenvironment in causing genetic

instability. Our laboratory has studied the role of ROS and RNS found in solid tumors in mutant induction in the MN-11 tumor model system. Our laboratory is the first to report an increased MF in cells grown as tumors, suggesting that the tumor microenvironment is mutagenic [1]. Reynolds et al. [43] have studied hypoxia in solid tumors using a tumorigenic mouse cell line (LN12) carrying a chromosomally based λsupF shuttle vector that grows *in vitro* and as s.c. tumor in athymic nude mice. Gal et al. [246] have studied the role of NO· in mutagenesis using a transplantable lymphoma (RcsX) to induce tumors in SJL mouse, stimulating NO· production by macrophages in spleen and lymph nodes. A significant increase in MF was found in the spleen (target) of tumor-bearing mice, suggesting a role of NO· in mutant induction.

MN-11 is a transplantable murine fibrosarcoma cell line that grows *in vitro* and as a s.c tumor in syngeneic mice (Chapter 2). This model system allows the *ex vivo* detection of mutants that may arise *in vivo*. Using this model, the frequency of mutants in MN-11 cells grown as tumor was found to be 3.64-fold higher than in the same cells maintained *in vitro* for an equivalent period. This data supports our hypothesis that factors present in the tumor microenvironment may be mutagenic and/or clastogenic. The mechanism underlying this observed increase in MF is unknown. My thesis investigates possible mechanisms. In this Chapter I describe the characterization of the MN-11 tumor with respect to morphology, growth curves and tumor infiltrating host cells.

3.2 MATERIALS AND METHODS

All materials, chemicals and solution compositions used in these experiments are found in Appendix II. Preparation of antibody and fixative solutions is found in Appendix III.

3.2.1 *Cell number needed for tumor formation*

To determine the minimum number of cells required to form tumors in animals, an experiment was conducted using different number of cells and six C57BL/6 female mice per group. Each group was injected with either 0.5, 1.0, 2.5 or 5 $\times$ 10^5 viable cells suspended in 0.1 mL PBS into the s.c. tissue of their flanks. Animals were watched for the development of any palpable tumors. If no palpable tumors were observed for 4 weeks, animals were sacrificed. A complete necropsy was performed on each animal, and the organs were examined for any signs of invasion and/or metastasis.

3.2.2 *Determination of tumor-doubling time*

A cell suspension of 5 $\times$ 10^5 viable cells was injected s.c. into the flanks of a group of mice. Tumor length, width and height were measured at various times following tumor cell inoculation with a caliper. No correction was made for skin thickness. Tumor volumes were calculated using the formula for the volume of a hemiellipsoid as described by Isaacs and Coffey [247]:

$$V = \tfrac{1}{2} (4 \pi/3) (l/2) (w/2) (h)$$

$$\text{tumor volume } (mm^3) = 0.5236 \times \text{length} \times \text{height} \times \text{width}$$

The data was plotted as days post tumor cell inoculation (x-axis) and the corresponding log tumor volume on the y-ordinate. The tumor volume-doubling time (in days) was then calculated by dividing the log 2 by the slope of the regression line determination.

3.2.3 *Detection of S-phase cells*

***(a) Labeling with 5-bromo-2'-deoxyuridine (BrdU)* in vivo**

Tumors were established by inoculation of 5×10^5 MN-11 cells s.c. into the flanks of C57BL/6 female mice. Tumors were allowed to form for 15, 19 or 21 days, respectively. BrdU was injected i.p. (30 mg/kg) in a volume of 0.2 mL PBS. Animals were sacrificed after 2 h and the tumors removed; small intestines from the same animal served as a control. Samples from tumors and small intestines were fixed in 10% neutral buffered formalin for 24 h, embedded in paraffin, sectioned at 3-5 μm and processed for immunohistochemistry as described below.

(b) Immunohistochemical detection

All antibodies were diluted in PBS without any sera added to reduce non-specific binding. Embedded tissues were first deparaffinized in xylene and rehydrated in a series of decreasing concentration of ethanol, starting with 100% ethanol. Sections were washed with distilled water and incubated with 50 mM tris-buffered saline, pH 7.6 (TBS) containing 1% H_2O_2 and 0.25% Triton X-100 for 15 min at room temperature to destroy endogenous peroxidase activity. For better antibody access, DNA was partially denatured with 4.0 N HCl for 20 min, Bouin's fixative at 60°C for 1 h or microwave heating for 10 min. The denaturation was quenched by immersion in 0.1 M sodium tetraborate, pH 9.2 for 10 min and then rinsed in TBS. Non-specific staining was blocked with 1% normal swine serum at room temperature for 30 min. Slides were blotted, 1:100 and 1:1000 dilution of mouse monoclonal anti-BrdU (Sigma Chem Co) was added and incubated at room temperature for 1 h. Detection of the primary antibody was achieved by incubating for 30 min at room temperature with horse anti-mouse biotinylated IgG (Dimension

Laboratories Inc.) (7.5 μg/mL), followed for 30 min at room temperature by avidin-peroxidase (Dimension Laboratories Inc.) (5 μg/mL). Slides were washed twice for 5 min in TBS between each step. Colour was developed using diaminobenzidine tetrahydrochloride (0.02% DAB) for 10 min, washed again with TBS, counterstained lightly with Mayer's haematoxylin and coverslips affixed with permount.

(c) Counting of S-phase cells

In cells in which BrdU had been incorporated, the nucleus was completely stained with a dark brown precipitate formed by the DAB-H_2O_2-peroxidase reaction. The BrdU labeling index (BLI) was quantified by counting at least 10 fields using a 40 × objective with a calibrated eye piece (where 1 field is 1 mm^2 of a 100 mm^2 grid) at the periphery and in the core of the tumor. The total number of tumor cells per field (defined by the grid) was determined by counting tumor cells within the boundary of 100 grid squares using an Olympus BH-2 microscope. The total number of tumor cells counted varied with cell size, amount of stroma, and cellularity.

$$\text{BLI}\ (\%) = \frac{\text{number of BrdU labeled cells}}{\text{total number of tumor cells}} \times 100$$

3.2.4 *Histochemical assay for detecting tumor-infiltrating cells*

Tumor tissue sections were fixed and processed as described in section 3.2.3 (a) unless otherwise indicated. The infiltrating cells in the tumor were examined using haematoxylin and eosin (H & E) stained sections. Special stains were also used to confirm each cell type.

(a) Demonstration of endogenous peroxidase activity in granulocytes

Preparation of frozen sections: To identify granulocytes by their endogenous

peroxidase activity, frozen sections had to be used. Tumor tissue was washed in ice cold 100 mM phosphate buffer, pH 7.2 (PB) and exposed to a 2 h fixation at 4°C in a modified Zamboni's fixative [248,249]. Fixative was cleared with several rinses in prechilled PB. Fixed tissue was stored at 4°C in a 1:1 mixture of 10% sucrose (containing 0.1% sodium azide) and 3% Triton X-100 in PB for a minimum of 24 h prior to sectioning. Tumor tissue was then embedded in Optimal Cutting Compound, frozen immediately in liquid nitrogen and stored at -80°C until analyzed. Cryosections were cut at 5 μm in thickness and mounted on 3-aminopropyl triethoxy silane (AES) coated slides (preparation described in Appendix III).

Detection of peroxidase activity: Enzyme activity was demonstrated by incubating frozen tumor tissue sections in TBS containing 0.02% DAB and 0.6% H_2O_2 for 10 min at room temperature with constant stirring. Sections were washed in running water, counterstained with haematoxylin and coverslips affixed with permount.

(b) Identification of macrophages by non-specific esterase activity

The α-naphthyl acetate method using the diazonium salt hexazonium pararosanilin was employed [250]. Frozen sections were incubated in the presence of equal volumes of 4% sodium nitrite and 4% pararosanilin for 20 min at 37°C, washed in running water and counterstained with haematoxylin.

(c) Identification of tissue mast cells by toluidine blue

Paraffin sections were processed as described in section 3.2.3 (b). Sections were stained in toluidine blue solution (1% toluidine blue in 50% isopropanol) for 10 min at room temperature. These were blotted and then placed in absolute isopropanol for 1 min, cleared and mounted as described above.

3.2.5 *Statistical analysis*

Data was analyzed using one-way ANOVA test. Following detection of a statistically significant F value, *post hoc* Dunnett's or Tukey-Kramer test was used. A 2 tailed p value of ≤ 0.05 was considered to be significant (shown as *) or $p \leq 0.01$ was considered to be highly statistically significant (shown as **).

3.3 RESULTS

3.3.1 *Tumorigenicity of MN-11 cells*

A total of 24 mice, 6 per group were injected with MN-11 cells (as indicated in section 3.2.1) and observed for the appearance of palpable tumors. Tumors first became palpable on day 8 following tumor cell inoculation. Figure 3-1 shows that on day 10, no tumors developed in animals injected with 0.5×10^5, 1×10^5 or 2.5×10^5 cells. However, 50% of the animals injected with 5×10^5 cells developed tumors. By day 14, the percentage of tumor-bearing animals increased in all the four groups (17% for animals injected with 0.5×10^5 cells, 67% each for animals injected with 1.0×10^5 and 2.5×10^5 cells and 100% for animals injected with 5×10^5 cells, respectively). No further increase in the percentage of tumor-bearing animals was seen after 16 days of tumor cell inoculation. As a result of this experiment, subsequent experiments were conducted using injections of 5×10^5 MN-11 cells. Tumor volumes, measured on day 18 were not significantly different in any of the groups (298 ± 70 mm^3 (animals injected with 0.5×10^5 cells) vs 239 ± 54 mm^3 (animals injected with 1.0×10^5 cells) vs 385 ± 60 mm^3 (animals injected with 2.5×10^5) vs 301 ± 64 (animals injected with 5×10^5); mean $\pm$ SEM, ANOVA, *post hoc* Tukey-Kramer test, $p > 0.05$).

Figure 3-1 **Tumor formation in C57BL/6 mice.** Animals were divided into four groups of six mice each, and injected s.c. with 0.5×10^5, 1.0×10^5, 2.5×10^5 and 5×10^5 viable MN-11 cells. Animals were monitored for the formation of palpable tumors on days 10, 14, 16 and 18, respectively.

Figure 3-1

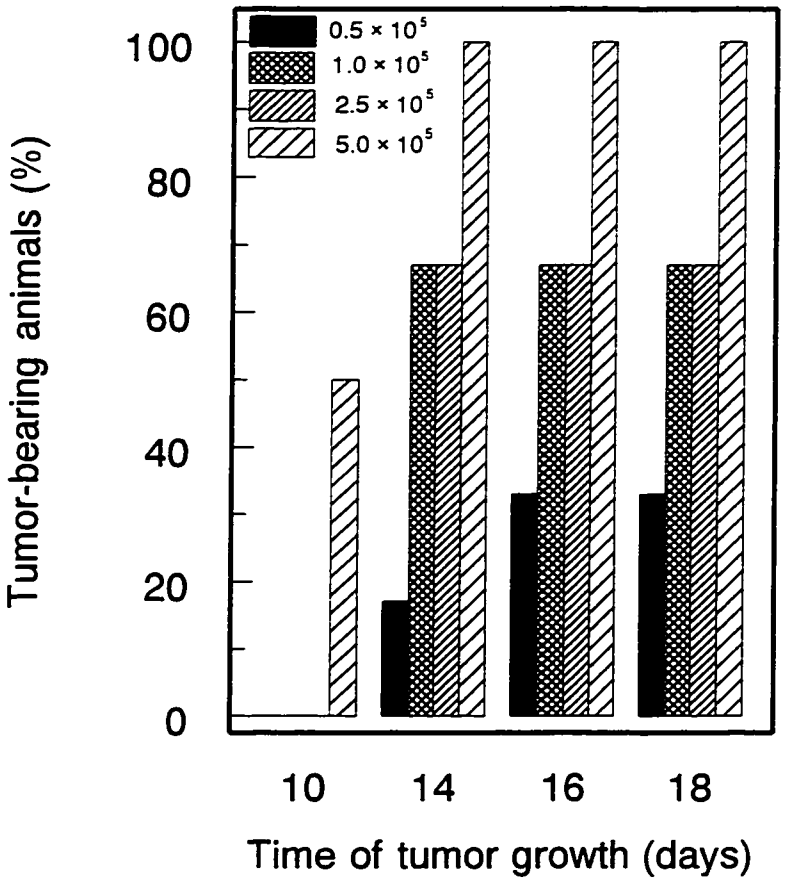
0.5 × 10^5
1.0 × 10^5
2.5 × 10^5
5.0 × 10^5
100
80
60
40
20
0
Tumor-bearing animals (%)
10
14
16
18
Time of tumor growth (days)

3.3.2 *Tumor volume-doubling time*

When 5×10^5 viable MN-11 cells were injected s.c. into C57BL/6 mice, tumors become palpable by day 14 in essentially 100% of the animals. The growth curve of these tumors is sigmoidal on a linear plot of tumor volume *versus* days post tumor inoculation (Figure 3-2A). The tumors had reached 87% of their volume by day 15. The growth curve was replotted as the log of the tumor volume *versus* days post tumor inoculation from which the tumor volume-doubling time was estimated to be 2.7 days calculated from the near-linear part of the curve (Figure 3-2B).

3.3.3 *Cell dynamics in MN-11 tumors*

The number of viable cells recovered from tumors decreases with the age of the tumor, after day 18 (data not shown). Tumor volume is likely to be a poor indicator of viable cell numbers. Therefore, the mitotic index (MI) and apoptotic index (AI) was examined as a function of the age of the tumor at the periphery and in the core of the tumor (counts were done as described in section 3.2.3 (c) for BrdU labeling index (BLI)) to obtain more information about the dynamics of cell growth and death in the tumor. Figures 3-3A and B show the features of mitotic and apoptotic cells in non-necrotic areas of the tumor. The AI increased with the age of the tumor, and it was highest by day 20. Peripheral areas showed a significant increase in the AI (ANOVA, *post hoc* Tukey-Kramer test, $p < 0.05$); the core exhibited a similar increase (ANOVA, *post hoc* Tukey-Kramer test, $p < 0.01$) (Figure 3-4). The MI showed a non-significant decrease with the age of the tumor both in the periphery and the core. MI was greater than the AI in day 12 and 14 tumors in the periphery ($p < 0.001$ in an unpaired Student's *t*-test); the core showed

Figure 3-2 **Tumor volume-doubling time of MN-11 tumors.** Linear (A) and semilogarithmic (B) growth plots of MN-11 tumor. C57BL/6 mice were inoculated with 5×10^5 viable MN-11 cells into the right flanks and monitored for tumor formation. Tumors were measured on days 9 through 18 using sliding caliper and tumor volumes were determined as described in section 3.2.2. Data is represented as mean $\pm$ SEM of a single experiment involving 6 mice. Where error bars are not shown, they are within the symbol.

Figure 3-2

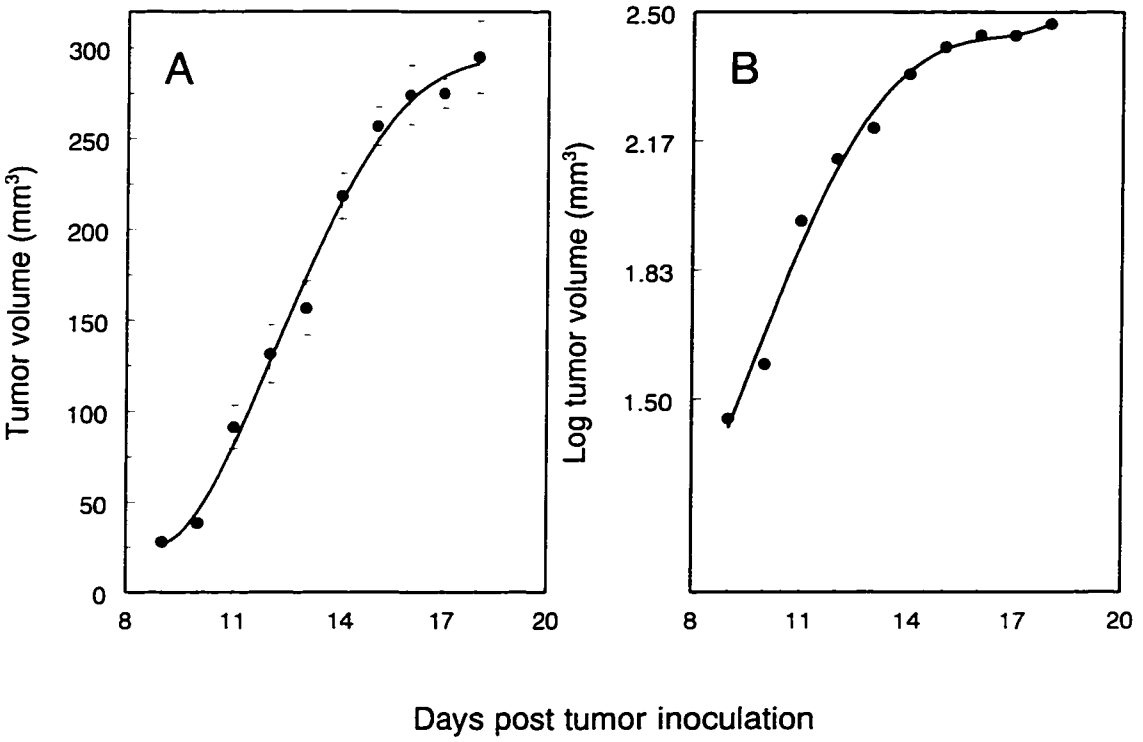
A
B
Tumor volume (mm3)
Log tumor volume (mm3)
300
250
200
150
100
50
0
2.50
2.17
1.83
1.50
8
11
14
17
20
Days post tumor inoculation

Figure 3-3 **Detection of mitotic and apoptotic cells in MN-11 tumors.** Representative photomicrographs of H & E stained sections showing the appearance of mitotic figures and apoptotic cells. (A), Cells in anaphase (small arrows), and metaphase (large arrows) , × 200; (B), Arrows points to apoptotic cells, identified by an eosinophilic cytoplasm and a clear halo, × 400.

Figure 3-3

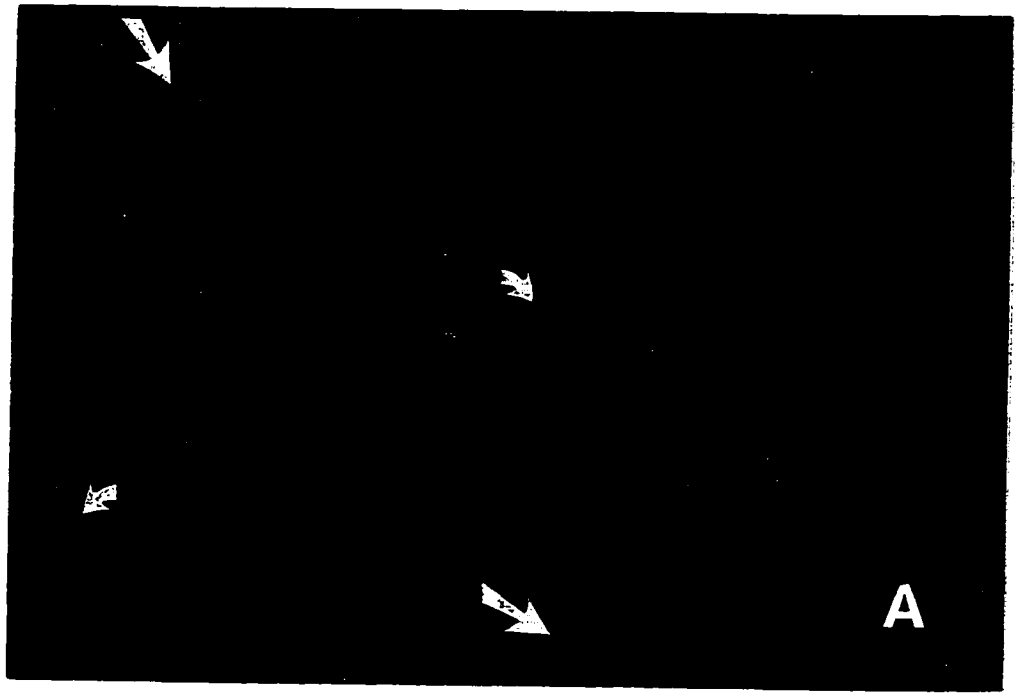

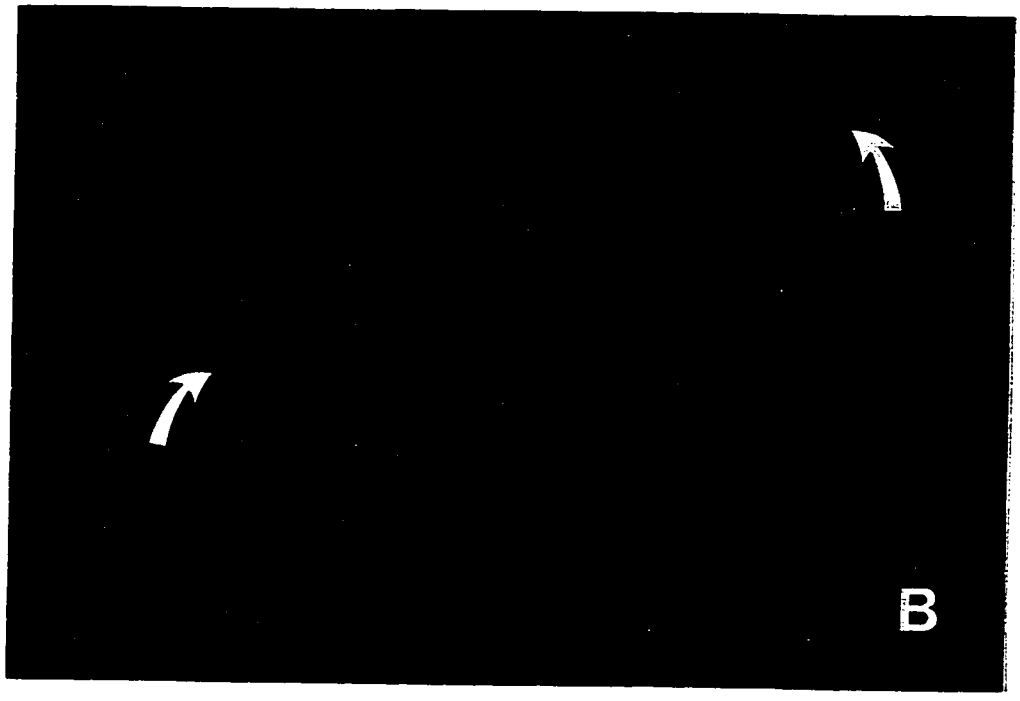

Figure 3-4 **Graph showing the apoptotic index (AI) and mitotic index (MI) of MN-11 tumors.** ■ and ▩, shows the respective AI or MI at the periphery; ▩ and ▧, shows the respective AI or MI in the core of the tumor. Tumors were excised on days 12, 14, 18 and 20 respectively, stained with H & E and the number of cells in mitosis and undergoing apoptosis were counted as described in section 3.2.3 (c). Data is represented as mean ± SEM of 4 tumors and in each case 10 fields were counted at the periphery and in the core of the tumor.

Figure 3-4

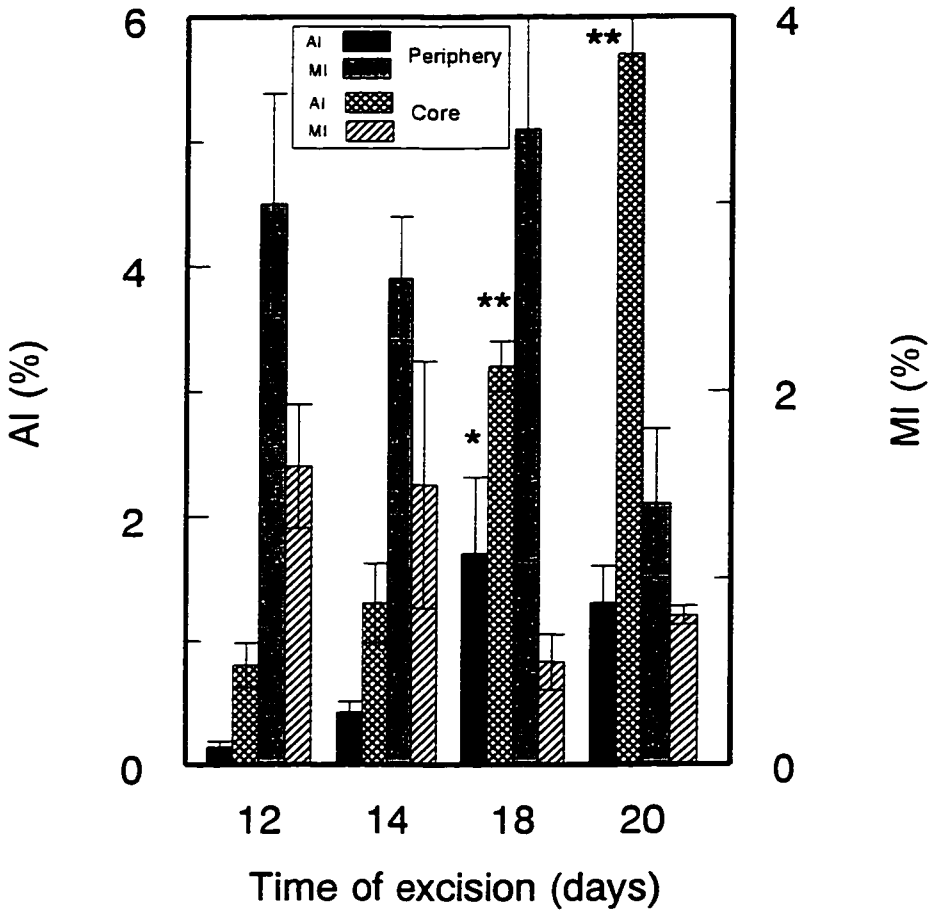
AI
MI
Periphery
AI
MI
Core
**
**
*
6
4
2
0
4
2
0
AI (%)
MI (%)
12
14
18
20
Time of excision (days)

a non-significant increase. However, the AI was significantly increased in the core ($p <$ 0.001 in an unpaired Student's *t*-test); the periphery showed a non-significant increase. Apoptotic cells occurred singly in young tumors but by day 18, they occurred as clusters of contiguous cells and by day 20, large zones of necrosis were observed. DNA extracted from day 14, 18 and 20 tumors was also analyzed by agarose gel electrophoresis for DNA fragmentation. The ladder pattern observed was not sharp and distinct, although it did show the presence of oligonucleosome size fragments and smearing, confirming coexistence of both apoptosis and necrosis (data not shown).

BLI was also examined as a function of the age of the tumor. Non-radioactive BrdU immunohistochemistry was used as a substitute for ^{3}H-thymidine autoradiography in localizing cells undergoing DNA synthesis (S-phase). DNA had to be denatured for easy antibody access; three methods of denaturation were tried. Intense BrdU nuclear labeling occurred following 4 N HCl denaturation in both tumor and small intestines, however, non-specific background staining was observed (data not shown). Following Bouin denaturation at 60°C for 60 min, nuclear labeling intensity was also strong; however, this was also accompanied by non-specific background staining (data not shown). In both cases, the background was greater over the cytoplasm than over the nucleus. Microwave heating resulted in markedly intense nuclear labeling of the tissues and the background staining in the tissues was eliminated (Figure 3-5A). It is important to note that a lower antibody dilution (1:100) was used for microwave treatment; higher dilutions (1:500 and 1:1000) produced weaker staining. However, the antibody was used at 1:1000 for the other two methods. Figure 3-5A shows that both lightly and darkly labeled nuclei were observed in the tumor sections, presumably because of completion or initiation of

Figure 3-5 **Detection of BrdU labeled cells in MN-11 tumors.** (A), Representative photomicrograph of MN-11 tumor labeled with BrdU and visualized by monoclonal anti-BrdU antibody. Labeled (S-phase) DNA appears brown, while non labeled DNA appears blue (counterstain haematoxylin, × 200). The large arrows point to darkly stained nuclei and small arrows point to lightly stained nuclei. The curved arrow points to a cell in metaphase. (B). Graph showing BrdU labeling index (BLI) of MN-11 tumors. Tumors were allowed to form and animals were injected with 30 mg/kg BrdU on days 15, 19 and 21, respectively. DNA was denatured using the microwave treatment and stained as described in section 3.2.3 (b). Labeled cells were detected using anti-BrdU antibody and scored microscopically as described in section 3.2.3 (c). Data is represented as mean ± SEM of 4-8 tumors and in each case 10 fields were counted at the periphery and in the core of the tumor.

Figure3-5

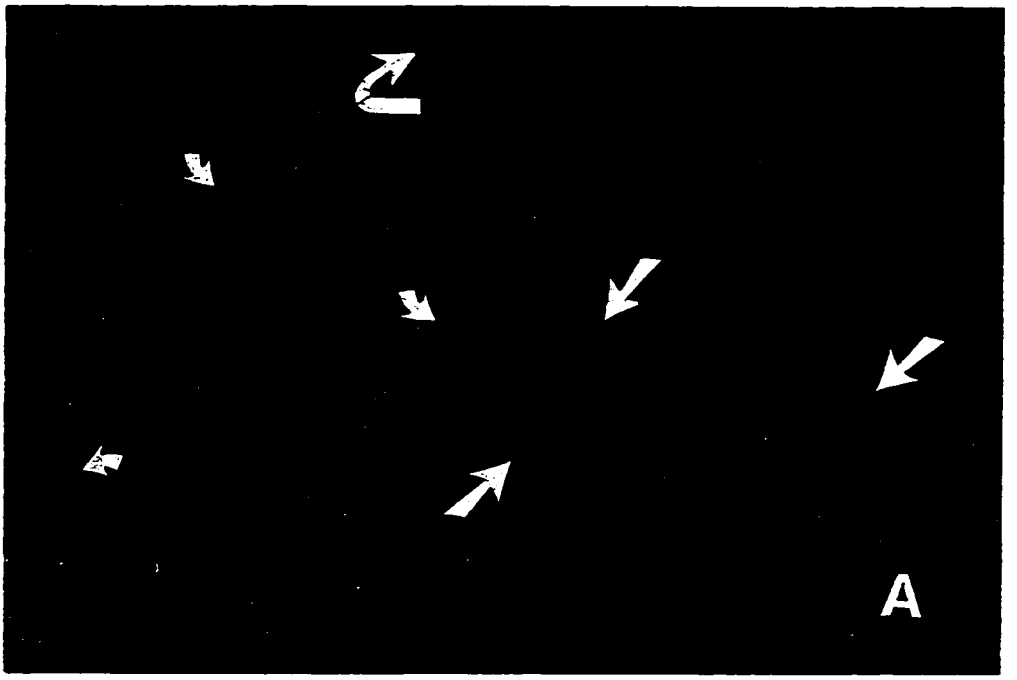

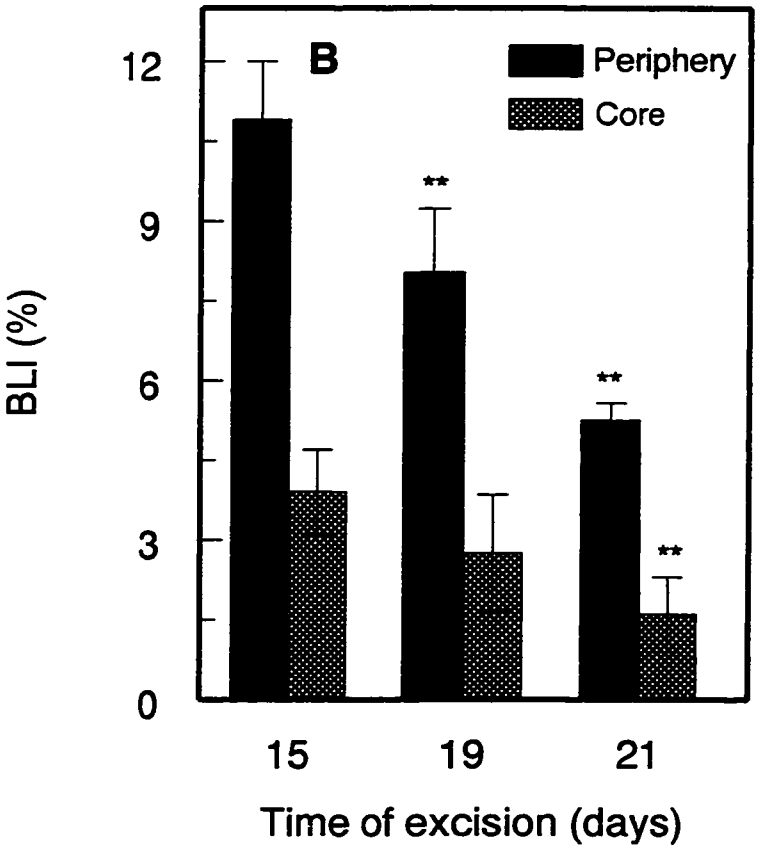

DNA synthesis during the labeling time.

The DNA was denatured with microwave treatment and stained as described above. The periphery and the core of the tumor were scored for the percentage of cells in the S-phase (BLI) (Figure 3-5B). The peripheral areas had a higher BLI than the core of the tumor. A statistically significant decrease in BLI in the peripheral area was observed after day 15 (ANOVA, Dunnett's test, $p < 0.01$). Similar results were obtained for the core of the tumor, showing statistically significant decrease for day 21 tumors (ANOVA, Dunnett's test, $p < 0.01$)

3.3.4 *Tumor Histopathology*

The exponentially growing tumors (day 11-day 16) are approximately 200 $\pm$ 50 mm^3 in volume, and are histologically described as fibrosarcomas with essentially no areas of necrosis (Figure 3-3A). Increased number of cells in mitosis are observed (showing cellular proliferation); an occasional cell in tripolar mitosis was also seen (data not shown). Tumor cells appear to have a high ratio of nucleus to cytoplasm, suggesting that the fibrosarcoma is poorly differentiated. A great variation in nuclear size between tumor cells and a greater variation in overall cell size is also observed. The tumors are very vascular (supplied with many blood vessels) accompanied by a peripheral nerve. The blood vessels occur more frequently at the periphery than the core of the tumor. In addition, formation of new blood vessels (angiogenesis) is seen at the periphery of the tumor (data not shown). These newly formed blood vessels are important to support the nutritional and respiratory needs of growing tumors. Tumor larger than 200 mm^3 in volume have an increase in the proportion of the tumor tissue that is necrotic. Blood

Figure 3-6 **Granulocytic infiltration in MN-11 tumors.** Representative photomicrographs depicting acute inflammatory response, characterized by increased infiltration with granulocytes. (A), Early vascular changes are evident as blood vessels filled with granulocytes (**G**), (H & E, × 400). Note, also in this illustration, the looseness and swelling of the connective tissue around the vessel. (B), Once out in the extravascular space, granulocytes are found mainly in the necrotic zones. They can be recognized by their lobed nuclei, disintegrating granulocytes are recognized by the condensation (pyknosis) or fragmentation (karyorrhexis) of their nuclei and cytoplasmic disintegration. The fibrin (**F**) is stained pink and is sparse in this micrograph (H & E, × 200).

Figure 3-6

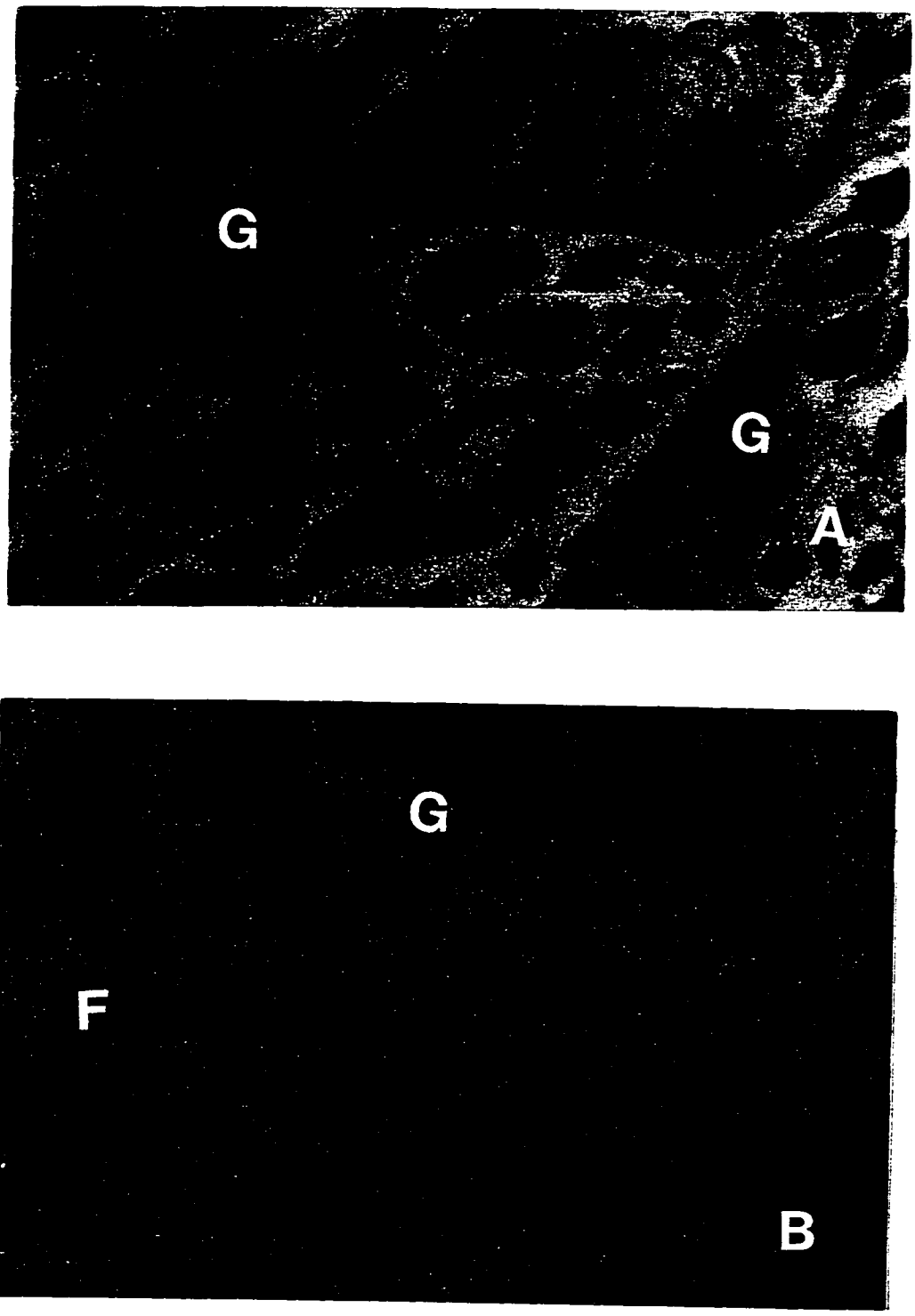

vessels become filled with granulocytes (Figure 3-6A). These white blood cells become adherent to the endothelium, this process is known as margination. They extravasate and seem to travel to areas of tissue damage; since necrotic areas show heavy infiltration of granulocytes (Figure 3-6B), with accompanying erythema and edema. Once the tumor develops necrosis, large acellular areas with very few tumor cells are observed. Necrotic areas may be next to large areas where tumor cells are perfectly maintained with no evidence of cellular death. Hence, the tumor mass represents an inflammatory lesion in which progressive tumor growth serves as a stimulus for phagocytic recruitment.

Invasion and metastasis: Tumors < 200 mm^3 are surrounded by an intact capsule (Figure 3-7A) composed of mainly collagen and fibroblasts. However, in tumors larger than 200 mm^3, tumor cells break through the capsule and can be seen invading the surrounding smooth muscle tissue (Figure 3-7B). No metastases have been observed in the organs (lungs, liver, kidneys and intestines) examined. Histopathological studies were carried out in collaboration with pathologists, Drs. Susan Robertson and George Wenckebach of the Anatomical Pathology Division, Ottawa General Hospital, Ottawa.

3.3.5 *Tumor infiltrating leukocytes*

To explore cellular sources of ROS and RNS that were postulated to contribute to the observed increase in MF, tumor tissue was analyzed histochemically for infiltrating inflammatory cells. Using H & E stained sections, the most abundant infiltrating cell type in MN-11 tumors was identified to be granulocytes. This cell type was confirmed by the presence of the endogenous peroxidase activity (brown precipitate by DAB reaction) in frozen sections (Figure 3-8A). Granulocytes were found mainly in the necrotic zones, less

Figure 3-7 **Invasiveness of MN-11 tumors.** (A), shows a tumor < 200 mm^3 with a well circumscribed fibrous capsule (**C**). Note that the tumor shows no evidence of local invasion (H & E, × 50). (B), shows a tumor > 200 mm^3. Note that the tumor has an irregular outline with arrows pointing to tumor cells invading the surrounding smooth muscle tissue (**SM**) of the flank.

Figure 3-7

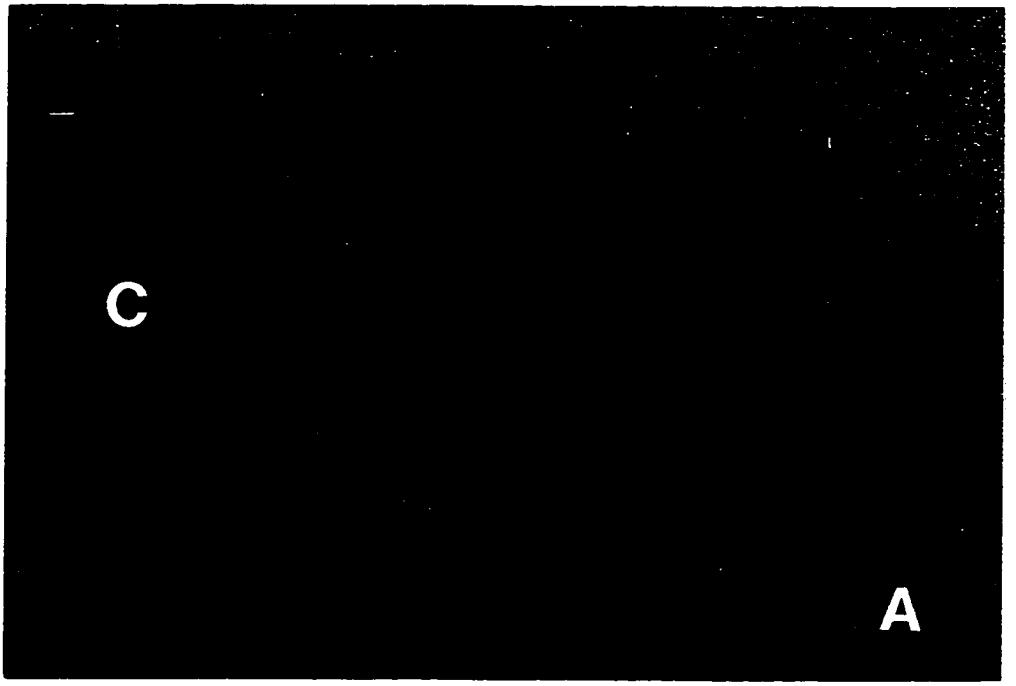

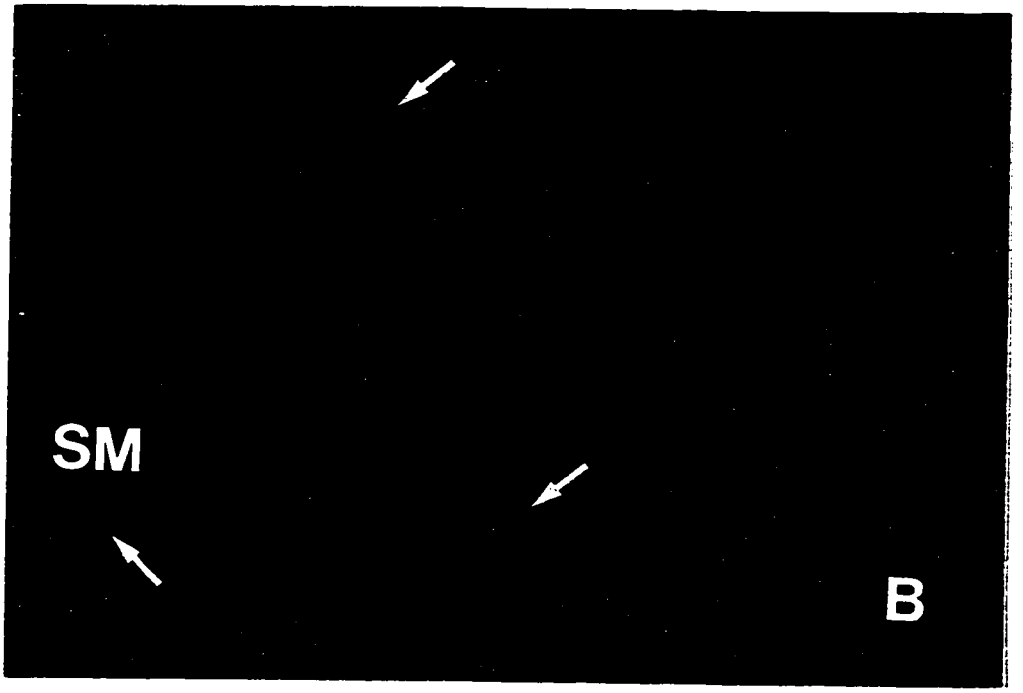

frequently in the non-necrotic, and at the periphery of the tumor. Both intact granulocytes and disintegrating granulocytes stain for the presence of the peroxidase activity. Positive staining of the macrophages was less frequent. Non-specific esterase activity identified the presence of macrophages only at the periphery of tumors (Figure 3-8B). However, in the core of older tumors (day 21), monocytes migrating from blood vessels were also observed, presumably to phagocytose dead tumor cells and granulocytes. Mast cells were seen, using toluidine blue stained sections, particularly at the periphery of the tumor (Figure 3-8C). Some tumors also showed the presence of lymphocytes toward the peripheral tumor mass on H & E stained sections (Figure 3-8D).

3.4 DISCUSSION

The MN-11 tumor model system was developed to explore the hypothesis that intratumor phagocytic cells such as macrophages and granulocytes may contribute to genomic instability and tumor progression by generating ROS and RNS. To improve our understanding the contribution of these factors the biology of the tumor was studied. MN-11 cells formed tumors rapidly in syngeneic animals; palpable tumors were observed by day 8 and by day 14 they were > 200 mm^3. 5×10^5 viable cells formed tumors in essentially 100% of the animals. MN-11 tumors grow with a tumor volume-doubling time of 2.7 days, reaching a plateau volume by day 18. However, tumor volume itself is a poor indicator of viable cell number, since tumors consist of a heterogeneous population of proliferating, nongrowing and dying cells. Therefore, MI, AI and BLI was used to study the dynamics of cell growth and death in this tumor.

Typically apoptosis affects scattered single cells in tumors, as in normal tissues,

Figure 3-8 **Characterization of tumor infiltrate.** Representative photomicrographs of different cell types identified in MN-11 tumors are shown. (A), endogenous peroxidase activity demonstrating the presence of granulocytes (counterstain haematoxylin, × 100). (B), Arrows point to nonspecific esterase activity detected in macrophages at the periphery of the tumor (counterstain haematoxylin, × 400). (C), Arrows point to toluidine blue stained mast cells toward the periphery of the tumor (counterstain haematoxylin, × 400). The characteristic feature of mast cells is an extensive cytoplasm packed with many granules. When stained with blue basic dyes such as toluidine blue, the granules bind to the dye changing its colour to red. This property is called *metachromasia*. (D), Section showing the presence of lymphoid cells, of which lymphocytes (L) are easily identified in the supporting connective tissue, (H & E, × 400).

Figure 3-8

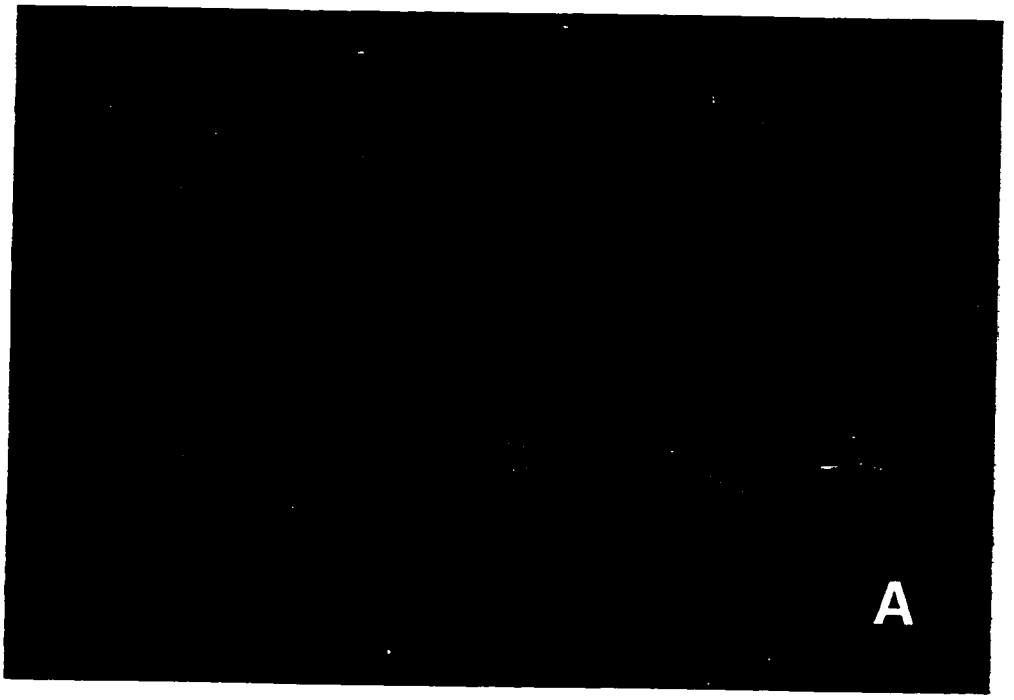

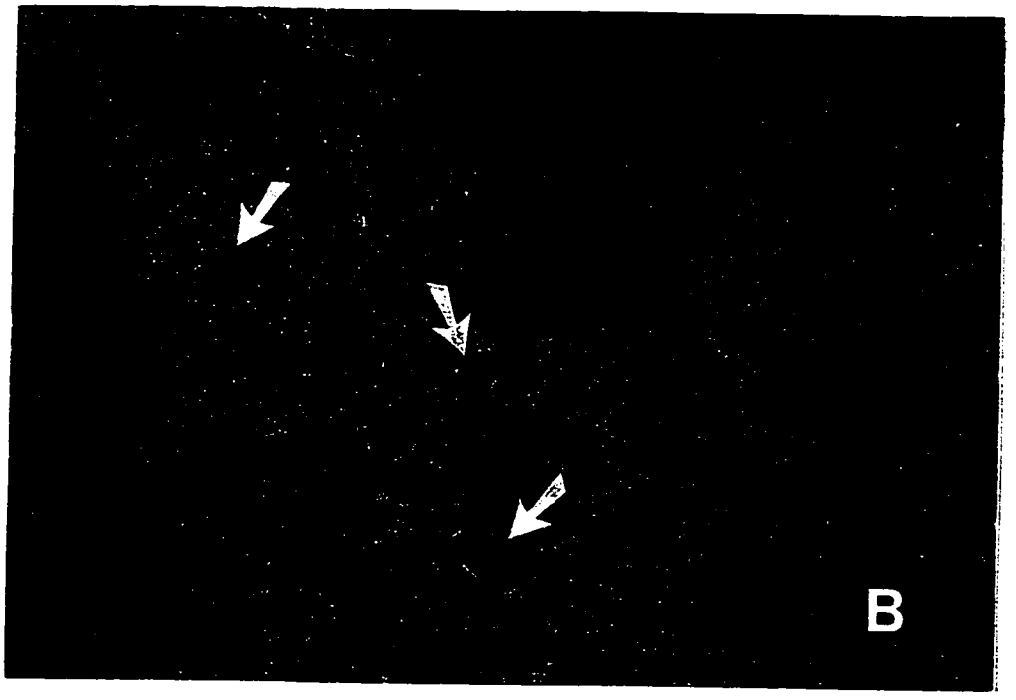

Figure 3-8

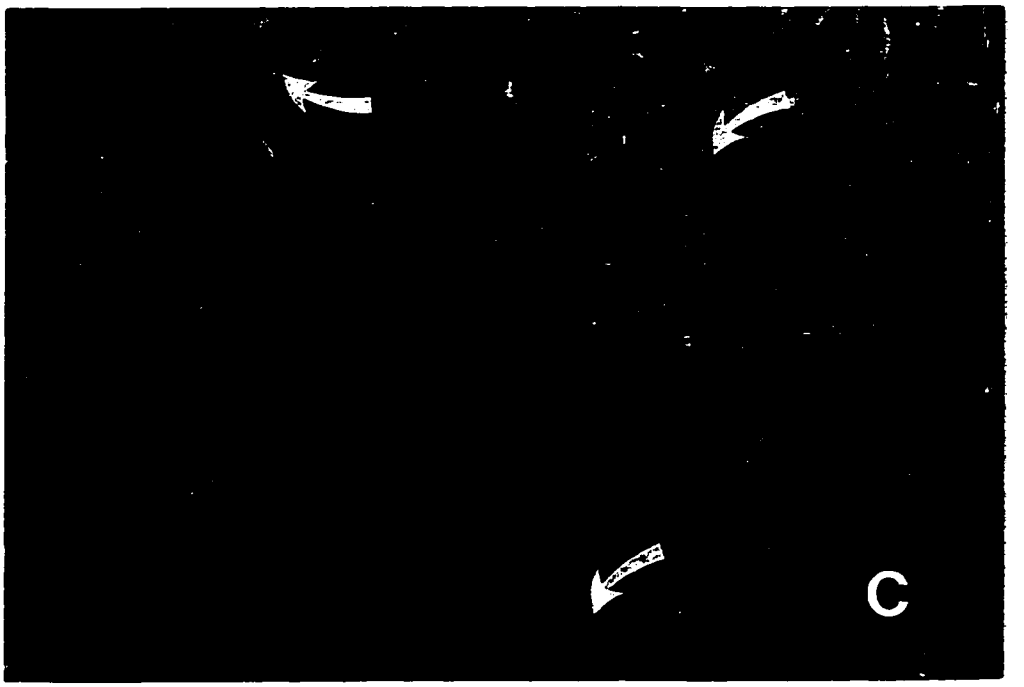

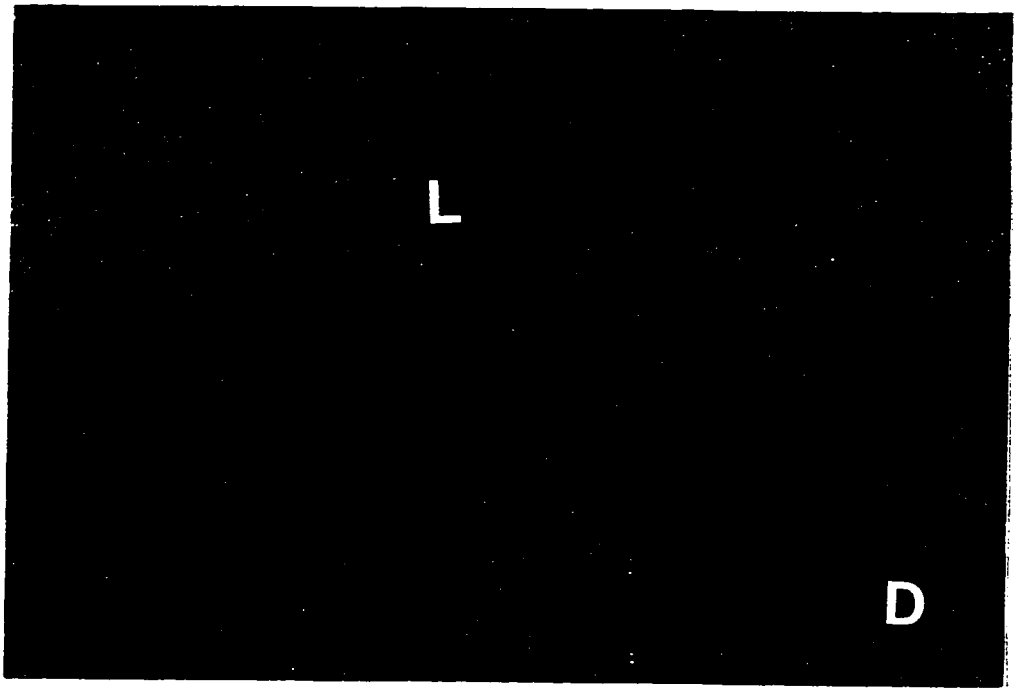

although in some tumors, especially with a high apoptotic rate, clusters of contiguous cells may be involved [251]. A cell undergoing apoptosis has a markedly shrunken nucleus and cytoplasm, irregularly beaded chromatin, deeply eosinophilic cytoplasm and are separated from adjacent tumor cells by a halo-like clear zone. Evaluation of apoptosis provides a useful measure of tumor cell kinetics and biologic behavior. In MN-11 tumors, AI increased with the age of the tumor and a more pronounced increase was observed in the core (Figure 3-4). By day 20, the AI was as high as 5.7% in the core of the tumor. Tumor histopathology also shows the presence of necrotic zones mainly in the core of the tumor. Agarose gel electrophoresis of tumor DNA is consistent with both forms of cell death in this tumor. Hypoxia (regions of low oxygen) and necrosis are common features of solid tumors. It is generally believed that, in fast growing tumors, the core of the tumor may be more hypoxic than the peripheral areas, since most of the blood vessels are found toward the periphery. It has been recently shown that *p*53 is induced in response to hypoxia [252,253] and *p*53 induction in turn is associated with apoptosis [254-256]. This implies that MN-11 cells may have wild type *p*53, although this warrants further investigation.

MI has long been used as a prognostic index in certain soft tissue tumors (especially leiomyosarcoma) and many solid tumors [251,257]. The central phases of mitosis, metaphase and anaphase were more easily recognized than cells in early prophase and late telophase. The number of mitotic figures was more frequent at the periphery than the core of the tumor. MI was greater than AI in tumors excised on days 12 and 14 both at the periphery and in the core, although a statistically non-significant decrease was observed with the age of the tumor. As an index of cell proliferation, mitotic figure counting is the

easiest method. However, it is only a crude reflection of the growth fraction.

A complementary approach for the measurement of tumor cell kinetics is the determination of the proportion of the tumor cell population in the S-phase of the cell cycle. Labeling of S-phase cells with BrdU has previously been used as a substitute for *in vivo* ^{3}H-thymidine labeling [258]. The DNA of S-phase tumor cells was labeled by a 2 h administration of an i.p. dose of BrdU to tumor-bearing mice. BrdU is incorporated into the DNA and detected using a mouse monoclonal anti-BrdU antibody. Localization of BrdU in fixed tissues requires that DNA be denatured to single strands capable of being recognized by antibodies. Three methods of denaturation were tried of which microwave treatment for 10 min worked the best (Figure 3-5A). It reduced the non-specific background staining found when mouse a monoclonal antibody is used on mouse tissues. Another study reported similar findings using mouse tissues, however, they had used a 1:50 dilution of the antibody with a 5 min microwave treatment [259]. The mechanism by which microwave treatment works is unclear, but it is possible that it removes proteins from DNA and allows better physical access of the antibody to the antigen.

A 50% reduction in the BLI was observed in day 21 as compared with day 15 tumors, both at the periphery and in the core (Figure 3-5B). The increase in AI and necrosis and decrease in MI and BLI explains the lower cloning efficiency observed in older tumors. Most of the MF experiments were conducted using young tumors (days 14 and 15). As expected from the cell cycle, BLI in the tumors was generally greater than MI. One possible explanation why BLI exceeds MI is that mitosis is completed more rapidly than DNA synthesis. The *in vitro* doubling time of MN-11 cells is 16 h (Chapter 2). A 2 h labeling time used *in vivo* should have labeled most of the cells in S-phase. If

the S-phase is assumed to be 8 h, any cell whose doubling time is 8 h or more would have been labeled. Cells in the S-phase or beginning to enter the S-phase would be detected as darkly stained nuclei. The weakest signal (lightly stained nuclei) detected would be at the G_1-S and at the S-G_2 junction. The probability of a cell being missed is if at the time of labeling it is in the G_1 or G_2 phase. As per the above model the probability of detecting cells in S-phase should be 8 times more sensitive than counting cells in mitosis. However, comparison of the BLI and MI (Figures 3-4 & 3-5) shows that our ability to count S-phase cells is lower because some cells may not have been labeled and are missed during counting. This could be due to technical problems. Although one can determine the fraction of cells that are cycling but none of the methodologies provides estimates of the growth rate of cells *in vivo*. Making a precise estimate of growth rate of cells *in vivo* is difficult, since tumors contain a mixture of growing, non-growing and dying cells.

Most solid tumors contain inflammatory cell infiltrates [54,195,197,260-267]. MN-11 tumors are also characterized by increased infiltration with inflammatory cells consisting primarily of granulocytes followed by macrophages, mast cells and lymphocytes (Figure 3-7). It is well known that granulocytes are recruited at the sites of inflammation by a variety of chemotactic agonists elaborated by intrinsic tissue cells and leukocytes. This activates them in the blood vessels and induces their migration across the vessel wall into the extra-vascular space. Four classes of agonists have been identified, which includes C5a, FMLP, leukotriene B_4 (LTB_4) and PAF. Recent studies have demonstrated other polypeptide mediators (chemotactic cytokines), are also synthesized during inflammation that elicit massive and long-lasting granulocytic infiltration. These chemotactic cytokines include neutrophil activating peptide (NAP-1), interleukin-8 (IL-8),

monocyte chemoattractant protein 1 (MCP-1), macrophage inflammatory protein 2 (MIP-2), G-CSF (granulocyte colony-stimulating factor), and MGSA (melanoma growth-stimulatory activity) [268-272]. A malignant fibrous histiocytoma cell line has been shown to promote granulocytic chemotaxis and to express mRNA for the cytokines, GM-CSF (granulocyte-macrophage colony stimulating factor) and IL-8 [273]. It may be possible that MN-11 cells may produce chemotactic cytokines that may attract granulocytes to the tumor tissue. The presence of lymphocytes and mast cells in this tumor also suggests that these cells may release a large repertoire of cytokines with granulocyte chemoattractant properties. The cytokines produced within the tumor microenvironment that attracts phagocytic cells have not yet been tested in MN-11 cells and warrants further investigation. This would help to understand the factors in the tumor microenvironment that could be further manipulated to increase granulocytes.

There is considerable evidence for the presence of hypoxia in human and experimental tumors. MN-11 tumors show zones of necrosis mainly in the core accompanied by heavy granulocytic infiltration. This may be due to the presence of hypoxia in these tumors. The possibility that necrosis may produce chemotactic factors that may attract granulocytes to these sites cannot be excluded. The presence of the inflammatory infiltrate within and adjacent to the tumor mass suggests an on-going "inflammatory" reaction. Whether these infiltrates result simply from a response of the host to the tumor or from an active part of the tumor ecosystem is uncertain.

CHAPTER 4

MUTAGENICITY AND CYTOTOXICITY OF REACTIVE OXYGEN AND NITROGEN SPECIES IN MN-11 CELLS

ABSTRACT

There is increasing evidence that endogenously generated ROS and RNS at sites of inflammation and in tumors may be genotoxic. This chapter describes an *in vitro* study of the ability of ROS and RNS to induce mutations in MN-11 cells. Radiation and radiomimetic drugs were used as positive controls; they caused a dose-dependent increase in MF. At D_0, streptonigrin and bleomycin induced about 50 and 95 mutants per 10^5 viable cells, respectively. ROS (H_2O_2) induced a lower frequency of mutants, 20-30 per 10^5, for enzymatically generated or bolus, respectively. Incubation with human granulocytes induced a low frequency of mutants (about 15 per 10^5 at 50% survival). RNS was tested using a series of NO-donating drugs. MF at 50% survival is shown. Spermine/NO· induced cytotoxicity but no mutants, while *S*-nitroso-*N*-acetylpenicillamine induced a low level, 10 per 10^5. Both release nitrogen monoxide spontaneously, with a $t_{1/2}$ <3 h. Glyceryl trinitrate and sodium nitroprusside are two drugs that were slowly metabolized by MN-11 cells (>12 h) to release nitrogen monoxide. Glyceryl trinitrate induced about 20 per 10^5 while nitroprusside induced 50 per 10^5. Our results indicate that RNS can induce mutations readily detectable in MN-11 cells. At equicytotoxic doses, the MF varied considerably for different drugs, suggesting that different states of nitrogen monoxide (such as NO^- or NO·) may be generated and these may vary in their mutagenic/cytotoxic potential. These data support the notion that ROS and/or RNS in tumors may be mutagenic and thereby contribute to genetic instability of tumors.

4.1 INTRODUCTION

The ability to detect mutations in mammalian cells can vary considerably depending upon

the locus studied [227,228,232,274]. Most detection systems utilize a single-copy (hemizygous or heterozygous) gene, whose inactivation by a mutagen causes a detectable phenotype. This requires either creating a heterozygous gene on an autosome, such as *TK*$^{-/-}$, or using a hemizygous gene on the X chromosome, such as *HPRT*. (In females, one copy of the X chromosome is inactive, creating a functionally hemizygous state). While both systems allow detection of small-scale events such as small deletions, transitions or transversions, a disadvantage of using the *HPRT* locus is that some large scale, multi-locus deletion mutants may be non-viable. It is believed that concomitant loss of a fragment of the chromosome that extends into neighbouring essential genes is responsible for the observed low recovery of this class of mutants in murine L5178Y cells [227]. MN-11 is a murine tumor cell line that uses the *HPRT* locus for detecting mutants but overcomes the limitations of a hemizygous system [1]. This cell contains multiple copies of the X chromosome but only one functional *HPRT* locus, that is, it is a heterozygous (*HPRT*$^{-/-/-}$) locus. MN-11 cells were used to study mutations induced by ROS and RNS.

ROS and RNS may be generated at high concentrations by activated phagocytes and other cells at sites of inflammation and within tumors [45,195,275]. These species have been shown to be genotoxic in a variety of cell types and mutagenic at several different loci. ROS generated chemically, enzymatically or by phagocytes were mutagenic in *Salmonella typhimurium* and produced sister chromatid exchanges, transformation and mutations at the *HPRT* locus in mammalian cells [70-74]. In V79 cells, high concentrations of H_2O_2 induced mutations at the *HPRT* locus but lower concentrations did not [77,78]. Using a hemizygous bacterial *GPT* transgene introduced onto an autosome in CHO cells, Hsie et al. [79,80] were able to detect mutants following exposure to ROS. NO· and related species have also been

examined for their mutagenic potential. NO· and NO_2 gases and GTN were mutagenic in *S. typhimurium* [178]. In rat lung cells, exposure *in vivo* to these gases could induce mutants and NO_2 could induce chromosomal aberrations [62]. High concentrations of NO· gas induced DNA strand breaks and mutations at both the *HPRT* and *TK* locus in TK6 human lymphoblasts [158]. High concentrations of NO· gas can also cause chemical changes in free DNA. Saturated solutions of NO· deaminate deoxyribonucleosides, nucleotides, purines and calf thymus DNA [157,158]. Exposure of naked plasmid DNA to NO· gas or $ONOO^-$, followed by transfection into human Ad293 cells or *Escherichia coli*, also resulted in deaminations [176,177]. $ONOO^-$ was shown to produce DNA strand breaks in rat thymocytes [161]. A variety of drugs that can spontaneously or metabolically generate NO· have also been tested for their mutagenicity in various biological systems. Felley-Bosco et al. [180] failed to show mutant induction at the *HPRT* locus in human epithelial cells by DEA/NO·, a spontaneous generator of NO·. Spermine/NO· and DEA/NO· were strongly mutagenic in *S. typhimurium* while GTN and sodium nitrite ($NaNO_2$) were weakly mutagenic [157,179]. Thus, a variety of evidence indicates that ROS as well as RNS may be genotoxic and mutagenic. This chapter shows that radiomimetic drugs, hydrogen peroxide and some but not all NO-donating drugs can induce mutants in MN-11 cells.

4.2 MATERIALS AND METHODS

A listing of the materials, chemicals suppliers and solution compositions is found in Appendix II.

4.2.1 *Cells and culture conditions*

Peripheral blood polymorphonuclear cells were isolated from freshly drawn blood

of normal human donors as previously described [276], except that sterile solutions and procedures were employed. MN-11 cells were grown in non-selective medium, HAT-medium, HT-medium or 6-TG-medium as defined previously (Appendix IV, section IV.1).

4.2.2 *Cytotoxicity and Mutagenicity of ROS and RNS Treatments*

Exponentially growing cultures were trypsinized and 5×10^5 cells (as determined by trypan blue exclusion) per 10 cm dish were allowed to attach overnight. The cultures were subjected to one of the following treatments in serum-free medium unless otherwise indicated (concentrations are shown in the figures): H_2O_2 and glucose oxidase for 1 h; Fe(III)-bleomycin complex for 1 h and streptonigrin for 6 h; NO-donating drugs were added for 24 h in non-selective complete medium. In co-culture experiments, MN-11 cells were incubated for 24 h in non-selective medium with either TPA (2×10^{-8} or 2×10^{-7} M) alone, or with granulocytes in the presence of TPA or vehicle (0.1% dimethyl sulfoxide). After the indicated treatments, cytotoxicity and MF was determined. Cultures were washed twice with PBS, trypsinized and split into two sets of dishes. For determination of cytotoxicity, 200 cells/6 cm dish were seeded in non-selective medium (up to 600 cells where low survival was expected). After 7 days, colonies (> 50 cells) were scored. Following all treatments described, MF was determined by plating 5 to 10×10^5 cells/10 cm dish in non-selective medium and an 8 day expression time was used. Cells were subcultured as needed to maintain them in log phase of growth, keeping at least 5×10^5 cells at each transfer. Mutant cells were detected by plating 1×10^5 cells per 10 cm dish in the presence of 50 μM 6-TG. Cloning efficiency was determined by seeding 200 cells/6 cm dish. 6-TG-resistant colonies (>50 cells) were scored after 10 days. MF is expressed as mutants per 1×10^5 viable cells,

where viability was determined from the cloning efficiency.

4.2.3 *Species generated by SNP and GTN*

To assess the effect of cyanide released by SNP, a cyanide scavenging system (8 units/mL of rhodanese + 5 mM $Na_2S_2O_3$) was added [277] to 5×10^5 cells. The contribution of H_2O_2 or $O_2^{\cdot-}$ to the effects seen with SNP and GTN was assessed by inclusion of catalase (50 μg/mL) or SOD (50 μg/mL) at the time of treatment. To verify that effects of SNP were due to NO·, oxyhaemoglobin (oxyHb; HbO_2) was used as a specific scavenger. 5×10^5 cells were plated in 10 cm dishes and allowed to attach overnight; cultures were treated with SNP in the presence of 100 μM oxyHb. Following incubation at 37°C for 24 h, cultures were washed twice with PBS; cytotoxicity and MF was determined. The production of NO· in cultures treated with SNP was monitored by the spectral conversion of oxyHb to methaemoglobin (metHb) using a Perkin-Elmer (Lambda 14) UV/VIS spectrometer at 350-700 nm.

4.2.4 *Preparation of OxyHb*

OxyHb may contain some metHb. Pure oxyHb was prepared by treating 1.0 mM solution with small amounts of dithionite ($Na_2S_2O_4$) until the solution turned blue. Oxygen was then gently bubbled through the solution until it turned bright red colour. Excess dithionite was removed by dialysis against PBS at 4°C. The concentration and purity of the oxyHb solution was determined spectrophotometrically (λ_{max} = 576 nm, 541nm; ϵ = 14,600, 13,800) [278].

4.2.5 *Measurement of nitrite*

Nitrite (NO_2^-) is a fairly stable product of more reactive nitrogen intermediates that

can be readily measured chemically. To quantify the amount of NO released by various drugs, the amount of NO_2^- which accumulated in the culture medium was measured. Replicate cultures of 2×10^5 cells in 1 mL of phenol red-free non-selective medium were established in 24 well plates. Different NO-donating drugs were added. Every 2 h, the cell supernatant was removed and mixed with an equal volume of Griess reagent [279]. Griess reagent is prepared by mixing equal volumes of 0.1% *N*-(1-napthyl)-ethylenediamine dihydrochloride in water and 1% sulphanilamide in 5.0% H_3PO_4 immediately before use. Ten min after addition of Griess reagent, absorbance at 540 nm was measured. The concentration of NO_2^- was calculated from a standard curve using $NaNO_2$.

4.2.6 *Statistical analysis*

Data were analyzed using one-way factorial ANOVA or Student's *t*-test, as applicable. Following detection of a statistically significant *F* value, *post hoc* Dunnett's *t*-test of significance was used. A value of $p \leq 0.05$ was considered to be significant. A statistically significant result is indicated by * ($p \leq 0.05$) or ** ($p \leq 0.01$).

4.3 RESULTS

4.3.1 *Radiomimetic drugs*

Certain drugs are considered to be radiation-like in their mode of action. These so-called radiomimetic drugs generate ROS such as OH· [280] and were expected to be mutagenic in the MN-11 system. The effects of streptonigrin (Figure 4-1A) and bleomycin (Figure 4-1B) on cytotoxicity and mutant induction were studied. In contrast to ^{137}Cs and ^{60}Co γ-irradiation, both drugs generated survival curves without detectable shoulders. The

Figure 4-1 **The effects of radiomimetic drugs cytotoxicity and mutagenicity on MN-11 cells.** (A), Streptonigrin (nM); (B), Fe (III) bleomycin complex (μM). Cytotoxic (●) and mutagenic (○) effects are shown. Cultures were exposed to Streptonigrin for 6 h and Fe (III) bleomycin complex for 1 h in serum free medium at 37°C. Following each treatment, cultures were washed with PBS, cytotoxicity and mutagenicity determined as described in Materials and Methods. Mean absolute cloning efficiency of untreated cultures was 51 ± 1.7% for (A) and 40 ± 9.9% for (B). Error bars indicate mean ± SEM (n = 2-5 independent experiments, each involving 4-6 replicate dishes per experimental point).

Figure 4-1

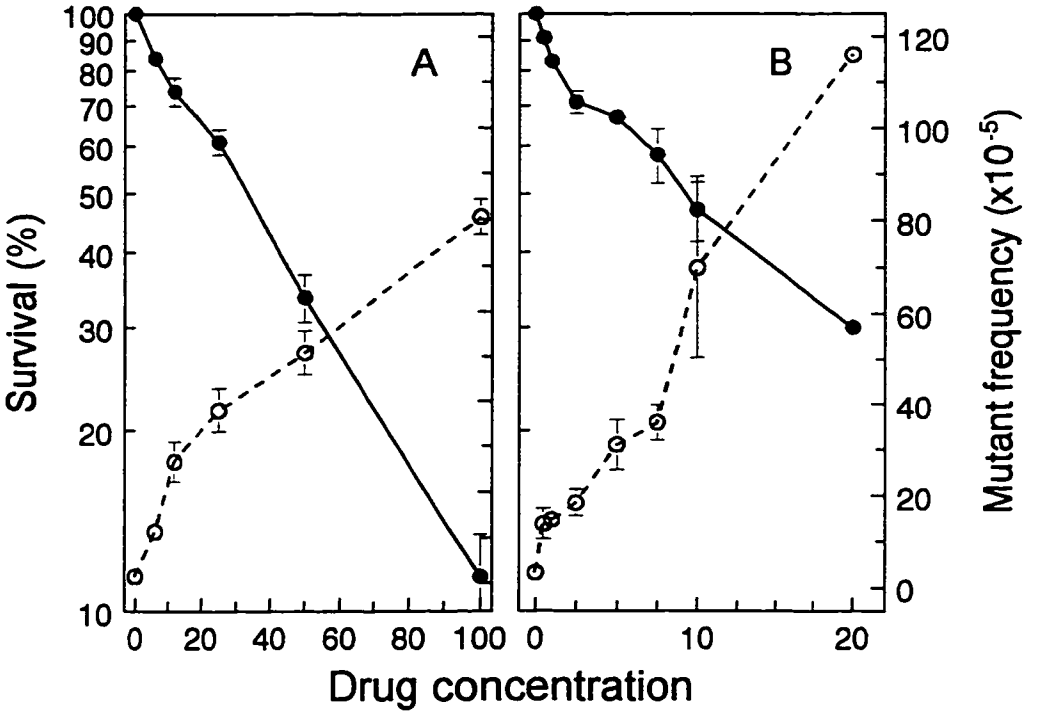
A
B
Survival (%)
Mutant frequency (x10-5)
Drug concentration
100
90
80
70
60
50
40
30
20
10
0
20
40
60
80
100
120
10

D_0 dose was 46 nM and 16 μM for streptonigrin and bleomycin, respectively. At D_0, the number of mutants induced by streptonigrin and bleomycin was about 50 and 95 per 10^5 cells, respectively.

4.3.2 *Hydrogen peroxide*

H_2O_2 is a relatively weak mutagen that is known to cause DNA strand breaks in cells [78]. To test its effect as a mutagen in MN-11 cells, H_2O_2 was added either as a bolus (Figure 4-2A) or generated enzymatically with glucose oxidase (Figure 4-2B) for 1 h in serum-free medium. In both cases, survival curves showed no detectable shoulder. The D_0 for H_2O_2 added as a bolus was 122 μM and generated enzymatically was 57 mU/mL. At these doses, the number of mutants induced were significantly lower (20 to 30 per 10^5 cells) than radiation or radiomimetic drugs. In both cases, a dose-dependent increase in MF was observed.

4.3.3 *Human granulocytes*

Human granulocytes elaborate ROS, which have been shown to cause mutations in bacteria [71] and mammalian cells [72]. Figure 4-3 shows the effects of unstimulated and TPA-stimulated granulocytes on cytotoxicity and mutation induction in MN-11 cells. Increasing numbers of unstimulated granulocytes (from 5 to 20 × 10^6 cells per 5 × 10^5 MN-11 cells) caused a progressive decrease in cloning efficiency of MN-11 cells with a maximum increase in MF of about 20 per 10^5. At 50% survival, the MF was about 15 per 10^5 cells, compared to the control (no granulocytes) of 3 per 10^5 cells. TPA was used to stimulate the respiratory burst of granulocytes, with the expectation of an increase in cytotoxicity and mutagenicity [281]. TPA at 2 × 10^{-7} M, in the absence of granulocytes, resulted in statistically significant cytotoxicity (survival of 39.9 ± 4.4%; n = 4; 2 tailed $p <$

Figure 4-2 **The effects of hydrogen peroxide on MN-11 cells.** (A), Bolus (μM); (B), Glucose oxidase (milliunits/mL). Cytotoxic (●) and mutagenic (○) effects are shown. Cultures were exposed to hydrogen peroxide (bolus) or generated enzymatically using glucose oxidase (flux) for 1 h in serum free medium at 37°C. Following each treatment, cultures were washed with PBS, cytotoxicity and mutagenicity determined as described in Materials and Methods. Mean absolute cloning efficiency of untreated cultures was 35 ± 11.5% for (A) and 37 ± 12% for (B). Error bars indicate mean ± SEM (n = 3-4 independent experiments, each involving 5-6 replicate dishes per experimental point).

Figure 4-2

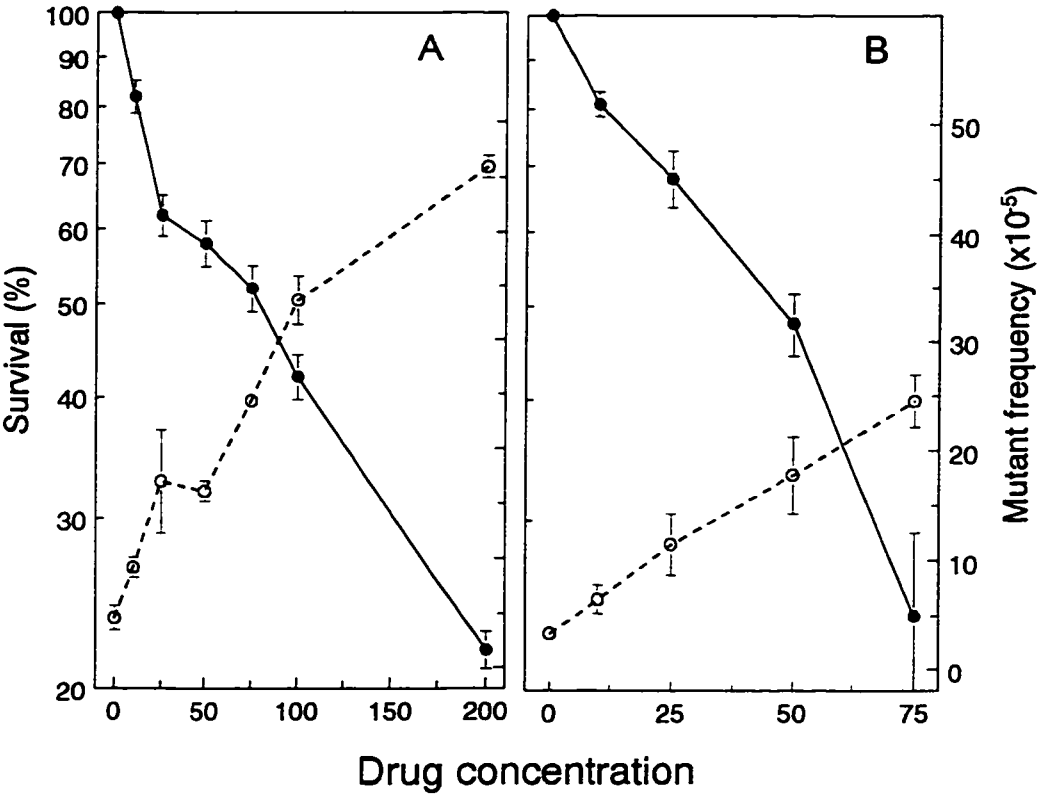
A
B
Survival (%)
Mutant frequency (x10^{-5})
Drug concentration
100
90
80
70
60
50
40
30
20
0
50
100
150
200
0
25
50
75
50
40
30
20
10
0

Figure 4-3 **Cytotoxic and mutagenic effects of human granulocytes, in the absence or presence of TPA.** Following treatment for 24 h (in the presence (▲, Δ), or absence (●, ○) of TPA), cultures were washed with PBS, cytotoxicity (●, ▲) and mutagenicity(○, Δ) determined. Mean absolute cloning efficiency of untreated cultures was 37 ± 11%. Error bars indicate mean ± range (n = 2 independent experiments, each involving 5-8 replicate dishes per experimental point) (n=4 for TPA with no granulocytes). Granulocyte concentration (as indicated, $\times 10^6$ per dish); target MN-11 cells (5×10^5 per dish). Treatment with vehicle (0.1% (v/v) dimethyl sulfoxide) had no cytotoxic or mutagenic effect (data not shown).

Figure 4-3

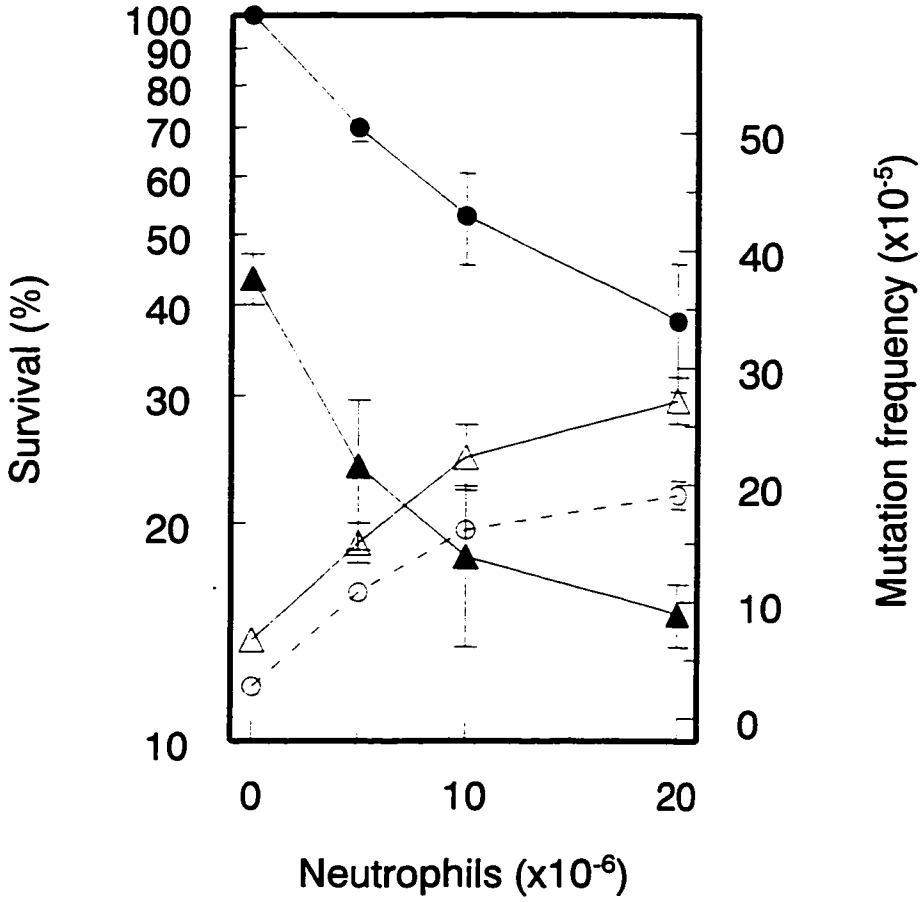
100
90
80
70
60
50
40
30
20
10
Survival (%)
50
40
30
20
10
0
Mutation frequency (x10-5)
0
10
20
Neutrophils (x10-6)

0.03). There was also a small increase in MF ($p < 0.05$ in a paired t-test). At a concentration of 2×10^{-8} M, TPA also caused a low level of cytotoxicity (survival of 76.5 ± 1.5%; n = 2) but no detectable change in MF. The combination of TPA and granulocytes was not significantly more cytotoxic than the sum of each individually. That is, the products of the respiratory burst activated by TPA appeared to have little additional cytotoxicity. Similarly, only a small increase in MF could be attributable to the respiratory burst.

4.3.4 *NO-donating drugs*

RNS have previously been shown to have a variety of genotoxic effects. Their cytotoxic and mutagenic potentials for MN-11 cells were tested by exposing cells to a variety of NO-donating drugs. SPER/NO· and SNAP are known to release NO· spontaneously, that is, without a requirement for cellular metabolism. SPER/NO· caused a dose-dependent decrease in cell viability with increasing drug concentration, but no detectable increase in MF in the dose range tested (Figure 4-4A). Spermine, the polyamine decomposition product of SPER/NO·, caused no cytotoxicity at concentrations up to 1 mM (data not shown). SNAP was also cytotoxic, but in contrast with SPER/NO· a statistically significant increase (ANOVA, *post hoc* Dunnett's t-test, $p < 0.05$) in the MF was observed (about 10 mutants per 10^5 cells above controls at 50% survival, Figure 4-4B).

GTN and SNP are two clinically useful smooth muscle relaxing drugs that yield a nitrogen monoxide species after metabolic activation [282,283]. GTN caused a dose-dependent decrease in cell viability together with a clear increase in MF (Figure 4-4C). At 50% survival, about 20 mutants per 10^5 cells were induced. The survival curve of SNP was similar to GTN. However, the MF at 50% survival was appreciably higher, over 50 mutants

Figure 4-4 **The effects of nitric oxide-donating drugs on MN-11 cells. (A), SPER/NO· ; (B), SNAP ; (C), GTN ; (D), SNP.** Cytotoxic (●) and mutagenic effects (○) are shown. Cultures were exposed to the respective nitric oxide-donating drug for 24 h in complete medium at 37°C. Following each treatment, cultures were washed with PBS, cytotoxicity and mutagenicity determined. Mean absolute cloning efficiency of untreated cultures for A, B, C and D was 30.5 ± 12%, 38.3 ± 2.5%, 39.8 ± 0.3 and 39 ± 6.6%, respectively. For A and B, data shown are mean± range (n = 2 independent experiments, each involving 3-8 replicate dishes per experimental point). For C and D, data shown are mean ± SEM (n = 3-6 and n = 3-5, respectively). Drug concentrations are shown in mM.

Figure 4-4

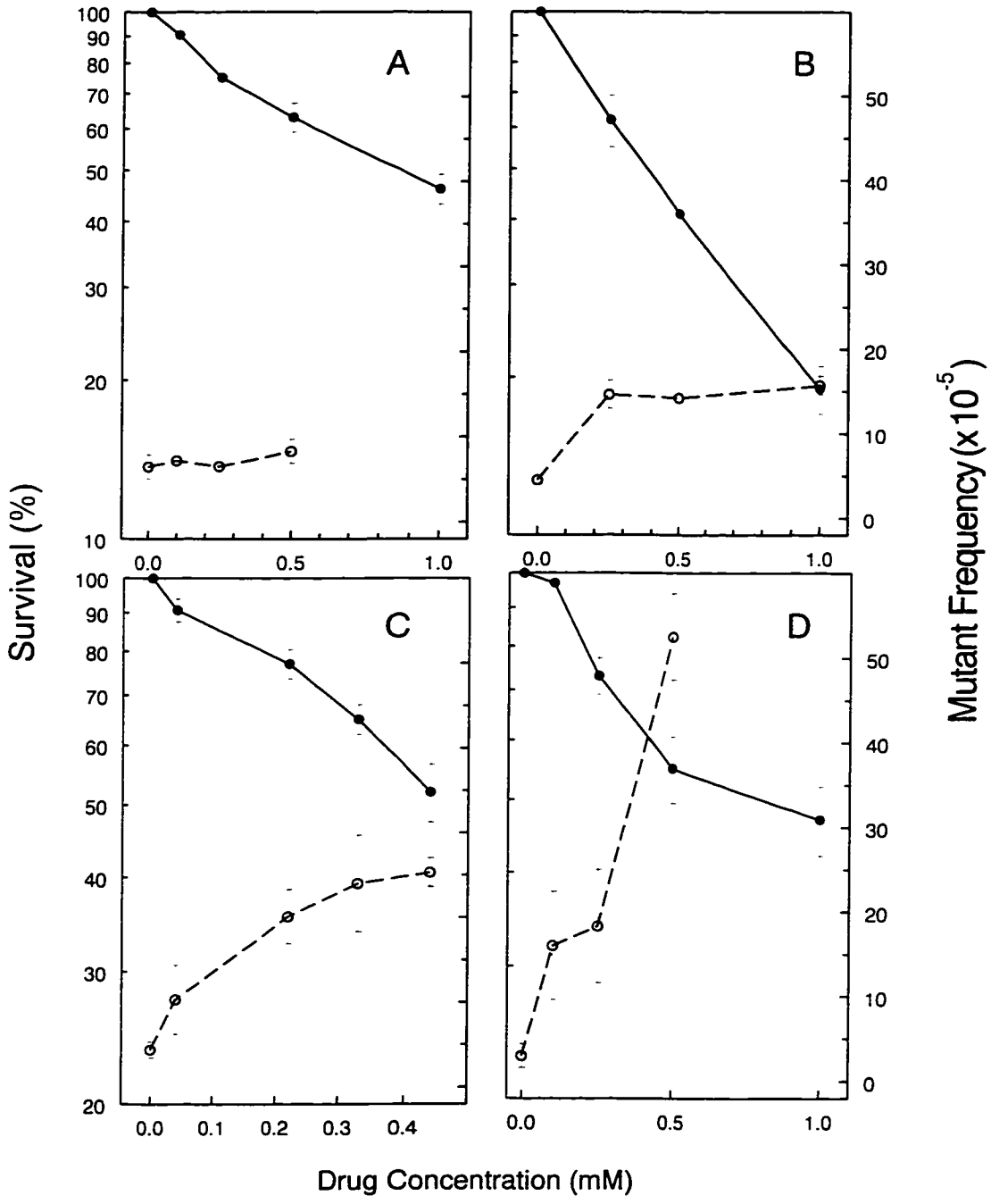
A
B
C
D
Survival (%)
Mutant Frequency (x10^{-5})
Drug Concentration (mM)
100
90
80
70
60
50
40
30
20
10
0
0.0
0.1
0.2
0.3
0.4
0.5
1.0

per 10^5 cells (Figure 4-4D). When cells were exposed to the same 2 drugs for 6 hours instead of 24 hours, no detectable increase in MF was observed, although a low level cytotoxicity was observed (data not shown).

Molsidomine (MOL) (1-10 mM) and persidomine (25-200 μg/mL), which require cellular metabolism to release NO· [284,285] were found to exert no cytotoxic or mutagenic effect in MN-11 cells (Table 4-1).

The effect of caffeine (a known repair inhibitor) was also investigated on GTN induced cytotoxicity and mutagenicity. As previously shown (Chapter 2, section 2.3.5) caffeine was not itself a significant mutagen. GTN (0.44 mM) was cytotoxic (54% survival), a further decrease (non-significant) in survival was observed in the presence of caffeine. GTN induced about 15 mutants per 10^5 cells, a slight non-significant increase (2 tailed $p = 0.2961$) in MF was observed in the presence of caffeine (Figure 4-5). Thus, caffeine does not appear to alter the cytotoxicity or mutagenicity associated with GTN. To rule out the possibility that caffeine may have altered the growth of MN-11 cells, the growth rate was determined by seeding 2×10^4 cells (as described in Chapter 2, section 2.2.9). No differences were found in the doubling times of cells with (16.4 h) or without (16.6 h) caffeine.

4.3.5 *Nitrite accumulation in response to NO-donating drugs*

The different NO-donating drugs tested produced similar cytotoxicity (at equivalent concentrations) but very different mutagenicity. As an indicator of NO production, the amount of NO_2^- produced when MN-11 cells were incubated in the presence of these drugs was determined. NO species gives rise primarily to NO_2^- and not nitrate in aqueous solution [286]. As shown in Figure 4-6, incubation of 2×10^5 MN-11 cells with GTN or SNP (which

Table 4-1 **Cytotoxic and mutagenic effects of MOL and persidomine on MN-11 cells.** Cell cultures were exposed to MOL or persidomine for 24 h in complete medium at 37°C. Following treatment cultures were washed with PBS and replaced with complete medium. The absolute cloning efficiency of cells in the absence of any drug was in the range of 39.5-51.5% (43.08 ± 4.6) in most experiments. MF is expressed as 6-TG^R cells per 1×10^5 viable cells. Data shown represent the mean ± SEM of 3-4 independent experiments, each using 3 separate dishes.

Table 4-1

Treatment	Dose	Survival (%)	MF
Molsidomine (mM)	0	100	3.0 ± 0.7
	1.0	98.3 ± 0.9	6.1 ± 2.1
	2.5	99 ± 0.6	4.7 ± 1.4
	5.0	96.8 ± 0.8	5.3 ± 0.7
	10	97 ± 1.2	3.8 ± 1.3
Persidomine (μg/mL)	0	100	3.0 ± 0.7
	25	98 ± 1.5	5.4 ± 0.4
	50	99.3 ± 0.3	4.2 ± 0.96
	100	93.5 ± 3.5	4.2 ± 1.1
	200	95.8 ± 0.8	4.1 ± 1.3

Figure 4-5 **Effect of caffeine on GTN induced cytotoxicity and mutagenicity on MN-11 cells.** Cultures were seeded at 5×10^5 cells per 10 cm dishes, exposed to GTN with or without caffeine for 24 h in complete medium at 37°C. Following treatment, cultures were washed with PBS, cytotoxicity and mutagenicity determined as described in Materials and Methods. Mean absolute cloning efficiency of untreated cultures with and without caffeine was 34.9% and 22.2%, respectively. Error bars show the mean ± SEM of 16-20 independent dishes, each analyzed in triplicate for MF. Dark bars represent survival and light bars represent MF.

Figure 4-5

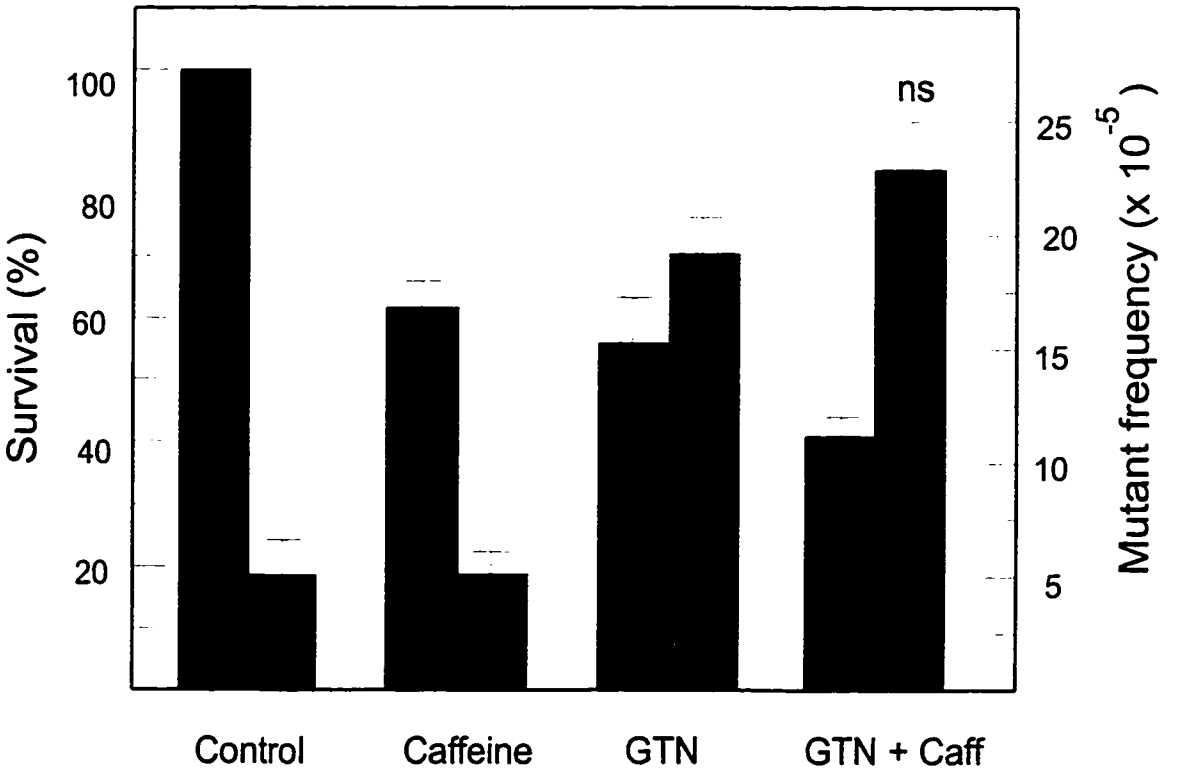
Survival (%)
100
80
60
40
20
ns
25
20
15
10
5
Mutant frequency (x 10^{-5})
Control
Caffeine
GTN
GTN + Caff

Figure 4-6 **Time course of NO_2^- accumulation by different NO-donating drugs in the presence of 2×10^5 MN-11 cells.** Basal level of NO_2^- accumulation at 24 h by MN-11 cells in the absence of drug was 0.5 ± 0.03 μM. No additional NO_2^- accumulation was detected with MOL (10 mM, □) and persidomine (200 μg/mL, ◆). SNP (0.5, ● and 1.0 mM, ○) and GTN (0.12 , ▲ and 0.25 mM, Δ) both produced a time-dependent increase in NO_2^-. Data shown are mean ± SEM (n = 3 experiments, each in triplicate). Results with SNAP (0.1 mM, ▼) are from a single experiment in duplicate.

Figure 4-6

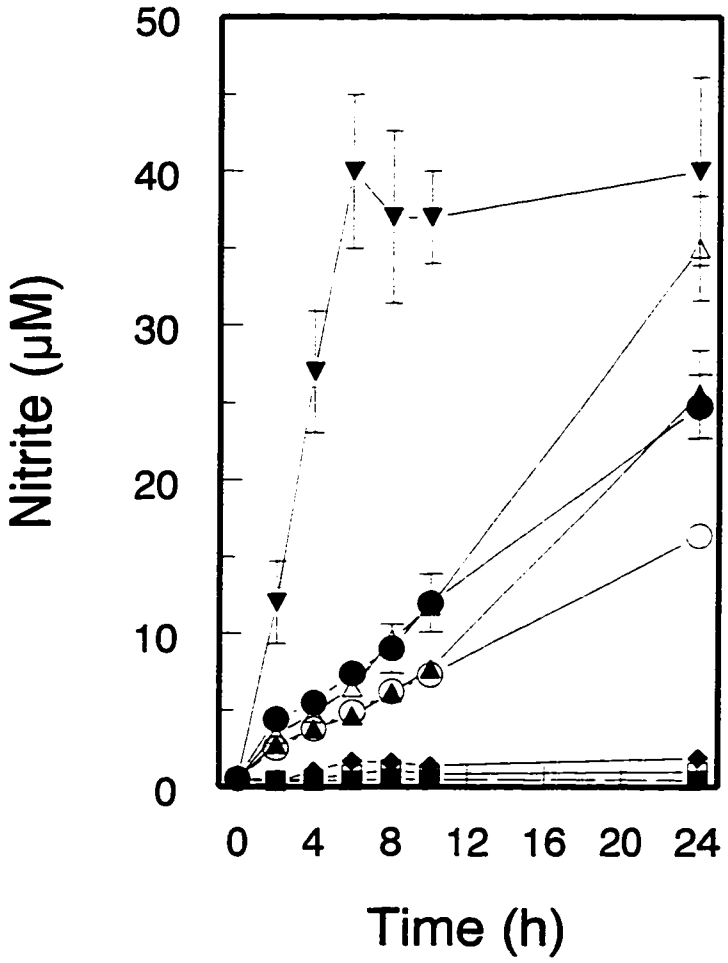

require bioactivation) caused a concentration and time-dependent increase in the accumulation of NO_2^-, with a fairly linear increase for at least 24 h. Incubation of 5×10^5 MN-11 cells with GTN approximately doubled the amount of NO_2^- accumulated. However, addition of SNAP (which does not require bioactivation) produced a much more rapid increase, reaching an apparent plateau at about 5 h. MOL and persidomine produced little or no accumulation of NO_2^- up to 24 h. To assess the contribution of NO_2^- to the observed cytotoxicity and mutagenicity of the NO-donating drugs, the effect of exposure to $NaNO_2$ ($\leq$ 5 mM) for 24 h was tested; <20% cytotoxicity and <5 mutants per 10^5 cells were induced (Table 4-2).

4.3.6 *Examination of the RNS generated by SNP and GTN*

(a) ***Effect of a cyanide scavenger.*** SNP showed the strongest mutagenic potential in MN-11 cells of all NO-donating drugs tested (Figure 4-4D). To assess the relative contribution of cyanide to cytotoxicity and mutagenicity, a cyanide scavenging system (rhodanese + thiosulphate) [277] was used (Figure 4-7A). SNP, at 0.5 mM, caused 60% survival, which was increased to 90% by the scavenging system (2 tailed $p < 0.0001$). Exposure to sodium cyanide itself at concentrations up to 2 mM for 24 h, produced surprisingly little cell killing (survival of 61 ± 2.8%; n = 2), compared to <1% survival of pancreatic islet cells [277]. This is presumably due to the high level of anaerobic glycolysis in MN-11 tumor cells compared to mitochondrial respiration in normal cells. SNP, at 0.5 mM, caused a marked increase in MF in MN-11 cells. The addition of the scavenging system caused a statistically significant reduction in MF, suggesting that cyanide might partially contribute to the observed mutagenesis (2 tailed $p < 0.002$). Although sodium cyanide at 0.5, 1.0, 1.5 and 2 mM did produce a small increase in MF, the effect did not

Table 4-2 **Cytotoxic and mutagenic effects of sodium cyanide and $NaNO_2$ on MN-11 cells.** Cell cultures were exposed to sodium cyanide or $NaNO_2$ for 24 h at 37°C in complete medium. Following treatments cultures were washed with PBS and replaced with complete medium. The absolute cloning efficiency of cells in the absence of any drug was in the range of 29.7-40% (33.1 ± 5.9) in most experiments. MF is expressed as 6-TG^R cells per 1×10^5 viable cells. Data shown represent the mean ± range of 2 independent experiments, each using 2-4 separate dishes.

Table 4-2

Treatment	Dose (mM)	Survival (%)	MF
Sodium cyanide	0	100	8.3 ± 1.3
	0.25	93 ± 0	16.1 ± 13.8
	0.50	84 ± 4.2	12.2 ± 5.0
	1.0	76.5 ± 4.9	6.2 ± 0.71
	1.5	73.5 ± 3.5	15.1 ± 7.6
	2.0	61 ± 2.8	20.9 ± 10
Sodium nitrite	0	100	8.3 ± 1.3
	0.5	97 ± 1.5	7.8 ± 0.5
	1.0	93 ± 0.3	4.9 ± 1.6
	2.5	90 ± 4.5	15.0 ± 4.2
	5.0	83 ± 2.8	7.7 ± 1.4

Figure 4-7 **Effect of scavengers of cyanide on cytotoxicity and mutagenicity of SNP.** (A), cyanide scavengers: rhodanese + thiosulfate (+) in the presence of indicated concentrations of SNP. (B), SNP in the absence or presence (+) of oxyHb (0.1 mM). The absolute cloning efficiency of untreated cells was 28-49% for (A) and 20-45% for (B). Other details as described in Materials and Methods. Data shown are mean ± SEM (n = 5-10 independent treatments, each analyzed in duplicate, using a single lot of MN-11 cells). The cytotoxic (light bar) and mutagenic (dark bar) effects of SNP are shown. Statistically significant differences (* or **) are as described in Results.

Figure 4-7

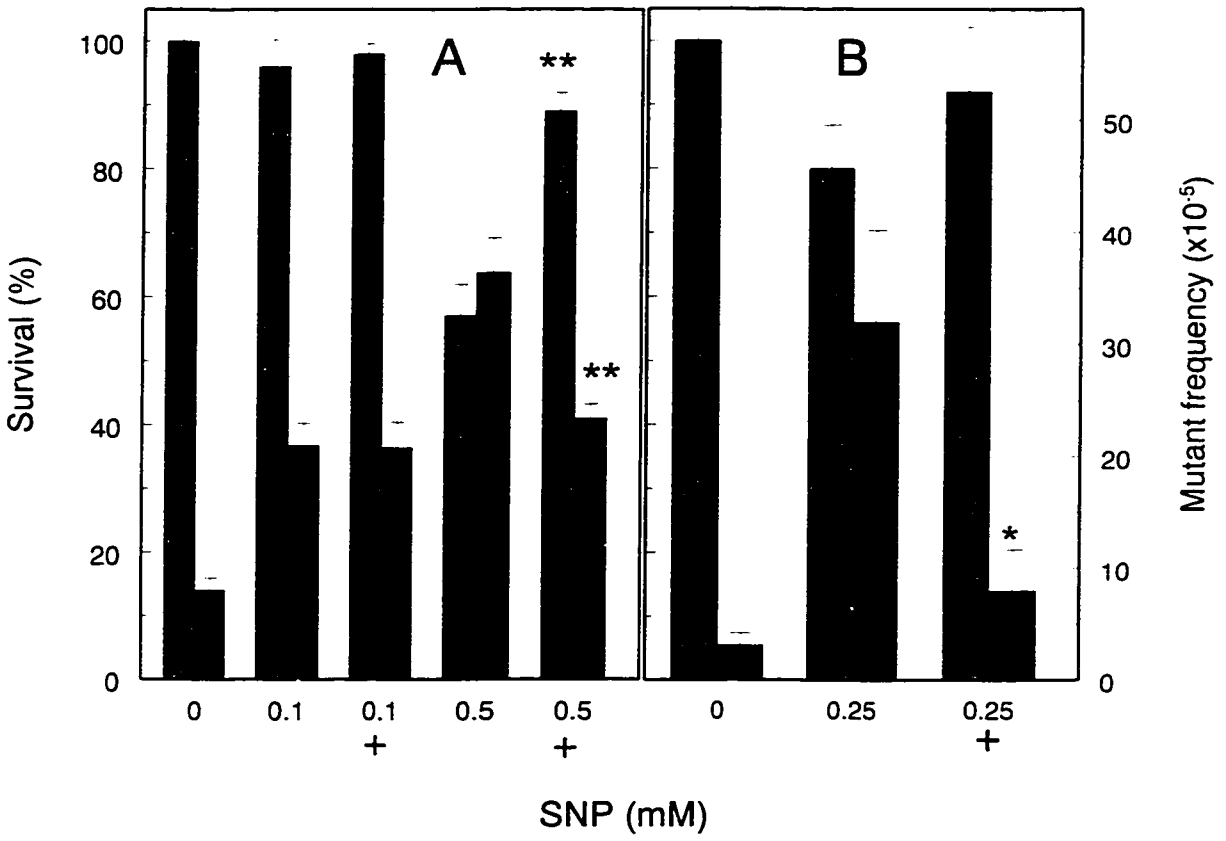
A
B
**
**
*
Survival (%)
Mutant frequency (x10-5)
100
80
60
40
20
0
50
40
30
20
10
0
0
0.1
0.1
+
0.5
0.5
+
0
0.25
0.25
+
SNP (mM)

appear to be dose-dependent (Table 4-2).

(b) ***Effect of oxyHb.*** To explore the relative effect of NO· on the observed cytotoxicity and mutagenicity of 0.25 mM SNP, the effect of oxyHb, a known NO· scavenger (Figure 4-7B) was tested. The addition of 100 μM oxyHb produced no statistically significant change in the cytotoxicity caused by SNP ($p = 0.24$) but did protect against mutagenicity (2-tailed $p < 0.02$). OxyHb alone caused no cytotoxicity (data not shown). When 100 μM oxyHb was incubated with 0.25 mM SNP in the presence of cells at 37°C, a spectral change was observed as oxyHb was converted to metHb indicating the release of NO· from SNP (Figure 4-8). The spectra for oxyHb and metHb resemble those reported by others [287]. The reaction of oxyHb to yield metHb occurs as follows [287,288]:

$$HbO_2 + O_2 \rightarrow \text{metHb} + NO_3^-$$

Looking at this reaction in more detail, the component reactions are

$$HbO_2(Fe^{3-}O_2^-) + NO\cdot \rightarrow [Hb(Fe^{3-}OONO^-)]$$

$$[Hb(Fe^{3-}OONO^-)] \rightarrow Hb(Fe^{3-}) + NO_3^-$$

(c) ***Effect of SOD and catalase.*** NO· can react with ROS such as H_2O_2 and $O_2^{\cdot-}$ to produce peroxynitrite ($OONO^-$). To determine if the cellular effects seen with SNP and GTN involve either ROS, the influence of catalase (a H_2O_2 scavenger) and SOD (a superoxide scavenger) was tested. Neither enzyme modified the cytotoxicity or mutagenicity produced by the two drugs (Table 4-3).

Figure 4-8 **Absorption spectra of oxyHb before and after reaction with 0.25 mM SNP in the presence of cells at 37°C.** Spectra of 100 μM oxyHb immediately before addition of SNP (solid line) and 4 h after addition of 0.25 mM SNP (broken line).

Figure 4-8

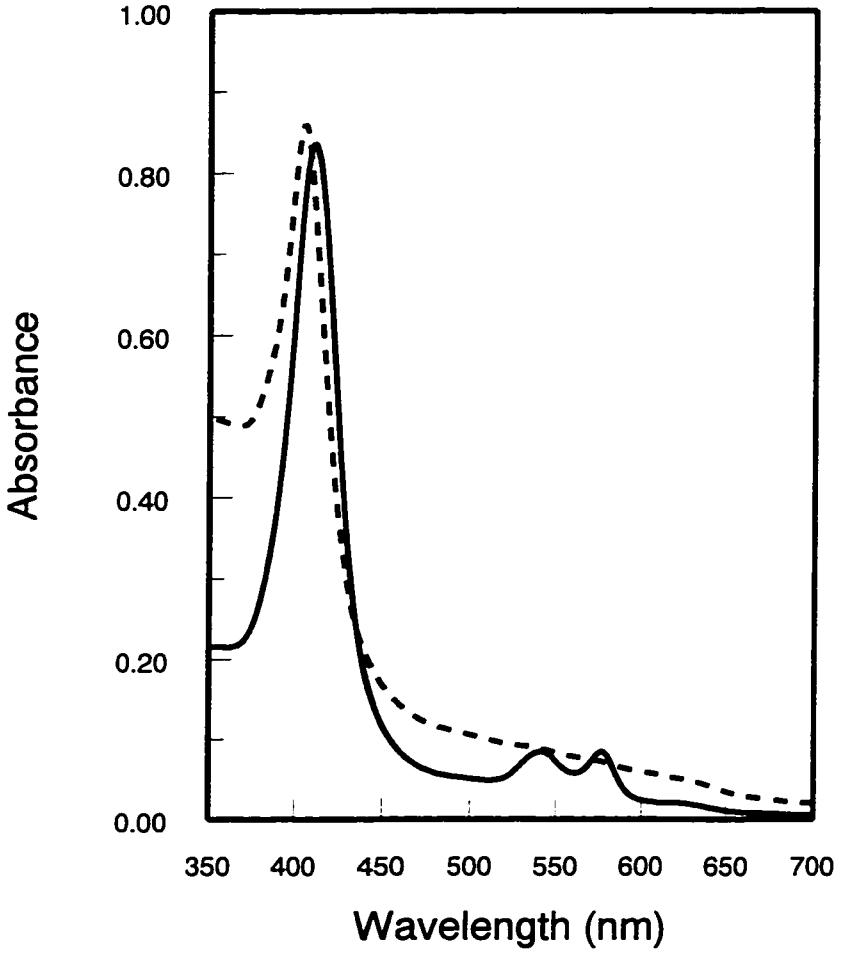
1.00
0.80
0.60
0.40
0.20
0.00
Absorbance
350
400
450
500
550
600
650
700
Wavelength (nm)

Table 4-3 **Effects of scavenger enzymes on cytotoxic and mutagenic effects of SNP and GTN.** Cultures were treated with either SNP or GTN in the presence of the scavenger enzymes for 24 h in complete medium. Following treatments cultures were washed with PBS, cytotoxicity and mutagenicity determined. Where indicated, SOD and catalase were each added at 50 μg/mL. Mean absolute cloning efficiency of untreated cultures was 45 $\pm$ 5%. MF is expressed as 6-TG^R cells per 1×10^5 viable cells. Values shown represent the mean $\pm$ range of duplicate experiments, each using 3 separate dishes.

Table 4-3

	Survival (%)			MF		
Treatment		*SOD*	*Catalase*		*SOD*	*Catalase*
Control	100	-	-	4.7 ±2.0	-	-
SNP (0.5 mM)	54 ±4.2	47 ±9.2	49 ±4.2	39 ±5.7	37.5 ±6.4	42.5 ±6.4
GTN (0.44 mM)	50 ±6.4	50 ±6.4	50 ±3.5	24 ±4.2	20.5 ±3.5	23.5 ±3.5

4.4 DISCUSSION

Genomic instability is a characteristic of malignant tumors, but the underlying mechanisms are only partially understood. It has been our hypothesis that there exists factors in the tumor milieu, such as ROS and RNS, that can be genotoxic and promote genetic instability. My earlier work showed a 3.64-fold increase in MF in MN-11 cells grown as s.c. tumors compared with the MF of cells grown in culture (Chapter 2, section 2.3.5). To explore the possibility that reactive species within the tumor might be involved, a number of ROS and RNS-generating compounds were tested to determine their mutagenic potential at the *HPRT* locus in MN-11 cells *in vitro*. Radiomimetic drugs (bleomycin and streptonigrin) were shown to induce mutants. Both drugs are known to be effective clastogenic agents, which induce large-scale deletion mutations at hemizygous or heterozygous loci [80,229,280,289,290]. These experiments lend further support to the notion that the apparent high frequency of mutant induction in MN-11 cells is due to their ability to survive despite suffering large-scale deletions at the *HPRT* locus.

H_2O_2 has been reported to be a relatively weak mutagen in other cells when tested at the X-linked *HPRT* locus [78,291]. In MN-11 cells, H_2O_2 (both bolus and flux generated by glucose oxidase) was a moderately strong mutagen, as also observed by Hsie *et al.* [79,80]. These workers compared mutations at the endogenous X-linked *HPRT* locus of Chinese hamster cells with an exogenous bacterial *GPT* gene introduced at an autosomal location in AS52 cells. Mutations were induced about 100-fold more readily at the *GPT* locus than at the *HPRT* locus by both potassium superoxide (which readily converts to H_2O_2) and by bolus H_2O_2. It thus appears that, although H_2O_2 almost exclusively induces single-strand rather than double-strand DNA breaks [292], it can also give rise to large-scale

deletions that are detectable in suitable systems, such as where the target locus is heterozygous.

Granulocytes are frequently seen within MN-11 tumors, particularly around necrotic areas (Chapter 3). The ability of granulocytes to induce mutations were tested in MN-11 cells. The resultant cytotoxicity and mutagenicity was very similar to that observed with H_2O_2, about 15 induced mutants per 10^5 cells at 50% survival. When TPA (a known potent stimulator of the respiratory burst [281]) was added to increase the production of ROS, TPA itself was found to be cytotoxic, with little additional mutagenicity. This phenomenon has not been further investigated. The mutagenicity and perhaps cytotoxicity of unstimulated granulocytes in our model system is likely due to the slow release of H_2O_2 that is known to occur when such cells are put into plastic tissue culture dishes [293]. The mutagenicity of human granulocytes at the *HPRT* locus of CHO cells was lower than in MN-11 cells [72], presumably because mutations arising as a result of large-scale deletions are more likely to cause lethality in CHO cells. H_2O_2 is likely to be the relevant mutagenic species since human granulocytes cannot produce RNS unless stimulated with cytokines [294]. However, other reactive species, such as hypochlorous acid, might be involved.

There has been in recent years considerable interest in the wide spectrum of biological effects of NO· and related species. However, there have been relatively few studies on their genotoxicity in mammalian systems. Since MN-11 cells appear to be sensitive for detecting large-scale deletion mutants as well as small-scale events, these cells were used to determine whether a variety of NO-donating drugs could cause this type of mutation. It was found that, at equitoxic doses, different NO-donating drugs varied widely in their mutagenic potential. There is considerable controversy as to the exact nature of the

molecular species present in cells or in medium after addition of these drugs. Of the drugs tested, it is generally agreed that SPER/NO· and SNAP will spontaneously release nitric oxide (NO·). SNP is a complex of Fe^{2+}, 5 CN^- and NO^- that does not spontaneously release NO· but may do so after bioactivation in a reaction involving a sulfhydryl [282]. GTN likewise requires bioactivation in a sulfhydryl-dependent reaction [295]. It has been proposed that some of the biological effects of SNP and GTN may involve NO^- [142]. The observed variation in the ratio of cytotoxic and mutagenic effects of different NO-donating drugs may be attributable to the different species that they generate. Reaction of NO· with $O_2^{\cdot-}$ leads to the formation of $ONOO^-$, which is generally considered to be a cytotoxic species. MOL, persidomine and SPER/NO· had no detectable mutagenic effect. The lack of mutagenic (and cytotoxic) effect of MOL and persidomine can be attributed to their failure to be metabolized to NO· [284,285], since no NO_2^- accumulation was detectable (Figure 4-5). It therefore appears that MN-11 cells are incapable of converting MOL to its active metabolite, SIN-1. However, polymorphonuclear cells have been shown to convert MOL enzymatically to SIN-1 or another NO-releasing compound [296]. As was the case of SPER/NO· in MN-11 cells, DEA/NO· was reported to be cytotoxic but not mutagenic in a human bronchial epithelial cell line [180]. Both generate NO· spontaneously ($t_{1/2}$ = 39 min and 2 min, respectively [297]). High concentrations (10-20 mM) of NO· gas were cytotoxic (90% killing) and were able to induce $HPRT^-$ and TK^- mutants in human TK6 cells [158], about 1 to 1.5 per 10^5 cells above background at both loci. SNAP is a nitrosothiol that can generate NO· spontaneously ($t_{1/2}$ = 4.2 h, [298]; $t_{1/2}$ = 3.0 h for NO_2^-, Figure 4-5) but may also have NO^- character; it was strongly cytotoxic but weakly mutagenic in MN-11 cells. The drugs (GTN and SNP) requiring bioactivation in thiol-mediated reactions, exhibited the

highest MF at relatively low cytotoxicity. This suggests that an intermediate in the metabolism of GTN and SNP with intracellular thiols, perhaps a NO^--like species, is responsible for mutagenicity in MN-11 cells. Base change mutations by RNS have been demonstrated following *in vitro* treatment of a plasmid-based shuttle vector, which was subsequently introduced into mammalian cell [176,177].

Of the NO-donating drugs tested, most of them were shown to produce NO_2^-. Metabolism of SNP and GTN by MN-11 cells produced a sustained release of NO_2^- over a 24 h period. By contrast, GTN is metabolized much more rapidly (<1 h) in endothelial and smooth muscle cells, [299]. To our knowledge, this is the first report showing GTN metabolism by a tumor cell. NO_2^- is not likely to be the cytotoxic or mutagenic species for MN-11 cells liberated by these drugs since $NaNO_2$ did not induce mutants (Table 4-2).

SNP was the most potent of the NO-donating drugs tested as a mutagen in MN-11 cells, but it can release CN^- as well as NO. A cyanide scavenger partially blocked mutagenicity, suggesting that CN^- itself or in combination with NO may be weakly mutagenic. The latter seems more probable since neither our data nor that of others showed that CN^- alone is appreciably mutagenic [300]. A majority of its mutagenicity appears to be due to its ability to release NO·, since mutagenicity was blocked by oxyHb (Figure 4-6B), a known NO· scavenger [299,301]. The spectrum of the derivative formed with the reaction of NO· (released from SNP) with oxyHb resembles that of metHb. Hence, the protection afforded against mutagenicity could therefore be associated with the ability of oxyHb to react with and bind NO·. OxyHb also afforded little protection against cytotoxicity. It is therefore possible that part of the observed cytotoxicity of 0.5 mM SNP was due to CN^- and that the protection afforded by oxyHb was due to contaminating methaemoglobin, which can

bind CN^-.

The detailed mechanism involved in mutant induction by RNS in MN-11 cells is uncertain. Neither catalase nor SOD had an effect on SNP or GTN-induced mutagenicity or cytotoxicity, suggesting that extracellular H_2O_2 or $O_2^{\cdot-}$ /$ONOO^-$ was not involved. NO_2^- is not likely to be the major cytotoxic species, since NO_2^- appears to be cytotoxic only at 100× higher concentrations [302]. Mutagenicity in MN-11 cells did not correlate with NO_2^- levels nor did added $NaNO_2$ induce mutants. Because NO· is a short-lived radical that can give rise to other reactive species, determination of the actual molecule responsible for any given biological effect can be difficult. For example, while it is accepted that NO· can give rise to NO_2^- and NO_3^-, the precise pathway seems to depend upon the specific conditions employed [286]. NO· can react with $O_2^{\cdot-}$ or H_2O_2 to produce $ONOO^-$, which can cause thiol oxidation and DNA strand breaks [116,158,161]. NO· and $ONOO^-$ have been shown to cause damage to DNA bases [157,177,303]. The mechanism of mutagenicity by NO· and NO-donating drugs appears to be complex. In assays sensitive to detection of base change mutations, NO· gas and NO-donating drugs are reasonably effective mutagens. In MN-11 and TK6 cells, which are sensitive to detection of large scale deletion mutations, NO· appears to be a less effective mutagen while drugs requiring bioactivation with thiols are much more effective. Metabolism of SNP and GTN by MN-11 cells may generate a species capable of causing large scale deletion mutations. Once such species are identified, it may then be possible to determine whether the same species are generated intracellularly by nitric oxide synthases. Our experiments using these model compounds may therefore provide insight into the mechanism of genotoxicity which is presumed to underlie the known association between inflammatory states and cancer.

CHAPTER 5

EXPRESSION OF INDUCIBLE NITRIC OXIDE SYNTHASE IN GRANULOCYTES INFILTRATING MN-11 TUMORS GENERATE NO· THAT MAY BE MUTAGENIC

ABSTRACT

Inducible nitric oxide synthase is an enzyme that can produce relatively large amounts of NO·, a free radical species implicated in many pathophysiological conditions. Our hypothesis is that phagocytic cells found within solid tumors may contribute to tumor progression by generating NO· and/or other related species that may be genotoxic and mutagenic. The MN-11 tumor model system was developed to test this hypothesis. An increased MF was demonstrated in MN-11 cells recovered from s.c. tumors in mice than in identical cells grown *in vitro*. In this chapter, the possible contribution of endogenous NO· in inducing mutations was assessed by examining NOS activity and expression of iNOS in MN-11 tumors. Immunohistochemical investigations with a polyclonal NOS antibody revealed immunolabeling predominantly of tumor-infiltrating granulocytes and to a lesser extent, in macrophages. No immunolabeling was found of tumor cells, lymphocytes or vascular endothelial cells. Western blot analysis of tumor tissue confirmed the presence of iNOS in tumor tissue. A positive correlation was observed between granulocytic infiltration and MF. Necrosis also correlated positively with granulocytic infiltration. Biochemical measurements of NOS activity in a large number of individual tumors demonstrated a positive correlation between MF and NOS activity. These results are consistent with a model in which NO· or a related species generated by infiltrating granulocytes in MN-11 tumors, may be mutagenic and contribute to the observed increase in MF in these tumors.

5.1 INTRODUCTION

Nitric oxide is an inorganic free radical synthesized from L-arginine by a family of isoenzymes called nitric oxide synthases [304]. Two of these are constitutively expressed

(eNOS and nNOS) and a third is inducible by various physiological stimuli (iNOS). The NO· released by the constitutive enzymes acts as a signalling molecule in the cardiovascular and nervous systems [305-308]. NO· released by iNOS is generated in large amounts by cells of the immune system and may have a cytostatic/cytotoxic role [122,127,246].

Increasing evidence suggests that chronic inflammatory conditions may predispose to cancer [45,55,131]. This increased incidence is presumed to be mediated by agents released by phagocytic cells at sites of inflammation. Recent data have shown that NO· present in these inflammatory conditions may be responsible for increase in cancer [155,241,309]. Several *in vitro* studies have demonstrated that NO· can induce cellular damage and mutations [157,158,178,194,310-312]. There has been only one study of mutagenicity by NO· *in vivo* using an experimental model system [182]. The precise role of NO· in tumor biology is not well understood. Solid tumors are a population of heterogeneous cell types, including endothelial cells of the tumor vasculature, fibroblasts of the supporting stroma, tumor-infiltrating immune cells (macrophages, polymorphonuclear cells and T-lymphocytes), and tumor cells themselves. Most of these cell types have been shown to generate NO· *in vitro* [313-315]. The presence of cNOS in endothelial cells and iNOS induced by cytokines in macrophages has been documented [89,316]. Various tumor cell lines have been reported to contain either cNOS, iNOS or both isoenzymes [136,317,318]. Recently, the presence of NOS has been demonstrated in human tumor tissue, where it is localized to the tumor cells [136,137] and to the stroma of breast cancers [135]. However, whether NO· had a positive, negative or no effect on the progression of these tumors is unknown.

Using the MN-11 tumor model system, a 3.64-fold increase in MF was observed in

s.c. tumors as compared to parallel *in vitro* cultures (Chapter 2, [1]). More recently, it was shown that NO· can induce mutations in MN-11 cells *in vitro* (Chapter 4, [194]). In this chapter, the contribution of endogenously generated NO· to the observed increase in MF was investigated in MN-11 tumors. The presence and cellular localization of NOS and a correlation between NOS activity and MF in tumor homogenates is described.

5.2 MATERIALS AND METHODS

All materials, chemicals and the compositions of solution used in these experiments are found in Appendix II.

5.2.1 *Cells and culture conditions*

MN-11 cells were grown in non-selective medium, HAT-medium, HT-medium or 6-TG-medium as defined previously (Appendix IV, section IV.1). Mouse peritoneal macrophages were prepared by injecting 1 mL of 2% sterile starch i.p. into 8-10 weeks old C57BL/6 mice. After 4 days, peritoneal lavage was performed by using 5 mL of PBS. Macrophages were cultured in 1 mL of phenol red-free non-selective medium for 4 h in 24-well dishes (1×10^5 cells/well) for NO_2^- measurement or in 10-cm petri dishes (5×10^5 cells) for mutant induction. Nonadherent cells were removed and fresh non-selective medium was added before the treatments.

5.2.2 *Co-culture of MN-11 cells with macrophages and stimulation with cytokines*

In co-culture experiments involving mutation induction, 5×10^5 MN-11 cells were added to the macrophage cultures and incubated in non-selective medium for 4 h at 37°C.

Macrophages were then stimulated for 24 h with TPA (2×10^{-7} M), LPS, or various cytokines. At the end of co-culture, G418-medium was added to the cultures to kill the macrophages after which cytotoxicity and MF was determined as described in Appendix IV, section IV.2. In some cultures, L-NMMA (1 mM), a specific inhibitor of NOS was added to verify the effects observed were due to NO·. For NO_2^- determinations, 1×10^5 MN-11 cells/well were added to the macrophage cultures, stimulated as above and NO_2^- measured in the culture supernatant as described below. As a control, MN-11 cells were stimulated for 24, 48, 72 and 96 h with cytokines and culture supernatant collected. Usually culture supernatant was stored frozen at -20°C until NO_2^- determinations were performed.

5.2.3 *Measurement of NO_2^- and nitrate (NO_3^-)*

NO_2^- is a fairly stable end product of NO· biosynthesis, but it may convert to NO_3^-. To quantify the amount of NO· released by stimulated macrophages, the amount of NO_2^- and NO_3^- that accumulated in the culture medium was measured. One hundred µL aliquots were removed from conditioned medium and the concentration of NO_2^- determined as described in chapter 4, section 4.2.5. NO_3^- was measured by enzymatically reducing NO_3^- to NO_2^- with nitrate reductase. Samples were incubated with nitrate reductase (25 milliunits) and β-NADPH (20 µM) for 30 min at 37°C and then NO_2^- measured using the Griess reagent [279].

5.2.4 *Nicotinamide adenine dinucleotide phosphate diaphorase (NADPH-d) staining*

Frozen sections were prepared as described previously (Chapter 3, section 3.2.4 (a)). Cryostat sections were cut at 5 µm, air dried and then washed with 100 mM PB for 5 min.

Sections were then incubated in a mixture of β-NADPH (1 mM), nitro blue tetrazolium (0.3 mM) and 0.2% Triton X-100 in 10 mM PB, pH 8.0 in a humid chamber for 1 h at 37°C. The slides were washed with 100 mM PB, air dried and mounted in permount [249]. Controls were processed without β-NADPH. In some incubations, L-NMMA (1 mM) was included in order to study the selectivity of this assay. Cultured MN-11 cells were grown on 0.1% gelatin coated coverslips and stained as above. P19 cells obtained from Dr. M. W. McBurney were used as positive controls.

5.2.5 *Assay of NOS Activity*

Tumor sections were snap frozen in liquid nitrogen and stored at -80°C until analyzed. Sections were thawed on ice and extracted by homogenization (with a Polytron homogenizer) in 2.5 volumes of a homogenization buffer (Appendix II). Tumor homogenates were centrifuged at 14,000 rpm at 4°C for 30 min and NOS activity was assessed in the supernatants by the conversion of L-[^{14}C]arginine to [^{14}C]citrulline [319]. Briefly, 2.5 volumes of assay buffer (Appendix II) was added to the tumor homogenates and enzymatic reactions were conducted at 37°C for 20 min. Reactions were terminated by addition of 1 mL ice-cold 1 mM CDTA, a chelator. These samples were then applied to columns (1 c.c. syringe) containing 0.4 mL Spectra/Gel, cation exchange 50W-X8, Na form, to remove unconverted arginine. Columns were eluted with 3 × 1 mL of 1 mM CDTA into scintillation vials. Scintillation fluid (Aquasol-2), (12 mL) was added to each vial and samples were counted in a 1600 TR Packard liquid scintillation counter. The activity of the calcium-dependent enzyme was determined from the difference between the [U-^{14}C]citrulline generated from control samples and samples containing 1 mM EGTA; the

activity of the calcium-independent enzyme was determined from the difference between samples containing 1 mM EGTA and samples containing both 1 mM EGTA and 1 mM L-NMMA. NOS activity is expressed as pmol/min/mg protein.

Protein content of tumor homogenates was determined spectrophotometrically (Beckman DU 640) with Bradford reagent [320], using bovine serum albumin as standard.

5.2.6 *Immunohistochemistry*

Paraffin wax-embedded tumor tissue was deparaffinized in xylene and rehydrated in a series of decreasing concentration of ethanol. Endogenous peroxidases and nonspecific immunoglobulins were inactivated as previously described in chapter 3, section 3.2.3 (b). Sections were blotted and incubated in a humid chamber with 1:100 dilution (2.5 μg/mL) of rabbit polyclonal antibody to macrophage iNOS (Transduction Laboratories). After overnight incubation at 4°C the sections were rinsed with TBS and incubated at room temperature for 30 min with 1:200 (7.5 μg/mL) goat anti-rabbit biotinylated IgG (Dimension Laboratories Inc.). The biotinylated conjugate was detected by incubating sections with avidin-peroxidase 1:1000 dilution (5 μg/mL) at room temperature for 30 min. Immunolabeling was detected as described earlier in chapter 3, section 3.2.3 (b). MN-11 cells and macrophages (unstimulated and stimulated) were grown on 0.1% gelatin-coated coverslips and stained for iNOS as described above for tumor tissue.

5.2.7 *Western Blot Analysis*

Tumor homogenates were prepared as described in section 5.2.5. Protein concentration was determined using the method of Bradford. Samples were diluted by

addition of equal volume of 2 × SDS sample loading buffer (Appendix II) and denatured by boiling for 5 min. Five μL of the mouse macrophage lysate treated with IFN-γ and LPS for 12 h provided by Transduction Laboratories was used as a positive control. An equal amount of protein (50 μg) from each tumor was loaded into each well and size-fractionated by 6% SDS-polyacrylamide gel electrophoresis for 16 h at 50 V. Resolved proteins were transferred electrophoretically to a Immobilon-P membrane (Millipore Corp.), overnight at 14 V as described in [321]. The membrane was blocked for 1 h with 5% nonfat milk in TBS at room temperature, washed once with TBS-T (TBS containing 0.05% Tween-20) and then incubated with rabbit anti- iNOS (1:1000) for 1 h at room temperature. The membrane was washed extensively with TBS-T and incubated with anti-rabbit horseradish peroxidase (1:6000) for 45 min at room temperature. Immunoreactive bands were visualized by enhanced chemiluminescence (ECL) using the LumiGLO™ substrate kit. Membrane was washed extensively in TBS-T overnight and as a loading control probed with anti β-tubulin (1:10, provided by Dr. M. W. McBurney). Immunolabeling was demonstrated with goat anti-mouse horseradish peroxidase (1:6000) and detected by ECL.

5.2.8 *Histological grading of granulocytic infiltration and necrosis*

A 2-mm grid was drawn on the tumor section. Using 40 × objective with a calibrated eye piece (1 mm index with 100 square grid) the top left and right or bottom left and right corners on the 2-mm grid were counted. In all tumor sections 5-14 areas were scored and in each section, granulocyte and necrosis counts were obtained in parallel.

5.2.9 *Statistical analysis*

The *in vitro* data was analyzed for significance by the one-way factorial ANOVA or Student's *t*-test, as applicable. Following detection of a statistically significant *F* value, *post hoc* Tukey-Kramer test was used. The *in vivo* data were analyzed by non-parametric tests, Kruskal-Wallis ANOVA, followed by a *post hoc* Dunn's test or Spearman rank test as applicable. A value of $p \leq 0.05$ was considered to be significant (shown as *) or $p \leq 0.01$ was considered to be highly statistically significant (shown as **).

5.3 RESULTS

5.3.1 *Induction of NOS activity in MN-11 cells*

The incubation of tumor cells with cytokines and/or LPS can induce the production of various mediators, among which is NO· [317]. To determine whether cytokines or LPS can induce NOS activity in MN-11 cells, these cells were incubated with different concentrations of IFN-γ (25-100 units/mL), IL-1β (25-100 units/mL), TNF-α (25-100 units/mL), or LPS (1.0-5.0 μg/mL), alone or in combinations. Following incubations for up to 96 h NOS activity, NO_2^- and NO_3^- accumulations were measured. Control MN-11 cells exhibited a basal level of NOS activity of 2.05 ± 0.07 pmol/min/mg, 46% was identified to be calcium-independent (iNOS) and 54% was calcium-dependent (cNOS). No further increase in NOS activity was observed up to 96 h. Basal level of NO_2^- accumulation at 24 h by MN-11 cells without any stimulant was 0.65 ± 0.05 μM, respectively. No significant increase in NO_2^- or NO_3^- was detected up to 96 h (1.0 ± 0.3 for NO_2^- and 1.2 ± 0.32 for NO_3^-, respectively, n = 3). IFN-γ, IL-1β, TNF-α or LPS were ineffective as single stimuli. Any combination of LPS and/or cytokines also did not result in an increase in NOS

activity, NO_2^- or NO_3^- accumulation (data not shown).

5.3.2 *Mutation induction by macrophages in MN-11 cells*

NO· is a major cytotoxic mediator secreted by activated macrophages [96,322] which has been shown to cause mutations in bacteria [323] and induce DNA strand breaks in tumor cells [324,325]. The ability of mouse peritoneal macrophages (elicited with 2% starch) to induce mutations in MN-11 cells was tested by co-culturing macrophages with MN-11 cells with and without an exogenous stimulant. Figure 5-1 shows the effect of stimulated macrophages on cytotoxicity and mutation induction in MN-11 cells. Incubation of MN-11 cells with TPA at 2×10^{-7} M, in the absence of macrophages, resulted in statistically significant cytotoxicity (survival of 44.5 ± 1.5%, n = 2; ANOVA, *post hoc* Tukey-Kramer test, $p < 0.001$). There was also a small increase in MF ($p = 0.0469$) as shown in chapter 4, section 4.3.3. Incubation of MN-11 cells with macrophages alone caused a non-significant decrease ($p = 0.06$) in cloning efficiency of MN-11 cells with a non-significant increase in MF ($p = 0.1390$). Macrophages were stimulated with TPA, IFN-γ (100 units/mL) and LPS (5 μg/mL) alone or a combination of these stimulants. The combination of TPA and macrophages was significantly more cytotoxic (Survival of 30 ± 2.5%, n = 2; $p < 0.01$) than each of them individually. That is, the products of the respiratory burst activated by TPA appear to be more cytotoxic. Treatment of macrophages with IFN-γ or LPS did not cause any further increase in cytotoxicity or MF. The combination of IFN-γ and LPS was slightly more cytotoxic than single stimuli, but a significant increase in MF (10.1 ± 1.2, n =2; $p < 0.05$) was observed. In the presence of L-NMMA (a NOS inhibitor) there was a significant increase in survival and a decrease in MF

Figure 5-1 **Cytotoxic (A) and mutagenic effects (B) of mouse peritoneal macrophages stimulated with TPA, LPS and/or IFN-γ in MN-11 cells.** Following treatment for 24 h, cultures were washed with PBS, cytotoxicity and mutagenicity determined. Mean absolute cloning efficiency of untreated cultures was 46.7 ± 6.2%. Black bars represent cytotoxicity and mutagenicity in control cells normalized to 100%. Hatched bars represent cytotoxicity and mutagenicity of TPA on MN-11 cells. Grey bars represent incubations in the presence of macrophages stimulated with the indicated agents. Error bars indicate mean ± SEM (results are from a single experiment, n = 2, each analyzed in triplicate). Macrophages and MN-11 cells were incubated at a 1:1 ratio. Treatment with vehicle (0.1% (v/v) dimethyl sulfoxide) had no cytotoxic or mutagenic effect (second set of bars). Other details as in Materials and Methods. Statistically significant differences (*) are as described in Results.

Figure 5-1

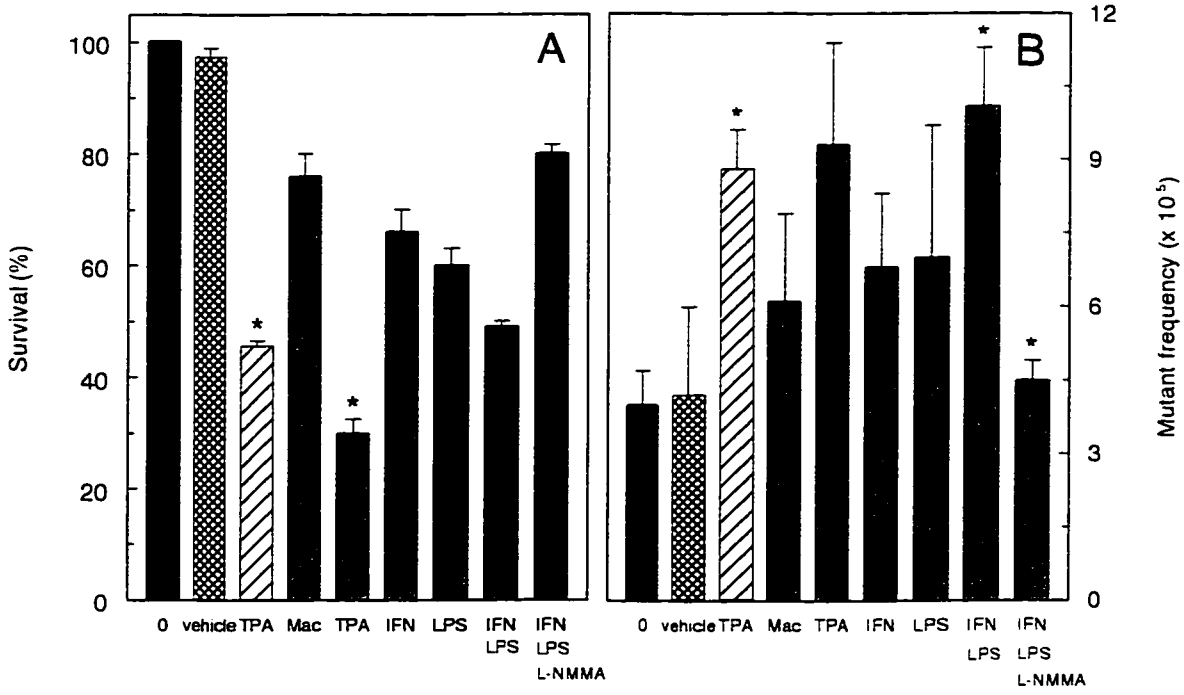
A
B
Survival (%)
Mutant frequency (x 10⁻⁵)
100
80
60
40
20
0
12
9
6
3
0
0
vehicle
TPA
Mac
TPA
IFN
LPS
IFN LPS
IFN LPS L-NMMA
*

when cells were cultured with both IFN-γ and LPS.

To test the hypothesis that NO· is generated under these conditions, NO_2^- and NO_2^- + NO_3^- accumulated in culture medium was measured (Figure 5-2). No detectable accumulation of these metabolites occurred when macrophages were cultured in the absence of immunostimulants. No further increase in accumulation of these metabolites was observed when macrophages were stimulated with TPA. As expected, treatment with IFN-γ or LPS showed a small but non-significant increase in production of these metabolites ($p > 0.05$, for both NO_2^- and NO_2^- + NO_3^-) which was further increased by co-treatment with IFN-γ and LPS ($p = 0.0274$). The NOS inhibitor significantly reduced the accumulation of these metabolites ($p = 0.0372$).

5.3.3 *Staining for NADPH-d activity*

NADPH-d is a histochemical marker for NOS activity [326,327] that stains all three isoforms of nitric oxide synthases. The diaphorases are a group of enzymes that in a histochemical medium can use an electron such as NADPH to reduce the soluble reagent nitro blue tetrazolium to produce diformazan dye. Figure 5-3A shows the blue formazan precipitate in MN-11 cells confirming NOS activity in these cells. This method labels both cNOS and iNOS. When L-NMMA was included in the reaction mixture, all activity was abolished. P19, an embryonal carcinoma cell line, was included as a positive control to demonstrate NOS activity. These cells were allowed to differentiate into neurons with retinoic acid (1 mM) [328,329] and stained with the NADPH-d technique; positive staining was observed (data not shown). MN-11 subcutaneous tumors also showed positive staining; both light and dark stained cells were observed (Figure 5-3B).

Figure 5-2 **Effects of various stimulants (TPA, LPS and/or IFN-γ) on the production of nitrite and nitrite + nitrate by murine peritoneal macrophages.** 2% starch-elicited, macrophages were co-cultured with MN-11 cells (1:1 ratio) and stimulated with the indicated stimulants. The amount of nitrite and nitrite + nitrate released by macrophages was measured after 24 h of incubation using the Griess reagent. Data shown are mean ± SEM from a single experiment analyzed in duplicate. Other details as in Materials and Methods. Statistically significant differences (*) are as described in Results.

Figure 5-2

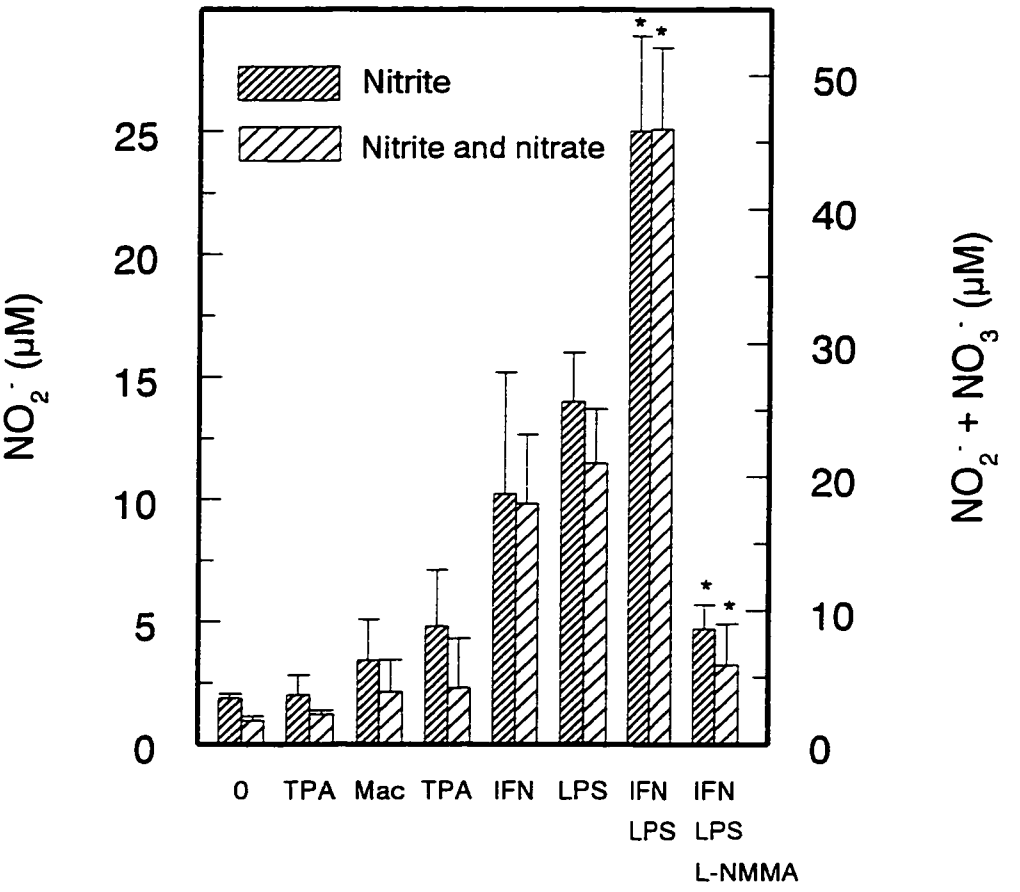
Nitrite
Nitrite and nitrate
NO_2^- (μM)
$NO_2^- + NO_3^-$ (μM)
0
5
10
15
20
25
0
10
20
30
40
50
0
TPA
Mac
TPA
IFN
LPS
IFN LPS
IFN LPS L-NMMA

Figure 5-3 **Histochemical evaluation of NADPH-d activity in MN-11 tumors.** (A), NADPH-d activity in cultured MN-11 cells. Positive activity is shown as blue deposits in the cytoplasm. (B), NADPH-d activity in subcutaneous tumors. Large arrow points to darkly stained cells and small arrow to lightly stained cells (× 200).

Figure 5-3

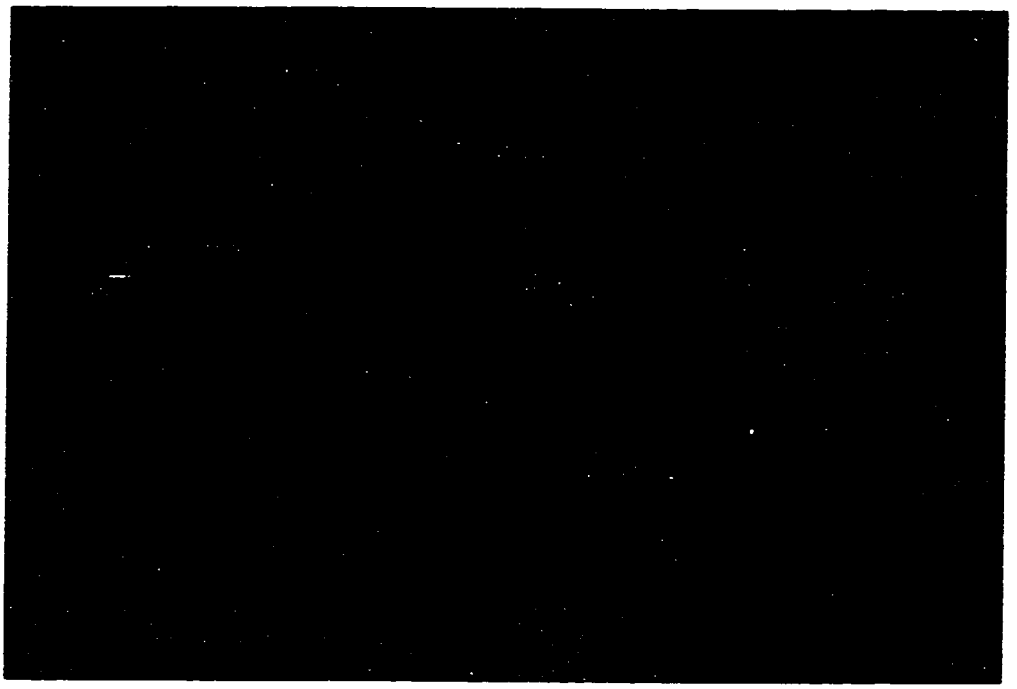

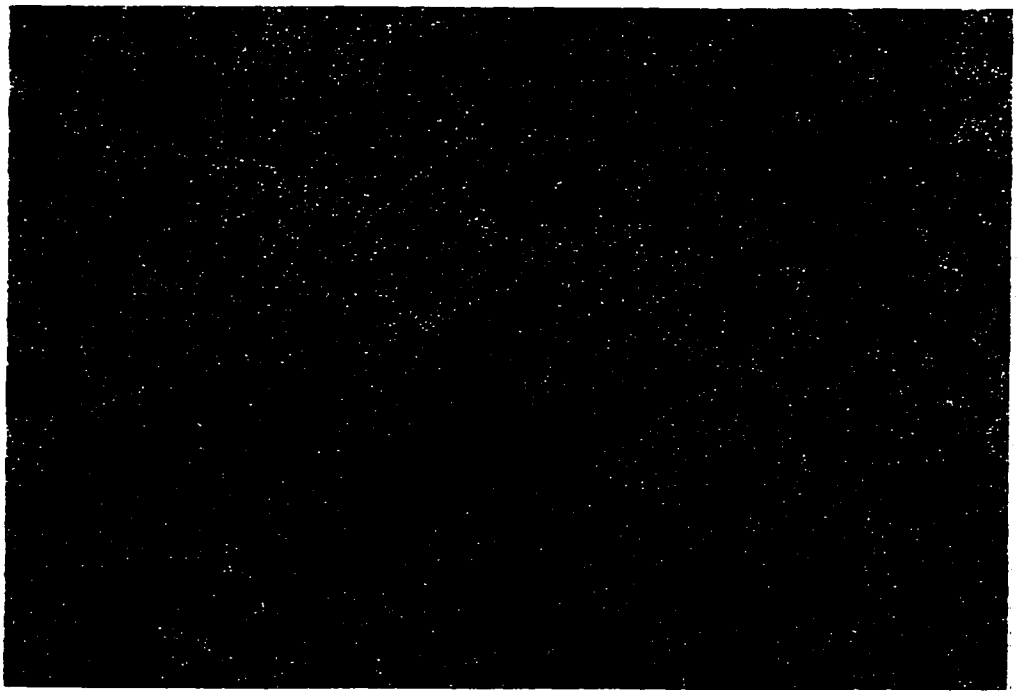

5.3.4 *Correlation between MF and NOS activity*

Fifty-seven tumors (15-22 days of *in vivo* growth) were examined biochemically for NOS activity and, in parallel, the MF was determined. Figure 5-4A shows that the total NOS activity varied widely between different tumors (range 1.1-33.7 pmol/min/mg protein). A positive correlation was observed between total NOS activity and MF ($r = 0.68$, 2 tailed $p < 0.001$(non-parametric Spearman rank test)). Calcium-independent (iNOS) activity also showed a positive correlation with MF (Figure 5-4B, $r = 0.60$, $p < 0.0001$). cNOS activity was between 1.0-4.2 pmol/min/mg protein for all the tumors examined; no correlation was found with MF (data not shown). Both total NOS and iNOS was analyzed as a function of the age of the tumor. No statistically significant differences were observed between the total NOS or iNOS activity and the age of the tumor (Kruskal-Wallis ANOVA, *post hoc* Dunn's test, $p > 0.05$).

5.3.5 *Immunohistochemical analysis of iNOS in MN-11 tumors*

Cultured MN-11 cells stain positively with anti-iNOS antibody (Figure 5-5A). Mouse peritoneal macrophages stimulated with IFN-γ and LPS for 24 h were used as a positive control to show iNOS staining (Figure 5-5B), whereas unstimulated macrophages showed no immunostaining. In MN-11 tumors, positive staining for iNOS was present mainly at sites of inflammatory cell infiltration. Granulocytes are the predominant cells staining positively. Immunolabeling of granulocytes was detected in both necrotic and non-necrotic regions of the tumor (Figure 5-6A & B). Macrophages and mast cells found at the periphery of the tumor also labeled positively (data not shown). No labeling was observed in tumor cells, lymphocytes or endothelial cells of the tumor vasculature. Normal rabbit

Figure 5-4 **Relationship between NOS activity and MF in MN-11 tumors.** (A), Total NOS activity *versus* MF. (B), iNOS activity *versus* MF. Tumors were excised after 15-22 days of *in vivo* growth and MF determined. A section of the tumor was snap frozen in liquid nitrogen and analyzed for NOS activity as described in Materials and Methods. All data are represented from fifty-seven individual tumors.

Figure 5-4

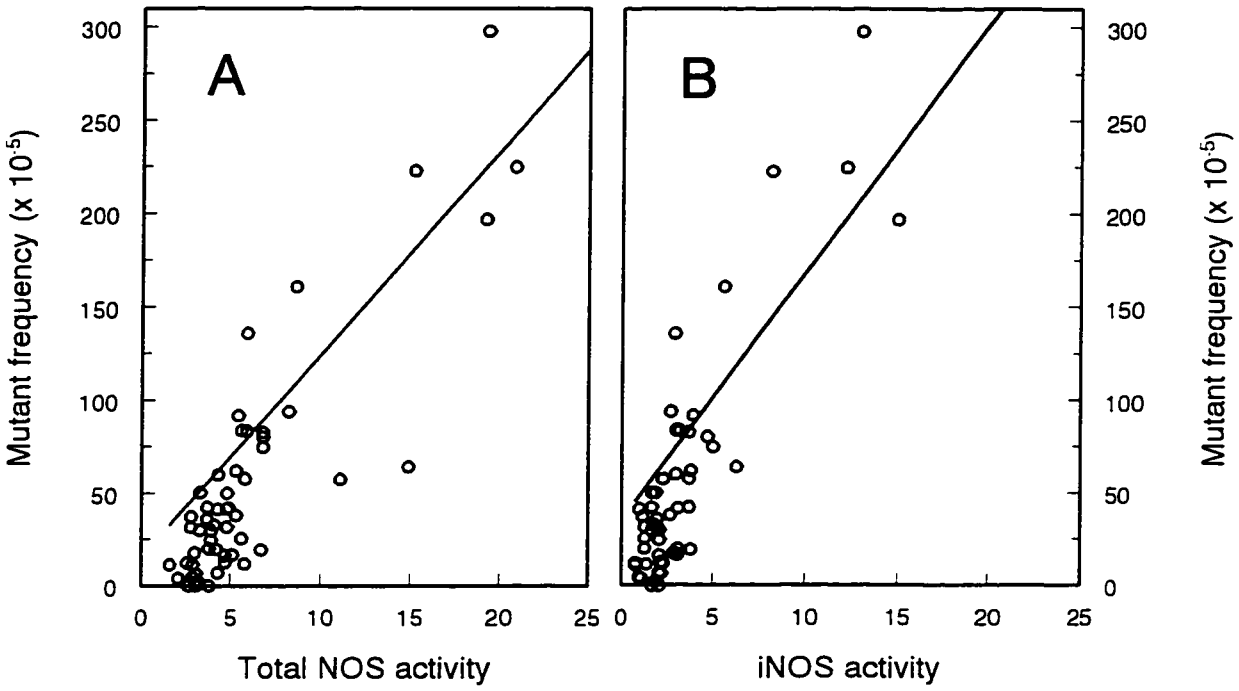
A
B
Mutant frequency (x 10-5)
Mutant frequency (x 10-5)
300
250
200
150
100
50
0
0
5
10
15
20
25
Total NOS activity
iNOS activity

Figure 5-5 **Immunohistochemical localization of iNOS using the anti-mac iNOS antibody.** (A), Cultured MN-11 cells, counterstain haematoxylin, × 400. (B), Mouse peritoneal macrophages stimulated with LPS plus IFN-γ, counterstain 2% Methyl green, × 400.

Figure 5-5

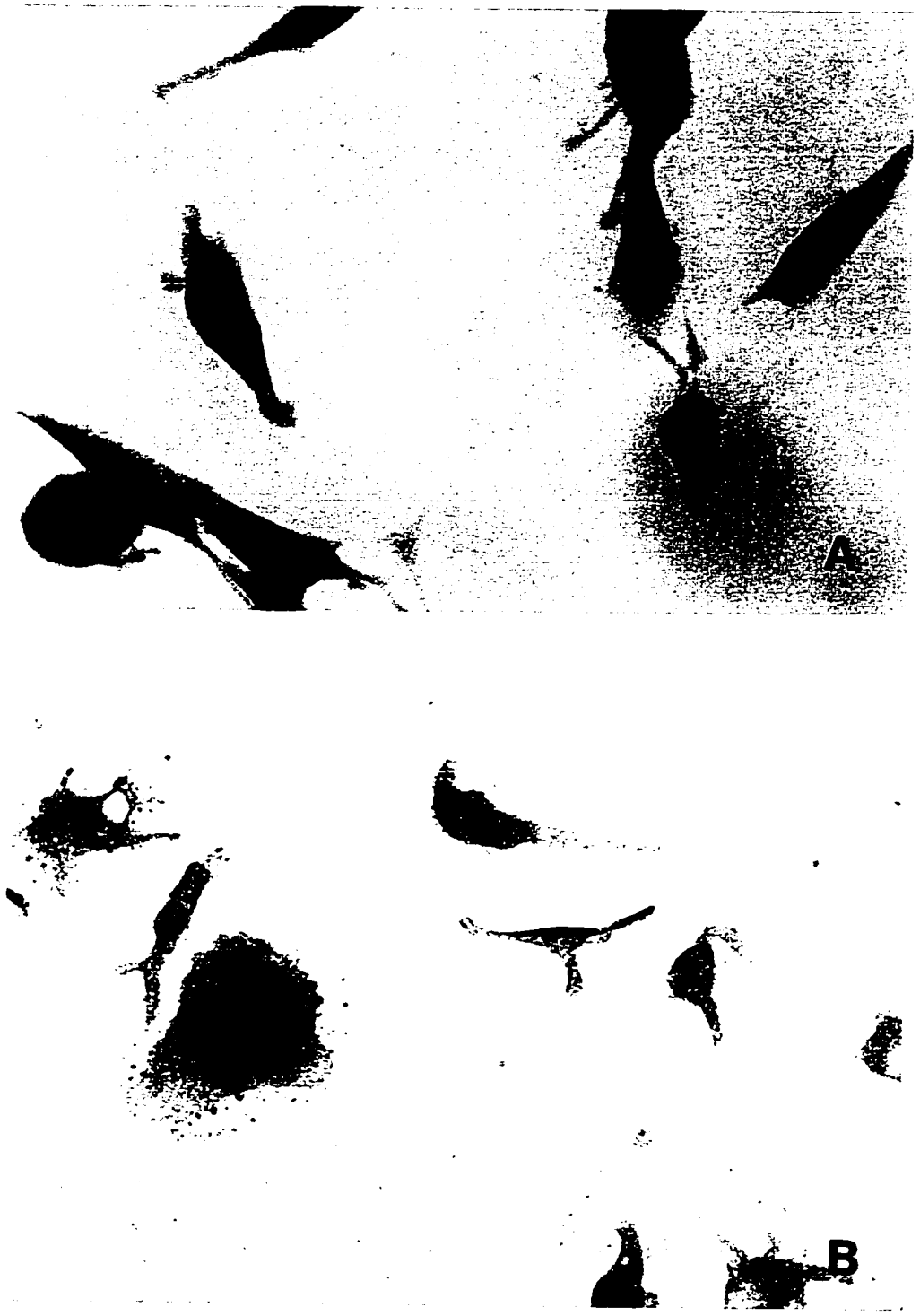

Figure 5-6 **Immunohistochemical localization of iNOS (using the anti-mac iNOS antibody) in MN-11 tumors.** (A), Granulocytes in the non-necrotic areas, iNOS (brown stain) counterstain, haematoxylin, × 200. Arrow points to the multi-lobed nuclei. (B) Granulocytes in the necrotic areas of the tumor, counterstain, haematoxylin × 400. No apparent immunostaining was detected in tumor cells.

Figure 5-6

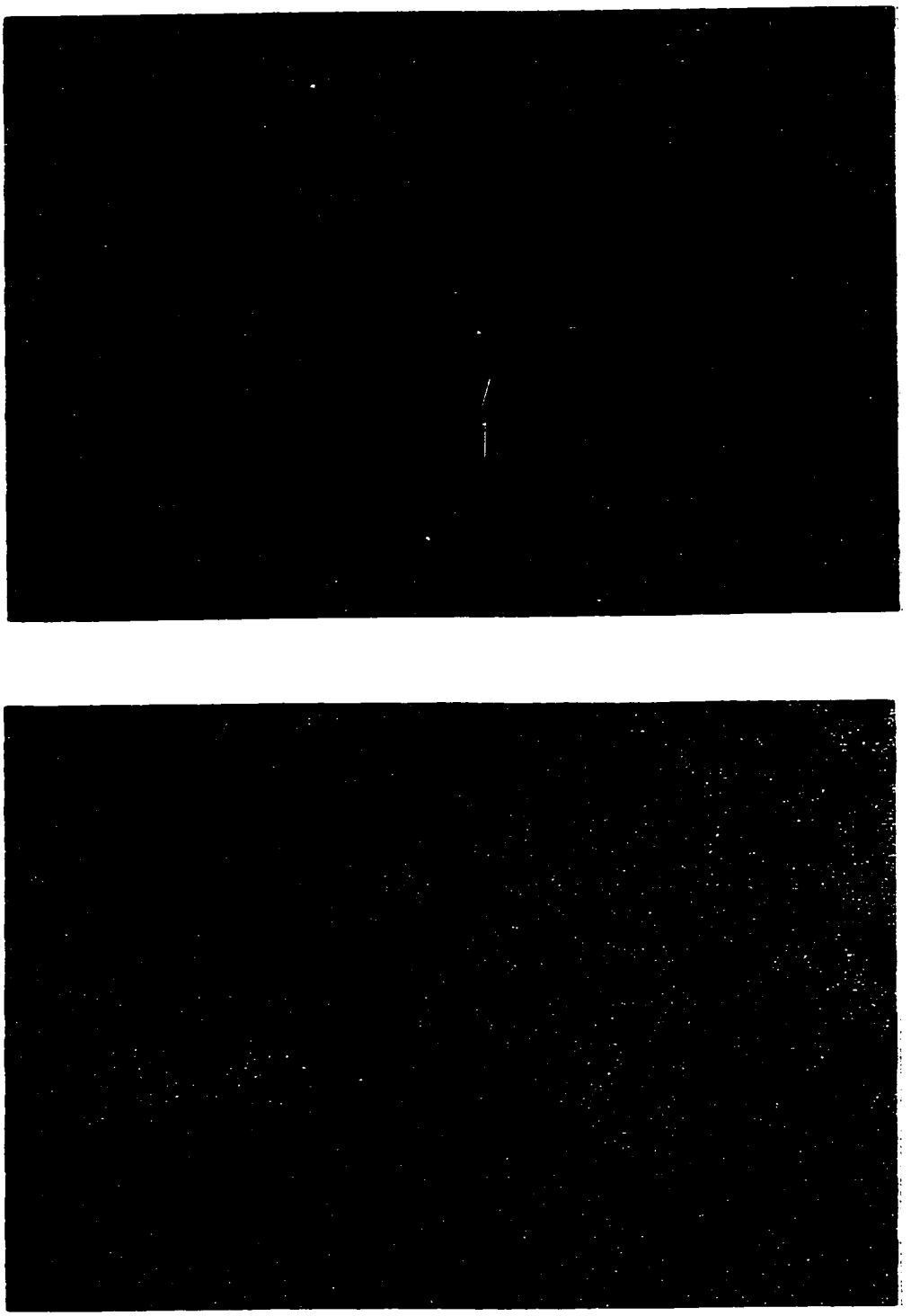

serum used as a negative control showed no staining of tumors or cultured cells.

5.3.6 *Demonstration of iNOS protein*

Immunohistochemical findings were confirmed by Western blot analysis of several tumor lysates. Gel electrophoresis identified an approximately 130 kDa protein using the anti-iNOS antibody in the control mouse macrophage lysate. Two of the 6 tumor lysates analyzed showed the presence of the 130 kDa protein (Figure 5-7). Parallel immunohistochemical analyses were not carried out.

5.3.7 *Correlation of MF with granulocytic infiltration*

The predominant host cell type of MN-11 tumors was granulocytes, identified using endogenous peroxidase activity (Chapter 3, section 3.3.5). To investigate the correlation between the number of these cells and MF, an experiment was conducted in which MF was determined in 20 control MN-11 tumors (14-19 days *in vivo* growth). In parallel, a section of the tumor tissue was frozen and quantified for granulocytic infiltration and necrosis. In four cases, the tumor was very small, sections were taken for granulocytic counts but the corresponding MF was not determined. Figure 5-8A shows a positive correlation between the number of infiltrating granulocytes and MF ($r = 0.70$, $p = 0.0007$ (non-parametric Spearman rank test)). Similar results were obtained for percent tumor necrosis and MF ($r = 0.76$, $p < 0.0001$, Figure 5-8B). When the same data was analyzed to correlate the number of infiltrating granulocytes and necrosis, a strong correlation was observed ($r = 0.66$, $p = 0.001$).

Figure 5-7 **Western blot analysis of MN-11 tumor lysates for iNOS.** Lane 1, contains positive control from mouse macrophage (RAW 264.7) cell line stimulated with IFN-γ plus LPS for 12 h provided by Transduction Laboratories. Lanes 2-7 contain protein lysates from MN-11 tumors. Loading control using antibody to β-tubulin showed equal protein in all lanes (data not shown).

Figure 5-7

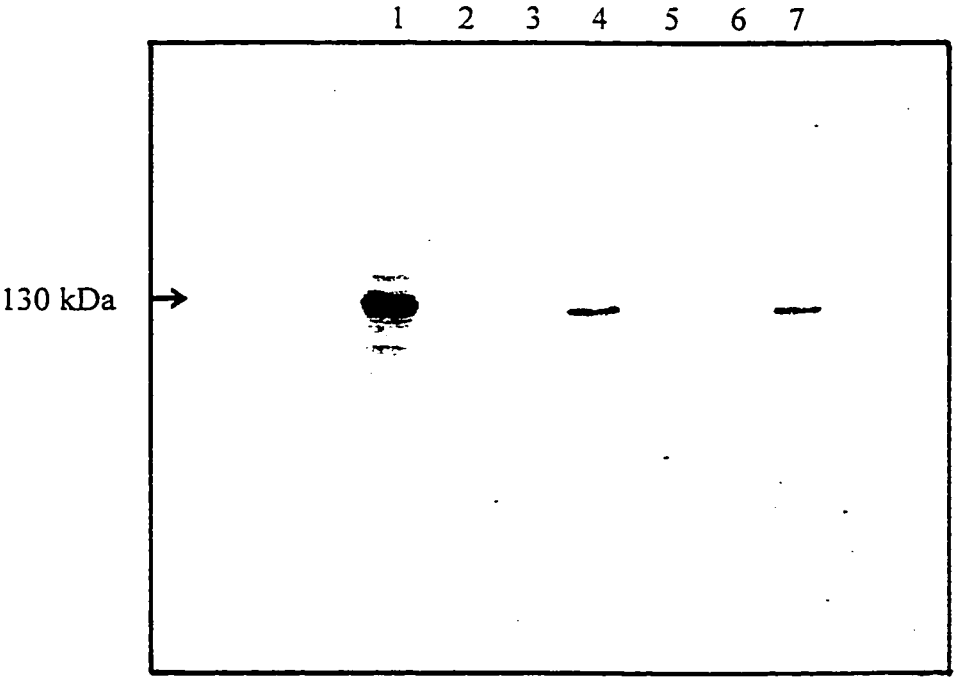

Figure 5-8 **Relationship between granulocytic infiltration (A), necrosis (B) and MF in MN-11 tumors.** Tumors were excised after 14-19 days of *in vivo* growth and MF determined. A section of the tumor was frozen and stained for endogenous peroxidase activity as described in Chapter 3, section 3.2.4 (a). Histological grading was done as described in section 5.2.8. All data are represented from 20 individual tumors.

Figure 5-8

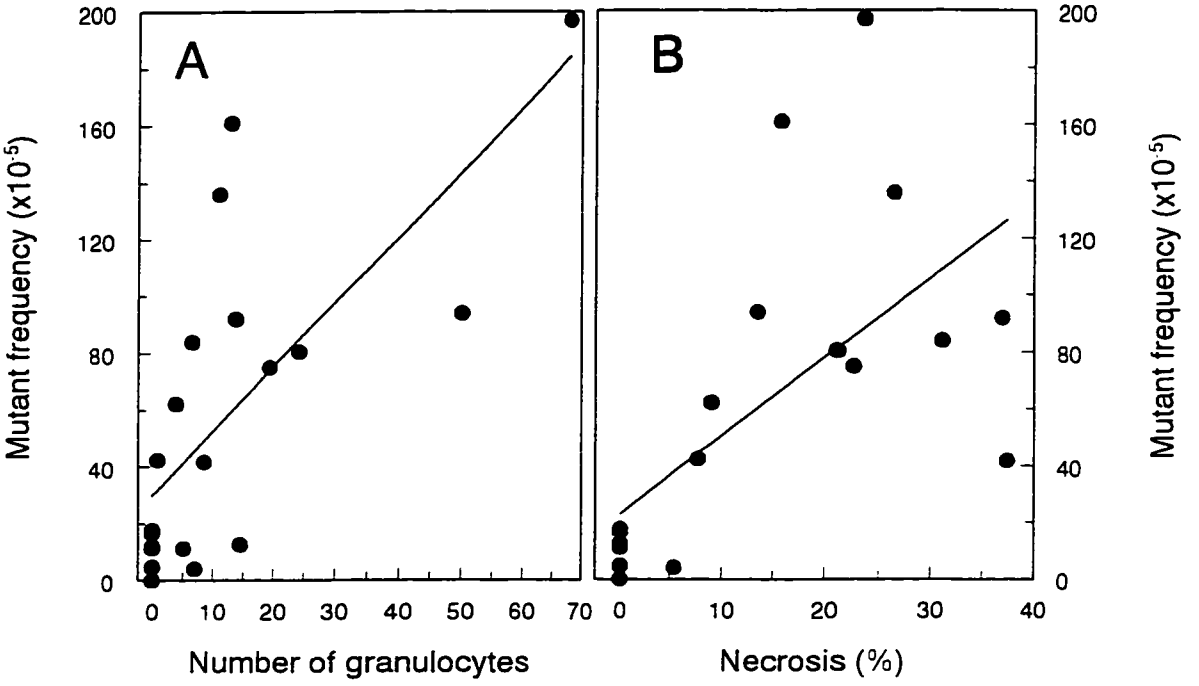
A
B
Mutant frequency (x10-5)
Mutant frequency (x10-5)
200
160
120
80
40
0
0 10 20 30 40 50 60 70
0 10 20 30 40
Number of granulocytes
Necrosis (%)

5.4 DISCUSSION

My earlier work has shown an increase in MF (3.64-fold) in cells recovered from tumors (Chapter 2, section 2.3.6) than in the same cells maintained in culture for an equivalent time. The inflammatory infiltrate consists primarily of granulocytes; however, macrophages, lymphocytes and mast cells were also found at the periphery of the tumor (Chapter 3, section 3.3.5). To investigate if the observed increase in MF might be due to RNS produced by infiltrating cells, tumors were characterized for iNOS expression and NOS activity.

Cultured MN-11 cells constitutively expressed both cNOS and iNOS enzymatic activities. The results of the histochemical study show the presence of NOS-related NADPH-d activity in cultured cells. Intense staining was also observed using the anti-mac iNOS antibody. When MN-11 cells were grown as tumors, they stained with NADPH-d. Both light and dark stained cells were observed. When tumors were stained with anti-mac iNOS antibody, staining was observed only in granulocytes and not in tumor cells. Taken together, this data suggests that the light stained cells may represent cNOS in tumor cells and the dark stained cells may represent iNOS in the phagocytic cells. Immunohistochemical localization of cNOS in tumor cells was not demonstrated. A number of studies have confirmed that nNOS can be labeled by NADPH-d technique [330-338]. NADPH-d activity is associated with all three forms of NOS (nNOS, eNOS and iNOS) and independent studies have shown that only different forms of NOS can withstand fixation with 4% paraformaldehyde [327]. In conclusion, NADPH-d histochemistry provides a simple and sensitive method to detect NOS-related activity. In cultured MN-11 cells, the expression of iNOS was not significantly increased after treatment with either combination of LPS and

cytokines or cytokines alone. Since very little accumulation of NO_2^- or NO_3^- was detected in culture supernatant of MN-11 cells it could be possible that these cells express an aberrant form of an enzyme that cannot be further induced. Studies have shown that other tumor cell lines can synthesize NO· [317,318,339]. A murine adenocarcinoma cell line expresses iNOS [339] and a neuroblastoma cell line contains cNOS. Human colon cancer cell lines also show a diverse pattern of expression of NOS and generation of NO·. SW-480 and SW-620 cells express iNOS constitutively resulting in the production of NO·. DLD-1 cells also produce NO·, but only after the induction of iNOS with LPS and/or cytokines. WiDr cells, however, appear not to produce NO· either before or after stimulation with a variety of LPS and/or cytokines combinations. SW-620 (metastatic) cells produce less NO· than SW-480 (non-metastatic) cells and this is due to the existence of an endogenous inhibitor of NOS [317]. Since MN-11 cells cannot be induced by the combination of LPS and/or cytokines tested, the possibility that these cells may contain endogenous inhibitors of cNOS or iNOS cannot be excluded. It may also be possible that the correct combination of LPS and/or cytokines was not determined in these experiments. Whether the failure of MN-11 cells to generate NO· is due to genetic abnormality or a deficiency in protein kinases that regulate NOS expression [340] remains unclear.

Macrophages were identified at the periphery of the tumor on the basis of non-specific esterase activity (Chapter 3, section 3.3.5). The presence of iNOS was shown in these cells, suggesting that they are activated. The contribution of NO· generated by tumor-associated macrophages in producing cytotoxicity and mutagenicity was explored *in vitro* by co-culture experiments (Figure 5-1). Unstimulated macrophages did not cause any significant increase in cytotoxicity and MF, suggesting no elaboration of any toxic

metabolites. No release of NO· occurred, confirmed by no accumulation of NO_2^- or NO_2^- + NO_3^-. When TPA was used to stimulate the respiratory burst, an increase in cytotoxicity and MF was observed. This increase may be attributed to the release of ROS and not RNS, since no NO_2^- or NO_2^- + NO_3^- accumulation occurred in the culture supernatant. Other reactive species, such as H_2O_2 and arachidonic acid metabolites may also have contributed to cytotoxicity and MF [325,341]. In another study, TPA stimulated macrophages showed induction of 5,6-ring-saturated thymine bases in NIH 3T3 cells [342], due to release of ROS. In MN-11 cells, a combination of IFN-γ plus LPS resulted in a 2.5-fold increase in cytotoxicity and MF. This increase may in part be explained by the finding that macrophages are major producers of NO·, since increased accumulation of NO_2^- or NO_2^- + NO_3^- was observed in culture supernatant of macrophages stimulated with IFN-γ plus LPS. That NO_2^- or NO_2^- + NO_3^- production and the observed cytotoxicity and MF was inhibited by L-NMMA, suggested that NO· produced by stimulated macrophages may mediate tumor cell cytotoxicity and mutagenicity. Other workers, using resident, periodate, casein or thioglycollate-elicited macrophages, have also reported that co-treatment with IFN-γ and LPS was a more potent inducer of NO· production than either alone [313,341,343]. NO· has been implicated as a major cytolytic and cytostatic factor in macrophage-mediated tumor cell cytotoxicity under *in vitro* conditions [96,166,322]. These experiments suggest that NO· generated by tumor-associated macrophages can cause cytotoxicity and mutagenicity in MN-11 cells. However, activation of macrophages with LPS also leads to the generation of numerous proinflammatory cytokines (IL-1, TNF-α, IFN-γ) or PAF, which may have effected these results.

A weak but significant correlation was found between total NOS, iNOS activity and

MF. This suggests that endogenously generated NO· by infiltrating granulocytes and macrophages in MN-11 tumors may contribute to the increase in MF. Western blot studies revealed a protein band of 130 kDa that corresponds to the known macrophage iNOS [344]. However, only 2 of the 6 tumors analyzed showed the presence of the iNOS protein, suggesting it is due to infiltration of inflammatory cells in these tumors. These data do not show the cell types that may be involved. Immunohistochemistry suggests that the source of NO· was iNOS in the inflammatory infiltrate, predominantly in granulocytes and to a lesser extent in macrophages and mast cells. No immunoreactivity was observed in tumor cells, lymphocytes or vascular endothelial cells. This contrasts with our *in vitro* observation showing positive staining for iNOS and NADPH-d in MN-11 cells. A possible explanation for this could be that there exist factors in the fetal calf serum that may cause induction of iNOS. Alternatively there may be factors in the tumor milieu that may inhibit iNOS in MN-11 cells. The regulation of iNOS is complex and occurs at transcriptional and posttranscriptional levels [345] which may reflect its nature to be turned on and off in the presence/absence of different factors.

The cause of relatively high levels of iNOS expression and iNOS activity in MN-11 tumors is not known. Mice with various infections show increased NO· production [346], but it is unlikely that our results were affected by infection. No correlation was observed between the NOS activities in tumors on the right and left flanks (data not shown), suggesting that systemic factors were not influencing MF. Each tumor may contain a variable number of inflammatory cells that may be responsible for the variation in MF observed in different tumors.

Granulocytes are the primary infiltrate of MN-11 tumors (Figure 5-6 A & B). A

positive correlation between number of infiltrating granulocytes and MF suggests that the NO· generated by iNOS expressed in these cells may contribute to an increase in MF observed *in vivo*. The chemokines that may increase the infiltration of inflammatory cells and their cellular source remains to be identified in MN-11 tumor. IL-8 is a member of the chemokine family that is a potent chemoattractant for granulocytes and stimulates granulocytic adhesion, respiratory burst, and degranulation [347]. Other cytokines like TNF-α and IFN-γ can act synergistically to stimulate NO· generation by induction of iNOS [348]. MN-11 cells were derived from a male C57BL/6 mouse treated with methylcholanthrene [197,198]. It is possible that these cells produce TNF-α since other methylcholanthrene induced fibrosarcomas are known to produce both TNF-α and IL-1 [349] and these cytokines can in turn induce iNOS.

Macrophages have also been shown to cause mutagenicity and induce DNA strand breaks [323-325,350-352] in tumor cells. These cells not only produce ROS but mouse macrophages have been shown to express iNOS that produces NO· in large amounts [159, 353-356]. Our data also shows that macrophages can induce cytotoxicity and mutagenicity in MN-11 cells in co-culture experiments. Nonspecific esterase staining showed that MN-11 tumors have very few macrophages compared with granulocytes and they are predominantly confined to the periphery of the tumor. Thus, it is more likely that granulocytes and not macrophages in MN-11 tumors provide a significant contribution to the observed increase in MF.

The preliminary data presented in this chapter suggests that NO· produced by granulocytes may be involved in the increase in MF observed in MN-11 tumors. The importance of NO· has been shown in inflammatory diseases [118,121,122,124,125,130,

347,356-361] and in tumor-associated macrophages [135]. The infiltration of granulocytes in MN-11 tumors could be increased by injecting cytokines to the tumor-bearing animals. The role of NOS could be tested by blocking endogenous production of NO· by specific inhibitors of iNOS to determine its effect on MF. These experiments would strengthen our hypothesis that increased granulocytic infiltration may be responsible for the increase in MF and are currently underway in our laboratory.

CHAPTER 6

VITAMIN E INHIBITS CYTOTOXICITY AND MUTAGENICITY OF NITRIC OXIDE-DONATING DRUGS *IN VITRO* AND *IN VIVO*

ABSTRACT

There is considerable interest in the pathophysiological role of NO·. This reactive nitrogen species is generated enzymatically by NOS but also released by nitrovasodilators. *In vivo* mutagenicity by such drugs has never previously been demonstrated. The MN-11 tumor model system appears to allow recovery of chromosomal mutations (multi-locus deletions) that would otherwise be lethal because the cells are unusual in that they are heterozygous at the X-linked *HPRT* locus. In this chapter, I show that NO-donating drugs are mutagenic in tumor-bearing animals. MF is expressed as mutants per 10^5 clonable cells. As a basis for comparison, animals bearing 12-day old tumors were exposed to ^{137}Cs γ-radiation and cisplatin, known DNA damaging agents. Each caused a dose-dependent increase in MF; radiation induced 103 mutants per Gy and cisplatin induced 59 mutants per mg/kg above background. The mutagenic effect of a single i.p. dose of NO-donating drugs administered at day 12 was tested. GTN (5 mg/kg) induced 310 ± 99 (mean ± SEM, n=14) mutants above background and MOL (100 mg/kg) induced 47 ± 8 (n=6) mutants. None of these treatments produced observable toxicity in the animals in the 2 day period between administration of radiation or drug and sacrifice of the animal. Protection against mutant induction by an antioxidant was tested. Animals were fed a dietary supplement of vitamin E (α-tocopherol acetate, 100 mg/kg/day) for 19 days prior to GTN treatment which resulted in a 82% decrease in MF. Vitamin E also decreased MF *in vitro*. Pretreatment of cells with 100 μM α-tocopherol for 24 h decreased GTN induced mutants by 84% and sodium nitroprusside induced mutants by 82%. Since NO· may be an important endogenous cancer risk factor, protection by vitamin E in our experiments may help to explain its anticancer action in humans.

6.1 INTRODUCTION

Nitric oxide and RNS are chemically reactive species that can have detrimental as well as beneficial roles. A relatively large amount of NO· is generated at sites of inflammation enzymatically by phagocytic cells (macrophages and polymorphonuclear cells) and other cell types, where it may be cytotoxic and genotoxic. NO·, delivered as gas or by nitrovasodilators is also used therapeutically [362]. Organic nitrates, such as nitroglycerin (GTN), and SNP have long been used as smooth muscle relaxants in the treatment of angina pectoris, coronary vasospastic disorders and hypertension. More recently, inhaled NO· (5-80 ppm) has been used as a pulmonary vasodilator in patients with pulmonary hypertension [363], adult respiratory distress syndrome and congenital diaphragmatic hernia [89]. Only a few studies of mutagenicity/carcinogenicity of GTN and NO-donating drugs in animals have been reported; evidence of carcinogenicity was reported in rodents, but only after massive doses and prolonged administration[310,364,365]. There is no prior evidence of mutagenicity/carcinogenicity of these agents in humans, although NO· produced by phagocytic cells (macrophages and polymorphonuclear cells), epithelial and endothelial cells has come under suspicion as a genotoxic species since chronic inflammatory conditions have long been known to be risk factors for cancer [45,55,155]. Nitrotyrosine, a marker of peroxynitrite damage, has also been shown to be present in inflamed tissues [132,241,309,366]. Mannick *et al.* [241] reported that patients recovering from *H. pylori* gastritis, who were given antioxidant vitamins (β-carotene and vitamin C), had a significantly decreased level of iNOS and nitrotyrosine in their gastric epithelial cells. Although NO· has been shown to be mutagenic *in vitro* [157,158,312], there has been no previous reports of mutagenicity by NO-donating drugs *in vivo*.

MN-11 cells grow as s.c. murine tumors and have been engineered to allow sensitive detection of mutations at the *HPRT* locus. Indirect evidence indicates that chromosomal mutations (multi-locus, large-scale deletions) can be detected at this site. Using this model system, a 3.64-fold increase in MF has been observed in s.c. tumors as compared to parallel *in vitro* cultures (Chapter 2, [1]). More recently, it was also shown that some NO-donating drugs (but not others) can induce $HPRT^-$ mutations in MN-11 cells *in vitro* (Chapter 4, [194]). In this chapter, I have shown, for the first time, that NO-donating drugs are mutagenic in tumor-bearing animals and that vitamin E (α-tocopherol) strongly protects against mutant induction, both *in vitro* and *in vivo*.

6.2 MATERIALS AND METHODS

All materials, chemicals and composition of solutions used in these experiments are found in Appendix II.

6.2.1 *Cell culture*

MN-11 cells were grown as described in Appendix IV, section IV.1. (R,R,R)α-tocopherol was dissolved in ethanol and absorbed to 10% fetal calf serum as described [367]at the indicated concentrations. The final concentration of ethanol in the samples with α-tocopherol was between 0.01-1%.

6.2.2 *Mutation induction by clastogenic and NO-donating drugs in tumor-bearing animals*

Experimental tumors were established by s.c. injection of MN-11 cells into the flanks of C57BL/6 female mice, 8-10 weeks of age, as described in Appendix IV, section IV.3.

Tumors were allowed to form for 12 days and then mice were exposed to one of the following conditions. Animals were whole-body irradiated with ^{137}Cs γ-rays (0-5 Gy) from a ^{137}Cs source at a dose rate of 1.15 Gy/min. Cisplatin and NO-donating drugs (GTN and MOL) were diluted in sterile PBS immediately before use and injected i.p. bilaterally. Control animals received vehicle (PBS) only. Dietary vitamin E (d-α-tocopherol acetate, 100 mg/kg/day) was administered by diluting it in soy oil and adding the liquid to dry laboratory chow pellets. Animals were isolated, 1 per cage, to ensure that the pellet was consumed. Control animals were treated similarly. Where indicated, this diet supplement was initiated 7 days prior to tumor cell injection and continued throughout the course of the experiment. Two days after mutagenic treatments, animals were sacrificed by cervical dislocation, tumors recovered and processed. For all experiments, an *ex vivo* expression period of 8 days was employed, following which MF was determined as described in Appendix IV, section IV.3.

6.2.3 *Cytotoxicity and mutagenicity of NO-donating drugs; effect of vitamin E*

Cultures were trypsinized and 5×10^5 viable cells per 10 cm dishes were allowed to attach overnight. Cells were preincubated for different time intervals with various concentrations of α-tocopherol (as shown in figure legends), washed twice with PBS and then exposed to NO-donating drugs for 24 h. Unless otherwise indicated, all experiments with SNP were done in the presence of the cyanide scavenging system (8 units/mL of rhodanese + 5 mM $Na_2S_2O_3$). Following exposure to the NO-donating drugs, cultures were washed twice with PBS, trypsinized and split into two set of dishes. Cytotoxicity and MF was determined as described in Appendix IV, section IV.2.

6.2.4 *Measurement of nitrite in MN-11 cells preincubated with vitamin E and treated with NO-donating drugs*

Replicate cultures of 2×10^5 cells in 1 mL of phenol red-free DMEM containing 10% fetal calf serum were allowed to attach for 6 h in 24 well dishes. Cells were washed once with PBS and fed with phenol red-free DMEM containing α-tocopherol (100 μM), prepared as described above (final ethanol concentration, 0.2 %) for 24 h. Cells were washed once again with PBS and fed with phenol red-free DMEM + 10% fetal calf serum containing the NO-donating drugs for 24 h. At the end of the incubation supernatant was collected and analyzed by Griess reagent essentially as described previously (Chapter 4, section 4.2.5).

6.2.5 *Characterization of Radiation and GTN induced mutants*

(a) 5-azacytidine treatment. In these experiments, the possibility that methylation of the *HPRT* gene was responsible for the $HPRT^-$ phenotype in GTN induced mutants was also tested. $6\text{-}TG^R$ colonies were obtained following treatment of the tumor-bearing animals with GTN (as described in section 6.2.2), cloned and established in culture. Prior to 5-Aza-Cyd treatment, all $6\text{-}TG^R$ clones were grown in non-selective complete medium for 30 days with subculturing as needed. The cytotoxic effect of 5-Aza-Cyd on mutant cells was determined by incubating 200-500 cells per 6 cm dishes in the presence of 0-5.0 μM 5-Aza-Cyd for 48 h. After 9 days, colonies were fixed, stained and scored as described in Appendix IV, section IV.4. Reactivation studies were carried out by seeding exponentially growing cultures into 10 cm dishes (2×10^5 cells per dish), allowing attachment for 6 h and then treating with the indicated concentration of 5-Aza-Cyd for 48 h. Following treatment, dishes were washed twice with PBS, cultured in non-selective medium for an additional 48

h, and split into two sets of dishes. 1×10^5 cells per 10 cm dishes were challenged with HAT to determine the reversion frequency. 200 cells per 6 cm dishes were seeded in parallel in non-selective complete medium to determine the plating efficiency. Cultures were refed with HAT-medium twice weekly. HAT^R ($HPRT^-$) colonies were fixed, stained and scored after 2 weeks. HAT^R colonies are expressed as colonies per 1×10^5 viable cells, where viability was determined from the plating efficiency. Control "reactivation" experiments were performed using C86AGM2 cells (obtained from Dr. M. W. McBurney) [368]. Survival and reversion frequencies were determined as described above.

(b) Karyotype analysis. Progenitors of MN-11 cells contain 3 copies of X chromosome [1]. It was suspected that a proportion of the $HPRT^-$ mutants might have lost one whole X chromosome. Chromosome preparations were prepared by culturing cells in 0.1 μg/mL colcemid for 2 h at 37°C, harvesting, and treating with 75 mM KCl for 15 min at 37°C before being fixed in three changes of methanol:acetic acid (3:1, v/v). The fixed cells were dropped onto wet slides and dried at 55°C for 2 h. Slides were then passed through ascending grades of ethanol to 100%, denatured at 70°C in 70% formamide/2× SSC for 2 min and again passed through ascending grades of ethanol to 100%. Prehybridization mix (50% formamide, 10% dextran sulfate, 2× SSC, 1 μg/mL salmon sperm DNA) was denatured at 70°C for 2 min, cooled on ice, and then applied to slides for 1 h at 37°C. Karyotype analysis was carried out using an X centromeric-specific probe (DXWas70) labeled with biotin by nick translation or random priming. Hybridization mixture was prehybridization mix including 100 ng of labeled probe, denatured at 75°C for 10 min and then transferred to ice. This mixture (10 μL) was applied to the slide under a 22 × 22 mm coverslip, sealed with rubber cement and incubated at 37°C for 16-20 h. Slides were then

washed three times in 50% formamide/2× SSC, three times in 2× SSC and twice in PN buffer (Appendix II) for 5 min at 45°C. Detection of biotinylated DNA was accomplished with two layers of avidin-FITC as described [369]. Representative cells were photographed using a Zeiss Axioskop 20 microscope. These experiments were done in collaboration with Dr. David Blakey at Bureau of Chemical Hazards, Environmental Health Directorate, Health and Welfare, Canada.

6.2.6 in vitro *growth rate determination*

Growth rate of MN-11 cells in the presence of 5-Aza-Cyd or NO-donating drugs was established by plating 2×10^4 cells per 6 cm dishes and measuring the increase in cell number with a Coulter counter over a 6 day period. Cell doublings were calculated from the logarithmic phase of the growth curve.

6.2.7 *Statistical analysis*

Data from animal experiments are expressed as mean ± SEM, but were analyzed using a non-parametric Mann-Whitney test. A 2 tailed p value of ≤ 0.05 was considered to be statistically significant (shown as *) or $p \leq 0.01$ was considered to be highly statistically significant (shown as **).

6.3 RESULTS

6.3.1 *Induction of mutants in tumor-bearing animals by known clastogenic agents*

Ionizing radiation and the antitumor drug cisplatin are well known chromosome and DNA breaking agents. Our previous *in vitro* studies have shown that MN-11 cells are

sensitive to mutant induction by both ^{60}Co γ-rays and ^{137}Cs γ-rays (Chapter 2 & 4). As a measure of the sensitivity of MN-11 tumors for detecting mutants *in vivo*, tumor-bearing animals were either exposed to ^{137}Cs γ-radiation or injected with cisplatin. In Figure 6-1A, the effects of ^{137}Cs γ-radiation on mutant induction are shown. MF increased with dose of ^{137}Cs γ-rays; cells were challenged with 6-TG on day 8 post-irradiation. Mutant induction was almost undetectable when cells were challenged on day 4 post-irradiation (data not shown). The calculated increase in MF from regression analysis was 103 mutants per Gy. The *in vitro* cytotoxic and mutagenic effects of cisplatin in MN-11 cells were also studied. The survival curve showed no detectable shoulder. A dose-dependent increase in cytotoxicity and mutation induction was observed. The D_0 dose was 0.45 μg/mL and the number of mutants induced was about 90 per 10^5 cells (Figure 6-1B, inset). As expected, cisplatin was also found to be mutagenic (Figure 6-1B), causing a dose-dependent increase in MF. The calculated increase in MF was 59 mutants per mg/kg. The cloning efficiency of cells recovered from tumors treated with 5 mg/kg cisplatin and 5 Gy of radiation was significantly lower than the vehicle-treated tumors (data not shown).

6.3.2 *Mutant induction by NO-donating drugs in tumor-bearing animals*

Exposure of rats to NO· and NO_2 gases has previously been shown to induce ouabain-resistant mutants in explanted lung cells [62]. There are no previous studies of the mutagenicity of NO-donating drugs *in vivo*. The ability of two clinically used nitrovasodilators, GTN and MOL, to induce mutants in MN-11 tumor-bearing animals was tested. GTN produced an increase in MF with non-linear dose-response kinetics (Figure 6-2A); a threshold was observed with a significant increase seen at 5 mg/kg. At this dose, the

Figure 6-1 **Mutation induction by DNA damaging agents in tumor-bearing animals.** (A), ^{137}Cs γ-radiation; (B), cisplatin. Four to 8 animals were treated at each dose. Treatments were on day 12 after tumor cell inoculation. Tumors were excised on day 14, cells were cultured for 8 days and challenged with 50 μM 6-TG to determine MF. The symbols and error bars represent means ± SEM. Where no error bars are shown, they are within the symbol. Inset in (B) shows the cytotoxic and mutagenic effects of cisplatin in cultured MN-11 cells. Cell cultures were exposed to cisplatin for 24 h in complete medium at 37°C. Following treatment cultures were washed with PBS and replaced with complete medium. Cytotoxicity and mutagenicity was determined as described above. Error bars indicate the mean ± SEM of 2-5 independent experiments involving 4-5 dishes at each experimental point.

Figure 6-1

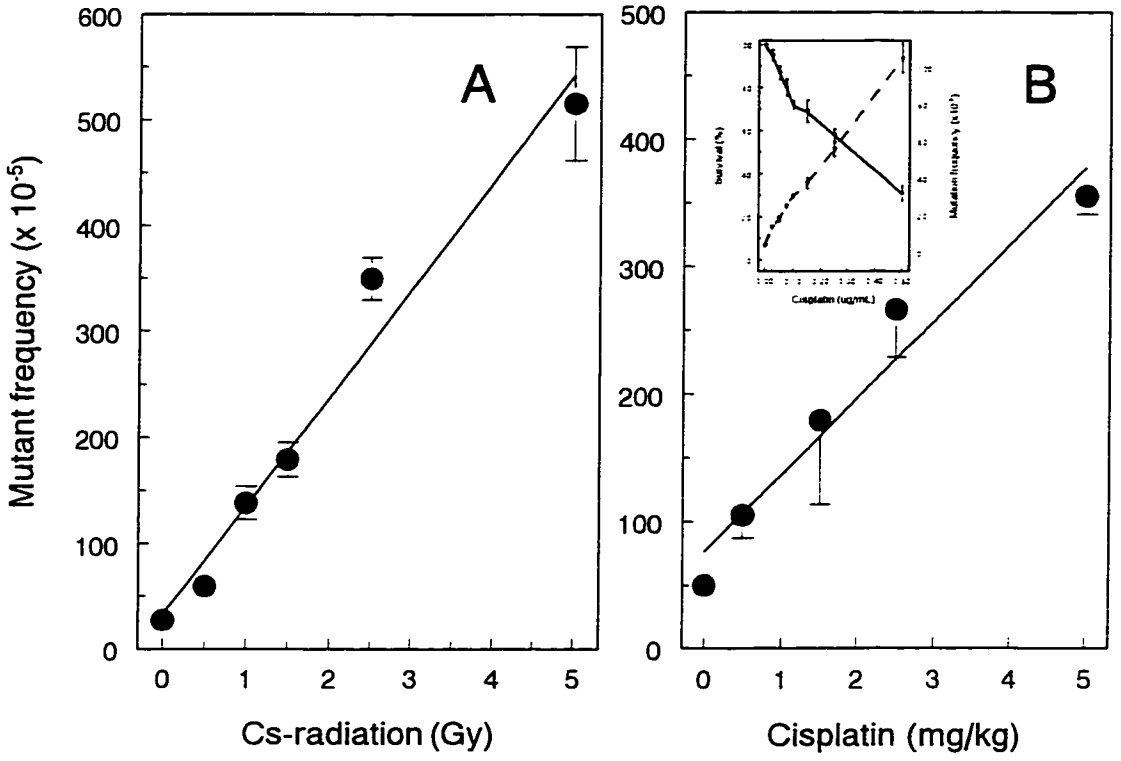
A
B
Mutant frequency (x 10-5)
Cs-radiation (Gy)
Cisplatin (mg/kg)
600
500
400
300
200
100
0
0
1
2
3
4
5

Figure 6-2 **Mutation induction by NO-donating drugs in tumor-bearing animals.** In panels (A) and (B), 5 animals were used for each dose; the mean MF ± SEM are shown.. On day 12, animals were injected i.p. with the respective NO-donating drug, tumors excised on day 14, established in culture and MF determined. (A) GTN. At the highest dose, the mean MF was 146.2×10^{-5}, calculated for 4 tumors. A fifth tumor, whose MF was very much higher (1333×10^{-5}), is shown separately as a square symbol. (The median for the 5 tumors was 137×10^{-5}). Difference between control and GTN (5 mg/kg) treated group is statistically significant (Mann Whitney test, $p = 0.03$). (B), MOL. At the highest dose, the mean MF was 65.8×10^{-5} (median MF was 70.0×10^{-5}) (n = 5). Difference between control and MOL (100 mg/kg) treated group is statistically very significant (Mann Whitney test, $p = 0.004$).

Figure 6-2

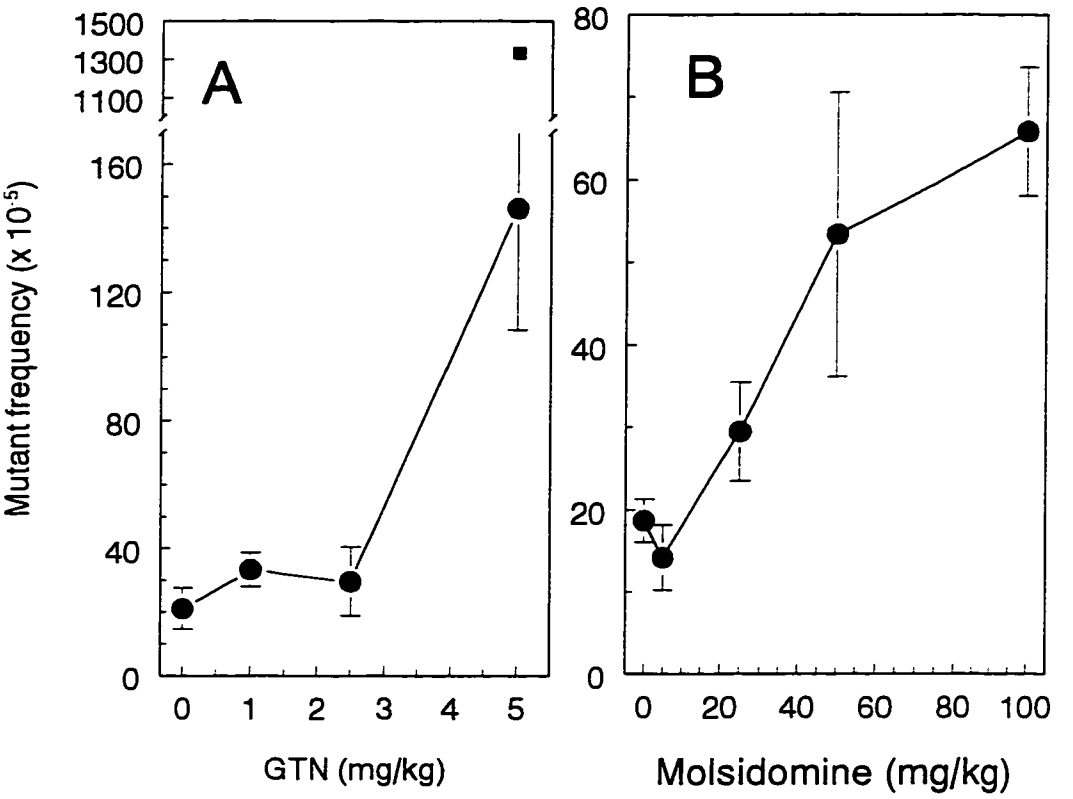
A
B
Mutant frequency (x 10⁻⁵)
1500
1300
1100
160
120
80
40
0
80
60
40
20
0
0 1 2 3 4 5
GTN (mg/kg)
0 20 40 60 80 100
Molsidomine (mg/kg)

MF was $146.2 \times 10^{-5} \pm 37.8 \times 10^{-5}$ (n = 4) (mean ± SEM). A fifth animal in this group showed a remarkably high MF (1333 per 10^5 cells) and is shown as a separate data point in the figure. Treatment with MOL showed an essentially dose-dependent increase in MF (Figure 6-2B). The MF observed at the highest dose, 100 mg/kg was $65.8 \times 10^{-5} \pm 7.8 \times 10^{-5}$ (n = 5) . Treated animals showed no obvious toxicity with either GTN or MOL. The cloning efficiency of cells derived from the tumors was unaffected by treatment with these drugs (data not shown). Histologically, there were no observed differences in either the vascularity of tumors or the number of infiltrating phagocytic cells in GTN-treated tumors compared to the vehicle-treated controls at the time of resection, 2-3 days after drug administration.

6.3.3 *Effect of dietary vitamin E on GTN induced mutations in tumor-bearing animals*

An experiment was carried out to explore whether a lipophilic antioxidant, vitamin E, could protect against mutagenicity induced by GTN (Figure 6-3A). One group of animals was fed normal laboratory chow and injected with 5 mg/kg GTN at day 12 after inoculation with tumor cells. A second group was provided with vitamin E dietary supplements (100 mg/kg per day) for 19 days prior to GTN treatment. A control group received no GTN and no vitamin E. In the absence of vitamin E supplements, the MF in GTN-treated animals was $329 \times 10^{-5} \pm 88.4 \times 10^{-5}$ (n = 9) (mean ± SEM). Vitamin E-supplemented animals had a markedly reduced MF, $92.5 \times 10^{-5} \pm 15.9 \times 10^{-5}$ (n = 11). The MF in the control group was $39.4 \times 10^{-5} \pm 7.0 \times 10^{-5}$ (n=7) . Inhibition of MF by vitamin E was 71.9% (81.7% if the MF of the control group is subtracted). The effects of vitamin E on the *spontaneous* MF was also tested in 3 independent trials (Figure 6-3B). Vitamin E reduced the MF by 47.3%,

Figure 6-3 **Effect of dietary vitamin E on induced and 'spontaneous' mutant frequencies in tumor-bearing animals.** (A), GTN and vitamin E. Three groups were subjected to the following treatments: I) injection with PBS; ii) injections with GTN (5 mg/kg) iii) Vitamin E supplemented diet (100 mg/kg/day for 19 days) and then injection with GTN. The mean MF in GTN-treated animals was 329×10^{-5} (n = 9) and 92.5×10^{-5} (n = 11) for vitamin E-supplemented animals. The respective median values were 255 and 98.5. The spontaneous mean MF was 39.4×10^{-5} (median MF was 34.1) (n = 7). Difference between GTN and GTN+vitamin E groups is statistically significant ($P = 0.05$). (B), Effect of vitamin E on the spontaneous MF. Three independent experiments carried out over the course of 1 year are shown. The number of animals in each group is shown in parentheses. Solid bars are animals treated with vitamin E as described in Materials and Methods. Differences between animals fed normal laboratory chow and those supplemented with vitamin E groups is statistically highly significant ($P = 0.0015$) for experiment 2 and statistically significant ($P = 0.03$) for experiment 3.

Figure 6-3

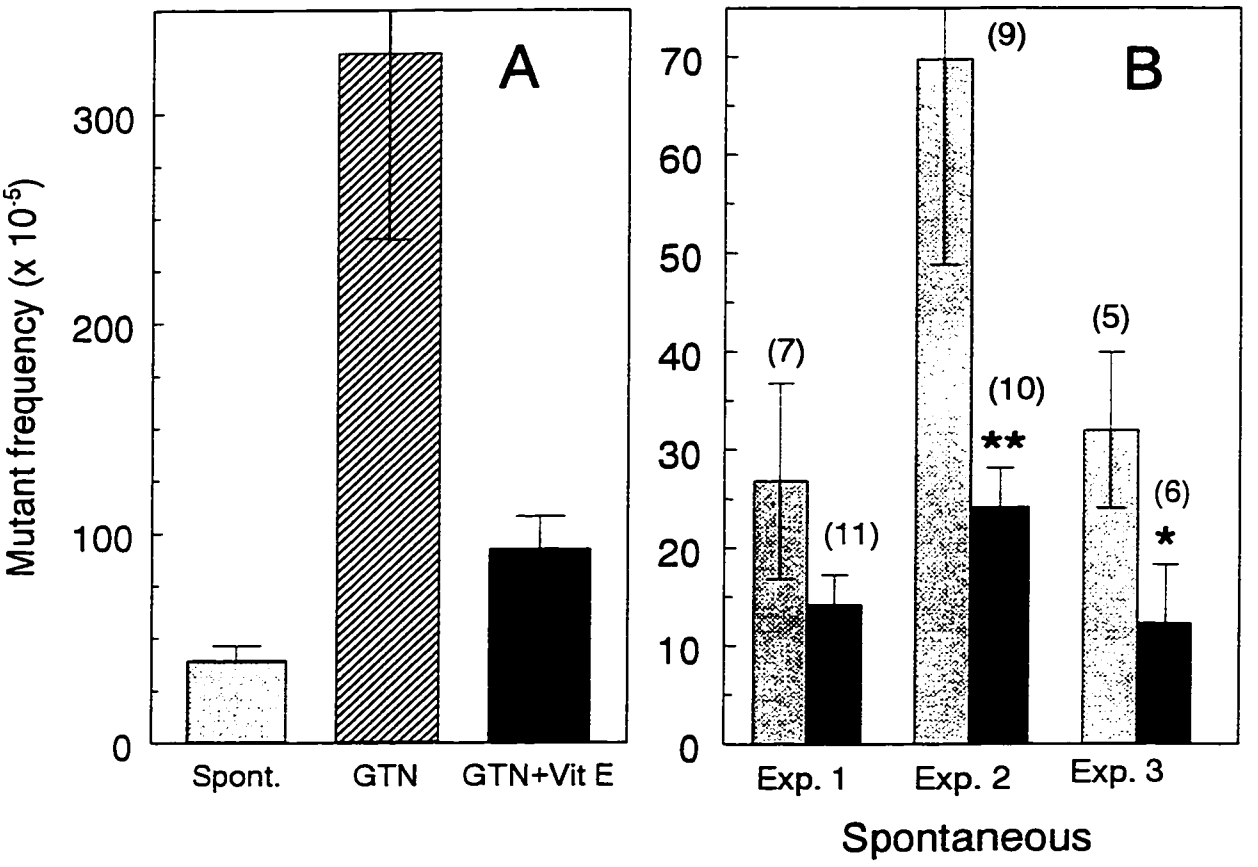
Mutant frequency (x 10-5)
300
200
100
0
A
Spont.
GTN
GTN+Vit E
70
60
50
40
30
20
10
0
B
(7)
(11)
(9)
(10)
**
(5)
(6)
*
Exp. 1
Exp. 2
Exp. 3
Spontaneous

65.4% and 61.9%, respectively, in the three trials. Vehicle (soy-oil) supplementation did not show any protection against GTN induced mutagenicity (data not shown).

6.3.4 *Effect of Vitamin E on mutagenicity and cytotoxicity induced by NO-donating drugs in vitro*

To better understand the mechanisms involved, *in vitro* cytotoxicity and mutagenicity studies were carried out. Treatment of MN-11 cells with 0.5 mM SNP for 24 h reduced survival to 56%. In the presence of a cyanide scavenging system, survival was increased to 82% (Figure 6-4A). α-Tocopherol was also tested for its possible protective activity against NO·-mediated cytotoxicity; the vitamin was added to MN-11 cells 24 h prior to addition of SNP at concentrations upto 1000 μM (Figure 6-4A). Preincubation with 1 or 10 μM failed to provide any significant protection while near-maximal effect was seen at 50 μM with little further protection at higher concentrations. GTN (0.44 mM) reduced survival to 51% (Figure 6-4B) which was significantly increased with 6 h preincubation with α-tocopherol (100 μM) and completely protective at 24 h. Preincubation of MN-11 cells with 25-1000 μM α-tocopherol for 24 h did not cause any cytotoxicity (Figure 6-4C).

SNP induced about 28 mutants per 10^5 cells in the presence of the cyanide scavenging system. α-Tocopherol at 100 μM did not protect against mutagenicity when added immediately prior to the addition of SNP. A slight decrease in MF was observed when MN-11 cells were preincubated with α-tocopherol for either 2 or 6 h, respectively (data not shown); however, 24 h preincubation reduced the MF by 82% (Figure 6-5). GTN at 0.44 mM induced about 20 mutants per 10^5 cells, which was also reduced by 84% when cells were preincubated with 100 μM α-tocopherol for 24 h (Figure 6-5).

Figure 6-4 **Effect of vitamin E on cytotoxicity of NO-donating drugs on MN-11 cells in culture.** Error bars represent mean ± SEM (n = 3 independent experiments, each involving 3 replicate dishes at each experimental point). (A), Dose-dependent protection of MN-11 cells from SNP (0.5 mM) induced cytotoxicity by α-tocopherol (solid bars). Increasing doses of α-tocopherol were added to MN-11 cells 24 h prior to addition of SNP. Survival was determined after 24 h of incubation. (0+), SNP in the presence of the cyanide scavenger (rhodanese + thiosulfate). Difference between MN-11 cells treated with SNP and those preincubated with 50 μM α-tocopherol and then treated with SNP is considered to be statistically significant (2 tailed p = 0.016). (B), Effect of preincubation of α-tocopherol (100 μM) on GTN (0.44 mM) induced cytotoxicity. MN-11 cells were preincubated at various time points with α-tocopherol, treated with GTN for 24 h and survival determined (solid bars). Difference between MN-11 cells treated with GTN and those preincubated with α-tocopherol for 6 h (p = 0.01) or 24 h (p = 0.0006) and then treated with GTN is statistically significant. Hatched bars in A and B represent survival (%) of MN-11 cells in the presence of SNP and GTN, respectively. (C), Effect of increasing concentrations of α-tocopherol on MN-11 cells. Treatment of vehicle (0.1-1% ethanol) had no cytotoxic effect (data not shown).

Figure 6-4

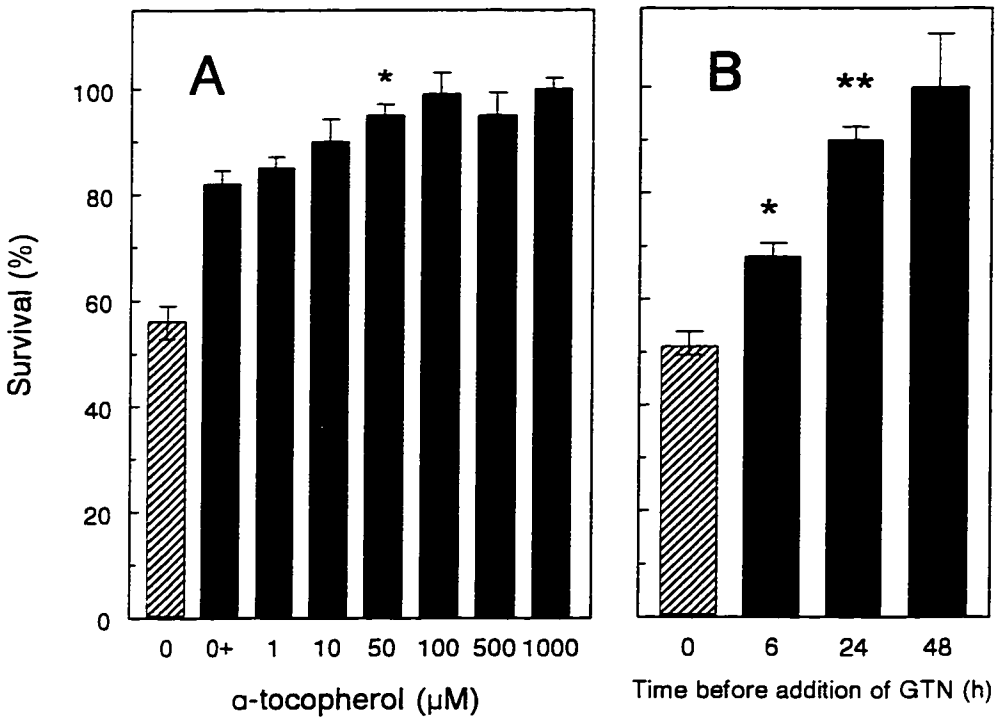
A
B
*
*
**
Survival (%)
100
80
60
40
20
0
0
0+
1
10
50
100
500
1000
α-tocopherol (μM)
0
6
24
48
Time before addition of GTN (h)

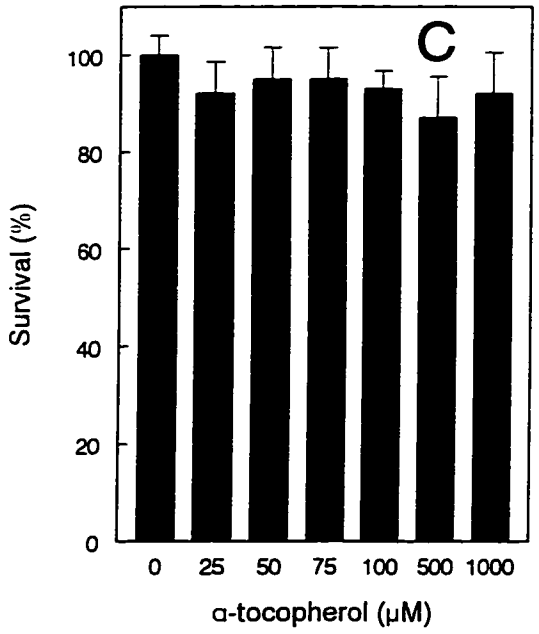
C
Survival (%)
100
80
60
40
20
0
0
25
50
75
100
500
1000
α-tocopherol (μM)

Figure 6-5 **Effect of vitamin E on mutagenicity of NO-donating drugs on MN-11 cells in culture.** Error bars represent mean ± SEM (n = 3 separate experiments, each involving 3 replicate dishes at each experimental point). Cultures were maintained in non-selective medium (hatched bars) or medium containing α-tocopherol (100 μM) (solid bars) for 24 h, washed with PBS, then exposed for 24 h to either GTN (0.44 mM) or SNP (0.5 mM). MF of vehicle (0.1% ethanol) treated cultures (labelled 'Spont') is also shown. Difference between GTN and GTN + α-tocopherol is statistically significant (2 tailed $p = 0.012$). Difference between SNP and SNP + α-tocopherol is also considered to be statistically significant ($p = 0.043$).

Figure 6-5

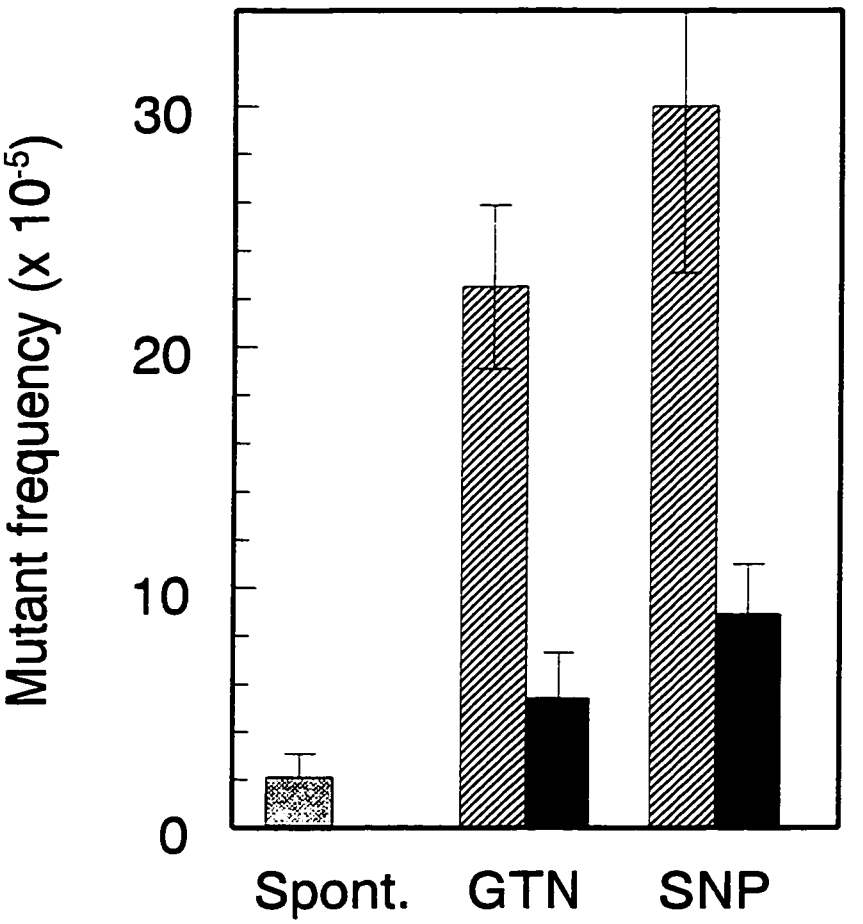

6.3.5 *Effect of Vitamin E on metabolic conversion of NO-donating drugs to nitrite by MN-11 cells*

I have previously shown that SNP and GTN were slowly metabolized by MN-11 cells ($t_{1/2}$ = 12 h) (Chapter 4) to produce nitrite, a more stable end-product of NO·. To rule out the possibility that the observed protection by α-tocopherol may be due to a down regulation of the enzymes responsible for metabolism of either SNP or GTN, its effect on the accumulation of nitrite was measured by Griess reaction. As shown in Table 6-1, no reduction in nitrite was observed: 235 vs 280 for GTN and 144 vs 168 for SNP(nmoles nitrite per 10^6 cells per 24 h for control and α-tocopherol treated, respectively).

6.3.6 *Characterization of mutants*

(a) ***Reactivation studies.*** Treatment of cells with 5-Aza-Cyd inhibits DNA methyltransferase activity thereby causing demethylation of DNA [370]. Table 6-2 shows that 5-Aza-Cyd caused a dose-dependent decrease in cloning efficiency of C86AGM2 and GTN induced mutant cells. C86AGM2 cells carry one active and one inactive X chromosome with an inactive *HPRT* gene on the active X chromosome. At concentrations of 2.5 and 5.0 μM, it reduced survival to 60.5 ± 1.96% and 45.4 ± 2.05% (mean ± SEM, n = 11), respectively, and these concentrations were used for reactivation studies. C86AGM2 cells formed colonies in HAT-medium with a spontaneous reversion frequency of $6.4 \times 10^{-5} \pm 1.3 \times 10^{-5}$ (mean ± SEM). 5-Aza-Cyd treatment of these cells dramatically increased the frequency of HAT^R colonies in a dose-dependent manner; $95 \times 10^{-5} \pm 5.0 \times 10^{-5}$ with 2.5 μM and $280 \times 10^{-5} \pm 7.2 \times 10^{-5}$ with 5.0 μM, respectively. No HAT^R colonies were detected following treatment of 6-TG^R MN-11 clones with 1.0, 2.5 or 5.0 μM 5-Aza-Cyd in GTN

Table 6-1 **Effect of Vitamin E on metabolic conversion of NO-donating drugs to nitrite by MN-11 cells.** 2×10^5 MN-11 cells were preincubated for 24 h in the presence of α-tocopherol (100 μM) and NO-donating drugs were added for 24 h. Nitrite was determined by the Griess reagent. Values shown are mean ± range of 2 independent experiments, each involving duplicate analysis. SNP was at 0.5 mM and GTN was at 0.12 mM, respectively.

Table 6-1

Nitrite accumulation by NO-donating drugs in the presence of vitamin E

Treatment	*Nitrite accumulated (μM)*
Cells alone	0.82 ± 0.4
GTN alone	47.0 ± 3.8
GTN + pre	56.0 ± 4.6
SNP alone	28.9 ± 1.1
SNP + pre	33.5 ± 2.5

Table 6-2 **5-Aza-Cyd induced cytotoxicity and reversion frequencies (HAT^R colonies) in C86AGM2 and GTN induced mutant cells.** 5-Aza-Cyd treatment was for 48 h; after which cultures were washed with PBS and fresh complete medium was added for a further 48 h. Mean absolute cloning efficiency of untreated cultures was $41.0 \pm 2.8\%$. Cell survival and reversion frequencies were determined as described in Materials and Methods. Reversion frequency is expressed as HAT^R cells per 1×10^5 viable cells. Data shown are mean ± SEM of 3 separate dishes analyzed in triplicate for each treatment.

Table 6-2

Cell line	Concentration of 5-Aza-Cyd (μM)							
	0		1.0		2.5		5.0	
	Survival (%)	HAT^R colonies	Survival (%)	HAT^R colonies	Survival (%)	HAT^R colonies	Survival (%)	HAT^R colonies
C86AGM2	100±2.2	6.4±1.3	79±4.0	N.D.	61±6.4	95±5.0	40±7.0	280±7.2
NG-1	100±7.8	0 ± 0	79±8.2	0 ± 0	69±19.4	0 ± 0	48±15.6	0 ± 0
NG-2	100±8.4	0 ± 0	74±8.0	0 ± 0	68±4.8	0 ± 0	50±14.0	0 ± 0
NG-3	100±4.3	0 ± 0	81±5.8	0 ± 0	64±3.6	0 ± 0	52±16.6	0 ± 0
NG-4	100±9.2	0 ± 0	84±5.9	0 ± 0	68±6.2	0 ± 0	54±14.6	0 ± 0
NG-5	100±2.7	0 ± 0	79±9.8	0 ± 0	61±19.7	0 ± 0	39±10.4	0 ± 0
NG-6	100±15	0 ± 0	83±4.0	0 ± 0	55±13.2	0 ± 0	31±5.9	0 ± 0
NG-7	100±8.0	0 ± 0	78±7.2	0 ± 0	53±6.1	0 ± 0	38±2.8	0 ± 0
NG-8	100±4.6	0 ± 0	85±7.3	0 ± 0	64±7.3	0 ± 0	48±6.9	0 ± 0
NG-9	100±0.7	0 ± 0	79±9.1	0 ± 0	51±3.1	0 ± 0	46±4.9	0 ± 0
NG-10	100±3.8	0 ± 0	88±6.8	0 ± 0	58±11.6	0 ± 0	47±5.5	0 ± 0
NG-11	100±6.6	0 ± 0	87±9.1	0 ± 0	55±5.1	0 ± 0	46±2.9	0 ± 0

N.D. = not determined

induced mutants (NG-1 to NG-11, n = 11, in 2 independent experiments) (Table 6-2).

(b) *Karyotype analysis.* Karyotype analysis, using the X centromeric-specific hybridization probe was performed on control, radiation (3 or 5 Gy) and GTN induced (5 mg/kg) mutants to determine if X chromosome loss was occurring. The probe detected 3 X-chromosomes and also X centromeric-sequences on chromosome 11 and a small fragment in all the mutant and control MN-11 cells (Figure 6-6). The results are summarized in Table 6-3. No loss of a total X chromosome was observed in any of the mutants tested (these results were obtained in collaboration with Dr. Blakey).

6.4 DISCUSSION

Our laboratory has developed an *in vitro/ex vivo* murine tumor model system in which the *HPRT* gene serves as a mutational target. Using this model system an increase in MF has been reported in MN-11 cells grown as s.c. tumors compared with the MF of cells grown in culture (Chapter 2, [1]). On the basis of this evidence, I hypothesized that ROS and RNS which may be produced by activated phagocytic cells within solid tumors, may be mutagenic and genotoxic. Earlier *in vitro* study has shown that NO-donating drugs (GTN and SNP) can readily induce mutations at the *HPRT* locus in MN-11 cells (Chapter 4, [194]). To explore the possibility that RNS generated within the tumors might be involved, I tested the mutagenic potential of NO-donating drugs in tumor-bearing animals and also if the mutation could be blocked by dietary vitamin E.

Ionizing radiation and the cancer chemotherapeutic drug, cisplatin, are well established DNA damaging and mutagenic agents. Ionizing radiation is an effective inducer of $HPRT^-$ mutants in MN-11 cells *in vitro* (Chapter 3). As a measure of the sensitivity of

Figure 6-6 **Detection of X centromeric-specific sequences by fluorescence *in situ* hybridization in MN-11, radiation and GTN-induced mutant cells.** Metaphase spreads of MN-11 (top) and NG-1 mutants (bottom) are shown. The orange arrows locate three X-chromosomes and the magenta arrows indicate X centromeric-specific sequences on chromosome 11. Yellow arrows point to an unidentified fragment. Radiation-induced mutants also demonstrated a similar pattern of X centromeric-specific sequences (data not shown).

Figure 6-6

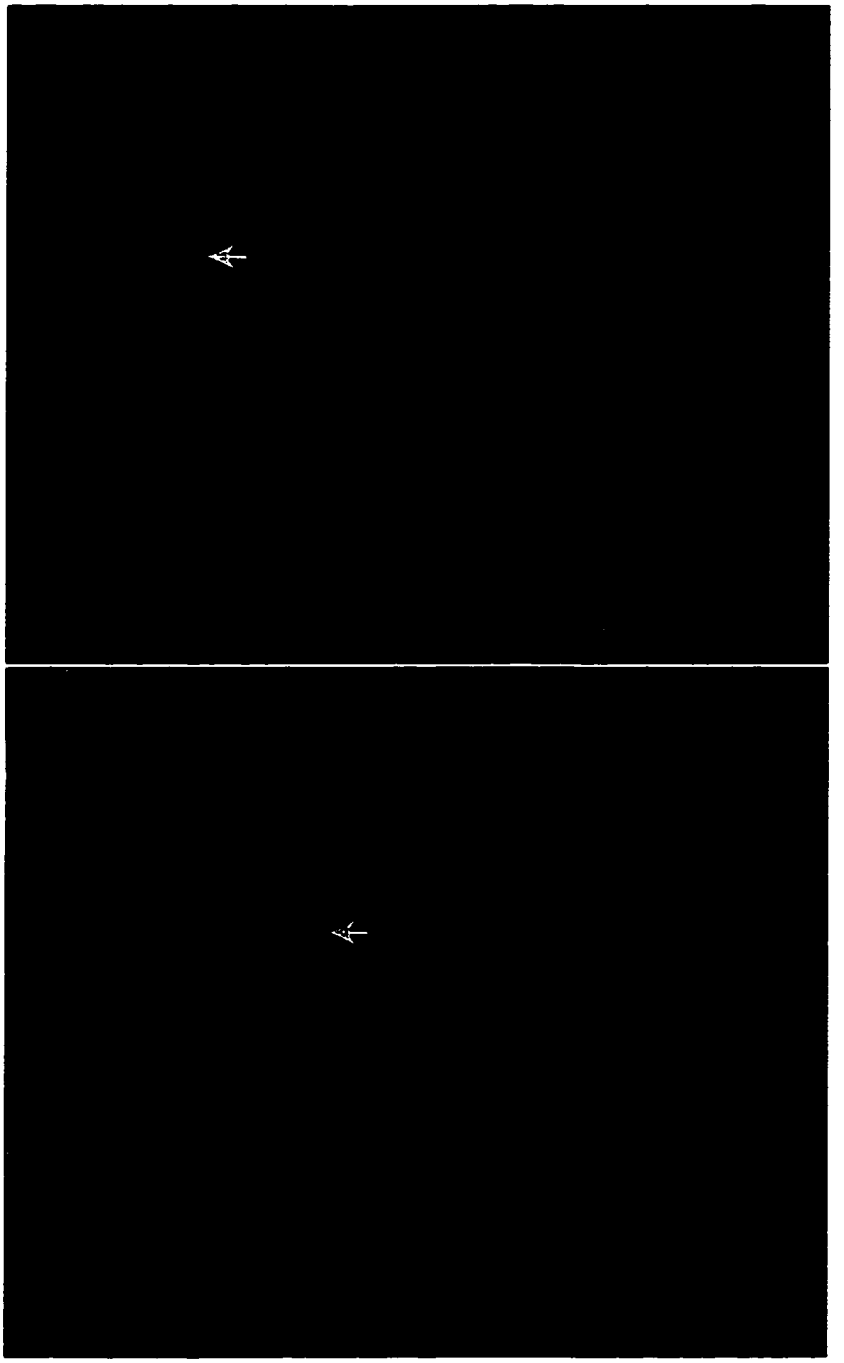

Table 6-3 **Karyotypes of MN-11, radiation and GTN-induced mutant cells.** Results represent the mean ± SD of separate samples. The differences in total number of chromosomes and the total number of signals detected by the X-centromeric probe are not statistically significant between the treatment and control MN-11 cells ($p > 0.05$, ANOVA., *post hoc* Dunnett's t-test).

Table 6-3

Sample	*Total number of chromosomes*	*Total number of signals*	*Number of X chromosomes*	***Number of other painted chromosomes*** *chromosome 11*	*unidentified Fragment*
MN-11 (n = 17)	72.8 ± 3.9	6.3 ± 0.6	3.0 ± 0	2.9 ± 0.34	0.41 ± 0.5
Radiation (n = 4)	74 ± 5.0	7.0 ± 0	3.0 ± 0	3.0 ± 0	1.0 ± 0
GTN (n = 4)	73.5 ± 3.0	6.8 ± 0.5	3.0 ± 0	2.8 ± 0.5	1.0 ± 0

MN-11 tumors for detecting mutants *in vivo*, tumor-bearing animals were either exposed to ^{137}Cs γ-radiation or injected with cisplatin. ^{137}Cs γ-radiation (single dose, 0.5-5.0 Gy) induced dose-dependent increase in MF in tumor-bearing animals. The MF increased about 100-fold with dose. Kataoka *et al.* [371] reported a MF of 1-2 × 10^{-5} per Gy in mice exposed to ^{60}Co γ-rays; compared to 103 per 10^5 cells per Gy in MN-11 tumors (Figure 4-1A). The differences in sensitivities to detect mutants in the two systems could be explained due to the differences in detecting chromosomal mutations. Cisplatin is an antitumor drug which acts by producing interstrand and intrastrand crosslinks of cellular DNA and has been shown to be mutagenic in CHO cells [372-374] and in T-lymphocytes of patients receiving cisplatin therapy [375]. It was found to induce mutants in cultured MN-11 cells (Figure 4-1B, inset). At equivalent cytotoxicities, ^{137}Cs γ-radiation was a more effective mutagen (Chapter 2) than cisplatin (170 compared to 90 mutants per 10^5 cells at D_0). As expected, it was also effective in inducing mutants *in vivo*, however, there was a large scatter in MF among different tumors at different doses. This could be attributed due to differences in the delivery of the drug to the tumor cells in different animals, metabolism of the drug or other factors. These experiments show that MN-11 tumor model system is also sensitive to detect mutations *in vivo*.

NO· has been shown to be mutagenic in both bacterial and mammalian systems. NO· gas was mutagenic in TK6 cells [158] and in explanted rat lung cells *in vivo* [62]. NO-donating drugs have been shown to be mutagenic in bacterial [157] and in MN-11 cells (Chapter 4). There are no earlier reports of mutagenicity of NO-donating drugs *in vivo*. Since MN-11 cells can grow both *in vitro* and as subcutaneous tumors, these cells were used to assess the mutagenic potential of NO-donating drugs in tumor-bearing animals.

Nitrovasodilators are prodrugs of NO· and have been used clinically for about 100 years in the treatment of angina pectoris, congestive heart failure, and hypertension [376]. GTN is enzymatically metabolized to NO· in the presence of a thiol group (especially cysteine) [295]. MOL is enzymatically metabolized by the liver to release SIN-1 (active metabolite of MOL), which is then converted non-enzymatically into SIN-1A, releasing NO· [284]. GTN has been shown to be metabolized by MN-11 cells, but MOL was not metabolized (Chapter 4, section 4.3.5). I show here for the first time that both GTN and MOL (single i.p. doses) induced HPRT$^-$ mutants in tumor-bearing animals. There is a threshold observed with GTN and a statistically significant increase was observed only at the highest dose tested. This could be because cellular and repair mechanisms responsible for detoxifying NO· have to be overwhelmed before the mutation can be induced. However, treatment with MOL produced an essentially dose-dependent increase in MF. It should be noted that these are not physiologically relevant doses of NO-donating drugs. MOL (4 mg/kg) [377] and GTN are used clinically in the treatment of patients with coronary artery disease and myocardial ischaemia. The large variance in MF found among different tumors could be explained by differences in metabolism of the drugs in individual tumors and or other factors. The differences in MF in individual tumors could not be attributable due to differences in tumor vasculature or increased infiltration of phagocytic cells in the GTN-treated tumors. Histochemical analysis of GTN-treated tumors did not reveal any differences in tumor vasculature or number of infiltrating phagocytic cells (data not shown). The increased MF observed in tumor-bearing animals exposed to NO-donating drugs could not be due to increased rate of cell replication. *In vitro* growth rates of MN-11 cells exposed to NO-donating drugs had a doubling time of 14 ± 2.4 h (data not shown), which is

essentially the same as untreated MN-11 cells (Chapter 2). SNP was not used *in vivo* since an earlier study has shown that acute overdoses of SNP in laboratory animals result in death by cyanide poisoning [378].

Previous investigations have shown that of the various lipid- and aqueous-phase antioxidants tested, only vitamin E (α-tocopherol) was found to be the most potent quencher of RNS. When MN-11 cells were exposed to NO-donating drugs both cytotoxicity and mutagenicity was observed. Pretreatment of MN-11 cells with α-tocopherol (100 μM) *in vitro* protected against NO· induced cytotoxicity and mutagenicity. Although the membrane concentration of vitamin E is not determined directly, it is likely that vitamin E is responsible for the observed protection. This is consistent with earlier reports where vitamin E was shown to protect pancreatic islet cells against cytotoxicity [379] and *Salmonella typhimurium* TA1535 against mutagenicity [178]. Interestingly, this study of NO· mutagenicity in bacterial cells showed little protection by other antioxidants besides α-tocopherol. The only other effective compound was β-carotene. Trolox, a water-soluble form of vitamin E analog was protective against peroxynitrite-mediated oxidative stress and apoptosis in rat thymocytes [380]. It was also shown to reduce nitric oxide synthase activity in tumor necrosis factor-α -treated hepatocytes [381] and protect against NO· mediated mitochondrial complex IV damage in cultured astrocytes [382]. In MN-11 cells, the protection afforded *in vitro* is not due to deregulation of enzymes responsible for metabolism of GTN and SNP, since nitrite accumulation was unaffected in cells preincubated with vitamin E. Animals fed with vitamin E supplemented diet (100 mg/kg/day) for 19 days prevented the mutagenic effect of GTN. Vitamin E did not have any cytotoxic nor mutagenic effects on MN-11 cells both *in vitro* and *in vivo*. Other workers have shown that

dietary supplementation with vitamin E is safe even at relatively high doses. Animal studies have shown that the toxicity of vitamin E is very low and it is not mutagenic, carcinogenic, or teratogenic [383,384]. Our data is in agreement with these observations. Because vitamin E protects against membrane lipid-peroxidation, it is possible that a membrane-derived lipophilic species may act as an intermediate in the cytotoxicity and mutagenicity observed in MN-11 cells. Recently, much attention has been paid to the role of DNA methylation in different stages of cancer development and carcinogenesis [385-387]. I have also tested if GTN induced mutant phenotype may be due to methylation of CpG sites in the promoter region of the *HPRT* gene. As a control C86AGM2 cells were used. Treatment of C86AGM2 cells with DNA demethylating agent, 5-Aza-Cyd, resulted in a large increase in reversion frequency. Our results obtained using these cells are essentially identical to those obtained by Hockey et al. [368]. Treatment of GTN induced mutants with 5-Aza-Cyd, induced no $HPRT^-$ revertants. These observations suggest that DNA methylation is not responsible for the $HPRT^-$ phenotype and majority of the mutants detected in MN-11 cells may be due to their ability to survive large-scale deletions on the *HPRT* gene. 5-Aza-Cyd did not alter the growth rate of MN-11 cells. The doubling times were 15 ± 2.3 h.

MN-11 cells contain 3 copies of the X-chromosome (Figure 6-6 and Table 6-3). The sensitivity to mutation induction by clastogenic agents (ionizing radiation and radiomimetic drugs) support the notion that MN-11 cells detect chromosomal mutations (as opposed to gene mutations) (Chapter 4). Tumor cells are genetically unstable [206] and therefore I expected to observe a total loss of X-chromosome in majority of the mutants. Karyotype analysis of radiation and GTN induced mutants using X centromeric-specific FISH probe showed no total loss of the X-chromosome. All the control and mutant cells examined

possess 3 X-chromosomes, suggesting that each of these 3 X-chromosomes may possess at least one essential gene, important for cell viability. Interestingly, all 3 X-chromosomes are maintained in all generations, further strengthening the notion of importance of essential genes on all 3 X-chromosomes. Hence, I suspect rearrangements, translocations, large deletions or small-scale deletions would be occurring in mutants but still maintaining the essential genes.

Our observations using NO-donating drugs add to the growing body of evidence that RNS may be mutagenic *in vivo* as well as *in vitro*. Vitamin E is a lipophilic antioxidant that appears to be protective in some studies. Epidemiological investigations suggest that vitamin E may lower the incidence of prostate and colorectal cancers and cardiovascular disease [388-393]. Our studies provide the first evidence that vitamin E can protect mammalian cells against mutagenicity of NO-donating drugs, both *in vitro* and *in vivo*. Furthermore, vitamin E inhibited the '*spontaneously*' arising mutants in tumor-bearing animals. The mechanism of inhibition of mutant induction is not known. However, few studies have shown that vitamin E may modify inflammatory responses by modifying the functions of activated neutrophils. An *in vivo* study demonstrated that neutrophils from rabbits receiving vitamin E were less adherent to the endothelium after exposure to the chemoattractant, N-formylmethionyl leucyl phenylalanine (FMLP) and they also demonstrated decreased capacity for production of H_2O_2 [394]. Another *in vitro* study has shown that vitamin E may inhibit superoxide generation by PMA-stimulated rat neutrophils [395]. NO· is produced by activated neutrophils [294,396]. Hence, infiltrating polymorphonuclear cells may result in reduced ROS and RNS production. NO· is postulated to be generated in inflammatory diseases that predispose to cancer [45,55,130,155,275,309]

and may be generated in MN-11 tumors by infiltrating neutrophils, macrophages or mast cells. iNOS has been shown to present in neutrophils and macrophages in MN-11 tumors (Chapter 5). Our findings are relevant to the *in vivo* situation and support the idea that increased dietary vitamin E supplementation may be important in preventing against NO· mediated damage.

CHAPTER 7

GENERAL DISCUSSION

Tumor progression refers to the progressive phenotypic changes frequently observed in growing tumors, including invasiveness, ability to metastasize and drug resistance. The mechanism by which these changes occur is not well understood, but is thought to be associated with genetic damage. Solid tumors are made up of a diverse population of cell types. These include vascular endothelial cells, fibroblasts of the stromal compartment, immune cells (lymphocytes, granulocytes and macrophages), mast cells and tumor cells. Although a number of immunohistochemical studies have demonstrated the presence of infiltrating phagocytic cells within or at the periphery of various tumors, there has been considerable debate as to their biological role(s). These cells release cytokines, arachidonic acid metabolites, ROS and RNS that can damage DNA and may be responsible for the genetic changes seen in tumor cells during tumor progression. To investigate the role of tumor-infiltrating phagocytic cells in solid tumors our laboratory has developed a new murine *in vitro/in vivo* tumor model system to study the frequency at which mutations arise *in vivo* within tumors. A tumor cell line was established from a methylcholanthrene-induced mouse tumor [198]. This line was then genetically modified to create a functionally heterozygous gene at the *HPRT* locus [1]. The work presented in this thesis describes the use of this cell line to study the contribution of the tumor microenvironment in promoting genomic instability underlying tumor progression and to identify such factors.

This thesis describes the development of a unique murine experimental model (MN-11cells, Figure 1-1) to study mutations that arise *in situ* in tumors. MN-11 cells exhibited a low spontaneous loss of the *HPRT* gene and an increased rate (> 1000-fold as compared to the parental line) of mutation detection, when exposed to a clastogenic agent, ^{60}Co γ-rays. The sensitivity of the system is comparable to the other heterozygous marker genes (*TK*,

APRT, and *GPT*) as reported by other workers [227,228,230,232], suggesting that the *HPRT* gene is located on a heterozygous chromosome (presumably X-chromosome). The conclusion from these experiments is that MN-11 cells can detect both gene mutations (small-scale deletions and point mutations) and chromosomal mutations (i.e., large-scale, multi locus deletions) at the *HPRT* locus. This data is also supported by the presence of both "large" and "small" colonies in HPRT$^-$ mutants induced by ^{60}Co γ-rays in MN-11 cells. The "small" colony phenotype has previously been described in literature and is associated with large-scale deletions at the *TK* locus in mouse L5178Y lymphoma cells [201-203]. MN-11 cells can also grow as s.c. tumors in syngeneic animals. The most significant observation to arise from these studies has been that the MF in cells grown as tumors in syngeneic mice was 3.64-fold higher than when they are grown *in vitro* under standard culture conditions. This is the first direct evidence of existence of mutagenic and/or clastogenic factors in the tumor milieu. These findings were recently supported from work from two different laboratories [42,43] who have also shown that the tumor microenvironment may promote genomic instability in tumors.

To explore factors in the tumor microenvironment that might be responsible for the observed increase in MF in MN-11 cells grown as tumors, tumors were studied histologically. The most abundant infiltrating cell type in MN-11 tumors is granulocytes, and to some lesser extent macrophages, mast cells and lymphocytes. Granulocytes were observed mainly in the necrotic areas of the tumors and to a lesser extent in the non-necrotic areas (Chapter 3). Immunohistochemical analysis of these tumors show that the local milieu of the tumor is conducive for iNOS expression in granulocytes, suggesting the cells may be activated. Macrophages and mast cells also show the presence of iNOS, present in very few

numbers at the periphery of the tumor. Biochemical analysis of tumor homogenates showed a positive correlation between iNOS activity and MF. These data suggest that granulocytes may be the primary cellular sources of RNS in MN-11 tumors. However, stimulated granulocytes likely also produce ROS that may interact with NO· and produce more potent genotoxic nitrating species such as peroxynitrite and nitrosating species such as nitrosonium ion (Chapter 1 (Figure 1-5), [114,397]). In this study I have not shown nitrotyrosine staining, a marker of peroxynitrite and other nitrating species in MN-11 tumors. This could be demonstrated using immunohistochemistry and study if its presence correlates with MF. This would provide evidence for the presence of such species. The results presented in this thesis also show a clear positive correlation between number of infiltrating granulocytes and MF (Chapter 5). This observation suggests that RNS and/or ROS generated by infiltrating granulocytes may be responsible for the observed increase in MF observed *in vivo*. Biochemical estimation of myeloperoxidase activity in tumor homogenates could be used as a quantitative measure of granulocytic recruitment in the tumor tissue. Such experiments would strengthen the correlation between granulocytes and mutant induction. Granulocytic infiltration is a common feature of solid human tumors and inflammatory diseases, but the function of these cells in the biology of tumors and their state of activation is uncertain. Tumor-associated macrophages have been shown to represent a major component of the cellular infiltrate in some experimental solid tumors where they have been postulated to have a role in the growth and metastasis of these tumors [323,324,350,352]. Recently, tumour-associated macrophages have been shown to express iNOS in human breast cancer [135]. These observations add to the growing list of functions for phagocytic cells and suggest that RNS generated by granulocytes may have a role in tumor progression.

A model is presented to summarize the results and provide a theoretical explanation for the observed increase in MF in MN-11 tumors (Figure 7-1). Synthesis of chemotactic cytokines by MN-11 cells, leukocytes or necrosis may contribute to the recruitment of granulocytes into the tumor tissue. This increased infiltration may lead to the production of ROS and/or RNS that may have cytotoxic and/or genotoxic effects on the neighbouring MN-11 cells, scored as $HPRT^-$ mutants in this system. Chemotactic factors, such as LTB_4, IL-1, G-CSF, IL-8, and the members of the IL-8 family NAP-1 and MIP-2 have been shown to increase neutrophilic granulocytes in different tissues [269,272,398-404]. Treatment of granulocytes *in vitro* with GM-CSF increases H_2O_2 production and causes enlargement of these cells [405]. The constitutive release of cytokines by tumor cells in which a cytokine gene has been inserted has been recently accomplished in mouse models [271,272,402,406-408]. More recently, human neoplastic cells may have also been successfully transduced with cytokine genes [273,409]. Yoshida et al. [273] have shown that granulocytic chemotactic factors are produced by a malignant fibrous histiocytoma cell line, suggesting the role of granulocytes in the disease progression. Most of the studies have shown the ability of granulocytes to kill tumor cells thereby suppressing tumorigenicity *in vivo* [272,404]. However, Pekarek et al. [403] have shown that granulocytes are required for tumor growth. They studied UV-induced cancers in mice; these cancers, when transplanted into normal syngeneic hosts, are usually rejected. A variant was derived that formed tumors in athymic nude mice and required host granulocytes for growth and elimination of host cells by an antigranulocyte antibody inhibited tumor growth. Using the MN-11 system, experiments carried out in our laboratory (detailed in the M.Sc thesis of Helen Privora) have shown that direct injections of IL-8 into MN-11 tumors, increases the

Figure 7-1 **Possible role of granulocytes in tumor progression.** Schematic depicts a multistep cascade of events that leads to granulocytic chemotaxis to sites of increased cytokine production. A blood vessel with red blood cells (**RBC**) and white blood cells mainly monocytes (**M**), granulocytes (**G**), and lymphocytes (**L**) is shown. Note also a tissue mast cell and macrophage (**Mac**), infiltrating tumor cells. The role of these cells in the biology of MN-11 tumor is not known. MN-11 cells may secrete cytokines, such as IL-1 or IL-8 that may attract granulocytes from the blood vessels. Conversely, necrotic areas in the tumor may also produce chemotactic factors that may cause granulocytic recruitment to the tumor. Granulocytes move from the blood to extravascular space via a multistep series of events that include selectin-dependent rolling and β_2-integrin (CD 18)-dependent adhesion and emigration [93]. These cells may in turn produce large amounts of ROS and RNS that can induce mutations at the *HPRT* locus in MN-11 cells.

Figure 7-1

POSSIBLE ROLE OF GRANULOCYTES IN TUMOR PROGRESSION

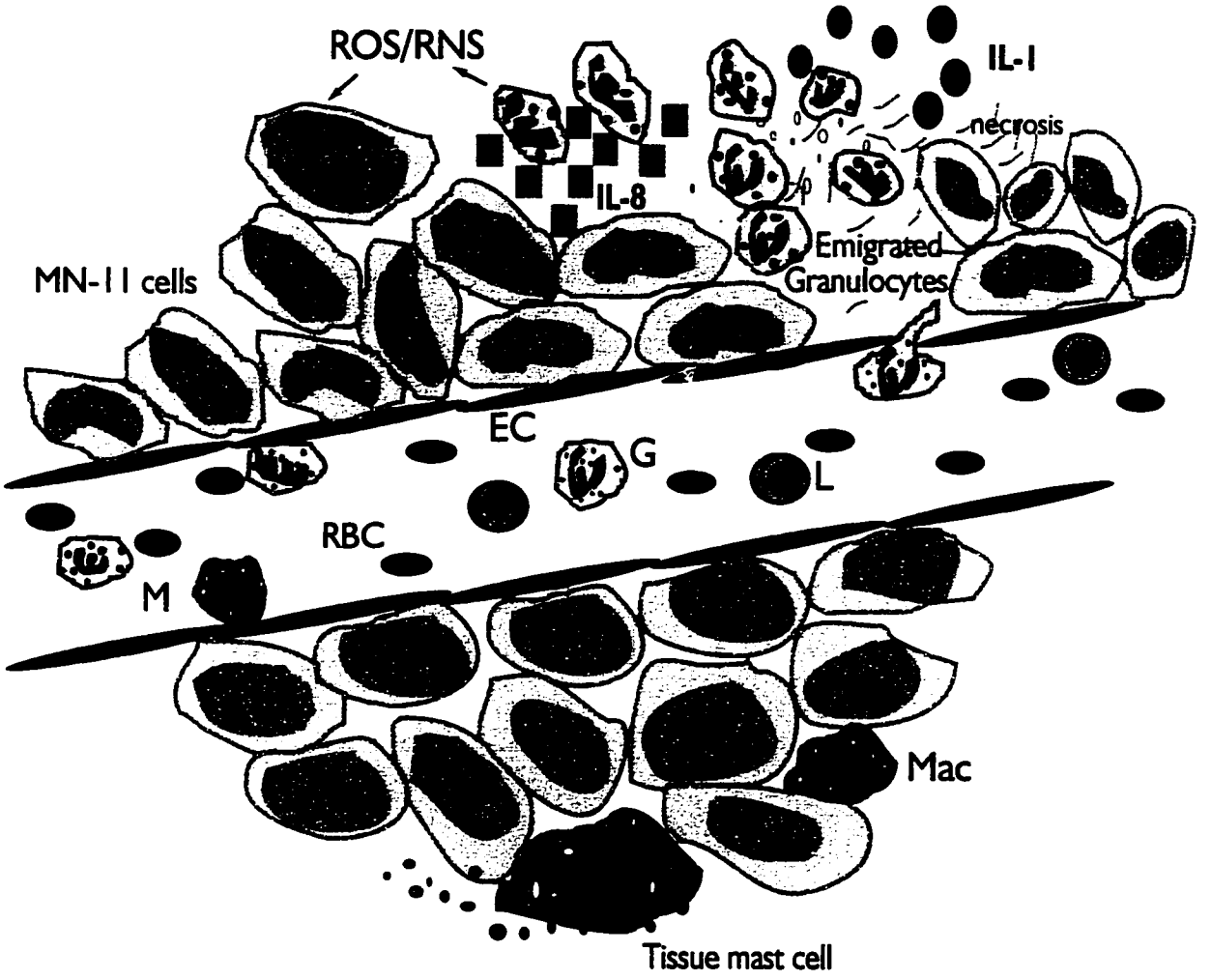

granulocytic content of the tumor. A positive correlation was observed between the number of infiltrating granulocytes and MF (Sandhu, Privora and Birnboim, ms. in preparation), but there was appreciable animal-to-animal variability. A more reliable method of increasing granulocytes in MN-11 tumors would be achieved by constructing permanent IL-8 expressing transfectants of MN-11. Although in principle this is straightforward, a complication is that excessive IL-8 expression can lead to extensive cytotoxicity mediated by increased granulocytic infiltration. Expression of this chemokine by tumor cells was shown markedly to decrease tumorigenicity of xenografts (and increase in granulocytic infiltration) in nude mice [270,271]. Therefore, another strategy would be to use an inducible expression vector. Once a reliable method to enhance the *in vivo* MF is established, a selective inhibitor of iNOS, aminoguanidine [410,411] would be administered to decrease the amount of NO· produced by granulocytes. These experiments would prove that NO· generated by granulocytes is responsible for the increase in MF.

Treatment of MN-11 cells *in vitro* by generators of ROS and RNS increased the MF (Chapter 4, [194]). Experiments using NO-donating drugs that liberate NO· spontaneously and rapidly (SPER/NO· and SNAP) produced cytotoxicity with little mutagenicity. Conversely, drugs that require bioactivation and liberate NO· slowly (GTN and SNP) were more mutagenic and less cytotoxic. Tamir et al. [412] have shown that a slow, controlled rate of release of NO· gas can increase toxicity, DNA damage and mutagenicity in a bacterial system. NO_2^-, a common end-product of many NO· reactions did not cause any cytotoxicity and/or mutagenicity in MN-11 cells (Table 4-2). These results suggest that different states of NO (such as NO^- or NO·) may be generated by these drugs that may vary in their mutagenic/cytotoxic potential [114,142,413]. To extend this study, other clinically used

organic nitrates, organic nitrites, NO· gas and spontaneous NO-donating drugs could be tested. The mechanism by which NO· generated by GTN and SNP caused mutant induction in MN-11 cells is unclear and is currently being investigated in our laboratory. Glutathione (GSH) is a principal intracellular non protein thiol and has been shown to protect cells against oxidative stress and free-radical damage including NO· [414-417]. Lowering of GSH levels *in vitro* and *in vivo* can readily be carried out by using BSO (L-buthionine SR-sulfoximine), which blocks γ-glutamylcysteine synthase, the first step in GSH biosynthesis. Depletion of GSH by BSO in a rodent and a human cell line was shown recently to sensitize cells to killing by NO· gas [418]. Similar results were obtained using MN-11 cells treated with GTN or SNP and BSO; NO-donating drugs alone increased GSH levels and BSO treatment increased cytotoxicity and mutagenicity (described in the M.Sc thesis of Helen Privora; Privora, Sandhu and Birnboim, ms. in preparation). The effect of GSH depletion on cytotoxicity and mutagenicity in tumor-bearing animals would help to determine its effect *in vivo*. These studies will allow us to understand and identify the chemical pathways that can lead to mutations by NO· in MN-11 cells.

NO-donating drugs (GTN and MOL) were shown to cause a dramatic increase in MF in tumor-bearing animals (Chapter 6, [419]). These data are the first to show mutagenic effects of NO-donating drugs *in vivo*. Administration of an antioxidant, vitamin E, to the diet of animals for 19 days before GTN treatment largely abolishes the MF. This is among the most dramatic *in vivo* protective effects demonstrated in a whole-animal system by dietary vitamin E. Vitamin E reduced the *spontaneous* MF, suggesting that the formation of the mutagenic species in the tumor environment could be abolished. Protection by vitamin E was also shown *in vitro* against GTN and SNP induced cytotoxicity and

mutagenicity. Although the data presented in this thesis shows the protective role of vitamin E against GTN and SNP induced cytotoxicity and mutagenicity, the species generated is unknown.

Characterization of the mutation induced is very important because the data suggests that MN-11 cells can detect chromosomal mutations, but this needed to be proven. In humans, the nearest essential genes to *HPRT* have been mapped by study of radiation induced mutants and lie approximately 2 Mb in the centromeric direction and 1.3 Mb in the telomeric direction [420]. In mice, equivalent mapping studies have not been done, but recovery of $HPRT^-$ mutants following radiation is similar to human cells, about 1-2 per 10^5 cells per Gy [227,421-423]. In MN-11 cells, recovery of $HPRT^-$ mutants is 100 × higher. This could be because MN-11 cells, as a result of non-disjunction event, have 3 active X chromosomes, converting this normally hemizygous locus to a heterozygous locus [1]. Using X centromere-specific FISH probe, no total loss of X chromosome is seen in any of the radiation or GTN-induced mutants (Chapter 6). This suggests that interstitial deletions or recombinations are likely occurring, of a size too small to be detected by standard karyotyping. Therefore, FISH probes that span the *HPRT* gene (approximately 40 kb) could be used. A 20 kb section of the mouse *HPRT* gene has been cloned and is available from Dr. M.W. McBurney. Long PCR has been used to produce other fragments comprising most of the gene. A large proportion of radiation-induced mutants are expected to show a reduction from 3 copies of the *HPRT* gene (2 non-functional + 1 functional) to 2 copies (both non-functional). If similar results are obtained for GTN-induced mutants, then this would be the first evidence that RNS can cause chromosomal mutations. Standard Southern blotting using *HPRT* cDNA as a probe does not work reliably because of the very small size

of most *HPRT* exons. Loss of the functional copy of the *HPRT* gene in mutants could not easily be detected because of the presumed presence of the 2 non-functional copies of the gene. Finally *HPRT* mRNA could be examined in mutant cells by RT-PCR. Transgenic mice now used for *in vivo* mutagenesis studies do not detect chromosomal mutations, because loss of the entire marker transgene cannot be scored [181,183]. Chromosomal mutations may be a common but an undetected event caused by RNS. Since such mutations are common in human tumors, this would help to establish a link between such mutations and ROS and RNS present in the tumor milieu.

In summary, this thesis documents that conditions within the tumor microenvironment are mutagenic. Tumor-infiltrating granulocytes may produce factors such as ROS and/or RNS that may produce mutagenic and/or clastogenic damage to DNA, commonly observed in solid tumors. In this manner, the tumor microenvironment may contribute to genetic instability in tumors leading to tumor progression.

REFERENCES

1. Wilkinson, D., *et al.* (1995). *Hprt* mutants in a transplantable murine tumour arise more frequently *in vivo* than *in vitro*. *Br. J. Cancer* 72: 1234-1240.

2. Foulds, L. (1954). The experimental study of tumor progression: a review. *Cancer Res.* 14: 327-339.

3. Nowell, P. C. (1976). The clonal evolution of tumor cell populations. *Science* 194: 23-28.

4. Nowell, P. C. (1978). Tumors as clonal proliferation. *Virchows Archiv* B. Cell Pathology. 145-150.

5. Nowell, P. C. (1980). Chromosomes and Tumor Progression. *Results & Problems in Cell Differentiation* 11: 102-106.

6. Loeb, L. A. (1991). Mutator phenotype may be required for multistage carcinogenesis. *Cancer Res.* 51: 3075-3079.

7. Nowell, P. C. (1989). Chromosomal and molecular clues to tumor progression. [Review] *Seminars in Oncology* 16: 116-127.

8. Nowell, P. C. (1991). Genetic instability and tumor development. *Basic Life Sci.* 57: 221-228.

9. Cheng, K. C. & Loeb, L. A. (1993). Genomic instability and tumor progression: Mechanistic considerations. *Adv. Cancer Res.* 60: 121-156.

10. Armitage, P. & Doll, R. (1954). The age distribution of cancer and a multi-stage theory of carcinogenesis. *Br. J. Cancer* 8: 1-12.

11. Fearon, E. R. & Vogelstein, B. (1990). A genetic model for colorectal tumorigenesis. [Review]. *Cell* 61: 759-767.

12. Poot, M. & Hoehn, H. (1993). DNA topoisomerases and the DNA lesion in human genetic instability syndromes. *Toxicol. Lett.* 67: 297-308.

13. Digweed, M. (1993). Human genetic instability syndromes: Single gene defects with increased risk of cancer. *Toxicol. Lett.* 67: 259-281.

14. Hollstein, M., *et al.* (1991). *p*53 mutations in human cancers. [Review]. *Science* 253: 49-53.

15. Hollstein, M. C., *et al.* (1993). *p*53 mutations and aflatoxin B_1 exposure in hepatocellular carcinoma patients from Thailand. *Int. J. Cancer* 53: 51-55.

16. Bennett, W. P., *et al.* (1992). *p53* Mutation and protein accumulation during multistage human esophageal carcinogenesis. *Cancer Res.* 52: 6092-6097.

17. Kahlenberg, M. S., *et al.* (1996). *p*53 tumor suppressor gene status and the degree of genomic instability in sporadic colorectal cancers. *J. Natl. Cancer Inst.* 88: 1665-1670.

18. Yin, Y., *et al.* (1992). Wild-type *p*53 restores cell cycle control and inhibits gene amplification in cells with mutant *p*53 alleles. *Cell* 70: 937-948.

19. Kastan, M. B., *et al.* (1992). A mammalian cell cycle checkpoint pathway utilizing *p*53 and *GADD45* is defective in ataxia-telangiectasia. *Cell* 71: 587-597.

20. Kuerbitz, S. J., *et al.* (1992). Wild-type *p*53 is a cell cycle checkpoint determinant following irradiation. *Proc. Natl. Acad. Sci. USA* 89: 7491-7495.

21. Blount, P. L., *et al.* (1993). Clonal ordering of 17p and 5q allelic losses in Barrett dysplasia and adenocarcinoma. *Proc. Natl. Acad. Sci. USA* 90: 3221-3225.

22. Reid, B. J., *et al.* (1993). Barrett's esophagus: cell cycle abnormalities in advancing stages of neoplastic progression. *Gastroenterology* 105: 119-129.

23. Motokura, T., *et al.* (1991). A novel cyclin encoded by a bcl1-linked candidate oncogene. *Nature* 350: 512-515.

24. Withers, D. A., *et al.* (1991). Characterization of a candidate bcl-1 gene. *Molecular & Cellular Biology* 11: 4846-4853.

25. Jiang, W., *et al.* (1993). Altered expression of the cyclin D1 and retinoblastoma genes in human esophageal cancer. *Proc. Natl. Acad. Sci. USA* 90: 9026-9030.

26. Xiong, Y., Zhang, H. & Beach, D. (1993). Subunit rearrangement of the cyclin-dependent kinases is associated with cellular transformation. *Genes & Development* 7: 1572-1583.

27. Livingstone, L. R., *et al.* (1992). Altered cell cycle arrest and gene amplification potential accompany loss of wild-type *p*53. *Cell* 70: 923-935.

28. Peltomaki, P., *et al.* (1993). Genetic mapping of a locus predisposing to human colorectal cancer. *Science* 260: 810-812.

29. Aaltonen, L. A., *et al.* (1994). Replication errors in benign and malignant tumors from hereditary nonpolyposis colorectal cancer patients. *Cancer Res.* 54: 1645-1648.

30. Perucho, M. (1996). Cancer of the microsatellite mutator phenotype. *Biol. Chem. Hoppe Seyler* 377: 675-684.

31. Fishel, R., *et al.* (1994). The human mutator gene homolog MSH2 and its association with hereditary nonpolyposis colon cancer. *Cell* 77: 167

32. Leach, F. S., *et al.* (1993). Mutations of a mutS homolog in hereditary nonpolyposis colorectal cancer. *Cell* 75: 1215-1225.

33. Bronner, C. E., *et al.* (1994). Mutation in the DNA mismatch repair gene homologue hMLH1 is associated with hereditary non-polyposis colon cancer. *Nature* 368: 258-261.

34. Papadopoulos, N., *et al.* (1994). Mutation of a mutL homolog in hereditary colon cancer. *Science* 263: 1625-1629.

35. Nicolaides, N. C., *et al.* (1994). Mutations of two PMS homologues in hereditary nonpolyposis colon cancer. *Nature* 371: 75-80.

36. Liu, B., *et al.* (1994). hMSH2 mutations in hereditary nonpolyposis colorectal cancer kindreds. *Cancer Res.* 54: 4590-4594.

37. Wooster, R., *et al.* (1994). Instability of short tandem repeats (microsatellites) in human cancers. *Nature Genet.* 6: 152-156.

38. Huddart, R. A., *et al.* (1995). Microsatellite instability in human testicular germ cell tumours. *Br. J. Cancer* 72: 642-645.

39. Loeb, L. A. (1994). Microsatellite instability: Marker of a mutator phenotype in cancer. *Cancer Res.* 54: 5059-5063.

40. Coleman, W. B. & Tsongalis, G. J. (1995). Multiple mechanisms account for genomic instability and molecular mutation in neoplastic transformation. *Clin. Chem.* 41: 644-657.

41. Honchel, R., *et al.* (1994). Microsatellite instability in Muir-Torre syndrome. *Cancer Res.* 54: 1159-1163.

42. Paquete, B. & Little, J. B. (1994). In vivo enhancement of genomic instability in minisatellite sequences of mouse C3H/10T1/2 cells transformed in vitro by X-rays. *Cancer Res.* 54: 3173-3178.

43. Reynolds, T. Y., Rockwell, S. & Glazer, P. M. (1996). Genetic instability induced by the tumor microenvironment. *Cancer Res.* 56: 5754-5757.

44. Templeton, A. C. (1975). *Persons at high risk of cancer: an approach to cancer etiology and* control. Edited by Fraumeni, J.F., Academic Press, New York. pp. 69-84

45. Ohshima, H. & Bartsch, H. (1994). Chronic infections and inflammatory processes as cancer risk factors: Possible role of nitric oxide in carcinogenesis. *Mutat. Res. Fundam. Mol.*

Mech. Mutagen. 305: 253-264.

46. Camisa, C. (1984). Squamous cell carcinoma arising in acne conglobata. *CUTIS* 33: 185-190.

47. Talley, N. J., *et al.* (1991). Gastric adenocarcinoma and Helicobacter pylori infection. *J. Natl. Cancer Inst.* 83: 1734-1739.

48. Eidt, S. & Stolte, M. (1995). The significance of Helicobacter pylori in relation to gastric cancer and lymphoma. *Eur. J. Gastroenterol. Hepatol.* 7: 318-321.

49. Houben, G. M. & Stockbrugger, R. W. (1995). Bacteria in the aetio-pathogenesis of gastric cancer: a review. *Scand. J. Gastroenterol. Suppl.* 212: 13-18.

50. Levine, M. S., *et al.* (1996). Helicobacter pylori and gastric MALT lymphoma. *Am. J. Roentgenol.* 166: 85-86.

51. Webb, P. M. & Forman, D. (1995). Helicobacter pylori as a risk factor for cancer. *Baillieres. Clin. Gastroenterol.* 9: 563-582.

52. Mera, S. L. (1995). Peptic ulcers and gastric cancer. *Br. J. Biomed. Sci.* 52: 271-281.

53. Liu, R. H. & Hotchkiss, J. H. (1995). Potential genotoxicity of chronically elevated nitric oxide: A review. *Mutat. Res. Rev. Genet. Toxicol.* 339: 73-89.

54. Rosin, M. P., Anwar, W. A. & Ward, A. J. (1994). Inflammation, chromosomal instability, and cancer: The schistosomiasis model. *Cancer Res.* 54 Suppl: 1929s-1933s.

55. Haswell-Elkins, M. R., *et al.* (1994). Liver fluke infection and cholangiocarcinoma: model of endogenous nitric oxide and extragastric nitrosation in human carcinogenesis. *Mutat. Res.* 305: 241-252.

56. Rosin, M. P., *et al.* (1994). Involvement of inflammatory reactions and elevated cell proliferation in the development of bladder cancer in schistosomiasis patients. *Mutat. Res. Fundam. Mol. Mech. Mutagen.* 305: 283-292.

57. Levin, B. (1992). Ulcerative colitis and colon cancer: biology and surveillance. *Journal of cellular biochemistry-Suppl.* 16G: 47-50.

58. Mellemkjær, L., *et al.* (1996). Rheumatoid arthritis and cancer risk. *Eur. J. Cancer.* 32A: 1753-1757.

59. Hennings, H., *et al.* (1987). Response of carcinogen-altered mouse epidermal cells to phorbol ester tumor promoters and calcium. *J. Invest. Dermatol.* 880: 60-65.

60. Potter, M. & Wiener, F. (1992). Plasmacytomagenesis in mice: model of neoplastic development dependent upon chromosomal translocations. [Review]. *Carcinogenesis* 13: 1681-1697.

61. Chester, J. F., *et al.* (1989). Colonic cancer induced by 1,2-dimethylhydrazine: promotion by experimental colitis. *Br. J. Cancer* 59: 704-705.

62. Isomura, K., *et al.* (1984). Induction of mutations and chromosome aberrations in lung cells following in vivo exposure of rats to nitrogen oxides. *Mutat. Res.* 136: 119-125.

63. Moilanen, E. & Vapaatalo, H. (1995). Nitric oxide in inflammation and immune response. *Ann. Med.* 27: 359-367.

64. Fridovich, I. (1989). Superoxide dismutases. An adaptation to a paramagnetic gas. *J. Biol. Chem.* 264: 7761-7764.

65. Halliwell, B. & Gutteridge, J. M. C. (1989). *Free radicals in biology and medicine.* 2nd ed. Edited by B. Halliwell and J. M. C. Gutteridge. Clarendon Press, Oxford.

66. Halliwell, B. & Gutteridge, J. M. C. (1990). Oxygen radicals in biological systems. Part B: Oxygen radicals and antioxidants. Role of free radicals and catalytic metal ions in human disease: An overview. *Methods Enzymol.* 186: 1-88.

67. Halliwell, B. (1991). Reactive oxygen species in living systems: Source, biochemistry, and role in human disease. *Am. J. Med.* 91 Suppl. 3C: 14S-22S.

68. Darley-Usmar, V., Wiseman, H. & Halliwell, B. (1995). Nitric oxide and oxygen radicals: A question of balance. *FEBS Lett.* 369: 131-135.

69. Halliwell, B. (1996). Antioxidants in human health and disease. *Annu. Rev. Nutr.* 16: 33-50.

70. Moody, C. S. & Hassan, H. M. (1982). Mutagenicity of oxygen free radicals. *Proc. Natl. Acad. Sci. USA* 79: 2855-2859.

71. Weitzman, S. A. & Stossel, T. P. (1981). Mutation caused by human phagocytes. *Science* 212: 546-547.

72. Weitzman, S. A. & Stossel, T. P. (1984). Phagocyte-induced mutation in Chinese hamster ovary cells. *Cancer Lett.* 22: 337-341.

73. Weitzman, S. A. & Weitberg, A. B. (1985). Phagocytes as carcinogens: Malignant transformation produced by human neutrophils. *Science* 227: 1231-1233.

74. Weitberg, A. B., *et al.* (1983). Stimulated human phagocytes produce cytogenetic

changes in cultured mammalian cells. *N. Engl. J. Med.* 308: 26-30.

75. Rosen, G. M., *et al.* (1995). Free radicals and phagocytic cells. *FASEB J.* 9: 200-209.

76. Phillips, B. J., James, T. E. & Anderson, D. (1984). Genetic damage in CHO cells exposed to enzymically generated active oxygen species. *Mutat. Res.* 126: 265-271.

77. Ziegler-Skylakakis, K. & Andrae, U. (1987). Mutagenicity of hydrogen peroxide in V79 Chinese hamster cells. *Mutat. Res.* 192: 65-67.

78. Bradley, M. O. & Erickson, L. C. (1981). Comparisons of the effects of hydrogen peroxide and X-ray irradiation on toxicity, mutation, and DNA damage/repair in mammalian cells (V-79). *Biochem. Biophys. Acta* 654: 135-141.

79. Hsie, A. W., *et al.* (1990). Molecular analysis of reactive oxygen-species-induced mammalian gene mutation. *Teratogenesis, Carcinogenesis, & Mutagenesis* 10: 115-124.

80. Hsie, A. W., *et al.* (1986). Evidence for reactive oxygen species inducing mutations in mammalian cells. *Proc. Natl. Acad. Sci. USA* 83: 9616-9620.

81. Emerit, I. & Cerutti, P. (1983). Clastogenic action of tumor promoter phorbol-12-myristate-13 acetate in mixed human leukocyte cultures. *Carcinogenesis* 4: 1313-1316.

82. Emerit, I., Khan, S. H. & Cerutti, P. A. (1985). Treatment of lymphocyte cultures with a hypoxanthine-xanthine oxidase system induces the formation of transferable clastogenic material. *J. Free Radic. Biol. Med.* 1: 51-57.

83. Emerit, I., *et al.* (1982). Activated oxygen species at the origin of chromosome breakage and sister chromatid exchanges. *Mutat. Res.* 103: 165-172.

84. Emerit, I. & Lahoud-Maghani, M. (1989). Mutagenic effects of TPA-induced clastogenic factor in Chinese hamster cells. *Mutat. Res.* 214: 97-104.

85. Emerit, I. (1994). Reactive oxygen species, chromosome mutation, and cancer: possible role of clastogenic factors in carcinogenesis. *Free Radic. Biol. Med.* 16: 99-109.

86. Ochi, T. & Cerutti, P. A. (1987). Clastogenic action of hydroperoxy-5,8,11,13-icosa tetraenoic acids on the mouse embryo fibroblasts C3H/10T1/2. *Proc. Natl. Acad. Sci. USA* 84: 990

87. Cerutti, P. A. & Trump, B. F. (1991). Inflammation and oxidant stress in carcinogenesis. *Cancer Cells* 3: 1-6.

88. Nathan, C. (1992). Nitric oxide as a secretory product of mammalian cells. *FASEB J.*

6: 3051-3064.

89. Kuo, P. C. & Schroeder, R. A. (1995). The emerging multifaceted roles of nitric oxide. *Ann. Surg.* 221: 220-235.

90. Ignarro, L. J. (1996). Physiology and pathophysiology of nitric oxide. *Kidney Int.* 49 Suppl. 55: S2-S5.

91. Feelisch, M. & Stamler, J. S. (1996). Donors of nitrogen oxides. Chapter 7. *Methods in Nitric Oxide Research.* Edited by M. Feelisch & J.S. Stamler. John Wiley & Sons, Inc. New York. pp. 71-115.

92. Morley, D., *et al.* (1993). Mechanism of vascular relaxation induced by the nitric oxide (NO)/nucleophile complexes, a new class of NO-based vasodilators. *J. Cardiovasc. Pharmacol.* 21: 670-676.

93. Beckman, J. S. (1995). *Nitric oxide: a modulator of cell-cell interactions in the microcirculation* Edited by P. Kubes. R.G. Landes Company, Texas. pp.1-18.

94. Kobzik, L., *et al.* (1994). Nitric oxide in skeletal muscle. *Nature* 372: 546-548.

95. Kobzik, L., *et al.* (1995). Endothelial type nitric oxide synthase in skeletal muscle fibers: Mitochondrial relationships. *Biochem. Biophys. Res. Commun.* 211: 375-381.

96. Stuehr, D. J. & Nathan, C. F. (1989). Nitric oxide. A macrophage product responsible for cytostasis and respiratory inhibition in tumor target cells. *J. Exp. Med.* 169: 1543-1555.

97. Bagasra, O., *et al.* (1995). Activation of the inducible form of nitric oxide synthase in the brains of patients with multiple sclerosis. *Proc. Natl. Acad. Sci. USA* 92: 12041-12045.

98. Park, S. K. & Murphy, S. (1994). Duration of expression of inducible nitric oxide synthase in glial cells. *J. Neurosci. Res.* 39: 405-411.

99. Borgerding, R. A. & Murphy, S. (1995). Expression of inducible nitric oxide synthase in cerebral endothelial cells is regulated by cytokine-activated astrocytes. *J. Neurochem.* 65: 1342-1347.

100. Hevel, J. M., White, K. A. & Marletta, M. A. (1991). Purification of the inducible murine macrophage nitric oxide synthase. Identification as a flavoprotein. *J. Biol. Chem.* 266: 22789-22791.

101. Marletta, M. A. (1994). Nitric oxide synthase: Aspects concerning structure and catalysis. *Cell* 78: 927-930.

102. Dawson, T. M. & Snyder, S. H. (1994). Gases as biological messengers: Nitric oxide

and carbon monoxide in the brain. *J. Neurosci.* 14: 5147-5159.

103. Nathan, C. & Xie, Q. (1994). Nitric oxide synthases: Roles, tolls, and controls. *Cell* 78: 915-918.

104. Lamas, S., *et al.* (1992). Endothelial nitric oxide synthase: molecular cloning and characterization of a distinct constitutive enzyme isoform. *Proc. Natl. Acad. Sci. USA* 89: 6348-6352.

105. McCall, T. B., *et al.* (1991). Identification of N-iminoethyl-L-ornithine as an irreversible inhibitor of nitric oxide synthase in phagocytic cells. *Br. J. Pharmacol.* 102: 234-238.

106. Olken, N. M., Osawa, Y. & Marletta, M. A. (1994). Characterization of the inactivation of nitric oxide synthase by N^G-methyl-L-arginine: Evidence for heme loss. *Biochemistry* 33: 14784-14791.

107. Bogle, R. G., *et al.* (1995). Induction of N^G-monomethyl-L-arginine uptake: A mechanism for differential inhibition of NO synthases. *Am. J. Physiol. Cell Physiol.* 269: C750-C756.

108. Connor, J. R., *et al.* (1995). Suppression of adjuvant-induced arthritis by selective inhibition of inducible nitric oxide synthase. *Eur. J. Pharmacol.* 273: 15-24.

109. Griffiths, M. J. D., *et al.* (1995). Aminoguanidine selectively decreases cyclic CMP levels produced by inducible nitric oxide synthase. *Am. J. Respir. Crit. Care Med.* 152: 1599-1604.

110. Nakane, M., *et al.* (1995). Novel potent and selective inhibitors of inducible nitric oxide synthase. *Mol. Pharmacol.* 47: 831-834.

111. Narayanan, K., *et al.* (1995). *S*-alkyl-L-thiocitrullines. Potent stereoselective inhibitors of nitric oxide synthase with strong pressor activity *in vivo*. *J. Biol. Chem.* 270: 11103-11110.

112. Rachmilewitz, D., *et al.* (1995). Experimental colitis is ameliorated by inhibition of nitric oxide synthase activity. *Gut* 37: 247-255.

113. Reif, D. W. & McCreedy, S. A. (1995). *N*-nitro-L-arginine and *N*-monomethyl-L-arginine exhibit a different pattern of inactivation toward the three nitric oxide synthases. *Arch. Biochem. Biophys.* 320: 170-176.

114. Stamler, J. S., Singel, D. J. & Loscalzo, J. (1992). Biochemistry of nitric oxide and its redox-activated forms. *Science* 258: 1898-1902.

115. Stamler, J. S., *et al.* (1992). Nitric oxide circulates in mammalian plasma primarily as an *S*-nitroso adduct of serum albumin. *Proc. Natl. Acad. Sci. USA* 89: 7674-7677.

116. Pryor, W. A. & Squadrito, G. L. (1995). The chemistry of peroxynitrite: A product from the reaction of nitric oxide with superoxide. *Am. J. Physiol. Lung Cell. Mol. Physiol.* 268: L699-L722.

117. Squadrito, G. L. & Pryor, W. A. (1995). The formation of peroxynitrite in vivo from nitric oxide and superoxide. *Chem. Biol. Interact.* 96: 203-206.

118. Barnes, P. J. & Liew, F. Y. (1995). Nitric oxide and asthmatic inflammation. *Immunol. Today* 16: 128-130.

119. Iadecola, C., *et al.* (1995). Inducible nitric oxide synthase gene expression in brain following cerebral ischemia. *J. Cereb. Blood Flow Metab.* 15: 378-384.

120. Brosnan, C. F., *et al.* (1994). Reactive nitrogen intermediates in human neuropathology: An overview. *Dev. Neurosci.* 16: 152-161.

121. Barnes, P. J. (1995). Nitric oxide and airway disease. *Ann. Med.* 27: 389-393.

122. Nussler, A. K., Billiar, T. R. & Simmons, R. L. (1995). Inducible nitric oxide synthase: Its role in inflammation, sepsis, and shock. *Prog. Surg.* 20: 33-50.

123. Amin, A. R., *et al.* (1995). The expression and regulation of nitric oxide synthase in human osteoarthritis-affected chondrocytes: Evidence for up-regulated neuronal nitric oxide synthase. *J. Exp. Med.* 182: 2097-2102.

124. McDaniel, M. L., *et al.* (1996). Cytokines and nitric oxide in islet inflammation and diabetes. *Proc. Soc. Exp. Biol. Med.* 211: 24-32.

125. Wong, M. L., *et al.* (1996). Inducible nitric oxide synthase gene expression in the brain during systemic inflammation. *Nature Med.* 2: 581-584.

126. Evans, C. H., Stefanovic-Racic, M. & Lancaster, J. (1995). Nitric oxide and its role in orthopaedic disease. [Review]. *Clin. Orthop.* 275-294.

127. Evans, C. H. (1995). Nitric oxide: what role does it play in inflammation and tissue destruction. [Review]. *Agents Actions Suppl.* 47: 107-116.

128. Belvisi, M., *et al.* (1995). Nitric oxide synthase activity is elevated in inflammatory lung disease in humans. *Eur. J. Pharmacol.* 283: 255-258.

129. Buttery, L. D. K., *et al.* (1996). Inducible nitric oxide synthase is present within human atherosclerotic lesions and promotes the formation and activity of peroxynitrite. *Lab. Invest.*

75: 77-85.

130. Cattell, V. & Jansen, A. (1995). Inducible nitric oxide synthase in inflammation. *Histochem. J.* 27: 777-784.

131. Nussler, A. K. & Billiar, T. R. (1993). Inflammation, immunoregulation, and inducible nitric oxide synthase. *J. Leukocyte Biol.* 54: 171-178.

132. Kaur, H. & Halliwell, B. (1994). Evidence for nitric oxide-mediated oxidative damage in chronic inflammation. Nitrotyrosine in serum and synovial fluid from rheumatoid patients. *FEBS Lett.* 350: 9-12.

133. Rachmilewitz, D., *et al.* (1995). Enhanced colonic nitric oxide generation and nitric oxide synthase activity in ulcerative colitis and Crohn's disease. *Gut* 36: 718-723.

134. Haddad, I. Y., *et al.* (1994). Quantitation of nitrotyrosine levels in lung sections of patients and animals with acute lung injury. *J. Clin. Invest.* 94: 2407-2413.

135. Thomsen, L. L., *et al.* (1995). Nitric oxide synthase activity in human breast cancer. *Br. J. Cancer* 72: 41-44.

136. Thomsen, L. L., *et al.* (1994). Nitric Oxide Synthase Activity in Human Gynecological Cancer. *Cancer Res.* 54: 1352-1354.

137. Chhatwal, V. J. S., *et al.* (1994). Aberrant expression of nitric oxide synthase in human polyps, neoplastic colonic mucosa and surrounding peritumoral normal mucosa. *Carcinogenesis* 15: 2081-2085.

138. Moochhala, S., *et al.* (1996). Nitric oxide synthase activity and expression in human colorectal cancer. *Carcinogenesis* 17: 1171-1174.

139. Cobbs, C. S., *et al.* (1995). Expression of nitric oxide synthase in human central nervous system tumors. *Cancer Res.* 55: 727-730.

140. Hara, E., *et al.* (1996). Expression of heme oxygenase and inducible nitric oxide synthase mRNA in human brain tumors. *Biochem. Biophys. Res. Commun.* 224: 153-158.

141. Ellie, E., *et al.* (1995). Differential expression of inducible nitric oxide synthase mRNA in human brain tumours. *Neuroreport* 7: 294-296.

142. Lipton, S. A., *et al.* (1993). A redox-based mechanism for the neuroprotective and neurodestructive effects of nitric oxide and related nitroso-compounds. *Nature* 364: 626-632.

143. Dawson, V. L. & Dawson, T. M. (1996). Nitric oxide in neuronal degeneration. *Proc. Soc. Exp. Biol. Med.* 211: 33-40.

144. Soares, H. D., *et al.* (1995). Inflammatory leukocytic recruitment and diffuse neuronal degeneration are separate pathological processes resulting from traumatic brain injury. *J. Neurosci.* 15: 8223-8233.

145. Youdim, M. B. H., Lavie, L. & Riederer, P. (1994). Oxygen free radicals and neurodegeneration in Parkinson's disease: A role for nitric oxide. *Ann. NY Acad. Sci.* 738: 64-68.

146. Dawson, V. L. & Dawson, T. M. (1996). Nitric oxide neurotoxicity. *J. Chem. Neuroanat.* 10: 179-190.

147. Vodovotz, Y., *et al.* (1996). Inducible nitric oxide synthase in tangle-bearing neurons of patients with Alzheimer's disease. *J. Exp. Med.* 184: 1425-1433.

148. Bukrinsky, M. I., *et al.* (1995). Regulation of nitric oxide synthase activity in human immunodeficiency virus type 1 (HIV-1)-infected monocytes: Implications for HIV-associated neurological disease. *J. Exp. Med.* 181: 735-745.

149. Lipton, S. A. & Gendelman, H. E. (1995). Nitric oxide and AIDS dementia. Reply. *N. Engl. J. Med.* 333: 522

150. Degroot, C. J. A., *et al.* (1997). Immuncytochemical characterization of the expression of inducible and constitutive isoforms of nitric oxide synthase in demyelinating multiple sclerosis lesions. *Journal of Neuropathology & Experimental Neurology* 56: 10-20.

151. Merrill, J. E., *et al.* (1993). Microglial cell cytotoxicity of oligodendrocytes is mediated through nitric oxide. *J. Immunol.* 151: 2132-2141.

152. Visser, J. J., Scholten, R. J. P. M. & Hoekman, K. (1994). Nitric oxide synthesis in meningococcal meningitis. *Ann. Intern. Med.* 120: 345-346.

153. Thomsen, L. L., *et al.* (1993). Arterial supersensitivity of nitric oxide (nitroglycerin) in migrane sufferers. *Cephalalgia* 13: 395-399.

154. Kosaka, H., *et al.* (1989). Nitrosation by stimulated macrophages. Inhibitors, enhancers and substrates. *Carcinogenesis* 10: 563-566.

155. Tamir, S. & Tannenbaum, S. R. (1996). The role of nitric oxide (NO.) in the carcinogenic process. *Biochim. Biophys. Acta Rev. Cancer* 1288: F31-F36.

156. Tamir, S., *et al.* (1996). DNA damage and genotoxicity by nitric oxide. *Methods Enzymol.* 269: 230-243.

157. Wink, D. A., *et al.* (1991). DNA deaminating ability and genotoxicity of nitric oxide and its progenitors. *Science* 254: 1001-1003.

158. Nguyen, T., *et al.* (1992). DNA damage and mutation in human cells exposed to nitric oxide in vitro. *Proc. Natl. Acad. Sci. USA* 89: 3030-3034.

159. DeRojas-Walker, T., *et al.* (1995). Nitric oxide induces oxidative damage in addition to deamination in macrophage DNA. *Chem. Res. Toxicol.* 8: 473-477.

160. Ischiropoulos, H., Zhu, L. & Beckman, J. S. (1992). Peroxynitrite formation from macrophage-derived nitric oxide. *Arch. Biochem. Biophys.* 298: 446-451.

161. Salgo, M. G., *et al.* (1995). DNA damage and oxidation of thiols peroxynitrite causes in rat thymocytes. *Arch. Biochem. Biophys.* 322: 500-505.

162. Uppu, R. M., *et al.* (1996). Competitive reactions of peroxynitrite with 2'-deoxyguanosine and 7,8-dihydro-8-oxo-2'-deoxyguanosine (8-oxodG): Relevance to the formation of 8-oxodG in DNA exposed to peroxynitrite. *Free Radic. Biol. Med.* 21: 407-411.

163. Salgo, M. G., Squadrito, G. L. & Pryor, W. A. (1995). Peroxynitrite causes apoptosis in rat thymocytes. *Biochem. Biophys. Res. Commun.* 215: 1111-1118.

164. Drapier, J. C. & Hibbs, J. B.,Jr. (1986). Murine cytotoxic activated macrophages inhibit aconitase in tumor cells. Inhibition involves the iron-sulfur prosthetic group and is reversible. *J. Clin. Invest.* 78: 790-797.

165. Drapier, J. C. & Hibbs, J. B.,Jr. (1988). Differentiation of murine macrophages to express nonspecific cytotoxicity for tumor cells results in L-arginine-dependent inhibition of mitochondrial iron-sulfur enzymes in the macrophage effector cells. *J. Immunol.* 140: 2829-2838.

166. Kwon, N. S., Stuehr, D. J. & Nathan, C. F. (1991). Inhibition of tumor cell ribonucleotide reductase by macrophage-derived nitric oxide. *J. Exp. Med.* 174: 761-767.

167. Filep, J. G., *et al.* (1996). Involvement of nitric oxide in target-cell lysis and DNA fragmentation induced by murine natural killer cells. *Blood* 87: 5136-5143.

168. Amber, I. J., *et al.* (1991). Activated macrophage conditioned medium: identification of the soluble factors inducing cytotoxicity and the L-arginine dependent effector mechanism. *J. Leukocyte Biol.* 49: 610-620.

169. Lysiak, J. J., *et al.* (1995). α_2-Macroglobulin functions as a cytokine carrier to induce nitric oxide synthesis and cause nitric oxide-dependent cytotoxicity in the RAW 264.7 macrophage cell line. *J. Biol. Chem.* 270: 21919-21927.

170. Damoulis, P. D. & Hauschka, P. V. (1997). Nitric oxide acts in conjunction with proinflammatory cytokines to promote cell death in osteoblasts. *J. Bone Miner. Res.* 12:

412-422.

171. Everett, S. A., *et al.* (1996). Nitric oxide involvement in the toxicity of hydroxyguanidine in leukaemia HL60 cells. *Br. J. Cancer* 74 Suppl. 27: S172-S176.

172. Gehrmann, J., Matsumoto, Y. & Kreutzberg, G. W. (1995). Microglia: Intrinsic immuneffector cell of the brain. *Brain Res. Rev.* 20: 269-287.

173. Le, W.-D., *et al.* (1995). Cell death induced by β-amyloid 1-40 in MES 23.5 hybrid clone: The role of nitric oxide and NMDA-gated channel activation leading to apoptosis. *Brain Res.* 686: 49-60.

174. Tamir, S., *et al.* (1995). Nitric oxide production in relation to spontaneous B-cell lymphoma and myositis in SJL mice. *Cancer Res.* 55: 4391-4397.

175. Szabó, C., *et al.* (1996). DNA strand breakage, activation of poly(ADP-ribose) synthetase, and cellular energy depletion are involved in the cytotoxicity in macrophages and smooth muscle cells exposed to peroxynitrite. *Proc. Natl. Acad. Sci. USA* 93: 1753-1758.

176. Juedes, M. J. & Wogan, G. N. (1996). Peroxynitrite-induced mutation spectra of pSP189 following replication in bacteria and in human cells. *Mutat. Res. Fundam. Mol. Mech. Mutagen.* 349: 51-61.

177. Routledge, M. N., Wink, D. A., Keefer, L. K. & Dipple, A. (1993). Mutations induced by saturated aqueous nitric oxide in the pSP189 *supF* gene in human Ad293 and *E. coli* MBM7070 cells. *Carcinogenesis* 14: 1251-1254.

178. Arroyo, P. L., *et al.* (1992). Mutagenicity of nitric oxide and its inhibition by antioxidants. *Mutat. Res. Lett.* 281: 193-202.

179. Maragos, C. M., *et al.* (1993). Mutagenicity of glyceryl trinitrate (nitroglycerin) in Salmonella typhimurium. *Mutat. Res.* 298: 187-195.

180. Felley-Bosco, E., *et al.* (1995). Nitric oxide and ethylnitrosourea: Relative mutagenicity in the *p53* tumor suppressor and hypoxanthine-phosphoribosyltransferase genes. *Carcinogenesis* 16: 2069-2074.

181. Dolle, M. E., *et al.* (1996). Evaluation of a plasmid-based transgenic mouse model for detecting in vivo mutations. *Mutagenesis* 11: 111-118.

182. Gal, A. & Wogan, G. N. (1996). Mutagenesis associated with nitric oxide production in transgenic SJL mice. *Proc. Natl. Acad. Sci. USA* 93: 15102-15107.

183. Gossen, J. A., *et al.* (1995). Spontaneous and X-ray-induced deletion mutations in a LacZ plasmid-based transgenic mouse model. *Mutat. Res.* 331: 89-97.

184. Heim, S. (1996). Clonal chromosome abnormalities in neoplastic cells: Evidence of genetic instability. *Cancer Surv.* 28: 247-260.

185. Yunis, J. J. (1983). The chromosomal basis of human neoplasia. *Science* 221: 227-236.

186. Murnane, J. P. (1996). Role of induced genetic instability in the mutagenic effects of chemicals and radiation. *Mutat. Res. Genet. Toxicol.* 367: 11-23.

187. Loeb, L. A. & Christians, F. C. (1996). Multiple mutations in human cancers. *Mutat. Res. Fundam. Mol. Mech. Mutagen.* 350: 279-286.

188. Liu, B., *et al.* (1995). Genetic instability occurs in the majority of young patients with colorectal cancer. *Nature Med.* 1: 348-352.

189. Sweezy, M. A. & Fishel, R. (1994). Multiple pathways leading to genomic instability and tumorigenesis. *Ann. NY Acad. Sci.* 726: 165-177.

190. Fishel, R., *et al.* (1994). Binding of mismatched microsatellite DNA sequences by the human MSH2 protein. *Science* 266: 1403-1405.

191. Fishel, R. (1996). Genomic instability, mutators, and the development of cancer: Is there a role for p53. *J. Natl. Cancer Inst.* 88: 1608-1609.

192. Birnboim, H. C. (1983). *Radioprotectors and anticarcinogens.* Edited by O.F. Nygaard & M.G. Simic. Academic Press, New York. pp. 539-556.

193. Bennett, S. A. L., Leite, L. C. C. & Birnboim, H. C. (1993). Platelet activating factor, an endogenous mediation of inflammation, induces phenotypic transformation of rat embryo cells. *Carcinogenesis* 14: 1289-1296.

194. Sandhu, J. K. & Birnboim, H. C. (1997). Mutagenicity and cytotoxicity of reactive oxygen and nitrogen species in the MN-11 murine tumor cell line. *Mutat. Res.* 379: 241-252.

195. Weitzman, S. A. & Gordon, L. I. (1990). Inflammation and cancer: role of phagocyte-generated oxidants in carcinogenesis. *Blood* 76: 655-663.

196. Troll, W. & Wiesner, R. (1985). The role of oxygen radicals as a possible mechanism of tumor promotion. *Annu. Rev. Pharmacol. Toxicol.* 25: 509-528.

197. Kadhim, S. A. & Rees, R. C. (1984). Enhancement of tumor growth in mice: Evidence for the involvement of host macrophages. *Cell. Immunol.* 87: 259-269.

198. Kadhim, S., Burns, B. F. & Birnboim, H. C. (1987). In vivo induction of tumor variants by phorbol 12-myristate 13-acetate. *Cancer Lett.* 38: 209-214.

199. Trosko, J. E. & Chang, C.-C. (1984). *Mechanisms of tumor promotion. vol. IV. Cellular responses to tumor promoters*. Edited by T.J. Slaga. CRC Press, Boca Raton, Florida. pp.119-145.

200. Nishi, Y., Hasegawa, M. M. & Inui, N. (1984). Forward mutation assay of V79 cells to 6-thioguanine resistance in a soft agar technique that eliminates effects of metabolic co-operation. *Mutat. Res.* 125: 105-114.

201. Zhang, L. S., *et al.* (1996). Chromosome painting analysis of spontaneous and methyl methanesulfonate-induced trifluorothymidine-resistant L5178Y cell colonies. *Mutat. Res.* 370: 181-190.

202. Ashby, J., *et al.* (1994). Potent clastogenicity of the human carcinogen etoposide to the mouse bone marrow and mouse lymphoma L5178Y cells: comparison to Salmonella responses. *Environ. Mol. Mutagen.* 24: 51-60.

203. Davies, M. J., Phillips, B. J. & Rumsby, P. C. (1993). Molecular analysis of mutations at the tk locus of L5178Y mouse-lymphoma cells induced by ethyl methanesulphonate and mitomycin C. *Mutat. Res.* 290: 145-153.

204. McGuinness, S. M., *et al.* (1995). Mutant quantity and quality in mammalian cells (AL) exposed to cesium-137 gamma radiation: effect of caffeine [published erratum appears in Radiat Res 1997 Jan;147(1):120]. *Radiat. Res.* 142: 247-255.

205. Speit, G., *et al.* (1992). Cytogenetic and molecular characterization of the mutagenicity of chlorambucil in V79 cells. *Mutat. Res.* 283: 75-81.

206. Bringuier, P. P., *et al.* (1993). DNA ploidy status and DNA content instability within single tumors in renal cell carcinoma. *Cytometry* 14: 559-564.

207. Nielsen, J. L., *et al.* (1993). Evidence of gene amplification in the form of double minute chromosomes is frequently observed in lung cancer. *Cancer Genet. Cytogenet.* 65: 120-124.

208. Risinger, J. I., *et al.* (1993). Genetic instability of microsatellites in endometrial carcinoma. *Cancer Res.* 53: 5100-5103.

209. Brison, O. (1993). Gene amplification and tumor progression. *Biochim. Biophys. Acta Rev. Cancer* 1155: 25-41.

210. Shibata, D., *et al.* (1994). Genomic instability in repeated sequences is an early somatic event in colorectal tumorigenesis that persists after transformation. *Nature Genet.* 6: 273-281.

211. Shridhar, V., *et al.* (1994). Genetic instability of microsatellite sequences in many

non-small cell lung carcinomas. *Cancer Res.* 54: 2084-2087.

212. Han, H.-J., *et al.* (1993). Genetic instability in pancreatic cancer and poorly differentiated type of gastric cancer. *Cancer Res.* 53: 5087-5089.

213. Augenlicht, L. H., *et al.* (1996). Evidence for genomic instability in human colonic aberrant crypt foci. *Oncogene* 12: 1767-1772.

214. Kahlenberg, M. S., *et al.* (1996). *p*53 tumor suppressor gene status and the degree of genomic instability in sporadic colorectal cancers. *J. Natl. Cancer Inst.* 88: 1665-1670.

215. Farid, N. R. (1996). Molecular pathogenesis of thyroid cancer: The significance of oncogenes, tumor suppressor genes, and genomic instability. *Exp. Clin. Endocrinol. Diabetes* 104 Suppl. 4: 1-12.

216. Habuchi, T., *et al.* (1994). Oncogene amplification in urothelial cancers with *p*53 gene mutation or MDM2 amplification. *J. Natl. Cancer Inst.* 86: 1331-1335.

217. Eyfjörd, J. E., *et al.* (1995). *p53* abnormalities and genomic instability in primary human breast carcinomas. *Cancer Res.* 55: 646-651.

218. Donehower, L. A., *et al.* (1995). Deficiency of *p53* accelerates mammary tumorigenesis in *Wnt-1* transgenic mice and promotes chromosomal instability. *Genes Dev.* 9: 882-895.

219. Tainsky, M. A., Bischoff, F. Z. & Strong, L. C. (1995). Genomic instability due to germline *p*53 mutations drives preneoplastic progression toward cancer in human cells. *Cancer Metastasis Rev.* 14: 43-48.

220. Albertini, R. J., *et al.* (1993). In vivo mutations in human blood cells: biomarkers for molecular epidemiology. *Environ. Health Perspect.* 99: 135-141.

221. Albertini, R. J., *et al.* (1990). In vivo somatic mutations in humans: measurement and analysis. *Annu. Rev. Genet.* 24: 305-326.

222. Branda, R. F., *et al.* (1993). Measurement of HPRT mutant frequencies in T-lymphocytes from healthy human populations. *Mutat. Res.* 285: 267-279.

223. Cariello, N. F. & Skopek, T. R. (1993). *In vivo* mutation at the human *HPRT* locus. *Trends Genet.* 9: 322-326.

224. Wurdeman, R. L., Douskey, M. C. & Gold, B. (1993). DNA methylation by N-methyl-N-nitrosourea: Methylation pattern changes in single- and double-stranded DNA, and in DNA with mismatched or bulged guanines. *Nucleic Acids Res.* 21: 4975-4980.

225. Shibata, M.-A., *et al.* (1994). DNA methylation adduct formation and H-*ras* gene

mutations in progression of *N*-butyl-*N*-(4-hydroxybutyl)nitrosamine-induced bladder tumors caused by a single exposure to *N*-methyl-*N*-nitrosourea. *Carcinogenesis* 15: 2965-2968.

226. Akagi, T., *et al.* (1993). Specificity of mutations induced by *N*-methyl-*N*-nitrosourea in a cDNA of the *hprt* gene. *Carcinogenesis* 14: 725-729.

227. Evans, H. H., *et al.* (1986). Locus specificity in the mutability of L5178Y mouse lymphoma cells: the role of multilocus lesions. *Proc. Natl. Acad. Sci. USA* 83: 4379-4383.

228. Schwartz, J. L., *et al.* (1991). Differential locus sensitivity to mutation induction by ionizing radiations of different LETs in Chinese hamster ovary K1 cells. *Carcinogenesis* 12: 1721-1726.

229. Klein, C. B., *et al.* (1994). Transgenic *gpt*⁻ V79 cell lines differ in their mutagenic response to clastogens. *Mutat. Res. Fundam. Mol. Mech. Mutagen.* 304: 217-228.

230. Ikehata, H., Kimura, H. & Kato, T. (1989). Shuttle vector system for the analysis of mutational events in mammalian chromosomal DNA. *Mutat. Res.* 210: 237-247.

231. Schwartz, J. L., *et al.* (1994). Multiplex polymerase chain reaction-based deletion analysis of spontaneous, gamma ray- and alpha-induced *hprt* mutants of CHO-K1 cells. *Mutagenesis* 9: 537-540.

232. Bradley, W. E., Belouchi, A. & Messing, K. (1988). The aprt heterozygote/hemizygote system for screening mutagenic agents allows detection of large deletions. *Mutat. Res.* 199: 131-138.

233. Vrieling, H., *et al.* (1985). Mutations induced by X-rays at the HPRT locus in cultured Chinese hamster cells are mostly large deletions. *Mutat. Res.* 144: 281-286.

234. Selby, C. P. & Sancar, A. (1990). Molecular mechanisms of DNA repair inhibition by caffeine. *Proc. Natl. Acad. Sci. USA* 87: 3522-3525.

235. Zhen, W. & Vaughan, A. T. M. (1995). Effect of Caffeine on Radiation-Induced Apoptosis in TK6 cells. *Radiat. Res.* 141: 170-175.

236. Kendal, W. S. & Frost, P. (1988). Pitfalls and Practice of Luria-Delbruck Fluctuation Analysis: A Review. *Cancer Res.* 48: 1060-1065.

237. Kuhl, D. P. & Caskey, C. T. (1993). Trinucleotide repeats and genome variation. *Curr. Opin. Genet. Dev.* 3: 404-407.

238. Rockwell, S. (1980). In vivo-in vitro tumour cell lines: characteristics and limitations as models for human cancer. *British Journal of Cancer - Supplement* 41: 118-122.

239. Rockwell, S. (1977). In vivo-in vitro tumor systems: new models for studing the response of tumours to therapy. [Review] [67 refs]. *Laboratory Animal Science* 27: 831-851.

240. Yamada, T. & Grisham, M. B. (1991). Role of neutrophil-derived oxidants in the pathogenesis of intestinal inflammation. *Klin. Wochenschr.* 69: 988-994.

241. Mannick, E. E., *et al.* (1996). Inducible nitric oxide synthase, nitrotyrosine, and apoptosis in Helicobacter pylori gastritis: effect of antibiotics and antioxidants. *Cancer Res.* 56: 3238-3243.

242. Petrone, W. F., *et al.* (1980). Free radicals and inflammation: Superoxide-dependent activation of a neutrophil chemotactic factor in plasma. *Proc. Natl. Acad. Sci. USA* 77: 1159-1163.

243. Tlsty, T. D. (1996). Regulation of genomic instability in preneoplastic cells. *Cancer Surv.* 28: 217-224.

244. Tlsty, T. D. (1995). Cell cycle control and genomic instability. *Cancer Metastasis Rev.* 14: 1-2.

245. Tlsty, T. D., *et al.* (1995). Genomic instability and cancer. *Mutat. Res. DNA Repair* 337: 1-7.

246. Gal, A., Tamir, S., Tannenbaum, S. R. & Wogan, G. N. (1996). Nitric Oxide Production in SJL Mice bearing the RCSX lymphoma - A model for in vivo toxicological evaluation of NO. *Proc. Natl. Acad. Sci. USA* 93: 11499-11503.

247. Isaacs, J. T. & Coffey, D. S. (1981). Adaptation versus selection as the mechanism responsible for the relapse of prostatic cancer to androgen ablation therapy as studied in the Dunning R-3327-H adenocarcinoma. *Cancer Res.* 4: 5070-5075.

248. Nichols, K., Staines, W., Wu, J.-Y. & Krantis, A. (1995). Immunopositive GABAergic neural sites display nitric oxide synthase-related NADPH diaphorase activity in the human colon. *J. Auton. Nerv. Syst.* 50: 253-262.

249. Nichols, K., Staines, W. & Krantis, A. (1993). Nitric oxide synthase distribution in the rat intestine: a histochemical analysis. *Gastroenterology* 105: 1651-1661.

250. Bancroft, J. D. & Cook, H. C. (1994). *Manual of histological Techniques and their diagnostic application.* Edited by R. Swan. Churchill Livingstone, London. pp. 289-322.

251. Staunton, M. J. & Gaffney, E. F. (1995). Tumor type is a determinant of susceptibility to apoptosis. *Am. J. Clin. Pathol.* 103: 300-307.

252. Graeber, T. G., *et al.* (1996). Hypoxia-mediated selection of cells with diminished

apoptotic potential in solid tumours. *Nature* 379: 88-91.

253. Graeber, T. G., *et al.* (1994). Hypoxia induces accumulation of *p53* protein, but activation of a G1-phase checkpoint by low-oxygen conditions is independent of *p53* status. *Molecular & Cellular Biology* 14: 6264-6277.

254. Yonish-Rouach, E., *et al.* (1991). Wild-type *p53* induces apoptosis of myeloid leukaemic cells that is inhibited by interleukin-6. *Nature* 352: 345-347.

255. Shaw, P., *et al.* (1992). Induction of apoptosis by wild-type *p53* in a human colon tumor-derived cell line. *Proc. Natl. Acad. Sci. USA* 89: 4495-4499.

256. Hooper, M. L. (1994). The role of the *p53* and *Rb-1* genes in cancer, development and apoptosis. *J. Cell Sci.* 107 Suppl. 18: 13-17.

257. Mooney, E. E., *et al.* (1995). Apoptotic and mitotic indices in malignant melanoma and basal cell carcinoma. *J. Clin. Pathol.* 48: 242-244.

258. Wynford-Thomas, D. & Williams, E. D. (1986). Use of bromodeoxyuridine for cell kinetic studies in intact animals. *Cell & Tissue Kinetics* 19: 179-182.

259. Dover, R. & Patel, K. (1994). Improved methodology for detecting bromodeoxyuridine in cultured cells and tissue sections by immunocytochemistry. *Histochem.* 102: 383-387.

260. Schultz, R. M., Chirigos, M. A. & Olkowski, Z. L. (1980). Stimulation and inhibition of neoplastic cell growth by tumor promoter- treated macrophages. *Cell. Immunol.* 54: 98-106.

261. Wei, W., *et al.* (1986). Characterization of lymphocytic infiltrates in normal, preneoplastic, and neoplastic mouse mammary tissues. *Cancer Res.* 46: 2680-85.

262. Lee, A. H. S., *et al.* (1996). Inflammatory infiltrate in invasive lobular and ductal carcinoma of the breast. *Br. J. Cancer* 74: 796-801.

263. Kirsch, I. R., *et al.* (1994). Lymphocyte-specific genetic instability and cancer. *Cold Spring Harbor Symp. Quant. Biol.* 59: 287-296.

264. McBride, W. H. (1986). Phenotype and functions of intratumoral macrophages. [Review]. *Biochim. Biophys. Acta* 865: 27-41.

265. Evans, R. (1982). Macrophages and neoplasms: new insights and their implication in tumor immunobiology. [Review] [81 refs]. *Cancer Metastasis Rev.* 1: 227-239.

266. Evans, R. (1972). Macrophages in syngeneic animal tumours. *Transplantation* 14: 468-473.

267. Lauder, I., *et al.* (1977). Macrophage infiltration of breast tumours: a prospective study. *J. Clin. Pathol.* 30: 563-568.

268. Watanabe, K., *et al.* (1989). The neutrophil chemoattractant produced by the rat kidney epithelioid cell line NRK-52E is a protein related to the KC/gro protein. *J. Biol. Chem.* 264: 19559-19563.

269. Harada, A., *et al.* (1994). Essential involvement of interleukin-8 (IL-8) in acute inflammation. [Review] [48 refs]. *J. Leukocyte Biol.* 56: 559-564.

270. Hoshino, Y., *et al.* (1995). Monocyte chemoattractant protein-1 stimulates tumor necrosis and recruitment of macrophages into tumors in tumor-bearing nude mice: increased granulocyte and macrophage progenitors in murine bone marrow. *Exp. Hematol.* 23: 1035-1039.

271. Hirose, K., *et al.* (1995). Chemokine gene transfection into tumour cells reduced tumorigenicity in nude mice in association with neutrophilic infiltration. *Br. J. Cancer* 72: 708-714.

272. Colombo, M. P., *et al.* (1991). Granulocyte colony-stimulating factor gene transfer suppresses tumorigenicity of a murine adenocarcinoma in vivo. *J. Exp. Med.* 173: 889-897.

273. Yoshida, M., *et al.* (1993). Neutrophil chemotactic factors produced by malignant fibrous histiocytoma cell lines. *Br. J. Cancer* 67: 508-513.

274. Liber, H. L., Yandell, D. W. & Little, J. B. (1989). A comparison of mutation induction at the tk and hprt loci in human lymphoblastoid cells; quantitative differences are due to an additional class of mutations at the autosomal tk locus. *Mutat. Res.* 216: 9-17.

275. Halliwell, B. (1995). Oxygen radicals, nitric oxide and human inflammatory joint disease. *Ann. Rheum. Dis.* 54: 505-510.

276. Birnboim, H. C. (1990). Fluorometric analysis of DNA unwinding to study strand breaks and repair in mammalian cells. *Methods Enzymol.* 186: 550-555.

277. Kallmann, B., *et al.* (1992). Toxicity of chemically generated nitric oxide towards pancreatic islet cells can be prevented by nicotinamide. *Life Sci.* 51: 671-678.

278. Ferioli, R., *et al.* (1995). A new class of furoxan derivatives as NO donors: Mechanism of action and biological activity. *Br. J. Pharmacol.* 114: 816-820.

279. Green, L. C., *et al.* (1982). Analysis of nitrate, nitrite, and [^{15}N]nitrate in biological fluids. *Anal. Biochem.* 126: 131-138.

280. Breen, A. P. & Murphy, J. A. (1995). Reactions of oxyl radicals with DNA. *Free*

Radic. Biol. Med. 18: 1033-1077.

281. DeChatelet, L. R., Shirley, P. S. & Johnston, R. B.,Jr. (1976). Effect of phorbol myristate acetate on the oxidative metabolism of human polymorphonuclear leukocytes. *Blood* 47: 545-554.

282. Bates, J. N., *et al.* (1991). Nitric oxide generation from nitroprusside by vascular tissue. Evidence that reduction of the nitroprusside anion and cyanide loss are required. *Biochem. Pharmacol.* 42 Suppl. S157-S165.

283. Feelisch, M. & Kelm, M. (1991). Biotransformation of organic nitrates to nitric oxide by vascular smooth muscle and endothelial cells. *Biochem. Biophys. Res. Commun.* 180: 286-293.

284. Bohme, E., Grossman, G. & Spies, C. (1983). Effects of molsidomine and other NO-containing vasodilators on cyclic GMP formation. [Review]. *Eur. Heart J.* 4 Suppl C: 19-24.

285. Wang, J., *et al.* (1993). Effects of an orally active NO-releasing agent, CAS 936, and its active metabolite, 3754, on cardiac and coronary dynamics in normal conscious dogs and after pacing-induced heart failure. *J. Cardiovasc. Pharmacol.* 22 Suppl 7: S51-8.

286. Ignarro, L. J., Fukuto, J. M., Griscavage, J. M., Rogers, N. E. & Byrns, R. E. (1993). Oxidation of nitric oxide in aqueous solution to nitrite but not nitrate: comparison with enzymatically formed nitric oxide from L-arginine. *Proc. Natl. Acad. Sci. USA* 90: 8103-8107.

287. Feelisch, M. & Kubitzek, D. (1996). The oxyhemoglobin Assay. Chapter 31. *Methods in Nitric Oxide Research.* Edited by M. Feelisch & J.S. Stamler. John Wiley & Sons, Inc. New York. pp. 455-478.

288. Ignarro, L. J. (1990). Biosynthesis and metabolism of endothelium-derived nitric oxide. *Annu. Rev. Pharmacol. Toxicol.* 30: 535-560.

289. Povirk, L. F., *et al.* (1994). Single base-pair deletions induced by bleomycin at potential double-strand cleavage sites in the *aprt* gene of stationary phase Chinese hamster ovary D422 cells. *J. Mol. Biol.* 243: 216-226.

290. Taylor, A. M., *et al.* (1983). Effects of the DNA strand-cleaving antitumor agent, streptonigrin, on ataxia telangiectasia cells. *Cancer Res.* 43: 2700-2703.

291. Nassi-Calò, L., Mello Filho, A. C. & Meneghini, R. (1989). *o*-Phenanthroline protects mammalian cells from hydrogen peroxide-induced gene mutation and morphological transformation. *Carcinogenesis* 10: 1055-1057.

292. Stamato, T. D. & Denko, N. (1990). Asymmetric field inversion gel electrophoresis: a new method for detecting DNA double-strand breaks in mammalian cells. *Radiat. Res.* 121: 196-205.

293. Schaiff, W. T., *et al.* (1992). HLA-DR associates with specific stress proteins and is retained in the endoplasmic reticulum in invariant chain negative cells. *J. Exp. Med.* 176: 657-666.

294. Evans, T. J., *et al.* (1996). Cytokine-treated human neutrophils contain inducible nitric oxide synthase that produces nitration of ingested bacteria. *Proc. Natl. Acad. Sci. USA* 93: 9553-9558.

295. Marks, G. S., *et al.* (1992). Biotransformation of glyceryl trinitrate by rat brain homogenate. *Can. J. Physiol. Pharmacol.* 70: 935-937.

296. Darius, H., Grodzinska, L. & Meyer, J. (1992). The effects of the nitric oxide donors molsidomine and SIN- I on human polymorphonuclear leucocyte function *in vitro* and *ex vivo*. *Eur. J. Clin. Pharmacol.* 43: 629-633.

297. Maragos, C. M., *et al.* (1991). Complexes of .NO with nucleophiles as agents for the controlled biological release of nitric oxide. Vasorelaxant effects. *J. Med. Chem.* 34: 3242-3247.

298. Kroncke, K. D., *et al.* (1993). Pancreatic islet cells are highly susceptible towards the cytotoxic effects of chemically generated nitric oxide. *Biochim. Biophys. Acta* 1182: 221-229.

299. Salvemini, D., *et al.* (1992). Metabolism of glyceryl trinitrate to nitric oxide by endothelial cells and smooth muscle cells and its induction by Escherichia coli lipopolysaccharide. *Proc. Natl. Acad. Sci. USA* 89: 982-986.

300. Owais, W. M., Janakat, S. & Hunaiti, A. (1985). Activation of sodium cyanide to a toxic but non-mutagenic metabolite in Salmonella typhimurium. *Mutat. Res.* 144: 119-125.

301. Maragos, C. M., *et al.* (1993). Nitric oxide/nucleophile complexes inhibit the in vitro proliferation of A375 melanoma cells via nitric oxide release. *Cancer Res.* 53: 564-568.

302. Tsuda, H. & Hasegawa, M. (1990). Malignant transformation of mouse BALB/c3T3 cells induced by NaNO2. *Carcinogenesis* 11: 595-597.

303. Schmutte, C., *et al.* (1994). Mutagenicity of nitric oxide is not caused by deamination of cytosine or 5-methylcytosine in double-stranded DNA. *Carcinogenesis* 15: 2899-2903.

304. Knowles, R. G. (1996). Nitric oxide synthases. *Biochem. Soc. Trans.* 24: 875-878.

305. Bredt, D. S., Hwang, P. M. & Snyder, S. H. (1990). Localization of nitric oxide synthase indicating a neural role for nitric oxide. *Nature* 347: 768-770.

306. Garthwaite, J. (1995). Neural nitric oxide signalling. *Trends in Neurosci.* 18: 51-52.

307. Liew, F. Y. (1994). Biology of nitric oxide in neuroimmunoregulation. *Ann. NY Acad. Sci.* 741: 39-45.

308. Jaffrey, S. R. & Snyder, S. H. (1995). Nitric oxide: A neural messenger. *Annu. Rev. Cell Biol.* 11: 417-440.

309. Singer, I. I., *et al.* (1996). Expression of inducible nitric oxide synthase and nitrotyrosine in colonic epithelium in inflammatory bowel disease. *Gastroenterology* 111: 871-885.

310. Keefer, L. K., *et al.* (1995). Experimental Tests of the Mutagenicity and Carcinogenicity of Nitric Oxide and Its Progenitors. *Methods: A Companion to Methods in Enzymology* 7: 121-130.

311. Christen, S., Gee, P. & Ames, B. N. (1996). Mutagenicity of nitric oxide in base pair-specific *Salmonella* tester strains: TA7000 series. *Methods Enzymol.* 269: 267-278.

312. Routledge, M. N., *et al.* (1994). DNA sequence changes induced by two nitric oxide donor drugs in the *supF* assay. *Chem. Res. Toxicol.* 7: 628-632.

313. Stuehr, D. J. & Marletta, M. A. (1987). Synthesis of nitrite and nitrate in murine macrophage cell lines. *Cancer Res.* 47: 5590-5594.

314. Shindo, T., *et al.* (1995). Nitric oxide synthesis in cardiac myocytes and fibroblasts by inflammatory cytokines. *Cardiovasc. Res.* 29: 813-819.

315. LeClaire, R. D., *et al.* (1995). Regulation of staphylococcal enterotoxin B-elicited nitric oxide production by endothelial cells. *Infect. Immun.* 63: 539-546.

316. Billiar, T. R. (1995). Nitric oxide: Novel biology with clinical relevance. *Ann. Surg.* 221: 339-349.

317. Radomski, M. W., *et al.* (1991). Human colorectal adenocarcinoma cells: Differential nitric oxide synthesis determines their ability to aggregate platelets. *Cancer Res.* 51: 6073-6078.

318. Jenkins, D. C., *et al.* (1994). Human colon cancer cell lines show a diverse pattern of nitric oxide synthase gene expression and nitric oxide generation. *Br. J. Cancer* 70: 847-849.

319. Knowles, R. G., *et al.* (1990). Differential induction of brain, lung and liver nitric oxide

synthase by endotoxin in the rat. *Biochem. J.* 270: 833-836.

320. Bradford, M. M. (1976). A rapid and sensitive method for the quantitation of microgram quantities of protein utilizing the principle of protein-dye binding. *Anal. Biochem.* 72: 248-254.

321. Towbin, H., Staehelin, T. & Gordon, J. (1979). Electrophoretic transfer of proteins from polyacrylamide gels to nitrocellulose sheets: procedure and some applications. *Proc. Natl. Acad. Sci. USA* 76: 4350-4354.

322. Hibbs, J. B.,Jr., Taintor, R. R. & Vavrin, Z. (1987). Macrophage cytotoxicity: role for L-arginine deiminase and imino nitrogen oxidation to nitrite. *Science* 235: 473-476.

323. Fulton, A. M., Loveless, S. E. & Heppner, G. H. (1984). Mutagenic activity of tumor-associated macrophages in Salmonella typhimurium strains TA98 and TA100. *Cancer Res.* 44: 4308-4311.

324. Chong, Y. C., *et al.* (1989). Macrophage-mediated induction of DNA strand breaks in target tumor cells. *Cancer Res.* 49: 6652-6657.

325. Fulton, A. M. & Chong, Y. C. (1992). The role of macrophage-derived TNFa in the induction of sublethal tumor cell DNA damage. *Carcinogenesis* 13: 77-81.

326. Beesley, J. E. (1995). Histochemical methods for detecting nitric oxide synthase. *Histochem. J.* 27: 757-769.

327. Wallace, M. N. (1996). NADPH diaphorase activity in activated astrocytes representing inducible nitric oxide synthase. *Methods Enzymol.* 268: 497-503.

328. Staines, W. A., *et al.* (1996). Retinoic acid treated P19 embryonal carcinoma cells differentiate into oligodendrocytes capable of myelination. *Neuroscience* 71: 845-853.

329. McBurney, M. W. (1993). P19 embryonal carcinoma cells. [Review] [55 refs]. *International Journal of Developmental Biology* 37: 135-140.

330. Lynn, R. B., *et al.* (1995). Colocalization of NADPH-diaphorase staining and VIP immunoreactivity in neurons in opossum internal anal sphincter. *Dig. Dis. Sci.* 40: 781-791.

331. Afework, M. & Burnstock, G. (1995). Colocalization of neuropeptides and NADPH-diaphorase in the intra-adrenal neuronal cell bodies and fibres of the rat. *Cell Tissue Res.* 280: 291-295.

332. Tharakan, T., *et al.* (1995). Appearance of neuropeptides and NADPH-diaphorase during development of the enteropancreatic innervation. *Dev. Brain Res.* 84: 26-38.

333. Huxlin, K. R. (1995). NADPH-diaphorase expression in neurons and glia of the normal adult rat retina. *Brain Res.* 692: 195-206.

334. Tassorelli, C. & Joseph, S. A. (1995). NADPH-diaphorase activity and Fos expression in brain nuclei following nitroglycerin administration. *Brain Res.* 695: 37-44.

335. Blottner, D., Grozdanovic, Z. & Gossrau, R. (1995). Histochemistry of nitric oxide synthase in the nervous system. *Histochem. J.* 27: 785-811.

336. Page, G. K. & Morton, A. J. (1995). Correlation of neuronal loss with increased expression of NADPH diaphorase in cultured rat cerebellum and cerebral cortex. *Brain Res.* 697: 157-168.

337. Chao, D. S., *et al.* (1996). Localization of neuronal nitric oxide synthase. *Methods Enzymol.* 268: 488-496.

338. Frandsen, U., Lopez-Figueroa, M. & Hellsten, Y. (1996). Localization of nitric oxide synthase in human skeletal muscle. *Biochem. Biophys. Res. Commun.* 227: 88-93.

339. Amber, I. J., *et al.* (1988). The L-arginine dependent effector mechanism is induced in murine adenocarcinoma cells by culture supernatant from cytotoxic activated macrophages. *J. Leukocyte Biol.* 43: 187-192.

340. Paul, A., Pendreigh, R. H. & Plevin, R. (1995). Protein kinase C and tyrosine kinase pathways regulate lipopolysaccharide-induced nitric oxide synthase activity in RAW 264.7 murine macrophages. *Br. J. Pharmacol.* 114: 482-488.

341. Ding, A. H., Nathan, C. F. & Stuehr, D. J. (1988). Release of reactive nitrogen intermediates and reactive oxygen intermediates from mouse peritoneal macrophages. Comparison of activating cytokines and evidence for independent production. *J. Immunol.* 141: 2407-2412.

342. Lewis, J. G. & Adams, D. O. (1985). Induction of 5,6-ring-saturated thymine bases in NIH-3T3 cells by phorbol ester-stimulated macrophages: Role of reactive oxygen intermediates. *Cancer Res.* 45: 1270-1275.

343. Ibuki, Y. & Goto, R. (1997). Enhancement of NO production from resident peritoneal macrophages by in vitro gamma-irradiation and its relationship to reactive oxygen intermediates. *Free Radic. Biol. Med.* 22: 1029-1035.

344. Stuehr, D. J. (1996). Purification and properties of nitric oxide synthases. *Methods Enzymol.* 268: 324-333.

345. Xie, Q. & Nathan, C. (1994). The high-output nitric oxide pathway: role and regulation. *J. Leukocyte Biol.* 56: 576-582.

346. Moncada, S., Palmer, R. M. & Higgs, E. A. (1991). Nitric oxide: physiology, pathophysiology, and pharmacology. [Review]. *Pharmacological Reviews* 43: 109-142.

347. Mclaughlan, J. M., *et al.* (1997). Interleukin-8 and inducible nitric oxide synthase mRNA levels in inflammatory bowel disease at first presentation. *J. Pathol.* 181: 87-92.

348. Zídek, Z. & Franková, D. (1995). Interferon-gamma/tumour necrosis factor-alpha synergism as a mechanism for enhanced nitric oxide production following *in vivo* administration of muramyl dipeptide (MDP) to mice. *Int. J. Immunopharmacol.* 17: 313-317.

349. Lonnroth, C., *et al.* (1990). Tumor necrosis factor-alpha and interleukin-1 alpha production in cachectic, tumor-bearing mice. *Int. J. Cancer* 46: 889-896.

350. Yamashina, K., Miller, B. E. & Heppner, G. H. (1986). Macrophage-mediated induction of drug-resistant variants in a mouse mammary tumor cell line. *Cancer Res.* 46: 2396-2401.

351. Lewis, J. G., Hamilton, T. & Adams, D. O. (1986). The effect of macrophage development on the release of reactive oxygen intermediates and lipid oxidation products, and their ability to induce oxidative DNA damage in mammalian cells. *Carcinogenesis* 7: 813-818.

352. Paul, L. A., Fulton, A. M. & Heppner, G. H. (1989). Reactive oxygen-mediated damage to murine mammary tumor cells. *Mutat. Res.* 215: 223-234.

353. Mozaffarian, N., Berman, J. W. & Casadevall, A. (1995). Immune complexes increase nitric oxide production by interferon-gamma-stimulated murine macrophage-like J774.16 cells. *J. Leukocyte Biol.* 57: 657-662.

354. Sheffler, L. A., *et al.* (1995). Exogenous nitric oxide regulates IFN-gamma plus lipopolysaccharide-induced nitric oxide synthase expression in mouse macrophages. *J. Immunol.* 155: 886-894.

355. Deguchi, M., *et al.*(1995). Exogenous and endogenous typ e I interferons inhibit interferon-gamma-induced nitric oxide production and nitric oxide synthase expression in murine peritoneal macrophages. *J. Interferon Cytokine Res.* 15: 977-984.

356. Wilson, K. T., *et al.* (1996). *Helicobacter pylori* stimulates inducible nitric oxide synthase expression and activity in a murine macrophage cell line. *Gastroenterology* 111: 1524-1533.

357. Ribbons, K. A., *et al.* (1997). The effect of inhibitors of inducible nitric oxide synthase on chronic colitis in the rhesus monkey. *Journal of Pharmacology & Experimental Therapeutics* 280: 1008-1015.

358. Thompson, M., *et al.* (1996). Expression of the inducible nitric oxide synthase gene in diaphragm and skeletal muscle. *J. Appl. Physiol.* 81: 2415-2420.

359. Moilanen, E., *et al.* (1997). Nitric oxide synthase is expressed in human macrophages during foreign body inflammation. *Am. J. Pathol.* 150: 881-887.

360. Goureau, O., *et al.* (1995). Increased nitric oxide production in endotoxin-induced uveitis: Reduction of uveitis by an inhibitor of nitric oxide synthase. *J. Immunol.* 154: 6518-6523.

361. Cannon, G. W., *et al.* (1996). Nitric oxide production during adjuvant-induced and collagen-induced arthritis. *Arthritis Rheum.* 39: 1677-1684.

362. Mizutani, T. & Layon, A. J. (1996). Clinical applications of nitric oxide. *Chest* 110: 506-524.

363. Roberts, J. D., *et al.* (1997). Inhaled nitric oxide and persistent pulmonary hypertension of the newborn. *N. Engl. J. Med.* 336: 605-610.

364. Ellis, H. V., *et al.* (1984). Subacute and chronic toxicity studies of trinitroglycerin in dogs, rats, and mice. *Fundament. Appl. Toxicol.* 4: 248-260.

365. Tamano, S., *et al.* (1996). Histogenesis of the role of p53 and K-ras mutations in hepatocarcinogenesis by glyceryl trinitrate (nitroglycerin) in male F344 rats. *Carcinogenesis* 17: 2477-2486.

366. Evans, C. H., Stefanovic-Racic, M. & Lancaster, J. (1995). Nitric oxide and its role in orthopaedic disease. *Clin. Orthop.* 312: 275-294.

367. Chan, A. C. & Tran, K. (1990). The uptake of (R,R,R)alpha-tocopherol by human endothelial cells in culture. *Lipids* 25: 17-21.

368. Hockey, A. J., Adra, C. N. & McBurney, M. W. (1989). Reactivation of hprt on the inactive X chromosome with DNA demethylating agents. *Somatic Cell & Molecular Genetics* 15: 421-434.

369. Blakey, D. H., *et al.* (1995). Cytogenetic mapping of lambda gt10 lacZ sequences in the transgenic mouse strain 40.6 (Muta Mouse). *Mutagenesis* 10: 145-148.

370. Jüttermann, R., Li, E. & Jaenisch, R. (1994). Toxicity of 5-aza-2'-deoxycytidine to mammalian cells is mediated primarily by covalent trapping of DNA methyltransferase rather than DNA demethylation. *Proc. Natl. Acad. Sci. USA* 91: 11797-11801.

371. Kataoka, Y., *et al.* (1992). Antimutagenic effects of radioprotector WR-2721 against fission-spectrum neurons and 60Co gamma-rays in mice. *Int. J. Radiat. Biol.* 61: 387-392.

372. Nagy, B., Dale, P. J. & Grdina, D. J. (1986). Protection against cis-diamminedichloro platinum cytotoxicity and mutagenicity in V79 cells by 2-[(aminopropyl)amino]ethanethiol. *Cancer Res.* 46: 1132-1135.

373. Pillaire, M. J., *et al.* (1995). Replication of DNA containing cisplatin lesions and its mutagenic consequences. *Biochimie* 77: 803-807.

374. Plooy, A. C., *et al.* (1985). Influence of treatment temperature on the genotoxic effects of cisplatin in CHO cells: cytotoxicity, mutagenicity and induction of lesions in DNA. *Mutat. Res.* 151: 129-136.

375. Perera, F. P., *et al.* (1992). Multiple biological markers in germ cell tumor patients treated with platinum-based chemotherapy. *Cancer Res.* 52: 3558-3565.

376. Gibaldi, M. (1993). What is nitric oxide and why are so many people studying it. *J. Clin. Pharmacol.* 33: 488-496.

377. Dikshit, M., Seth, P. & Srimal, R. C. (1993). Effect of molsidomine and free radical scavengers on the pulmonary thromboembolism in mice. *Thromb. Res.* 70: 317-327.

378. Smith, R. P. & Kruszyna, H. (1974). Nitroprusside produces cyanide poisoning via reaction with hemoglobin. *Journal of Pharmacology & Experimental Therapeutics* 191: 557-563.

379. Burkart, V., *et al.* (1995). Suppression of nitric oxide toxicity in islet cells by α-tocopherol. *FEBS Lett.* 364: 259-263.

380. Salgo, M. G. & Pryor, W. A. (1996). Trolox inhibits peroxynitrite-mediated oxidative stress and apoptosis in rat thymocytes. *Arch. Biochem. Biophys.* 333: 482-488.

381. Duval, D. L., Sieg, D. J. & Billings, R. E. (1995). Regulation of hepatic nitric oxide synthase by reactive oxygen intermediates and glutathione. *Arch. Biochem. Biophys.* 316: 699-706.

382. Heales, S. J., *et al.* (1994). Trolox protects mitochondrial complex IV from nitric oxide-mediated damage in astrocytes. *Brain Res.* 668: 243-245.

383. Bendich, A. & Machlin, L. J. (1988). Safety of oral intake of vitamin E. [Review]. *Am. J. Clin. Nutr.* 48: 612-619.

384. Kappus, H. & Diplock, A. T. (1992). Tolerance and safety of vitamin E: a toxicological position report. [Review]. *Free Radic. Biol. Med.* 13: 55-74.

385. Bird, A. P. (1996). The relationship of DNA methylation to cancer. *Cancer Surv.* 28: 87-101.

386. Laird, P. W. & Jaenisch, R. (1996). The role of DNA methylation in cancer genetics and epigenetics. *Annu. Rev. Genet.* 30: 441-464.

387. Counts, J. L. & Goodman, J. I. (1995). Alterations in DNA methylation may play a variety of roles in carcinogenesis. *Cell* 83: 13-15.

388. Bostick, R. M., *et al.* (1993). Reduced risk of colon cancer with high intake of vitamin E: the Iowa Women's Health Study. *Cancer Res.* 53: 4230-4237.

389. Albanes, D., *et al.* (1995). Effects of alpha-tocopherol and beta-carotene supplements on cancer incidence in the Alpha-Tocopherol Beta-Carotene Cancer Prevention Study. *Am. J. Clin. Nutr.* 62: 1427S-1430S.

390. Losonczy, K. G., Harris, T. B. & Havlik, R. J. (1996). Vitamin E and vitamin C supplement use and risk of all-cause and coronary heart disease mortality in older persons: the Established Populations for Epidemiologic Studies of the Elderly. *Am. J. Clin. Nutr.* 64: 190-196.

391. Paolisso, G., *et al.* (1995). Chronic intake of pharmacological doses of vitamin E might be useful in the therapy of elderly patients with coronary heart disease. *Am. J. Clin. Nutr.* 61: 848-852.

392. Anonymous. (1994). The effect of vitamin E and beta carotene on the incidence of lung cancer and other cancers in male smokers. The Alpha-Tocopherol, Beta Carotene Cancer Prevention Study Group. *N. Engl. J. Med.* 330: 1029-1035.

393. Machlin, L. J. (1995). Critical assessment of the epidemiological data concerning the impact of antioxidant nutrients on cancer and cardiovascular disease. [Review] [4 refs]. *Crit. Rev. Food Sci. Nutr.* 35: 41-50.

394. Lafuze, J. E., *et al.* (1983). *Biology of vitamin E.* Ciba Foundation symposium 101, London. pp. 130-146.

395. Kanno, T., *et al.* (1995). Inhibition of stimulus-specific neutrophil superoxide generation by alpha-tocopherol. *Free Radic. Res.* 22: 431-440.

396. Mikami, S., *et al.* (1996). Expression of nitric oxide synthase in a murine model of viral myocarditis induced by coxsackievirus B3. *Biochem. Biophys. Res. Commun.* 220: 983-989.

397. Radi, R., *et al.* (1991). Peroxynitrite oxidation of sulfhydryls. The cytotoxic potential of superoxide and nitric oxide. *J. Biol. Chem.* 266: 4244-4250.

398. Dias, V. C., Wallace, J. L. & Parsons, H. G. (1992). Modulation of cellular phospholipid fatty acids and leukotriene B4 synthesis in the human intestinal cell (CaCo-2). *Gut* 33: 622-627.

399. Perretti, M., *et al.* (1993). Pharmacology of interleukin-1-induced neutrophil migration. *Agents & Actions* 38 Spec No: C64-5.

400. Van Osselaer, N., *et al.* (1991). Increased microvascular permeability in vivo in response to intradermal injection of neutrophil-activating protein (NAP-2) in rabbit skin. *Am. J. Pathol.* 138: 23-27.

401. Rampart, M., *et al.* (1989). Granulocyte chemotactic protein/interleukin-8 induces plasma leakage and neutrophil accumulation in rabbit skin. *Am. J. Pathol.* 135: 21-25.

402. Lejeune, P., *et al.* (1994). Interleukin-8 has antitumor effects in the rat which are not associated with polymorphonuclear leukocyte cytotoxicity. *Cancer Immunology, Immunotherapy* 38: 167-170.

403. Pekarek, L. A., *et al.* (1995). Inhibition of tumor growth by elimination of granulocytes. *J. Exp. Med.* 181: 435-440.

404. Colombo, M. P., *et al.* (1992). Local cytokine availability elicits tumor rejection and systemic immunity through granulocyte-T-lymphocyte cross-talk. [Review]. *Cancer Res.* 52: 4853-4857.

405. Yuan, L., *et al.* (1993). An evaluation of the effects of cytokines on intracellular oxidative production in normal neutrophils by flow cytometry. *Exp. Cell Res.* 209: 375-381.

406. Colombo, M. P., *et al.* (1992). Granulocyte colony-stimulating factor (G-CSF) gene transduction in murine adenocarcinoma drives neutrophil-mediated tumor inhibition in vivo. Neutrophils discriminate between G-CSF-producing and G-CSF-nonproducing tumor cells. *J. Immunol.* 149: 113-119.

407. Colombo, M. P., Mattei, S. & Parmiani, G. (1992). Cytokine gene transfer in tumor cells as an approach to antitumor therapy. [Review]. *International Journal of Clinical and Laboratory Research* 21: 278-282.

408. Pekarek, L. A., *et al.* (1993). Footprinting of individual tumors and their variants by constitutive cytokine expression patterns. *Cancer Res.* 53: 1978-1981.

409. Colombo, M. P., *et al.* (1992). Expression of cytokine genes, including IL-6, in human malignant melanoma cell lines. *Melanoma Research* 2: 181-189.

410. Corbett, J. A. & McDaniel, M. L. (1996). Selective inhibition of inducible nitric oxide synthase by aminoguanidine. *Methods Enzymol.* 268: 398-408.

411. Wolff, D. J. & Lubeskie, A. (1995). Aminoguanidine is an isoform-selective, mechanism-based inactivator of nitric oxide synthase. *Arch. Biochem. Biophys.* 316: 290-301.

412. Tamir, S., *et al.* (1993). The influence of delivery rate on the chemistry and biological effects of nitric oxide [published erratum appears in Chem Res Toxicol 1994 May-Jun;7(3):469]. *Chem. Res. Toxicol.* 6: 895-899.

413. Stamler, J. S. (1995). S-nitrosothiols and the bioregulatory actions of nitrogen oxides through reactions with thiol groups. *Curr. Top. Microbiol. Immunol.* 196: 19-36.

414. Meister, A. (1981). Metabolism and functions of glutathione. *Trends 3 Biochem. Sci.* 6: 231-234.

415. Petit, J. F., *et al.* (1996). Protection by glutathione against the antiproliferative effects of nitric oxide -Dependence on kinetics of NO release. *Biochem. Pharmacol.* 52: 205-212.

416. Kuo, P. C. & Abe, K. Y. (1996). Nitric oxide-associated regulation of hepatocyte glutathione synthesis is a guanylyl cyclase-independent event. *Surgery* 120: 309-314.

417. Bolaños, J. P., *et al.* (1996). Nitric oxide-mediated mitochondrial damage: A potential neuroprotective role for glutathione. *Free Radic. Biol. Med.* 21: 995-1001.

418. Luperchio, S., Tamir, S. & Tannenbaum, S. R. (1996). NO-induced oxidative stress and glutathione metabolism in rodent and human cells. *Free Radic. Biol. Med.* 21: 513-519.

419. Sandhu, J. K. & Birnboim, H. C. (1998). *Vitamin E inhibits in vivo mutagenicity of nitric oxide-donating drugs in mouse MN-11 tumours* (submitted)

420. Nelson, S. L., *et al.* (1995). Mapping the end points of large deletions affecting the *hprt* locus in human peripheral blood cells and cell lines. *Radiat. Res.* 141: 2-10.

421. Lorenz, R., *et al.* (1994). Dose and dose-rate dependence of the frequency of *HPRT* deficient T lymphocytes in the spleen of the ^{137}Cs gamma-irradiated mouse. *Int. J. Radiat. Biol.* 66: 319-326.

422. Kataoka, Y., Perrin, J. & Grdina, D. J. (1993). Induction of *hprt* mutations in mice after exposure to fission-spectrum neutrons or ^{60}Co gamma rays. *Radiat. Res.* 136: 289-292.

423. Zhou, P. K., *et al.* (1993). Cultured mouse SR-1 cells exposed to low dose of gamma-rays become less susceptible to the induction of mutagenesis by radiation as well as bleomycin. *Mutagenesis* 8: 109-111.

APPENDIX I: DEVELOPMENT OF MN-11 TUMOR MODEL SYSTEM

Methylcholanthrene

↘

C57BL/6 MALE MOUSE

↓

MC1A FIBROSARCOMA
(maintained by transplantation in syngeneic animals)

↓

MC1A-C1
(clonal variant of MC1A which is tissue culture adapted)
($HPRT^-$, HAT^R, $6\text{-}TG^S$)
$HPRT^{+/+/-}$ or $HPRT^{+/+/+}$ genotype

N-methyl-*N*-nitrosourea (MNU) ↗ ↓

MC-TGR17
($HPRT^-$, HAT^S, $6\text{-}TG^R$)
$HPRT^{-/-/-}$ genotype

↓

MC-TGS17-51
($HPRT^-$, HAT^R, $6\text{-}TG^S$)
$HPRT^{+/-/-}$ genotype

infection with a retroviral construct ↗ ↓

carrying the *neo* gene

MN-SERIES
($HPRT^-$, HAT^R, $G418^R$, $6\text{-}TG^S$)
$HPRT^{+/-/-}$ genotype

APPENDIX II: LIST OF CHEMICALS, SUPPLIERS AND SOLUTION COMPOSITION

α-napthyl acetate	Sigma Chemical Co
AES	ICN
Aminopterin	Sigma Chemical Co; stored at -20°C as a stock solution of 4×10^{-5} M
Assay buffer	1 mM KH_2PO_4, 0.2 mM $CaCl_2$, 1 mM $MgCl_2$, 1 mM β-NADPH, 6 mM L-valine, 18 μM L-arginine, 1 μCi ^{14}C-L-arginine (Amersham)
5-Aza-Cytidine	Sigma Chemical Co; Stock solution of 0.5 mM was prepared in complete medium immediately before use
β-NADPH	Sigma Chemical Co
Bleomycin sulfate	3 units/mL, (Blenoxane); Bristol-Meyers Squibb Canada
5-Bromo-2'-Deoxyuridine	Sigma Chemical Co
Caffeine	BDH
Catalase	Sigma Chemical Co; (EC 1.11.1.6) from bovine liver
Cisplatin	1 mg/mL solution; David Bull Lab (Canada)
Colcemid	10 μg/mL stock; Gibco BRL
DAB	Sigma Chemical Co., Stock solution of 2.4% DAB prepared in TBS , aliquoted and frozen at -80 °C
(dl)-α-tocopherol acetate	deCiba-Geigy, Canada
DMEM	Gibco BRL
DMSO	J.T. Baker
Ferric chloride	Fischer
Fetal Calf Serum	Flow Laboratories, Inc.
Geneticin (G418)	Gibco BRL, New York, USA; stored at -20°C as a 50 mg/mL stock in 10 mM Tris-HCl, pH 6.0
Glucose oxidase	Sigma Chemical Co; stored as a stock solution of 150 units/mL in H_2O at -20 °C
GTN	5 mg/mL (22 mM); David Bull Lab (Canada) Inc; dilution was made in PBS, immediately before use in subdued light
Homogenization buffer	320 mM sucrose, 10 mM HEPES, 1 mM D,L-thiothreitol, 1 mM EDTA, 10 μg/mL soybean trypsin inhibitor, 10 μg/mL leupeptin, and 2 μg/mL aprotinin, pH 7.4
Hydrogen peroxide	Fischer; 7.98 M stock stored at 4°C; dilution was made in H_2O, immediately before use
Hypoxanthine	Sigma Chemical Co; see Appendix II.1 for preparation procedure
Lipopolysaccharide	Sigma Chemical Co; from *E. coli* 0128:B12
LumiGLO™ substrate kit	Kirkegaard & Perry Laboratories, Maryland, USA
Methyl Green	J.T. Baker
Molsidomine	Hoechst-Roussel Canada Inc., Montreal or Sigma; 0.05 M stock in complete medium prepared fresh in subdued light, filtered through 0.2 μm filter and used immediately

N-(1-napthyl)-ethylene-diamine dihydrochloride	Sigma Chemical Co; Stored as a stock solution of 0.1% in H_2O at 4°C protected from light
N^G-monomethyl-L-arginine	Toronto Research Chemicals, Inc; stored at -20°C as a stock of 50 mM in H_2O
Nitrate reductase	Sigma Chemical Co; (EC 1.6.6.2) from *Aspergillus* species
Nitroblue tetrazolium	Sigma Chemical Co
Oxyhaemoglobin	Sigma Chemical Co (bovine haemoglobin type I)
Phosphate buffered saline	2.7 mM KCl, 1.5 mM KH_2PO_4, 137 mM NaCl, 4.3 mM Na_2HPO_4, pH 7.4
Persidomine	Hoechst-Roussel Canada Inc., Montreal
PN buffer	100 mM sodium phosphate, 0.05% Nonidet P-40, pH 8.0
Rhodanese	Sigma Chemical Co
(R,R,R) α-tocopherol	Gift from Dr. Alvin Chan
Sample loading buffer	125 mM Tris-HCl, pH 6.8, 4% SDS, 20% glycerol, 2% bromophenol blue, 10% v/v freshly added β-mercaptoethanol
SNAP	Toronto Research Chemicals, Inc.
SNP	Aldrich Chemicals; 100 mM stock in serum free medium was prepared immediately before use in subdued light
Sulfanilamide	Sigma Chemical Co; stored as a stock solution of 1.0% in 5% phosphoric acid at 4°C
Superoxide dismutase	DDI Pharmaceuticals, Mount View, CA; (EC 1.15.1.1) from bovine liver
Sodium cyanide	J.T. Baker
Sodium nitrite	Fischer
Sodium thiosulfate	Fischer
SPER/NO	Toronto Research Chemicals, Inc.
2X SSC	150 mM NaCl, 15 mM sodium citrate, pH 7.0
Streptonigrin	Sigma Chemical Co
6-TG	Sigma Chemical Co; stored at -20 °C as a stock solution of 10 mM in H_2O
TBS (Tris buffered saline)	50 mM Tris-HCl (pH 8.0), 150 mM NaCl, Adjust pH to 7.6
Thymidine	Sigma Chemical Co
TPA	12-*O*-Tetradecanoylphorbol-13-acetate, LC Services Corp., Woburn, MA; stored at -20°C as a stock solution of 1×10^{-4} M in dimethyl sulfoxide
Trypan blue stain	Mix 4 parts 0.2% trypan blue with1 part 4.25% NaCl prior to use; mix cells in a 1:1 (v/v) ratio
Toluidine blue O	Fischer
Wright's stain	BDH; 1.7 g wright's stain in 1 litre of methanol

II.1 Preparation of HAT-medium

II.1.1 HT-medium: Stock (100 ×) contains hypoxanthine and thymidine at a concentration of 1×10^{-2} M and 1.5×10^{-3} M, respectively.

Weigh 0.1361 g of hypoxanthine and dissolve in 40 mL of dd H_2O. Similarly weigh 0.036

g of thymidine separately and dissolve in 40 mL of dd H_2O. Combine the two drugs in a 250 mL beaker, add a stir bar and add 2-3 drops of 10 N NaOH completely to dissolve HT. Make volume to 100 mL with dd H_2O. Filter sterilize through 0.2 μm filter and dispend into 1.5 mL autoclaved microfuge tubes. Store at -20°C. Add 100 μL to 10 mL of non-selective medium so that the final concentration of hypoxanthine and thymidine are 1×10^{-4} M and 1.5×10^{-5} M, respectively.

II.1.2 Aminopterin: Stock (100 ×) contains aminopterin at a concentration of 4×10^{-5} M. Weigh 1.76 mg of aminopterin and dissolve in 100 mL of dd H_2O. Completely dissolve aminopterin by adding 2-3 drops of 10 N NaOH. Filter sterilize through 0.2 μm filter and dispend into 1.5 mL autoclaved microfuge tubes. Store at -20°C covered with tin foil since aminopterin is light sensitive. Add 100 μL to 10 mL of non-selective medium so that the final concentration is 4×10^{-7} M.

HAT-medium is non-selective medium supplemented with hypoxanthine, aminopterin and thymidine at concentrations of 1×10^{-4} M, 4×10^{-7} M and 1.5×10^{-5} M, respectively.

APPENDIX III: PREPARATION OF FIXATIVE AND ANTIBODY SOLUTIONS

Preparation of reagents used for histochemical studies and staining techniques is described in reference [250].

Modified Zamboni's fixative

paraformaldehyde	4%
picric acid	0.4%
160 mM PB, pH 6.9	

Dissolve 40 g paraformaldehyde in 300 mL distilled H_2O by heating in a fume hood, stirring constantly until only a faint cloudiness persists. Clarify this solution by adding 10 N NaOH drop by drop until the solution is clear. Cool to room temperature, then at 4°C and filter. Add sufficient 0.5 M NaH_2PO_4 (stock) to about 250 mL 0.5 M Na_2HPO_4 (stock) to bring the pH to 7.1. Take 320 mL of this phosphate buffer, and add 140 mL of saturated picric acid. To this solution, add the paraformaldehyde solution, filter and adjust pH to 6.9 and make up to 1 L. Fixative should be cleared from the tissue in several washes of 100 mM PB, pH 7.2.

ANTIBODY SOLUTIONS

Non-specific activity blocker

Bovine serum albumin	4.0 g
Sucrose	10 g
Normal swine serum	1 mL
50 mM TBS, pH 7.6	100 mL

Filter sterilize through 0.45 μm filter and store at 4°C.

Primary and Secondary antibody diluent

Bovine serum albumin	4.0 g
Sucrose	10 g
50 mM TBS, pH 7.6	100 mL
Sodium azide	0.1%

Filter sterilize through 0.45 μm filter and store at 4°C.

PREPARATION OF AES COATED SLIDES

Dip slides in 10% Extran 300 solution overnight. Wash slides in hot running water for 30 min. Dry them at 60°C for 20 min and bring to room temperature. Prepare fresh solution of 2% AES with dry acetone and place slides for 2 min. Dry acetone is prepared by adding sodium sulfate to acetone and filtering with a coarse filter. Wash slides in dry acetone (few dips) and then in distilled water thoroughly. Dry at 42°C overnight and use.

APPENDIX IV: GENERAL METHODS

IV.1 *Cells and Culture conditions*

Cells (MC1A-C1, MC-TGS17-51 and MN-series) were grown in 10 cm tissue culture dishes in non-selective medium (Dulbecco's Eagle medium (DMEM) supplemented with 10% fetal calf serum (FCS)) at 37°C in a humidified atmosphere of 5% CO_2/95% air. To remove any pre-existing mutants, cells were grown in HAT-medium for 7 days and transferred to HT-medium for 2 days to allow recovery from HAT treatment. If cells were transferred directly from HAT-medium to non-selective medium, the plating efficiency of the cells was only about 5%. Hence, when cells grown in HAT-medium needed to be transferred to non-selective medium they had to be cultured first in HT-medium for a minimum of 24 h, although 2 days was chosen in all experiments. For subculture, cells were detached with 0.05% trypsin and seeded at 2×10^5 cells per 10 cm dish in fresh medium.

IV.2 *Determination of* in vitro *mutant frequency*

Exponentially growing cultures were trypsinized and 5×10^5 cells (determined by trypan blue exclusion) per 10 cm tissue culture dish were allowed to attach overnight. Cultures were then subjected to either a physical or chemical agent (described in Chapters 2 and 3). Following treatments, cultures were incubated at 37°C for 24 h, unless otherwise indicated, washed with PBS and split into two sets of dishes. For determination of cytotoxicity, 200 cells/6 cm dish (unless otherwise indicated) were seeded in non-selective medium and were kept without any renewal of medium. Colonies were stained and scored (> 50 cells) after 7-9 days (MN-series) or 10 days (MC-TGS17-51), as described below. For determination of MF, $5\text{-}10 \times 10^5$ cells/10 cm dish were grown in non-selective medium for 8 days to allow the full expression of the mutant phenotype. The subculture was done twice or three times during the expression time to avoid confluence or a cell number lower than 5×10^5. Mutant cells were detected by plating 1×10^5 cells (determined from the reconstruction experiment as described in Chapter 2) per 10 cm dishes in 6-TG-medium. Twice weekly, culture medium was replaced with 6-TG-medium. 6-TG^R colonies (> 50 cells) were scored at either 10 days (MN-series) or 14 days for MC-TGS17-51. 6-TG-medium was non-selective medium supplemented with 5×10^{-5} M 6-thioguanine. In parallel, plating efficiency was determined by seeding 200 cells/6 cm dish. MF is expressed as mutants per 1×10^5 viable cells, where viability was determined from the plating efficiency.

IV.3 *Determination of* in vivo *mutant frequency*

Cells were grown and prepared for animal experiments as described above. 1×10^5 cells/10 cm dish (in triplicate) were seeded in 6-TG-medium to verify the effectiveness of HAT treatment. To determine the spontaneous MF, 5×10^5 cells/10 cm dish (in duplicate) were placed in non-selective medium, subcultured as needed, and challenged with 50 μM 6-TG. Tumors were formed by injecting 5×10^5 cells subcutaneously (0.1 mL suspension, using a 1 c.c. syringe #25 G⅝ needle) into the right flanks of syngeneic C57BL/6 female mice, 8-10 weeks of age (Charles River Laboratories). Animals were maintained on regular laboratory chow, 2-3 per cage (12 h light-dark cycle). When tumors reached approximately 1 cm in diameter (14 days after injection), animals were sacrificed by cervical dislocation.

Tumors were excised aseptically, dead and necrotic tissue as well as the encapsulating fibrous sheath (white in appearance) was removed. Single cell suspensions were prepared by finely mincing the tumor tissue with a scalpel blade (#22), and mechanically disaggregating further by triturating with 3 c.c syringes (without a needle). After centrifugation at 1000 rpm at 4°C, supernatants were removed by aspiration. The pellets were suspended in non-selective medium and transferred to 10 cm dishes. Following incubation for 24 h, non-adherent dead cells and tumor fragments were removed, cultures were washed with PBS and replaced with fresh non-selective medium. Cells were established in culture for 4-5 days. MF and plating efficiency was determined essentially as described above. To estimate the percentage of total cells which were $G418^R$, 200 cells/6 cm were seeded in G418-medium. G418-medium is non-selective medium containing 500 μg/mL G418. After 8 days, colonies were stained and scored. The number of $6\text{-}TG^R$ mutants was corrected for plating efficiency and for G418-resistance. All animal procedures were carried out in accordance with guidelines of the Canadian Council on Animal Care.

$$\text{Mutant frequency (corrected for } G418^R \text{ cells)} = \frac{\#\text{ of } 6\text{-}TG^R \text{ colonies}}{1 \times 10^5\ G418^R \text{ cells}}$$

$$\text{Mutant frequency (corrected for viable } G418^R \text{ cells)} = \frac{\#\text{ of } 6\text{-}TG^R \text{ (corrected for } G418^R\text{) colonies}}{1 \times 10^5 \text{ viable } G418^R \text{ cells}}$$

IV.4 ***Staining and scoring of colonies***

Following incubation, dishes were removed from the incubator, washed with PBS, colonies fixed with methanol for 15-20 min, rinsed with PBS and stained with Wright's stain for 5 min. Excess stain was removed by rinsing gently with running water. Colonies are scored after air drying overnight at room temperature. Colonies comprising > 50 cells (> 0.2 mm) were considered to be viable and could be readily scored under 2.5 × magnification.

APPENDIX V: LIST OF PUBLICATIONS

Refereed papers, published

1. **Sandhu, J. K.,** and Kahlon, S. S. Citric acid production by *Aspergillus niger*. Optimization of parameters. J. Res. PAU. 29, 350-354, 1992 (Published in India)
2. **Sandhu, J. K.,** and Birnboim, H. C. Fluorometric determination of DNA in Agarose gels: Usefulness for measurement of double-strand breaks in Non-labelled cells by pulsed-field gel electrophoresis. Radiation Research. 135, 3: 338-342, 1993
3. Wilkinson, D., **Sandhu, J. K.,** Breneman, J. W., Tucker, J. D. and Birnboim, H. C. *Hprt* mutants in a transplantable murine tumor arise more frequently *in vivo* than *in vitro*. British Journal of Cancer. 72, 1234-1240, 1995
4. Birnboim, H.C., and **Sandhu, J.K.** Levels of DNA Strand Breaks and Superoxide in Phorbol Ester-Treated Human Granulocytes. Journal of Cellular Biochemistry. 66, 219-228, 1997
5. **Sandhu, J. K.,** and Birnboim, H. C. Mutagenicity and Cytotoxicity of Reactive oxygen and Reactive nitrogen species in the MN-11 murine tumor cell line. Mutation Research. 379, 2: 241-252, 1997

Refereed papers, submitted

1. **Sandhu, J. K.,** and Birnboim, H. C. Vitamin E inhibits *in vivo* mutagenicity of nitric oxide-donating drugs in mouse MN-11 tumors.

ABSTRACTS

Refereed contributions

1. Wilkinson, D., **Sandhu, J. K.,** Birnboim, H. C., and Himms-Hagen, J. Construction of a transplantable mouse tumor cell line containing a selectable marker to allow sensitive determination of *in vivo* and *in vitro* clastogenic events. FASEB Journal. 7 (7), A1067, 1993
2. Wilkinson, D., **Sandhu, J. K.,** Reid, A., and Birnboim, H. C. A murine tumor with an *hprt* marker gene for detection of *in vitro* and *in vivo* clastogenic/mutagenic events: effect of an antifolate drug. Proceedings of American Association of Cancer Research. 36, A1034, 1995

Non-refereed contributions

1. Wilkinson, D., **Sandhu, J. K.,** Birnboim, H. C. Development of a tumor model system to detect spontaneous and induced *in vitro* and *in vivo* clastogenic events with high sensitivity. An AACR Special Conference in Cancer Research. (Dec. 7-12, 1992) Banff, Alberta, Canada
2. **Sandhu, J. K.,** Wilkinson, D., and Birnboim, H. C. A transplantable mouse tumor cell line genetically altered to allow sensitive determination of *in vivo* and *in vitro* clastogenic events. New directions in Cancer Research: A symposium in honour of Peter G.Scholefield (Sep 19-22, 1993) Honey Harbour, Ontario, Canada
3. **Sandhu, J. K.,** Wilkinson, D., and Birnboim, H. C. Sensitive detection of genomic instability *in vivo* as evidenced by gene loss in a transplantable murine tumor cell line. An AACR Special Conference in Cancer Research, Cancer: Perturbations in Cell Cycle Control and Genomic integrity (Feb. 19-24, 1994) Banff, Alberta, Canada

4. J. R. McLean, A. Thansandote, D. Lecuyer, M. Goddard, J. Kim, H. C. Birnboim, **J. K. Sandhu**, J. C. Scaiano and F. Johnson. The design of experiments to test the effect of 60 Hz magnetic fields on initiation, malignant conversion and progression in mouse tumor models. DOE's Contractors Review in Palm Spring, CA, Nov 11-16, 1995

5. **Sandhu, J. K.,** Privora, H. F., and Birnboim, H. C. Nitric oxide: Possible involvement in tumor progression. Resident Research Day, Department of Medicine, Ottawa, May 1-3, 1996

IMAGE EVALUATION
TEST TARGET (QA-3)

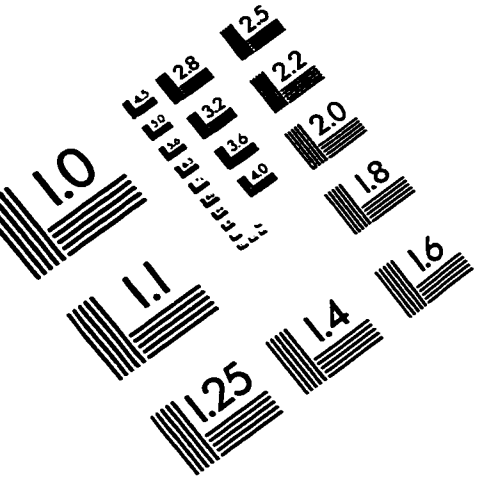

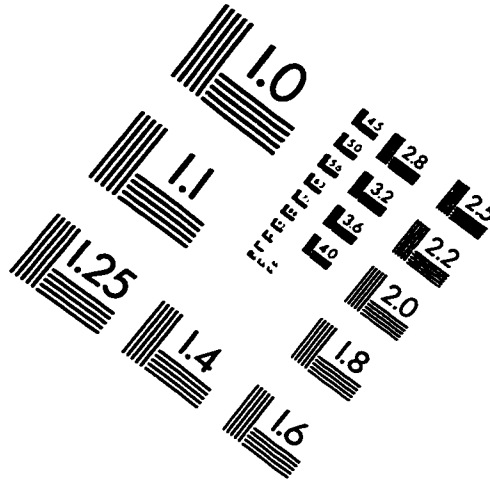

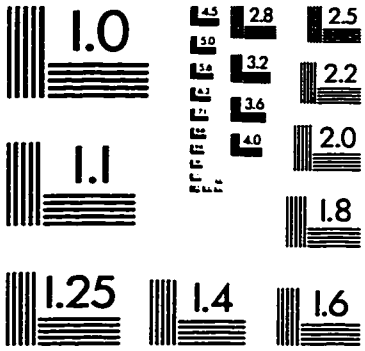

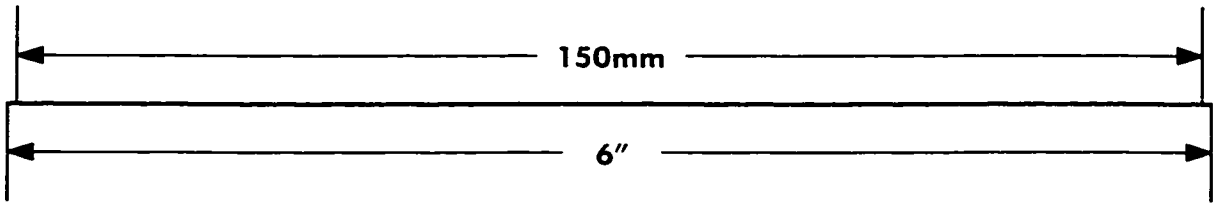

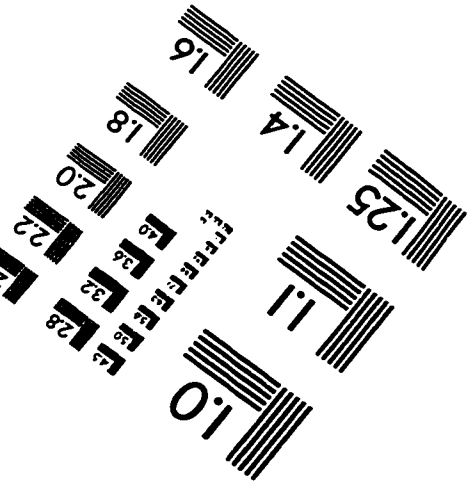

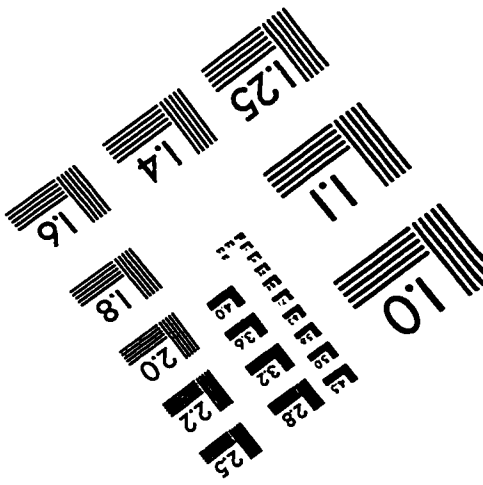

APPLIED IMAGE, Inc
1653 East Main Street
Rochester, NY 14609 USA
Phone: 716/482-0300
Fax: 716/288-5989